UV-RESISTANCE LOCUS 8 and UV-B Specific Signaling in *Arabidopsis thaliana*

By

Lauren R. Headland

Thesis submitted for the degree of Doctor of Philosophy

Division of Biochemistry and Molecular Biology
Faculty of Biomedical and Life Sciences
University of Glasgow

December, 2009

For Maman and Missy

Abstract

UV-B is a natural component of the sunlight spectrum. As a result of the potentially harmful effects of this radiation, plants have evolved a highly effective suit of protective and repair mechanisms. However, the signalling pathways that control such responses are not yet well known. For example while the photoreceptors responsible for red and blue light responses are well characterised, no such UV-B photoreceptor has yet been identified. Despite this particularly large gap in our knowledge, previous work identified the first UV-B specific signalling component which, unlike the more general stress-associated pathways often seen at high doses, specifically regulates expression of genes in response to even very low fluence rates of UV-B. This protein, UV-RESISTANCE LOCUS 8 (UVR8) regulates the induction of a number of photoprotective genes mostly via the transcription factors ELONGATED HYPOCOTYL 5 (HY5) and HY5 HOMOLOGUE (HYH). The end result of this pathway is the production of photoprotective compounds such as the flavonoids which enhance a plants ability to withstand UV-B stress. Thus UVR8 promotes plant fitness under these conditions.

While we know that UVR8 binds to chromatin in the promoter region of HY5 and that it accumulates in the nucleus under UV-B, many other questions about this particular protein remain unanswered. For example, we do not yet know if UVR8-mediated UV-B signalling involves other factors which interact with UVR8 nor do we understand the mechanism by which UVR8 localisation is mediated. In addition, although we are aware of the importance of UVR8 in UV-B acclimation, it is unclear what roles might be played by other genes and proteins acting independently of this pathway. Therefore, the aims of this study were to investigate low fluence UV-B pathways that may act independently of UVR8 and to further examine the UVR8 protein itself both in terms of its interactions with other proteins and also in the role of the N-terminal region in regulation of its localisation.

To achieve the first of these aims, RNA samples derived from plants treated with low fluence UV-B were submitted for microarray analysis. It was initially determined that the total number of genes induced was roughly equal in both low fluence treated samples and also to that found in the previous microarray performed by Brown *et al*. (2005) at a comparatively higher fluence. Thus, as only 72 genes have currently been linked to UVR8, there do appear to be many low-fluence UV-B induced pathways besides that regulated by UVR8. Several genes were analysed further using RT-PCR and qPCR methods in order to confirm their independence from the UVR8 signalling pathway components as well as assess their dependence on other hypothesised UV-B sensory

mechanisms. It was found that while some genes did seem to be expressed independently of known photoreceptors, DNA damage signals as well as UVR8, HY5, HYH and COP1; one gene was expressed in a COP1-dependent but UVR8 independent manner. It therefore appears that at least four classes of genes are induced by UV-B; low fluence UVR8/HY5/HYH independent COP1 dependent, low fluence UVR8/HY5/HYH/COP1 dependent, low fluence UVR8/HY5/HYH/COP1 independent and finally high fluence non-specific signalling.

The second portion of this thesis examined the structure and function of UVR8 in greater detail. To assist in this analysis, the BLAST sequence homology tool was used to probe both the Arabidopsis genome and available green plant sequences. It was found that 23 UVR8-like sequences exist in *Arabidopsis* but none of these appear to have similar N or C-terminal sequences to UVR8. As these two regions have previously been shown to be of vital importance in UVR8 function (Kaiserli and Jenkins, 2008; Kaiserli unpublished data) it is unlikely that any are acting in a redundant fashion to UVR8. A number of similar proteins to UVR8 can be found in other plant species. These potential homologues however fall into two categories based on their closer similarity with either UVR8 or its close homologue in humans REGULATOR OF CHROMATIN CONDENSATION 1 (RCC1). The wide variety of plant species that did show UVR8-like proteins suggests that this particular means of UV-B acclimation may have arisen relatively early with the colonisation of land plants. Interestingly, many of these likely homologues had a conserved N terminal.

The N-terminal of UVR8 has previously been show to have a role in UV-B dependent nuclear accumulation (Kaiserli and Jenkins, 2008). This was examined further in Chapter 4 through the generation of a number of deletion and addition constructs in both a stable *Arabidopsis uvr8-1* background as well as transiently in tobacco. From analysis of localisation of these constructs via confocal microscopy it was determined that the first 12 amino acids are sufficient but not necessary for nuclear accumulation, while the first 20 appear to be both necessary and sufficient. Indeed, it was shown that the initial 32 amino acids also confer constitutive localisation of a GFP tag in the nucleus regardless of light condition and despite the presence of a nuclear exclusion signal (NES). It therefore appears that this region, which shows strong conservation with UVR8-like proteins in other plant species, is of vital importance to the nuclear accumulation seen under UV-B.

Finally, in Chapter 5, the possibility that UVR8 may be acting as part of a complex was explored. This involved use of size exclusion chromatography to provide approximate sizes of the UVR8 protein complex. It was found that native UVR8 appears to exist in a

complex of about 70-90 kDa in size. This suggests that at least one other protein interacts stably with UVR8. Other fusion constructs were also analysed in this way, however the results were more difficult to interpret due the apparent artificial dimerisation of the GFP tag.

In summary, the work presented here has shown that although UVR8 dependent pathways are predominant, a variety of low fluence UV-B induced genes and pathways may exist. Homology searches and mutational analyses suggest that the N-terminal region of UVR8 plays a critical role in its function and localisation. Finally, size exclusion chromatography suggests that UVR8 forms a complex in vivo with as yet uncharacterised partner proteins.

In total these results provide further insight into the mechanisms UVR8 action and highlight new avenues for both UVR8 dependent and independent UV-B signalling.

Acknowledgements

I would firstly like to thank my supervisor Professor Gareth I. Jenkins for his guidance over the period of my studies. In addition, my thanks also go to the BBSRC for funding those studies. I am grateful to Dr John Christie for his valuable advice and suggestions over the course of this work. Special thanks must also go to Drs Julin Maloof and Neelima Sinha for providing a wonderful working environment which complimented my time writing this thesis. I owe a great deal to all the members of the Brian lab, both past and present for not only helping my labwork to go smoothly but also for excursions to the pub and acting as guinea pigs for my various baking experiments. In particular I want to mention Dr Bobby 'Ceilidh' Brown for his initial babysitting duties as well as his continuing help and support. Additional mentions to Drs Cat Cloix and Eirini Kaiserli for their constant input and their willingness to pass on some of their considerable knowledge. For technical help, plant-sitting and many a coffee break chat I am grateful to Jane Findlay and Peggy Ennis. Also my thanks go to Drs Stuart Sullivan, Cat Thomson, Andy Love and Bo Wang whose help from day to day was too extensive to list here.

Outside of the Brian Lab, my thanks go to Dr Gill Nimmo and Janet Laird for helping me to master both the qPCR and SEC machines. For his help formulating equations for the timecourse analysis I'm grateful to Mark Girolami.

Outwith of the world of science, my thanks go to Catherine Lee for providing a roof over my head as well as tolerating a near permanent layer of icing sugar over her kitchen. I am especially grateful to Matt for not only acting as a soundboard for my ideas but also for his unceasing encouragement and ability to make me smile no matter what. My final thanks go to Maman and Missy, who have helped in ways they could never imagine over the duration of my studies and for their love, friendship, support and for being an amazing mother and sister.

Publications

Parts of this thesis have been published in the following publication;

Brown BA, Headland LR and Jenkins GI (2009) "UV-B Action Spectrum for UVR8-Mediated *HY5* Transcript Accumulation in Arabidopsis." Photochemistry and Photobiology 85, 1147-55.

Contents

Figures

CHAPTER 1

CHAPTER 2

CHAPTER 3

CHAPTER 4

APPENDICES

Abbreviations

2-OG	2-oxoglutarate-dependent dioxygenase
6-4PP	Pyrimidine (6,4)-pyrimidinone
ANAC	*Arabidopsis* NAC domain containing protein
BLAST	Basic Local Alignment Search Tool
BR	Brassinosteroid
BSA	Bovine Serum Albumin
bZIP	b-helix zipper
ChIP	Chromatin Immunoprecipitation
CHS	Chalcone synthase
Chum	Chalcone synthase underexpressing mutant
Col	Columbia
COP	Constitutive photomorphogenic
CPD	Cyclobutane pyrimidine dimer
CRY	Cryptochrome
CSN	COP9 signalosome
Δ	Deletion
DAPI	4',6-Diamidino-2-phenylindole
DASH	*Drosophila Arabidopsis Synechocystis* Human
DDB1	Damaged DNA binding protein 1
DEPC	Diethyl pyrocarbonate
DET	De-etiolated
DMSO	Dimethyl sulfoxide
dNTPs	Deoxyribonucleotide triphosphates
ds	Double stranded
DTT	1,4-Dithiothreitol
EDTA	Ethylenediaminetetraactetic acid
ELIP	Early Light-Induced Protein
EtBr	Ethidium bromide
EtOH	Ethanol
FAD	Flavin adenine dinucleotide
FAH1	Ferrulic acid hydroxylase
FHY	Far-red elongated hypocotyl
FHL	Far-red elongated hypocotyl-like

FR	Far-red light
GEF	Guanine nucleotide Exchange Factor
GFP	Green Fluorescent Protein
HRP	Horseradish peroxidase
HSP	Heat shock protein
HY5	ELONGATED HYPOCOTYL5
HYH	*HY5* homologue
HW	High white light
ICX	Increased chalcone synthase expression
K_{av}	Gel-phase distribution coefficient
LB	Luria broth medium
L. *er*	Landsberg *erecta*
LOV	Light oxygen voltage
Luc	Luciferase
LW	Low white light
MAPK	Mitogen-activated protein kinase
MATE	Multi drug and toxin efflux
MES	2-(N-morpholino)ethanesulfonic acid
M_r	Molecular weight
NASC	Nottingham *Arabidopsis* Stock Centre
NCBI	National Center for Biotechnology Information
NER	Nucleotide Excision Repair
NES	Nuclear export signal
NLS	Nuclear localization signal
NAS	Nuclear accumulation signal
NO	Nitric oxide
OD	Optical density
P_{FR}	Far-red light absorbing form of phytochrome
P_R	Red light absorbing form of phytochrome
PAL	Phenylalanine Ammonia-Lyase
PAR	Photosynthetically active radiation
PCR	Polymerase chain reaction
pH	$-\log_{10}$ (hydrogen ion concentration)
PHOT	Phototropin
PHR1	*Arabidopsis* type II CPD photolyase

PHY	Phytochrome
PIF	Phytochrome interacting factor
PMSF	Phenylmethanesulphonylfluoride
PR	Pathogenesis-related
Pro	Promoter
qPCR	Quantitative polymerase chain reaction
RbcS	Ribulose-1,5-bisphosphate carboxylase small subunit
RCC1	Regulator of Chromatin Condensation 1
ROS	Reactive oxygen species
RPK	Receptor protein kinase
RPK-L	Receptor protein kinase like
RT	Reverse transcriptase
35S	Cauliflower mosaic virus 35S promoter
SA	Salicylic acid
SDS	Sodium dodecyl sulfate
SDS-PAGE	SDS-polyacrylamide gel electrophoresis
SEC	Size exclusion chromatography
ss	single stranded
tt	transparent testa
TAE	Tris-acetate EDTA
TBE	Tris-borate EDTA
TBS	Tris buffered saline
TBS-T	Tris buffered saline triton-X
TBS-TT	Tris buffered saline triton-X Tween
T-DNA	Transfer DNA
TEMED	N,N,N',N'-tetramethylethane-1,2-diamine
TF	Transcription factor
UV	Ultraviolet
UVR	UV resistance locus
v/v	Volume / volume
V_0	Void volume
V_C	Column volume
V_e	Elution volume
WRKY	WRKY transcription factor

Ws	Wassilewskija
WT	Wild type
w/v	Weight / volume

CHAPTER 1 INTRODUCTION

1.1 Introduction

The natural world can be a very hostile place in which to live. All organisms are subjected to a number of environmental stresses that can fluctuate on a seasonal, daily or even hourly basis. As a result, numerous morphological and biochemical adaptations have evolved across all species that promote survival in such conditions. However, a clear divide is apparent between plant and animal groups in their primary responses to stressful stimuli. Animals would seem to have the advantage over plants as they are mobile and thus can alter behaviour in order to escape unfavourable conditions. For example the problem posed by a hot day can be addressed by simply retreating into the shade. Plants on the other hand are sessile organisms and so have no means of escape. Instead they have had to develop a larger suite of mechanisms in order to neutralize the effects of stressful conditions and repair the inevitable damage. Consequently, through the process of acclimation, they can adapt to their environment to ensure maximal survival and reproduction. In high temperatures for example, some plant species make alterations in the position of their leaves (e.g. in paraheliotropic plants) to minimize exposure to the sun or produce heat shock proteins to preserve the integrity of essential protein molecules (Taiz and Zeiger 1998; Feder and Hofmann 1999).

In addition to immobility, plants have one further restriction that animals do not. The vast majority of plant species are autotrophs and hence rely on sunlight to provide the energy required to drive photosynthesis. Therefore, good access to sunlight is crucial for survival. However, sunlight has a hidden danger within its spectrum which can pose a problem for plants, namely UV radiation (see Figure 1.5). UV radiation is composed of wavelengths that are shorter than those of the visible part of the spectrum. Consequently, UV has a greater inherent energy and so is a potential agent of damage not only to plants but also many other organisms. The exact effects of such exposure to UV are wide ranging, extending from catalysis of DNA repair to severe damage of biomolecules. The precise nature of these effects is highly dependent on the wavelength of the radiation. The shorter wavelengths (and thus high energies) of UV-C radiation (100-280 nm) means that it has the ability to cause severe damage to multiple cellular components. Fortunately for both animals and plants however, all UV-C radiation is absorbed in the stratospheric ozone layer and so never reaches the Earth's surface. UV-A on the other hand consists of longer, less energetic wavelengths that can pass through the ozone layer, but this form of radiation

is not a threat to living systems. Indeed the reverse could be said to be true as UV-A is implicated in some plant DNA repair pathways used to correct damage induced by other UV qualities (Tuteja *et al.* 2001).

UV-B lies at the centre of the UV spectrum and shares characteristics with both UV-A and UV-C. Similarly to UV-A, some longer wavelength UV-B is able to pass through the ozone layer and reach the biosphere. However, like UV-C, these waves are more energetic and so have the capacity to cause damage (albeit to a lesser degree than UV-C). As a result UV-B can be considered as one of the many abiotic stresses which have an impact on plant life. The precise effects of this radiation have become an area of increased interest since the discovery in the 1980's that the ozone layer appeared to be thinning (Rozema *et al.* 2005). A reduced ozone layer means a reduced capacity to filter out UV-B, hence an increased amount reaching the Earth's surface (McKenzie *et al.* 2003). It is therefore apparent that we need to determine what mechanisms plants already have in place to cope with UV-B radiation and how they may respond under increasing ambient levels. The fact that plants rarely show signs of 'sunburn' highlights that they must already have efficient mechanisms in place to combat the damaging effect of UV-B. Nonetheless, evidence from areas in Southern Patagonia show that in *Gunnera magellanica*, increased levels of DNA damage can be closely linked to the passage of an 'ozone hole' over this area (Rousseaux *et al.* 2001). Therefore, by studying the physiological and biochemical changes that occur in plants that allow them to acclimate to this stress will help us to determine the possible effects on natural species should UV-B levels rise.

Although the effects of UV-B would seem to be an important area of study and despite extensive research, our current knowledge of the exact mechanisms of perception and signal transduction are incomplete. Therefore, the purpose of this study is to further examine the various signalling components that appear to have a role in UV-B responses in plants and, in particular, to investigate the role of the key protein UV-RESISTANCE LOCUS 8 (UVR8) in this environmental response.

1.2 The damaging effects of UV-B/High dose responses

1.2.1 DNA damage

Macromolecules such as proteins, lipids and DNA are prone to damage through absorption of UV-B or via the ROS generated by this stressor. In the case of DNA, direct absorption of UV-B radiation results in phototransformations, the most common of which are the

formation of cyclobutane-pyrimidine dimers (CPDs) and pyrimidine (6,4)-pyrimidinone photoproducts (6-4PPs). These lesions impair the action of DNA interacting enzymes and can halt transcription (Britt 2004). Therefore in order to neutralize this damage plants initiate a number of repair mechanisms including photoreactivation, nuclear excision repair and homologous recombination (Ries *et al.* 2000; Waterworth *et al.* 2002; Kimura 2004). The later two of these mechanisms are more general repair mechanisms which can occur under both light and dark conditions. The more frequent means of repair, photoreactivation, however is mediated through DNA photolyases. These enzymes are responsible for the specific recognition and direct repair of either CPDs or 6-4PPs (Britt 2004). This is mediated through binding to the damaged bases before absorption of energy from a blue or UV-A light source. This then initiates electron transfer and breaks the cylcobutane ring (Sancar 1994). As a result, DNA integrity is restored and normal transcription can resume.

CPDs and 6-4 photoproducts have strikingly different structures and so are repaired by different types of photolyases. CPDs account for the majority (approximately 75%) of the pyrimidine dimers formed through absorption of UV-B (Britt 2004). While both types of pyrimidine dimers have the ability to block transcription, it seems the more common lesions, CPDs, have the most detrimental effect on plant systems. Jiang *et al.* (1997) showed that the CPD deficient photolyase mutant *uvr2* exhibits a greater inhibition of root growth under UV-B conditions than the corresponding 6-4PP photolyase mutant (*uvr3*). Furthermore, an increase in homologous recombination was seen in plants lacking the CPD photolyase. This alternative mechanism of DNA repair allows the plant to compensate for the reduced capacity to mend these dimers through photoreactivation.

Another difference between these enzymes occurs in their differential expression patterns. CPD photolyases are induced by both white light and UV-B whereas levels of the 6-4PP photolyase remain relatively constant. Interestingly however, in the presence of continuous white light, high levels of the CPD photolyase are not maintained and instead the protein is degraded. It would therefore seem that appropriate regulation of this enzyme requires light-dark cycling (Waterworth *et al.* 2002; Britt 2004).

In addition to photolyases, plants share another set of mechanisms for DNA repair that are shared with other eukaryotes. Two protein kinases, ataxia telangiectasia-mutated (ATM) and ataxia telangiectasia-mutated and Rad3-related (ATR) are also implicated in DNA repair mechanisms via the regulation of cell cycle progression (Sancar *et al.* 2004; Culligan *et al.* 2006). Through recognition of damaged DNA, the cell cycle is temporarily arrested allowing time for the damage to be repaired (Sancar *et al.* 2004). ATM recognises

DNA double strand breaks and appears to have a more minor role in repair of DNA damage as mutants do not appear to be hypersensitive to UV-B radiation. Null ATR mutants on the other hand so seem to exhibit UV-B sensitivity, under such conditions they show increased root growth retardation in comparison to wild type plants (Culligan *et al.* 2004). The role of this kinase involves perception of single stranded DNA and situations where the replication fork has been blocked. Such single stranded DNA can occur when NER and homologous recombination repair mechanisms are in action while the formation of pyrimidine dimers by UV-B is one major source of such replication blocks (Culligan *et al.* 2004). This explains why mutants that are unable to recognise such blocks and regulate cell cycle progression in response are more sensitive to UV-B.

Therefore, while it can be seen that DNA damage could cause a significant problem to a plant cell, efficient mechanisms are already in place in order to fix breaks and inappropriate bonds. Indeed, in this respect plants are better adapted to exposure to UV-B radiation than mammals, as it appears that the latter have lost their photolyase enzymes and instead rely upon NER to repair UV-B induced damage (Cleaver 2001).

1.2.2 Ribosomes and transcription

In addition to damage to DNA which can inhibit transcription and replication processes, UV-B can also damage the translational machinery in plants. Exposure to this radiation can damage ribosomes by encouraging the formation of cross-links between ribosomal proteins and RNA (Casati and Walbot 2004). This can directly affect new protein synthesis thereby having a significant negative impact on plants. In maize at least, these negative effects appear to be ameliorated by the removal of damaged ribosomes and an increase in the synthesis of ribosomal proteins (Casati and Walbot 2004).

1.2.3 Generation of ROS/oxidative stress

Reactive oxygen species (ROS) are produced in UV-B irradiated plants through a number of different mechanisms. These include non-specific UV absorption, disrupted electron transfer in chloroplasts and production by enzymes including NADPH oxidase (Allan and Fluhr 1997; Hideg *et al.* 2002; Stratmann 2003). ROS in themselves can act as agents of damage as they have the capacity to react with molecules such as water and release free radicals as well as directly oxidize cellular components thereby compounding the damaging effect of exposure to UV-B. Therefore, a plant subjected to UV-B will produce antioxidants and antioxidant enzymes such as superoxide dismutase (SOD) in order to mop

up these free-radicals thereby preventing any further damage to molecules such as DNA (Stratmann 2003).

1.2.4 Photosynthesis

Most plants are strongly dependent on light, it drives photosynthesis and thus the synthesis of carbohydrates. The machinery involved in this process is therefore of vital importance, however it is also extremely sensitive to damage. UV-B is well known to degrade the two protein subunits, D1 and D2, at the core of PSII and has also been shown to decrease Rubisco, carotenoid and chlorophyll levels in some maize accessions (Jansen *et al.* 1998; Correia *et al.* 1999).

1.2.5 Whole plant effects

When considering the wider impacts of UV-B radiation it can be seen that some of these damaging effects may cumulatively cause changes in the overall biomass or yield. This is an especially important consideration as this can have a large impact on the productivity of crop species. For example, in maize it was shown that supplemental UV-B radiation could cause decreases of up to 30 %. Significant reductions were also seen for both the dry weight and the leaf area, thus showing that in addition to reproductive effect, this treatment has detrimental effects on vegetative aspects of the plant (Correia *et al.* 1998). This, similarly to the situation with the effects on photosynthesis, was ecotype dependent with some varieties showing increased tolerance to this stress stimulus. Interestingly, another study which showed decreases in biomass in *Arabidopsis* in response to UV-B also showed ecotype differences (Kalbina and Strid 2006). These differences could be explained by variations in the levels of UV-B seen in the locations from which these ecotypes are derived. Work by Casati *et al.* 2006 showed that maize varieties which naturally grow at higher altitudes (and thus exposed to increased levels of UV-B) show lower levels of expression of genes associated with UV-B responses than their lower altitude counterparts.

1.3 Signalling responses to high doses of UV-B

In a broad sense, plant responses to UV-B can be split into two groups, non-specific responses that are also stimulated by other abiotic or biotic stimuli and include stress responses to high doses (above ambient UV-B levels), and the specific photomorphogenic responses to lower fluence rates (Frohnmeyer 2003; Brown and Jenkins 2008; Jenkins

2009). In the following sections the signalling pathways that mediate responses to high and low (i.e. damaging and non-damaging) fluences of UV-B will be discussed. For an overview of these, see Figure 1.1.

1.3.1 High dose signalling

Firstly, high doses of UV-B are potentially a considerable problem to plants. Many cellular components such as DNA, proteins, membranes and photosynthesis machinery absorb UV-B readily. This can cause severe disruption of the cellular environment and can ultimately lead to necrosis. As a result, in plants we see an induction of more general stress responses designed to repair the inevitable damage caused. For example, in a study performed by Brown and Jenkins (2008), UV-B induced gene expression in *Arabidopsis* was initiated by distinct pathways operating at different fluence rates and a study involving maize similarly showed that some genes require different threshold doses of UV-B (Casati and Walbot 2004). The first of these different pathways in *Arabidopsis* was stimulated by low fluences of UV-B and mediated by UVR8/HY5/HYH (see Section 1.5 below). Secondly at higher fluence rates (> 1 μmol m^{-2} s^{-1}) a suite of genes are induced that are not dependent on these factors and whose functions are associated with other stressful stimuli. For example the WRKY30 transcription factor (At5g24110) is induced under these conditions and has previously also been associated with response to ROS and wounding (Taki *et al.* 2005; Brown and Jenkins 2008; Scarpeci *et al.* 2008). A study examining UV-B responses in *Nicotiana longiflora* also found an up-regulation of a WRKY transcription factor that is similarly induced in response to feeding by *Manduca sexta* larvae (Izaguirre *et al.* 2003). The WRKY transcription factors, especially those belonging to the sub-group III which includes WRKY30, seem to have a role in pathogen responses (Eulgem *et al.* 2000). While this particular gene was not induced by salicylic acid (SA), strong induction in expression was seen upon exposure to a number of different pathogens (Kalde *et al.* 2003). Thus it seems that this particular transcription factor may be induced by a diverse range of stimuli and has a role in response to both biotic and abiotic stresses.

1.3.2 Cross-talk with other stress pathways

In fact, it seems that as a result of UV-B stress, plants initiate a number of signalling cascades, many of which share components with other stress related transduction pathways. For example, there is considerable overlap with responses to pathogen attack or wounding. In this case, genes such as the *PATHOGENESIS RELATED* (*PR*) genes,

proteinase inhibitor genes and the defensin gene *PDF1.2* are all induced by high levels of UV radiation (Mackerness *et al.* 1999; Frohnmeyer 2003). In addition, UV-B stimulates the production of compounds associated with signal transduction in plants subjected to pathogen attack. That is, high levels of UV-B result in increased levels of salicylic acid (SA), ethylene and jasmonic acid (JA) (Mackerness *et al.* 1999; Mackerness *et al.* 2001). Furthermore, in *Arabidopsis* mutants that are insensitive to the hormones ethylene and JA (*etr-1* and *jar1*), in response to UV-B show reduced *PR1* expression in the former and both *PR1* and *PDF1.2* expression in the case of the latter mutant. These are obviously important processes in plant responses to UV-B stress as both hormone mutants also exhibited increased sensitivity to UV-B compared to the wild-type control (Mackerness *et al.* 1999).

The increase in expression of genes associated with pathogen/wounding responses may not be attributable solely to the increased levels of signalling compounds such as JA. ROS in addition to causing damage to cellular components can also themselves act as signalling molecules. For example the up-regulation of *PR-1* under high UV-B is regulated by H_2O_2, whereas *PDF1.2* is up-regulated by O_2^- (Mackerness *et al.* 2001).

Interestingly, *CHALCONE SYNTHASE (CHS)*, one of the genes induced by low fluences of UV-B is not regulated by ROS, thus adding weight to the hypothesis that there are at least two distinct low and high fluence signalling pathways (Mackerness *et al.* 2001).

Indeed it has been shown that exposure to UV-B can confer increased resistance to herbivory as well as cross tolerance to other stresses such as drought and cold (Gitz and Liu-Gitz 2003; Izaguirre *et al.* 2003; Stratmann 2003; Chalker-Scott and Scott 2004; Izaguirre *et al.* 2007). In tomato, it was found that responses elicited by UV-B strongly overlapped with those attributable to the signalling peptide systemin, usually associated with wounding responses. It was therefore suggested that the UV-B signal may be co-opting the receptors associated with perception of wounding in order to transmit the signal that the plant is experiencing stress and to induce or inhibit relevant genes (Stratmann 2003). For example, one group of genes that showed similar down-regulation in a microarray study examining the overlap between simulated herbivory and UV-B, included photosynthetic genes such as rubisco and *Lhcb* (Izaguirre *et al.* 2003). As mentioned above, photosynthesis is a highly UV-B sensitive process and therefore it is evident that co-opting a defence pathway that results in the down-regulation of this process may have beneficial effects. Another study showed that a down-regulation in the *Lhcb* gene can be reversed with the application of ascorbate, a compound with the ability to remove ROS

(Surplus *et al.* 1998). This therefore again demonstrates the involvement in these radicals in UV-B responses.

1.4 Photomorphogenic responses

1.4.1 Low fluence UV-B responses

The majority of the above responses mainly apply to the upper levels of ambient UV-B and above. Therefore it is the way in which plants respond to levels that are more common in natural environments (around 3.5 μmol $m^{-2}s^{-1}$ and lower) that are of particular interest. Although non-specific UV-B signalling pathways operate to some extend at normal ambient levels of UV-B, a UV-B specific pathway is also initiated. The end results of the specific pathway(s) include proteins and other components that allow plants to adapt to current UV-B conditions and also protect against any future higher doses. That is, here, UV-B is acting as an informational signal rather than just a source of damage.

Interestingly, these responses can be seen at very low levels of UV-B and in response to very short UV-B treatments. For example, a fluence rate of just 0.1 μmol m^{-2} s^{-1} is sufficient to suppress hypocotyl growth, a key morphological change seen after UV-B irradiation (Kim *et al.* 1998; Boccalandro *et al.* 2001). In addition, millisecond pulses have been shown to induce the transcription of the gene encoding *CHALCONE SYNTHASE* (*CHS),* a key enzyme in the flavonoid biosynthesis pathway (Frohnmeyer *et al.* 1999). These results indicate that responses to low doses of UV-B are highly specific. Consequently, exposing plants to low intensity UV-B allows us to dissect and trace the specific pathways involved. This can be achieved through both physiological studies such as addition of inhibitory compounds, and also through genetic means such as mutagenesis studies. In particular it seems that UV-B specific responses rely heavily upon transcriptional chances and thus studies using gene expression are very useful in dissecting the potentially numerous pathways involved.

However, it is worth bearing in mind that low and high level UV-B responses are not completely distinct so that at certain fluence rates an overlap may exist with both systems being utilized. Although we have an estimation of where this overlap between the two processes occurs (around the 1 μmol m^{-2} s^{-1} mark), the exact limits have not yet been determined (Brown and Jenkins 2008). Indeed, this may be an impossible task as the threshold values are likely to vary considerably depending on a plant's genotype, environment, age and whether it has been previously exposed to UV-B radiation. While we can make generalisations and state that high doses of UV-B elicit responses that are

primarily concerned with repairing the resulting damage and that low doses induce the photoprotective responses designed to acclimate the plant and prevent damage, it is likely that in the natural environment plants use a combination of these. Unlike in many experimental conditions, the natural environment fluctuates considerably and thus plants will be exposed to an ever changing dose of UV-B (Caldwell *et al.* 2003).

1.4.2 Morphological effects

Similarly to other light qualities, exposure to low doses of UV-B has an affect on the morphology of a plant. These changes mainly occur at low fluences whereas higher doses generally produce symptoms of cellular damage (Kim *et al.* 1998). For this reason the low level responses to UV-B are sometimes referred to as the photomorphogenic responses. When exposed to UV-B numerous morphological adaptations are seen which are an attempt to minimize exposure to radiation similar to that seen in high levels of white light (Kim *et al.* 1998); for example, leaf curling, increased leaf thickness, reduced leaf size and inhibition of root, hypocotyl and stem growth (Kim *et al.* 1998; Jansen 2002; Wargent *et al.* 2009). Also, on a slightly smaller scale, it has been observed that ambient levels of UV-B cause a decrease in both ad and abaxial cell size (Wargent *et al.* 2009). As plant hormones have a vital role in the morphology of a plant, it is no surprise that such phytohormones have been implicated in morphological responses to UV-B. Interestingly is has been suggested that UV-B screening flavonols may be implicated in these morphologies through alteration of polar auxin transportation (Jansen 2002; Kliebenstein 2004). That is, in the *tt4* mutant (a CHS null mutant) plants exhibit a two-fold increase in auxin transport levels. This is accompanied by changes in morphology that are usually associated with altered auxin levels such as a reduction in plant height and an increase in axiliary branching (Brown *et al.* 2001). However this result is difficult to reconcile with the observation that UV-B treated plants, with high flavonoid levels, have a similar phenotype at the *tt4* mutant, which lacks flavonoids.

1.4.3 Flavonoids and other screening compounds

Many studies have shown that UV-B induces the production of various secondary metabolites. For example, one of the first responses is the induction of pathways which lead to the production of flavonoids and other phenolics. These compounds accumulate in the epidermis and act as a sunscreen, absorbing the potentially harmful UV radiation without affecting the passage of the visible wavelengths needed for photosynthesis. In

addition to this, flavonoids also have the ability to scavenge the free radicals produced by UV radiation (Landry *et al.* 1995). If these pathways are disrupted through mutation, then an enhanced sensitivity to UV-B results. For example, it has been shown that mutants deficient in flavonoids or sinapate esters exhibit an increased occurrence of UV-B induced oxidative damage to proteins and membranes (Landry *et al.* 1995). Furthermore, chalcone isomerase (*chi)* mutants have a reduced biomass and *chs* mutants accumulate increased concentrations of DNA dimers (Li *et al.* 1993; Mazza *et al.* 2000). Therefore it can be seen that both flavonoids and sinapate esters have vital functions in the protection of plants from UV-B stress. A summary of the biosynthetic pathway that gives rise to these compounds is shown in Figure 1.2

In literature on the effects of UV-B on plants, CHS appears fairly regularly. This enzyme is one of the key elements in UV-B responses as it is the first committed step in the flavonoid biosynthesis pathway. It has proved to be a useful tool in both pharmacological and genetic tests. One of the reasons for this is the multiple factors, including other light qualities besides UV-B, which can influence its expression. Blue/UV-A exposure for example can lead to the induction of *CHS* expression, primarily through Cryptochrome 1 (cry1), but also to a lesser extent through Cryptochrome 2 (cry2). This effect can further be increased through pre-illumination with either red or far red wavelengths mediated through redundantly acting Phytochrome A (phyA) and Phytochrome B (phyB) (Wade *et al.* 2001). In addition, through co-action between phyB and cry1, this signal can be further amplified. If we incorporate UV-B into this model it can be seen that contrary to the case in blue light, phyB actually acts as an inhibitor of the UV-B mediated induction of *CHS* expression while supplementary illumination with blue or UV-A can act synergistically with UV-B to result in an increased induction of *CHS*. This latter effect is independent of cry1, cry2, phyA and phyB. A summary of this complex interaction is shown in Figure 1.3 (Fuglevand *et al.* 1996; Wade *et al.* 2001).

This network of regulation allows us to dissect components that are UV-B specific from those that are not. For example, if *CHS* induction is lost in a mutant when exposed to UV-B, but is retained under cry mediated conditions, we can conclude that the mutated gene encodes a UV-B specific element. Indeed this was the approached used by Brown and co-workers (2005) and enabled the discovery of the first UV-B specific signalling component, UV-RESISTANCE LOCUS 8 (UVR8).

1.5 UV-B specific signalling and UVR8

Despite the interest in this subject area, our knowledge of UV-B specific responses is still somewhat limited especially in comparison to that for other light signalling pathways. This is partly due to the complications of separating out more general stress responses from photomorphogenic ones. Nevertheless, some progress has been made with the identification of UVR8. Interestingly, in the screen performed by Brown et al. (2005) using a CHS *promoter*::Luciferase reporter line which identified several alleles of the *uvr8* mutation, no other mutant gene was discovered. Although this would suggest that the UV-B specific pathway is composed of relatively few components, functional redundancy may have masked additional mutants.

1.5.1 UV-RESISTANCE LOCUS 8

It was only within the last five years that an early UV-B signalling component was identified; the UVR8 protein. Mutant *uvr8* plants were first identified in a screen for UV-B hypersensitivity, and were shown have a reduced accumulation of flavonoids and an increase in the expression of PR1 and PR5 genes (normally associated with stress) under low level UV-B conditions (Kliebenstein *et al.* 2002). Further analysis showed that the role of this protein was in a UV-B specific pathway. It was demonstrated that *uvr8* mutant plants retain normal induction of *CHS* under UV-A/blue light in adult plants, and under far-red in seedlings but lack UV-B induction (Brown *et al.* 2005). Furthermore, *CHS* induction by other abiotic stimuli such as low temperature and elevated sucrose concentration was unaffected in the *uvr8* mutant. Thus, it can be seen in this mutant that only the signalling pathway associated with UV-B is affected. This was a key discovery as it identified the first gene involved exclusively in UV-B responses. Indeed its vital importance in the UV-B signalling pathway is evident when sensitivity assays are performed. Mutant plants, unlike wild types, are severely damaged when exposed to ambient UV-B and cannot survive in sunlight (Brown *et al.* 2005). It has also more recently been shown that mutants in this gene do show an altered morphology (i.e. a true photomorphogenic response) with respect to hypocotyl length when compared to wild type plants. Exposure to UV-B wavelengths normally elicits a suppression in hypocotyl growth in seedlings, however this response is absent in the *uvr8* mutant (Favory *et al.* 2009). This demonstrates that UVR8 has the ability to alter the structure of a plant very early on in its development in response to this form of radiation. In addition, mature *uvr8* plants have smaller leaves as a result of altered epidermal cell size (Wargent *et al.* 2009).

As well as a number of different mutant alleles of UVR8, several over-expressing lines have been generated (Favory *et al.* 2009). In line with results seen for UVR8 loss of function mutants, these exhibit enhanced *HY5* and *CHS* expression as well as enhanced levels of anthocyanins under UV-B conditions. In addition, young overexpressing plants that had been allowed to acclimate to low UV-B conditions showed increased tolerance to UV-B stress compared to their wild type or *uvr8* mutant counterparts. Interestingly, when over-expressing UVR8 lines were grown in conditions which simulated sun (and hence natural UV-B levels), adult plants showed a dwarfed and dark green phenotype (Favory *et al.* 2009). It is possible that the over-accumulation of flavonoids may have affected the auxin distribution thus giving rise to a dwarfed phenotype. However, we might expect that in this case, in line with results for a mutant exhibiting lower levels of flavonoids with a dwarfed phenotype, we would expect to see larger plants relative to the wild type (Brown *et al.* 2001). Thus although it is not yet clear what factors may be causing this phenotype in overexpressing lines it seems that these plants have features that may explain their increased tolerance to UV-B, that is a reduced surface area for exposure to UV-B and perhaps increased chlorophyll content or wax accumulation (not tested) in order to combat and reduce the damaging effects on photosynthetic machinery.

1.5.2 UVR8 and chromatin

As of yet, the function of UVR8 has not been fully resolved. However our knowledge of this important factor is fast accumulating and it should not be long before the complete picture is produced. Initially chromatin immunoprecipitation (ChIP) studies demonstrated that the protein binds to chromatin at specific regions and interacts with histones. One such region of interaction includes the promoter of *HY5*, a bZIP transcription factor up-regulated by UV-B (Brown *et al.* 2005). In addition, UVR8 has been shown to interact with chromatin immediately around the *HY5* gene. ChIP assays performed by Cloix and Jenkins (2008) demonstrated that while association of UVR8 could be found within the coding region as well as the 5' and 3' non-coding regions proximal to the gene, no association could be found at positions 5 kb up or downstream. It thus appears there may be a close link between UVR8 and some of the genes that it regulates. However, this does not appear to be universal for all UVR8 dependent genes, no association could be found for *HYH* which is closely related to *HY5* and is also regulated by UVR8 (Cloix and Jenkins 2008). Interestingly, the association of UVR8 with chromatin does not appear to be restricted to more up-stream UV-B signalling components such as *HY5*, an interaction was

also seen for *CRYD*, a gene that is itself regulated by *HY5*. An association was tested for *CHS*, but here again no association was seen.

Additional work by Cloix and Jenkins (2008) also showed that this association with chromatin occurs via histones and more specifically preferentially via interaction with H2B. Histones themselves are known to undergo a number of modifications such as acetylation, methylation and so forth that are associated with changes in trnscription. While no consistent pattern of acetylation or methylation was found in the Cloix and Jenkins study, it is a likely possibility that such modifications and variants have a role in UVR8 mediated UV-B signalling. It is possible that UVR8 may recognise certain variants or that it itself causes the modifications of histones, thereby regulating expression. It is interesting to note that the association of UVR8 with chromatin is not UV-B dependent. UVR8 can be found on the promoter region of *HY5* even when plants have never been exposed to UV radiation (Brown *et al.* 2005; Cloix and Jenkins 2008). It therefore seems that the activation of this protein requires an additional signal derived directly or indirectly from UV-B.

The association between UVR8 and chromatin is a characteristic shared with a homologous protein found in humans, RCC1 (REGULATOR OF CHROMATIN CONDENSATION) (Kliebenstein *et al.* 2002). Due to their similarities in sequence UVR8 is therefore predicted to adopt a similar seven-bladed propeller structure to RCC1 (Renault *et al.* 1998; Moore 2001; Brown *et al.* 2005). However despite this similar structure, it appears that the two proteins do not have shared functions as UVR8 does not exhibit the Ran/guanine nucleotide exchange activity characteristic of RCC1 (Moore 2001; Brown *et al.* 2005). It thus appears that UVR8 is unlikely to have similar roles to RCC1 in regulation of the cell cycle and nucleocytoplasmic transport. Interestingly, no true homologue of RCC1 protein, which is found in both mammals and yeast, has been found in plants. As this factor is necessary for cellular growth in both these groups it is likely that a homologue also exists in plants but as yet it remains elusive (Moore 2001).

1.5.3 UVR8 localisation

The presence of UVR8 bound to chromatin even under minus UV-B conditions would suggest a nuclear localisation. Studies using GFP however have demonstrated that under white light conditions although UVR8 detectable in the nucleus, UVR8 is mainly cytoplasmically localised. Upon UV-B exposure a strong nuclear accumulation is seen (Brown *et al.* 2005; Kaiserli and Jenkins 2007). This accumulation is specifically in response to wavelengths in the UV-B portion of the spectrum as red and UV-A light both

failed to elicit the same response. This appears to be yet another facet of the UV-B specificity of this protein (Kaiserli and Jenkins 2007). Finally, it was demonstrated that this change in localisation occurs at even very low fluence rates of UV-B (0.1 μmol m^{-2} s^{-1}) and after very short durations of treatment (10 mins), thereby supporting evidence for a role of UVR8 in non-damaging photomorphogenic responses to UV-B.

The work performed by Kaiserli and Jenkins (2007) was extended to test the effect of nuclear exclusion and localisation signals (NES and NLS) on the localisation of UVR8. These signals, derived from mammalian PK1 and the SV40 virus respectively have previously been shown to restrict phytochrome B to the cytoplasm and nucleus respectively (Matsushita *et al.* 2003). Results from these fusion studies showed that the NES tagged version was indeed excluded from the nucleus but under UV-B radiation was still able to accumulate in the nucleus thereby demonstrating the strength of the UV-B dependent accumulation. The addition of an NES tag to GFP-UVR8 therefore gives a more clear-cut mechanism to test the localisation of the protein. NLS tagged UVR8, although constitutively in the nucleus, still requires UV-B for activation. This observation complements the result obtained by Cloix and Jenkins (2008) where chromatin bound UVR8 still requires UV for activation. It thus appears that we are still missing a vital step in the action of UVR8 linking its histone associated presence in the nucleus with its subsequent activation. It is possible that the activation requires the influence of some other UV-B responsive element although it is interesting to note that such an element has not been detected in previous UV-B mutant screens (Kliebenstein *et al.* 2002; Brown *et al.* 2005).

In the Kaiserli and Jenkins study, the 23 most N-terminal amino acids were also removed from the construct and its ability to accumulate in the nucleus assessed. It was found that this construct showed a reduced ability to accumulate in the nucleus thus suggesting the presence of some nuclear accumulation signal within this region. When RCC1 and UVR8 sequences are aligned, there exists relatively little conservation in this region. Additionally, while RCC1 possesses a bipartate NLS, no such equivalent can be found in the corresponding UVR8 sequence. Hence, these results suggest the existence of some novel nuclear accumulation signal in the N-terminal region that enhances nuclear localisation after UV-B exposure.

1.5.4 N and C-terminal regions of UVR8

When UVR8 and RCC1 sequences are compared, in addition to the dissimilarity in the N-terminal regions, there is a 27 amino acid insertion towards the C-terminus of the UVR8

sequence relative to RCC1. This region was deleted by Kaiserli and Jenkins (unpublished data) and it was found, similarly to the N-terminal region, to be essential for normal UVR8 function. Unlike the N-terminal region however, it did not affect the localisation of a NES-GFP-ΔCUVR8 construct. Thus UVR8 possesses two characteristic regions that both confer functionality, albeit in yet unknown mechanisms, to the protein. This loss in functionality is not as a result of a loss in chromatin binding as ChIP assays demonstrated that this feature is retained in both deletion constructs. Therefore, the importance of the N-terminal may be associated with its localisation, but the role of the C-terminal insertion region remains entirely elusive.

1.5.5 UVR8 regulated genes

Through microarray analysis, it has been determined that UVR8 is able to regulate around 72 genes in response to UV-B, a relatively small component of the >500 genes induced by UV-B in the study by Brown *et al.* (2005). Nevertheless, this group of genes includes a number that encode factors that are vital in the acclimation of plants to this kind of stress. For example CHS, as mentioned above is a vital enzyme in the production of the UV-B screening compounds. Moreover, UVR8 regulates the expression of several other enzymes that act further downstream in this process, flavonol synthase (FLS), flavone 3-hydroxylase (F3H) and chalcone isomerase (CHI) (Debeaujon *et al.* 2001). In addition, the photolyase PHR1, responsible for repair of CPDs, the predominant form of UV-B induced DNA damage, is also under the regulation of UVR8 in UV-B conditions (Britt 2004). It is therefore clear why any plant lacking induction of such genes, as seen in *uvr8*, would be highly sensitive to UV-B radiation.

Another key element in the UV-B signalling process is the HY5 transcription factor (ELONGATED HYPOCOTYL5). This bZIP transcription factor was previously known to have a role in seedling photomorphogenesis but it has since been revealed to have an additional role in UV-B mediated responses through the generation of transgenic *HY5* promoter::Luc plants (Ulm *et al.* 2004). These plants were shown to luminesce strongly after UV-B illumination. This role of *HY5* in UV-B responses was further supported through microarray studies performed by Brown e*t al.* (2005). The results obtained showed firstly that *HY5* transcripts in UV-B treated *uvr8* plants were absent thereby supporting the results of chromatin immunoprecipitation assays which conclude that HY5 is a downstream effector of the UVR8 pathway. Secondly, around half of the genes regulated by UVR8 also appear to be regulated by HY5. This includes the genes encoding components of the flavonoid biosynthesis pathway and the PHR1 photolyase. Thus, *hy5*

mutants were observed to be highly sensitive to UV-B radiation similarly to *uvr8* mutants, hence demonstrating that this protein too is a vital component of the UV-B response pathway.

From the Brown *et al.* (2005) study it was concluded that at least two UV-B specific pathways existed, one that was dependent on both UVR8 and HY5 and one that seemingly only required UVR8. However, subsequent work by Brown and co-workers (2007) demonstrated that *HY5* still has a role in regulating the remaining half of the UVR8 regulated genes. In this study gene expression in the *hy5* mutant as well as a *hy5 hyh* double mutant was assessed. HYH (HY5 HOMOLOGUE) appears as a UVR8-regulated gene in the initial microarray study and it bears strong similarity to the HY5 transcription factor (49 % identical at the protein level) (Holm *et al.* 2002). It was shown that several of the genes initially thought to be UVR8-dependent HY5-independent showed loss of UV-B induction in the *hy5 hyh* double mutant. It thus appears that these two transcription factors act redundantly to regulate a subset of the UVR8-dependent genes (Brown and Jenkins 2008). While the *hy5 hyh* double mutant has yet to be submitted for microarray analysis to determine exactly which genes are dependent on this system, it seems that the remaining half of the UVR8-dependent genes are regulated in a HY5/HYH redundant mechanism. Consequently, it seems that of these two transcription factors, HY5 has the more major role in UVR8-mediated responses but that HYH has a limited capacity to compensate for some of these in the absence of functional HY5. When the sensitivity of the *hyh* mutant was tested, it could be seen that it exhibited very little sensitivity to UV-B exposure with plants resembling those of wild type rather than the strongly affected *uvr8*, *hy5* and *hy5 hyh5* mutants (Brown and Jenkins 2008). For a summary of the UVR8 pathway see Figure 1.4.

In conclusion, the current hypothesis for UVR8 action is that while present in the nucleus and associated with chromatin under minus UV-B conditions, in a manner akin to a “ready state”, exposure to UV-B causes a strong accumulation in the nucleus. This same radiation is some yet unknown way activates UVR8, possibly by the incorporation of other factors into a complex, thus facilitating transcription of the genes in the region of chromatin to which it is bound. This initiation of transcription may be via an increased availability of these UV-B responsive genes to transcription factors, thus allowing a rapid increase in expression. While some attempts have been made to find proteins that interact with UVR8, only one candidate, CONSTITUTIVELY PHOTOMORPHOGENIC 1 (COP1) has been found so far (Oravecz *et al.* 2006; Favory *et al.* 2009).

1.5.6 COP1

COP1, an E3 ubiquitin ligase, has a well characterized role in the repression of photomorphogenesis in dark grown seedlings. By targeting the destruction of positive regulators of the light grown phenotype such as HY5, COP1 prevents the suppression of hypocotyl growth and greening of the seedling. Therefore mutations in the COP1 gene can result in dark-grown plants adopting a light-grown phenotype as opposed the characteristic etiolated phenotype. In the case of UV-B responses however, the situation appears to be reversed with COP1 taking on a positive rather than negative role in photomorphogenesis. For example, the expression of *HY5* under UV-B actually requires the presence of functional COP1 in addition to UVR8, thus this ligase is now acting as a positive regulator of HY5. Interestingly a positive role for COP1 in gene induction appears to be true for a large number of UVR8-regulated genes. Roughly half of the genes found to be dependent on HY5 for UV-B induction were also shown to require COP1. It therefore appears that the UVR8, HY5 and COP1 pathways may be intimately connected, although it is not yet fully clear just how these components interact to give rise to UV-B responses.

Interestingly however, it does appear that there is a direct interaction between the UVR8 and COP1 proteins that is UV-B dependent (Favory *et al.* 2009). The two proteins can be co-immunoprecipitated and were shown to colocalize in the nucleus. It is therefore possible that this UV-B dependent association may act as the activating step required for the activation of a subset of the UVR8-dependent genes. If this is the case, then it would appear that in this situation COP1 is not utilising its E3 ubiquitin ligase function and is acting in some as yet unknown mechanism. In support of this, it does seem that different parts of the protein may be responsible for different responses. The cop^{eid6} mutant allele for example while still is hypersensitive to white light, is unlike *cop1-4* in that it exhibits an increased tolerance for UV-B with retained levels of *CHS* and *HY5* expression (Dieterle *et al.* 2003; Oravecz *et al.* 2006). The mutation in the cop^{eid6} allele, which results in the conversion of a conserved histidine residue to a tyrosine, causes a disruption in the RING-finger motif of the protein. It would therefore appear that while this motif, which confers ligase activity, is of vital importance for white light responses it is not necessary in the downstream processes of UV-B signalling.

It has been suggested that COP1 may be acting to remove some negative regulator of UVR8-mediated transcription specifically under UV-B conditions (Favory *et al.* 2009). That is, the action of UV-B, perhaps via a UV-B photoreceptor, causes a rapid interaction between UVR8 and COP1 that subsequently removes the hypothesised inhibitor. This then

allows the activation of the UVR8 protein already bound to chromatin, thereby initiating transcription of its associated genes.

While it is evident that COP1 has a role in UV-B responses, it is interesting to take into consideration some additional observations from these studies. Firstly, while it appears that YFP-tagged COP1 also accumulates in the nucleus under UV-B (in contrast to its exclusion from the nucleus after white light exposure) this process occurs more slowly than that seen for GFP-UVR8 (Favory *et al.* 2009). As the expression of some UV-B responsive genes can occur very rapidly, it is difficult to reconcile these two characteristics. That is, if the initiation of transcription requires the COP1 mediated removal of a negative regulator, it is difficult to explain why translocation of COP1 is slow while initiation of transcription is rapid.

Secondly, while the *cop1-4* mutant does exhibit some UV-B sensitivity, the effects are not as extreme as seen for either *uvr8* or *hy5* (Oravecz *et al.* 2006; Brown and Jenkins 2008). It therefore seems that similarly to HYH, this protein may have a more minor role in the responses of plants to UV-B. However, the reduced sensitivity seen may be as a result of an increased level of flavonoids present in *cop1-4* plants that are grown under white light (Oravecz *et al.* 2006). It therefore may be that these screening compounds are effectively reducing the dose that the plant experiences, thus preventing the same degree of damage seen in *hy5* or *uvr8* mutants.

Finally, it should be noted that it can be difficult to interpret results derived from use of the *cop1-4* mutant as this is not a null mutant. Such null mutants do not exist as COP1 is essential for plant survival and thus complete loss results in seedling lethality (Mcnellis *et al.* 1994). Therefore, while in this allele the protein is truncated so that the WD40 repeat domain (the site of interaction with other proteins such as HY5) has been lost, the N-terminal region including the RING finger (required for ligase activity) and the coiled-coil (dimerisation) domains remain (Yi and Deng 2005).

1.6 UVR8-independent pathways

In summary, work on the UV-B response in plants has shown that several separate signalling pathways exist. Firstly, one that is mainly associated with high fluences of UV-B and thus results in the induction of genes associated with general stress responses. Secondly there is a major class of low fluence UVR8 dependent genes which can be subdivided into those also dependent on COP1, HY5, HY5/HYH or a combination of the above. However, a microarray study performed by Brown and colleagues (2005) showed

that >500 genes are induced in response to UV-B and it seems unlikely that all of those that cannot be linked to the UVR8 pathway are associated with more general stress responses. It is more likely that a number of further low fluence UV-B responsive pathways exist that have roles (albeit more minor in comparison to UVR8) in responses to these wavelengths of radiation.

To date, only one example of a gene that belongs to this class exists. ANAC13 encodes a transcription factor so named for its NAC domain (which is itself named from the NAM, ATAF1/2 and CUC2 family members). This large group of transcription factors, >100 members in *Arabidopsis*, is plant specific with diverse roles in development as well as defence against biotic and abiotic stresses (Olsen *et al.* 2005). The characteristic N-terminal NAC domain consists of a DNA binding domain, while the highly diverse C-terminal region contains a transcriptional activation domain (Ooka *et al.* 2003). X-ray crystallography studies on ANAC1 has shown that instead of the classical conformation of helix-turn-helix motif, NAC domains adopt a novel transcription factor fold which consists of a twisted beta-sheet surrounded by a few helical elements (Ernst *et al.* 2004). However, despite the emerging important role of this large family of plant transcription factors in developmental and environmental responses our knowledge concerning this group is yet limited.

The role of ANAC13 in UV-B responses was first identified by Safrany *et al* (2008). In a combination of studies using the promoter fused to the LUC gene and through PCR analysis they determined that ANAC13 is induced by UV-B in a manner independent of both COP1 and UVR8. In addition they found this gene, similarly to *CHS*, to also be up-regulated by red-light. However, with closer examination of the promoter region it was found that these two responses could be separated out. While the red light response requires the promoter region between -1457 and -195 bp, UV-B responsiveness is only lost with deletion of bases between -146 and -110. This latter region was therefore examined more closely and it was found that elements similar to ACE^{CHS} (ACGT-containing element) and MRE^{CHS} (MYB responsive element) are present. In *CHS* these elements confer white and UV-B responsiveness (Hartmann *et al.* 1998). However, it was also determined that the UV-B responsiveness seen was not solely attributable to these elements. An exchange of the -110 to +24 bp region (downstream of the two elements termed ACE^{ANAC13} and MRE^{ANAC13}) for a minimal CaMV35S promoter severely compromised induction under UV-B. Through this, a novel responsive element which is both necessary and sufficient for UV-B induction was identified and named $UVBox^{ANAC13}$. Interestingly this new element confers responsiveness specifically to shorter wavelength

UV-B and is not induced by longer wavelengths nor other stress stimuli such as cold. This element was also found to be enriched in a number of other late UV-B responsive genes, thus suggesting a whole new pathway of UV-B regulation.

Although the identification of this new UV-responsive element provides an interesting new insight into UVR8-independent UV-B signalling, so far no downstream targets nor any upstream factors controlling ANAC13 up-regulation have been found. However, the identification of the UV^{ANAC13} box provides a stepping-stone to discovery of its upstream regulator.

1.7 Other signalling mechanisms

Finally, it seems that calcium signalling as well as protein kinases and phosphatases may be involved in UV-B signalling. Christie and Jenkins (1996) demonstrated that antagonists of calcium and calmodulin inhibit UV-B induction of *CHS* expression. In addition, millisecond pulses of UV-B result in a rise in cytosolic calcium in parsley cell culture (Frohnmeyer *et al.* 1999). However, artificial increases in cytosolic calcium alone are unable to generate an increase in *CHS* expression (Christie and Jenkins 1996). Therefore, it is possible that the UV-B induced rise in calcium is not cytosolic and instead occurs in another cellular location.

Additional pharmacological studies showed that inhibitors of protein kinases and phosphatases also result in a loss in UV-B mediated *CHS* expression (Christie and Jenkins 1996). This is an interesting observation, as receptor tyrosine kinases and receptor-directed tyrosine phosphatases (PTPs) have been implicated in perception of UV-B in animal cells (Groβ *et al.* 1999). In this case, it has been proposed that UV exposure leads to ligand-independent activation of receptor tyrosine kinases via the inhibition of PTPs. However, the exact roles which protein kinases and phosphatases play in the signal transduction of UV-B is not yet clear.

1.8 Known light signalling pathways

Recent work has lead to many advancements in our knowledge of UV-B signalling downstream of perception, but one significant gap yet remains, perception itself. To date no UV-B specific photoreceptor has been identified unlike for red and blue light pathways which have well characterised perception mechanisms. The perception of light signals is of vital importance as it leads to the optimisation of plant form to the specific environment

in which it finds itself. As a result, a number of different plant photoreceptors have evolved which have the ability to detect the quality, quantity and duration of light stimuli (see Figure 1.5 For a summary). It is likely that if such a UV-B photoreceptor exists, it will share features with those developed for responses to other wavelengths of the electromagnetic spectrum. Therefore this next section will summarise the photoreception and signalling responses to red and blue light stimuli before a discussion on the possible mechanisms of UV-B perception.

1.8.1 Cryptochromes

This family of blue light photoreceptors consists of two primary members. Cry1 and cry2 are mediators of various plant photomorphogenic responses to blue light including regulation of flowering time, stomatal opening, hypocoytl extension and cotyledon expansion (Spalding and Folta 2005; Li and Yang 2007). The inhibition of hypocotyl extension under blue light conditions is regulated by both cryptochromes but with different fluence rate dependency for each. Cry1 mediates the high fluence aspect and cry2 the low fluence (Ahmad and Cashmore 1993; Lin *et al.* 1998).

As is the case for the other plant photoreceptors mentioned below, perception of the light signal (in this case blue or UV-A) is mediated through chromophores associated with the light sensing domain of the protein. Cryptochrome proteins include two of these chromophores, flavin adenine dinucleotide (FAD) and pterin, at the N-terminal region of their sequence. The FAD chromophore alone is sufficient to absorb blue light wavelengths and it has been hypothesised that the pterin is present to act as an antenna complex, thereby increasing the range of wavelengths that can be sensed by these proteins (Hoang *et al.* 2008).

Upon exposure to blue light cry1 and cry2 become autophosphorylated, a process which seems to require homodimerization (Shalitin *et al.* 2002; Shalitin *et al.* 2003; Sang *et al.* 2005). The downstream signalling of cryptochromes then involves a direct interaction of their C-terminal domain with COP1 (Yang *et al.* 2001). This prevents COP1, a negative regulator of photomorphogenesis, interacting with and subsequently targeting to the proteosome factors such as *HY5* (Yang *et al.* 2001). This allows the up-regulation of various light-regulated responses.

In addition to their role in photomorphogenesis, cryptochromes have also been implicated in the circadian clock. Both *cry1* and *cry2* mutants exhibit altered circadian rhythms and are thus implicated in the input pathway of the molecular clock mechanisms (Somers *et al.* 1998). In addition to their role in regulating blue-light input to the clock, it

seems that cry1 is also implicated in red-light inputs via its interaction with phyA (Devlin and Kay 2000). Indeed it seems that in mammals cryptochromes may have been co-opted into the circadian system and form a vital component of the central oscillator (Harmer *et al.* 2001).

Cryptochromes are nuclear localised proteins. Cry2 appears to remain constitutively nuclear regardless of the light conditions. Cry1 on the other hand appears to be exported to the cytoplasm under blue light (Lin and Shalitin 2003).

A third cryptochrome, cry3 sometimes referred to as CRYD due to its similarity to *synechocystis* CRY DASH (for Drosophila–Arabidopsis-Synechocystis–Human), is also found in *Arabidopsis*. However, this example lacks the C-terminal domain seen in cry1 and cry2 and as such more closely resembles bacterial DNA photolyases (Kleine *et al.* 2003). Indeed, it seems that unlike cry 1 and cry2, cry3 has retained the ability to act as a photolyase and has been shown to repair CPDs in ssDNA (Selby and Sancar 2006). Also unlike the other two cryptochromes, cry3 is localised in the chloroplasts and mitochondria (Kleine *et al.* 2003). Therefore, despite their similar names, cry3 can be thought of as entirely separate from the cryptochrome photoreceptors.

1.8.2 Phototropins

Phototropins are a second group of plant photoreceptors that mediate responses in the blue and UV-A portion of the spectrum. Similarly to the cryptochromes, there are two members named phot1 and phot2. The phot proteins consist of an N-terminal region which includes two LOV (light oxygen or voltage sensing) domains. Each of these LOV domains incorporates a blue/UV-A light absorbing flavin mononucleotide (FMN). At the C-terminal end of the protein lies a serine/threonine kinase responsible for the autophosphorylation of the protein.

Phototropin mediated signal transduction occurs through the initial absorption of the light signal by the FMN chromophore. This results in the formation of a covalent adduct with a conserved cysteine residue of the LOV domain (Christie 2007). This ultimately leads to a conformational change in the protein, mediated via the Jα-helix, which in turn releases repression of the C-terminal serine/threonine kinase (Jones *et al.* 2007). Subsequently the phot autophosphorylates and in the case of phot1 results in the internalization of the photoreceptor from the plasma membrane, where it resides in minus blue light conditions, to the cytoplasm (Sakamoto and Briggs 2002; Kaiserli *et al.* 2009). Phot2 meanwhile has been shown to translocate from the plasma membrane to the golgi apparatus in response to blue light (Kong *et al.* 2006). However, the exact purpose of this

phototropin autophosphorylation and the downstream targets of the phototropins have yet to be determined.

The phototropin family were named for their defining photomorphogenic characteristic, namely the growth of the hypocotyl towards a blue light source (Christie *et al.* 1999). This response is mediated by both phototropins, however the two phototropins differ in their fluence responsiveness for this trait with phot1 regulating low fluence and phot2 high fluence responsiveness (Sakai *et al.* 2001). These two photoreceptors also have overlapping roles in chloroplast accumulation in response to low light conditions, cotyledon/leaf expansion, leaf movement and stomatal opening (Christie 2007). Separate roles nonetheless exist for chloroplast avoidance in high light conditions, which is regulated primarily by phot2, and both hypocotyl inhibition in the dark and mRNA stability for which phot1 is responsible (Christie 2007).

In addition to the separation of roles of the two phototropins, different functions can also be assigned to the two light sensing LOV domains of phot1. While LOV2, the more efficient light sensor seems to act to repress kinase activity in the dark, a role for the LOV1 domain remains more elusive. Experiments where the domains were exchanged showed that LOV1 cannot replace LOV2 as a repressor of kinase activity and additionally has a relatively poor light sensing efficiency (Kaiserli *et al.* 2009). However it has subsequently been revealed that LOV1 appears to have an essential role the arrest of chloroplast accumulation under high light intensities (Kaiserli *et al.* 2009).

1.8.3 Phytochromes

The phytochrome family of photoreceptors is somewhat larger than that for phototropins or cryptochromes, and consists of five members named phyA – phyE in *Arabidopsis* (Clack *et al.* 1994). Similarly to the phototropins and cryptochromes, different family members are responsible for different fluence rate responses, with phyA mediating very low fluence and high far-red (FR) irradiation responses. Phys B-E on the other hand regulate low fluence and high red (R) irradiance responses (Quail 2002).

Phytochrome proteins consist of a N-terminal photosensory domain which binds the chromophore phytochromobilin, and a C-terminal region which possesses several domains with functions in dimerisation, localisation and potentially also in downstream signalling (Jiao *et al.* 2007). When these photoreceptors are irradiated with red light, they undergo a conformational change which results in the formation of a physiologically active form known as P_{FR}. Upon subsequent FR illumination, phytochrome phyB-E revert back to the inactive R light absorbing form known as P_R. PhyA, unlike the other phytochromes

is not photostable and thus undergoes rapid degradation when in the P_{FR} form (Kevei *et al.* 2007).

Phytochrome subcellular localisation occurs mostly in the cytoplasm in the dark, with treatment with various fluences of light resulting in nuclear import (Kircher *et al.* 2002). Interestingly, both phyA and phyB have been shown to accumulate in 'speckles' within the nucleus, termed nuclear bodies (Yamaguchi *et al.* 1999; Kircher *et al.* 2002). While this is a well-known phenomenon, it is not clear what the purpose of these bodies may be and their role in downstream signalling events. COP1 was shown to colocalise with phyA in these nuclear bodies (Seo *et al.* 2004). As COP1 has been shown to have a role in the degradation of this protein, it is possible that these nuclear bodies may be involved in the desensitization mechanism of this photoreceptor (Seo *et al.* 2004).

One of the key photomorphogenic responses regulated by the phytochrome family of photoreceptors includes the shade avoidance response and the R:FR photoreversibility of phytochromes makes them particularly amenable to such a role. Plants growing under other vegetation experience a drop in the R:FR ratio of light as the photosynthetic machinery of the leaves above preferentially absorb R light while leaving the FR portions of the spectrum unaffected. This results in an enrichment in the FR portion of the spectrum under a vegetation canopy and it is by detecting such changes in spectral qualities that the phytochromes, and thus the plant, can sense the current light conditions and initiate the appropriate responses. The shade avoidance response is characterised by such changes in morphology as a rapid elongation in stems and leaves. This has the effect of increasing the chances that a plant may escape from the leaf canopy and emerge into more favourable light conditions (Franklin *et al.* 2005). This particular role for phytochromes in photomorphogenesis appears to be mainly associated with phyB which acts to inhibit the development of the shade avoidance response in plants under high R:FR ratios (Franklin *et al.* 2005).

1.8.4 A UV-B Photoreceptor?

Despite our considerable knowledge of the perception and downstream signalling events associated with blue/UV-A and red far-red light stimuli, there remain a number of holes in our understanding of UV-B responses. One such example of a gap in our comprehension concerns the perception of the UV-B signal. At first glance, the known photoreceptors would appear to be good candidates for these proteins because, similarly to the vast majority of proteins in general, they are able to absorb wavelengths in the UV-B region of

the spectrum. However, previous mutant studies have been able to eliminate their involvement. For example it has been shown that in *phyA, phyB* and *cry1, cry2* double mutants UV-B induction of several genes is unaltered (Boccalandro *et al.* 2001; Wade *et al.* 2001; Brosche and Strid 2003; Brown and Jenkins 2008). It would therefore seem that we are looking for a novel photoreceptor or family of photoreceptors.

One possible explanation for the inability to identify a UV-B specific receptor, is that no such protein actually exists. Instead it is possible that UV-B is perceived through some other mechanism. A prime candidate for this would be via DNA damage. It has already been shown that DNA readily absorbs radiation in the UV-B range which in turn results in the formation of dimers between neighbouring pyrimidine nucleotides (Jiang *et al.* 1997; Britt 1999). Thus, DNA damage could be seen to be the first step in UV perception that triggers the subsequent signalling cascade. However, evidence exists which seems to refute this for currently known UV-B responsive pathways. Wade *et al.* (2001) exposed plants to UV-B in conjunction with supplemental wavelengths in either the blue or UV-A range. Photolyases, the enzymes responsible for repair of UV-B induced lesions, are activated by both blue light and UV-A. Consequently, under the above conditions we might expect to see enhanced repair, thus reduced damage, a potentially reduced signal and as a result a reduced expression of UV-B induced genes such as *CHS*. The reverse however appears to be true so that increased expression of genes such as *CHS* are seen. That is, blue light and UV-A act synergistically to enhance *CHS* expression. This result suggests that we can rule out DNA damage as the mechanism of photoreception. Conversely, it is possible that it is the repair mechanisms instead that are responsible for initiation of the signal thus explaining why an increase in *CHS* expression was seen under photoreactivating conditions. However, this theory has yet to be tested, although it should be noted that mutants in DNA photolyases retain UV-B induction of CHS expression (Brown and Jenkins, unpublished data).

Action spectra have been used in the past to link peaks in responses with the absorption of candidate photoreceptor complexes, for example in the case of phototropins (Christie *et al.* 1999). Several action spectra for UV-B responses have been performed, however these have given different values for the peak of response. For example two studies examining stomatal opening in bean and *HY5* activation in *Arabidopsis* both cite values of 280 nm, while a third examining the induction of the *PHR* promoter in cucumber gives a peak of 300 nm (Eisinger *et al.* 2000; Ioki *et al.* 2008; Brown *et al.* 2009). Action spectra experiments can be particularly problematic for the UV-B region because many proteins, DNA as well at the photoprotective pigments such as flavonoids absorb in this

region. This therefore adds a layer of complexity when trying to perform such experiments. The Brown *et al.* (2009) study attempted to address one of these issues by conducting additional experiments in mutants lacking either sinapate esters or flavonoids. This resulted in very similar values to that found in wild type plants, thus providing supporting evidence that in the case of *HY5* induction, the peak in response is indeed at 280 nm.

One interesting possibility is that UVR8 itself may act as the UV-B photoreceptor. The protein has a relatively large number of tryptophans, more than in RCC1, which absorb UV-B wavelengths well (Brown *et al.* 2009). In addition, no other mutant alleles other than those for UVR8 were identified in mutant screens for UV-B responsiveness (Kliebenstein *et al.* 2002; Brown *et al.* 2005). This however could be due to a level of redundancy, thereby preventing the discovery of the photoreceptors with overlapping functions.

In mammalian UV-B perception it seems that there may be a role for cytosolic tryptophans as a chromophore. In this system, UV-B absorption by tryptophan results in the formation of 6-formylindolo[3,2-b]carbazole (FICZ) which acts as a ligand for the arylhydrocarbon receptor (AhR) (Fritsche *et al.* 2007). The subsequent translocation of the AhR receptor into the nucleus results in the initiation of UV-B downstream signalling (Fritsche *et al.* 2007). It is possible that a similar mechanism may exist in plants, although initial experiments suggest otherwise. (Brown and Jenkins, unpublished data).

The UV-B photoreceptor or UV-B sensing components in plants therefore remain elusive. It may be that different UV-B response pathways are regulated by different photosensory mechanisms. For the well defined UVR8 pathways however, it seems that we can exclude a role for known photoreceptors as well as DNA damage whereas the role of DNA repair or the theory that UVR8 itself may be the photoreceptor have yet to be fully tested.

1.9 Conclusions

UV-B is not only an agent of damage, it also acts as an important informational signal which regulates many aspects of plant metabolism and development. Indeed the effects of this 'stress' are wide reaching in that exposure to UV-B has been shown to enhance a plant's resistance to herbivores (Izaguirre *et al.* 2003; Paul and Gwynn-Jones 2003; Izaguirre *et al.* 2007), a phenomenon which may occur through the accumulation of secondary metabolites of which are distasteful to many herbivores.

When applying laboratory research to natural ecosystems, we have to consider that the effects of UV-B are generally milder in field conditions. A further complication in applying findings to the current and possible future UV-B climate lies in the fact that UV-B levels are rarely constant. A wide variety of factors including cloud cover, canopy thickness and seasonal variations can all alter the dose of UV-B experienced by a plant (Paul and Gwynn-Jones 2003).

One final consideration when examining the literature on UV-B responses in plants is that experimental conditions and methods used can vary widely between different laboratories. For example different groups use different model species e.g. *Arabidopsis*, tobacco, maize and others. In addition, even within a species diverse ecotypes are used. In *Arabidopsis* for instance it has already been demonstrated that different ecotypes have different responses. C24, Wassilewskija and Columbia-0 ecotypes all exhibited differences in the expression of the PR-5 protein (Kalbina and Strid 2006). Also, the Wassilewskija ecotype of *Arabidopsis* which is deficient in phyD, appears to have reduced expression of *HY5* and *CHS* in response to UV-B (Brown and Jenkins unpublished data).

In conclusion, although UV-B studies have progressed a long way in the past couple of decades, there are still considerable gaps in our knowledge. For example, identification of the photoreceptor/photosensory system would greatly enhance our understanding of the full perception/transduction/response cascade. Nevertheless, we can conclude that separate low fluence informational and high fluence stress related signalling systems do exist in plants. While high levels of UV-B obviously have a detrimental effect on plants, we now realize that low levels can allow a plant to adapt to its environment and so actually promote survival. Recent advances, particularly in the area of UVR8-mediated responses have furthered our knowledge of these specific photomorphogenic responses. However, it is still not clear what other pathways may be involved nor the exact mechanism of action of UVR8.

1.10 Aims of this study

While the downstream changes in gene expression arising from the action of UVR8 are becoming increasingly defined, we still have very little knowledge of other pathways that may act in such low fluence UV-B conditions. One of the first aims of this study therefore was to investigate and try to identify components of these other pathways. Samples treated with lower fluences of UV-B than used in the Brown *et al.* (2005) study were therefore submitted for microarray analysis so that candidate genes could be identified. A subset of

genes were then examined more closely using RT-PCR methods for dependence upon UVR8, HY5, HYH, COP1 as well as the major classes of known photoreceptors. Furthermore, the possibility that these genes may be induced as a result of DNA damage/repair was explored in addition to an assessment of their expression profiles under extended periods of UV-B treatment using qPCR.

Next attention was turned to the UVR8 protein itself. The sequences of proteins similar to UVR8 in *Arabidopsis* as well as other plant species were examined to assess their similarity. The C and particularly the N-terminal regions were focused on as these have previously been shown to be essential for UVR8 function (Kaiserli and Jenkins 2007). The role of the N-terminal region of UVR8 in localisation was then further tested using a number of deletion and addition constructs expressed stably in *Arabidopsis* or transiently in tobacco.

Finally, the possibility that UVR8 may be acting as part of a complex was explored. To address this, protein extracts from plants expressing a number of different UVR8 constructs were applied to a size exclusion chromatography column. From these experiments the approximate sizes of the complex could be obtained. The use of constructs targeted to different compartments as well as treatments in both plus and minus UV-B conditions allowed the determination of these factors on the overall size of the complex. Use of the *cop1-4* mutant and the previously described Δ23N UVR8 construct enabled the role of COP1 and of the N-terminal UVR8 sequences in formation of the UVR8 complex to be assessed.

In summary, a key aim of this study is to further understand the mechanism of UVR8 action through examination of its nuclear accumulation under UV-B and the presence of interacting partners. Through this work it was hoped to gain further insight into UVR8 action as a whole. Finally, while UVR8 is an important component of plant responses to UV-B, it is not the sole mechanism of acclimation to this factor. Therefore, work was undertaken to identify other potential UV-B specific signalling pathways.

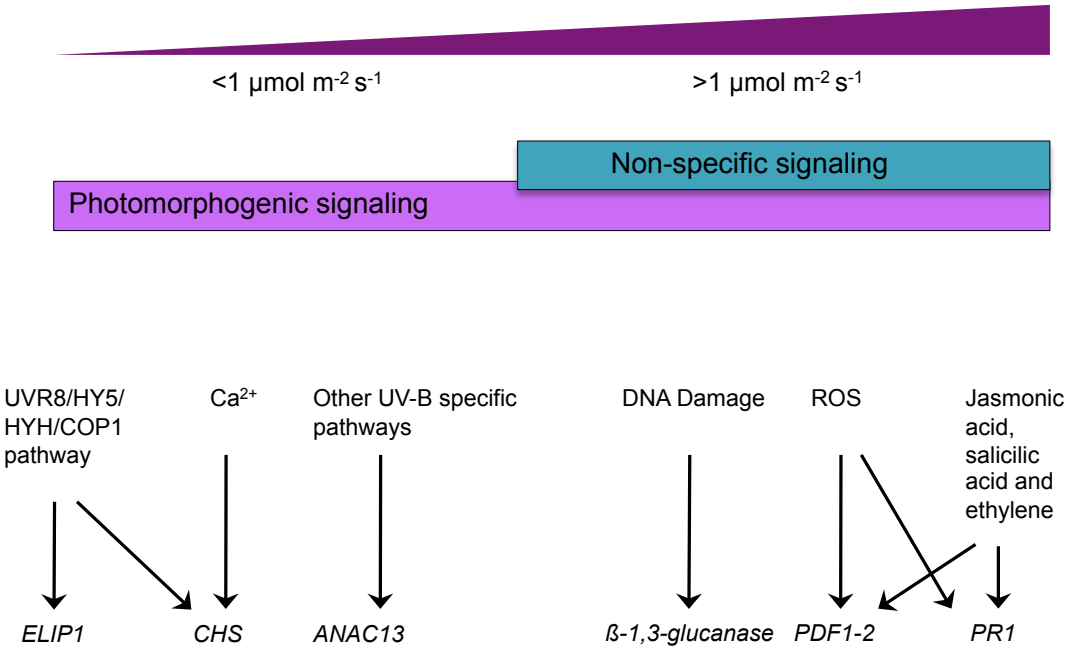

Figure 1.1 Signaling pathways elicited by UV-B radiation. Modified from Jenkins (2009) and Brosche and Strid (2003). A summary of both the high and low fluence UV-B induced pathways in plants with examples of genes whose expression is induced by these mechanisms. Example genes are as follows, EARLY LIGHT INDUCED PROTEIN1 (ELIP1), Chalcone synthase (CHS), Arabidopsis NAC transcription factor 13 (ANAC13), PLANT DEFENSIN1-2 (PDF1-2) and PATHOGENESIS RELATED 1 (PR1).

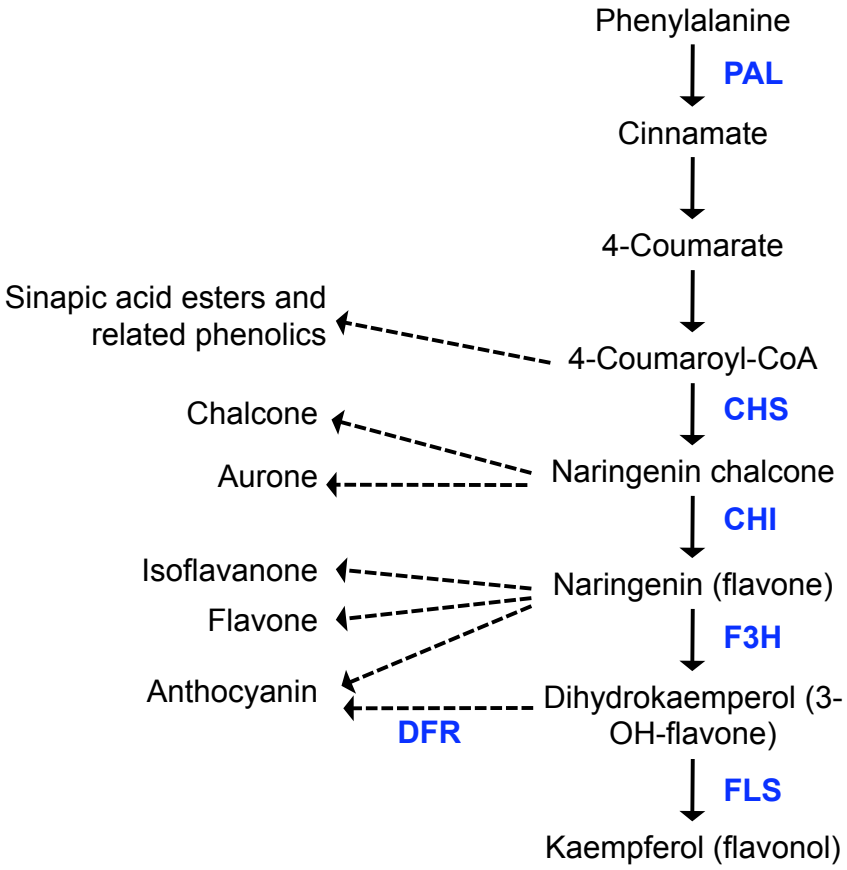

Figure 1.2 Pathway for Phenylalanine-derived secondary product biosynthesis in plants. Modified from Li *et al.* (1993) and Merhtens et al. (2005). A simplified pathway of some UV-B absorbing pigments showing key enzymes in blue. Phenylalanine ammonia-lyase (PAL) catalyses the first step in the synthesis of the secondary aromatic compounds which ultimately leads to the formation of sinapic esters and flavonoids. Chalcone synthase (CHS) is the first committed step in the flavonoid biosynthesis pathway. Chalcone isomerase (CHI) catalyses the reaction which produces isoflavones, flavones and anthocyanin. flavanone 3-hydroxylase (F3H) and flavonol synthase (FLS) catalyse further steps towards the production of kaempferol. Dihydroflavonol 4-reductase (DFR) meanwhile catalyses the first step of anthocyanin formation.

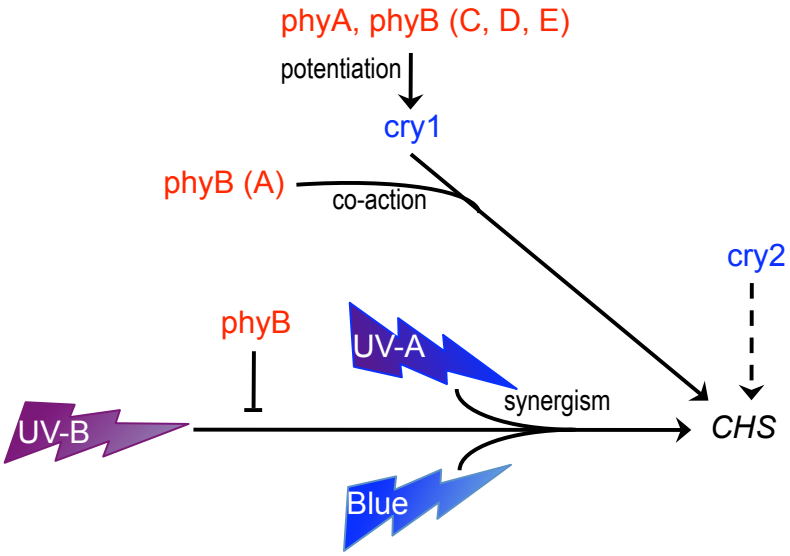

Figure 1.3. Model showing the network of photoreceptors regulating *CHS* expression. Blue/UV-A exposure induces *CHS* expression, primarily through cry1, but also to a lesser extent through cry2. Expression can be further increase with pre-illumination with red/far red light mediated through either phyA or phyB, or alternatively via co-action between phyB and cry1. While PhyB can inhibit UV-B mediated induction of *CHS* expression, supplementary illumination with blue/UV-A light synergistically enhances it in a cryptochrome and phytochrome independent fashion. Diagram modified from Wade *et al.* (2001)

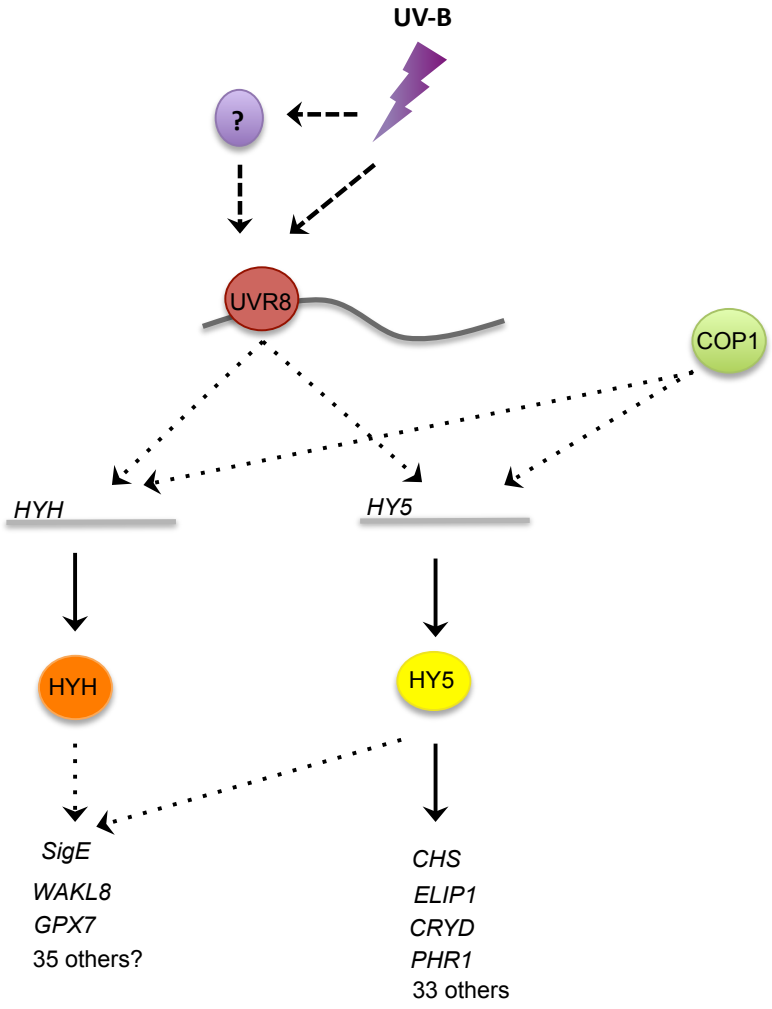

Figure 1.4 Downstream signalling of UVR8 and COP1 in UV-B. After activation by UV-B, possible via a UV-B photoreceptor (denoted by a ?), chromatin bound UVR8 induces the expression of genes such as HY5. HY5 and HYH transcription factors then in turn up-regulate other UV-B responsive genes. The expression of a total of 35 genes are dependent on function HY5 while three are known to rely on a HY5/HYH redundant mechanism. It is hypothesised that the remaining 37 UVR8-regulated genes are also under the control of the HY5/HYH mechanism although this has yet to be determined.

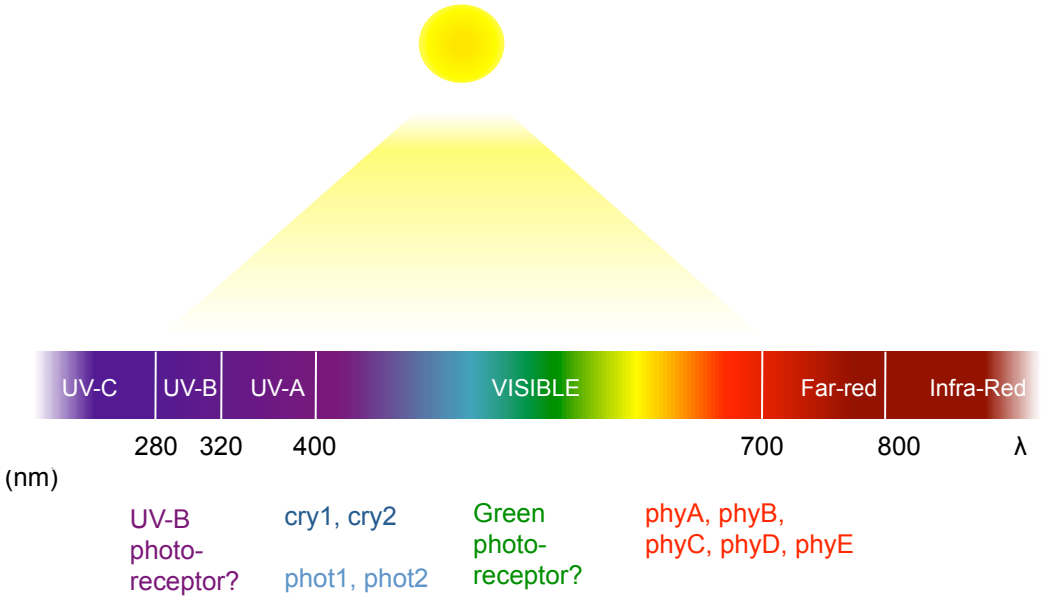

Figure 1.5 The electromagnetic spectrum of sunlight and the photoreceptors that mediate plant photomorphogenic responses. The major classes of known photoreceptors are shown below the portions of the spectrum at which they absorb maximally. The hypothesised UV-B and green ligh photoreceptors are also shown. λ = wavelength.

CHAPTER 2 MATERIALS AND METHODS

2.1 Materials

2.1.1 Chemicals

The chemicals used in the following experimental procedures were obtained from VWR International Ltd. (Poole, UK), Thermo Fisher Scientific UK Ltd. (IL, USA) and Sigma-Aldrich Inc. (St. Louis, USA) unless otherwise stated.

2.1.2 Enzymes

Enzymes used in DNA restriction, ligation, synthesis and DNA/RNA modification were purchased from Promega (Wisconsin, USA), New England Biolabs (Hitchin, UK) and Ambion Inc (Huntingdon, UK).

2.1.3 Primers

RT-PCR primers were custom made by either VH Bio Ltd. (Gateshead, UK) or Invitrogen (Paisley, UK) and purified using Reverse Phase Cartridge (RPC). All qPCR primers were obtained from VH Bio and were Reverse Phase High Performance Liquid Chromatography (HPLC) purified.

2.1.4 Antibiotics

Antibiotics were obtained from Sigma-Aldrich and were dissolved in distilled water. In the case of kanamycin a working concentration of 50 $\mu g\ ml^{-1}$ was used for *Escherichia coli* (*E. coli*), while for plants a concentration of 75 $\mu g\ ml^{-1}$ was utilised. For gentamycin a working concentration of 30 $\mu g\ ml^{-1}$ was used.

2.1.5 Antibodies

Anti-GFP antibodies were obtained from Clontech (California, USA). Both the N-terminal (MAEDMAADEVTAPP) and C-terminal (VPDETGLTDGSSKGN) anti-UVR8 antibodies

were custom made by Sigma-Aldrich. Secondary anti-rabbit (for use with UVR8 antibodies) and anti-mouse (for use with anti-GFP) antibodies conjugated to Horseradish Peroxidase (HRP) were obtained from Promega. All antibodies were used at a concentration of 1:5000.

2.1.6 Vectors

pEZR(K)L-C was sourced from Dr. Gert-Jan de Boer and was used to add a GFP tag to UVR8 constructs. pCR®2.1 vector was used in conjunction with One Shot® TOP10 cells for the purpose of PCR product cloning and was obtained from Invitrogen.

2.1.7 Bacterial strains

E. *coli* strains TOP10® (Invitrogen) and XL-1 Blue (Stratagene, CA, USA) were chemically transformed and used for sub-cloning, expression and amplification. To generate stable transgenic lines and for transient expression in tobacco, *Agrobacterium tumefaciens* strain GV3101 was used.

2.1.8 Other Reagents

All reagents used in this study for protein electrophoresis and quantification purposes were purchased from Bio-Rad Laboratories (Hercules, California, USA) unless otherwise stated.

2.2 Preparation of media and solutions

2.2.1 Measurement of pH

The pH of media and solutions was measured using a glass electrode connected to a Jenway 3320 pH meter (Jenway, Felsted, Essex).

2.2.2 Autoclave sterilisation

Equipment and solutions were sterilised using a benchtop autoclave (Prestige Medical, Model 220140).

2.2.3 Filter sterilisation

Heat sensitive solutions, those of small volume and those used in Size Exclusion Chromatography (see section 2.10) were sterilised by filtration through a 0.2 μM pore diameter Nalgene® filter (Thermo Fisher Scientific Inc.).

2.3 *Arabidopsis* plant material

2.3.1 Seed stocks

Wild-type *A. thaliana* cv Landsberg *erecta*, Col-3 and Ws-2 seeds were obtained from The European *Arabidopsis* Stock Centre (NASC, Nottingham, UK). The *hy5-1* mutant in the L. *er* ecotype was also acquired from the NASC. Additional mutants in a L. *er* background include the *cry1 cry2* mutant generated by Wade et al. (2001), *uvr8-1* mutant from Prof. D. Kliebenstein (U.C. Davis, USA) and the *phyA-1 phyB-1* mutant from Prof. Garry Whitelam (University of Leicester, UK). Dr. Roman Ulm provided the *cop1-4* mutant while *hy5-ks50, hyh* and *hy5-ks50 hyh* mutants (all in Ws) were supplied by Prof. Xing Wang Deng (Yale University, USA). Dr. John Christie (University of Glasgow, UK) provided the *phot1-5 phot2-1* mutant and Dr. Enrique Lopez-Juez (Royal Holloway, University of London, UK) the *hy1-100* (both Col). GFP-UVR8, NES-GFP-UVR8, NLS-GFP-UVR8 and ΔN-UVR8 seed (all in a *uvr8*-1 background) were generated in the Jenkins lab by Dr Eirini Kaiserli (Kaiserli et al., 2007). Dr. R. Sablowski (John Innes Centre, Norwich, UK) provided $35S_{pro}$GFP (L *er.*) seeds.

2.3.2 Growth of plants on compost

Plant pots were filled with compost (John Innes No.2 compost) and generous volumes of insecticide solution (0.15 g l^{-1} Intercept® (Scotts UK, Bramford, Ipswich)) added until soil was soaked through. *Arabidopsis* seeds were then sown onto the surface and covered with cling film, before transferral to 4 ºC in the dark for a stratification period of 2-4 days to ensure optimal germination. After this time, plants were moved to growth cabinets at 21 º C and with either low fluence rate (20 ± 5 μmol m^{-2} s^{-1}) or high fluence rate (100 ± 10 μmol m^{-2} s^{-1}) continuous white light according to experimental requirements. Cling film was removed after approximately one week of growth and if necessary, seedlings were thinned out to prevent overcrowding. In order to prevent a thrip infestation, plants were sprayed twice per week with the insecticide Conserve® (Fargo Ltd., Littlehampton, West

Sussex). Three week old plants were used for RT-PCR while protein extractions were performed on 12-21 day old seedlings.

2.3.3 Surface sterilisation of seed

A bleach solution of 50 % (v/v) sodium hypochlorite, 0.2 % (v/v Tween-20) was prepared fresh and 1 ml added to a small amount of *Arabidopsis* seeds. Tubes were shaken vigorously and left for five minutes. After this period, the bleach solution was drawn off and discarded. Seeds were then washed three times in 1 ml sterile distilled water before resuspension in approximately 0.5 ml sterile distilled water.

2.3.4 Growth on agar plates

After surface sterilisation, plants were grown on 0.8 % agar plates containing 2.15 g l^{-1} Murashige and Skoog salts with the pH adjusted to 5.7. For those plants that had been transformed, seeds were sown onto plates with the addition of 75 μg ml^{-1} kanamycin. In most cases, sterile filter paper discs were placed on the surface of the plates and individual seeds dotted on top. However, where large numbers of seeds were to be put onto plates, seeds were first mixed with a few millilitres of MS mixture (while still liquid and approximately body temperature) before being poured onto the plate and swirled to ensure good separation.

2.3.5 Harvesting of plant tissue

Where tissue was subsequently used for RNA extraction, leaves were removed from several plants, packaged into aluminium foil and immediately plunged into liquid nitrogen. Samples were then stored at -80 ºC. In the case of protein extraction, whole seedlings were directly transferred to an ice-cold pestle and mortar and extracted as described in section 2.8.1.

2.4 UV-B and other light treatments

2.4.1 Light fluence rate measurements

The fluence rate of white light (photosynthetically active radiation) in the plant growth chambers was measured using a quantum sensor that registers wavelengths ranging from

400 to 700 nm attached to a Skye RS232 meter (Skye Instruments, Powys, UK). To measure fluence rates of UV-B (280-315 nm) a SKU 430 sensor fitted to a RS 232 meter was used. Where more detailed measurements of light quality were required, a Macam Spectroradiometer Model SR9910 (Macam Photometrics Ltd., Livingstone, Scotland) with the capability of recording wavelengths between 240-800 nm was used.

2.4.2 Light sources

All light treatments in this study were conducted in growth chambers at 21 ± 1 °C. For white light treatments warm white fluorescent tubes L36W/30 (Osram, Munich, Germany) were used. UV-B was provided by Q-Panel UV-B 313 tubes (Q-Panel Co., USA). In order to eliminate the UV-C component emitted from this source, tubes were covered with one layer of cellulose acetate (Catalogue No. FLM400110/2925, West Design Products, Nathan Way, London). This filter was changed after 24 hours of use to prevent UV-C leaking through due to filter degradation. Where UV-B minus treatments were conducted, the same UV-B tubes were covered with a 'Clear 130' mylar filter (Lee Filters, Andover) instead of cellulose acetate. This filter cuts out UV-B wavelengths as well as UV-C. To achieve lower fluence rates of UV-B, tubes were wrapped in sections of thin black card. Dark treatments were conducted in the growth chamber without any light sources turned on.

2.5 DNA and RNA methods

2.5.1 Extraction of RNA from plant tissue

Approximately 0.4 g of plant tissue was hand ground in liquid nitrogen using a mortar and pestle until a fine powder was obtained. Powder was then transferred to a pre-cooled Eppendorf tube. Total RNA was subsequently extracted using the RNeasy® Plant Mini Kit (Qiagen, Crawley, UK) according to the manufacturer's instructions. Buffer RLT (containing 10 µl β-Mercaptoethanol per 1 ml buffer) was used in this study. Purified RNA was eluted from the RNeasy spin column with 30 µl RNase free water. Samples were stored at -80 ºC.

2.5.2 Quantification of DNA and RNA concentrations

To determine the concentration of extracted RNA and of DNA plasmids, 2 µl of the sample was diluted in 2 ml of RNase free dH_2O and mixed well. An equivalent volume of RNase free dH_2O was used to blank the spectrophotometer (Bio-Rad SmartSpec 3000). A reading of the absorbance of the DNA/RNA solution at 260 nm (OD_{260}) was recorded. The concentration of the sample was then determined by taking an OD_{260} of 1 to be equivalent to 50 µg ml^{-1} for DNA and 40 µg ml^{-1} for RNA. (Sambrook and Russell, 3rd Edition).

2.5.3 DNase treatment of RNA

In order to remove any DNA present prior to analysis using PCR methods, a DNAse treatment (DNA-free, Ambion) was performed on all samples. Approximately 5 µg of RNA (as determined using spectroscopy as described in 2.5.3) was incubated with 2 units of DNAse I, 1 x DNAse I buffer and sterile water up to a total volume of 35.5 µl at 37 °C for 30 mins. An additional 2 units of DNAse I were then added to the samples before a further incubation of 30 mins at 37 °C. DNAse inactivation reagent was then added to the samples and left for 2 mins at room temperature with occasional flicking of tubes to ensure the reagent was well suspended. Samples were then spun down at 13 000 rpm in an Eppendorf 5415D centrifuge for 1.5 mins to pellet inactivation reagent. To ensure the DNAse treatment had been effective, a 35 cycle PCR reaction using ACTIN2 primers was performed on 2.5 µl of each sample as well as a negative (sterile water) and positive (genomic DNA) control. If no PCR product was detectable, then samples were carried onto cDNA synthesis. If however DNA was still present, then DNAse treatment was repeated until no DNA could be detected.

2.5.4 Synthesis of cDNA

0.24 µM oligo dT ($dTTP_{15}$) was added to 10 µl of DNAsed RNA and incubated at 72 °C for 10 mins. Samples were then allowed to cool on ice while a master mix of 1 x AMV Reverse Transcriptase Reaction Buffer (Promega), 1 mM of each dNTP (VHBio), 24 units RNase inhibitor (Promega), 1 mM dithiothreitol, 10 units AMV Reverse Transcriptase (Promega) and RNAse free water up to a volume of 25 µl was made up and added to the sample. The sample was then incubated at 48 °C for 45 mins then 95 °C for a further 5 mins to inactivate the enzyme. The resulting cDNA samples were then stored at -20° C.

2.5.5 Microarray

Three independent RNA samples extracted as described in section 2.5.1 were submitted to the Sir Henry Wellcome Functional Genomics Facility (SHWFGF, University of Glasgow). RNA quality was checked using an Aligent RNA BioAnalyzer 2100 (Austin, TX). The samples were then reverse transcribed and biotinylated cRNA hybridised to Affymetrix *Arabidopsis* ATH1 GeneChips (High Wycombe, UK) as per manufacturers protocols. Subsequent washes and staining were performed using a Fluidics Station 400 (Affymetrix) according to manufacturer's instructions. The chips were scanned on the GeneArray Scanner 2500 (Affymetrix) and analysed by the SHWFGF using FUNALYSE version 2.0 (University of Glasgow, UK). Analysis involved normalization using Robust Multi Chip Average (Irizarry, 2003) and differentially expressed genes were determined using the Rank Products method (Breitling, 2004).

2.6 Semi-quantitative Polymerase Chain Reaction techniques

2.6.1 RT-PCR primers

All primers were designed using the Primer3 software (http://fokker.wi.mit.edu/primer3/input.htm). For each gene, at least two sets of primers were designed and then tested to determine which pair showed the best expression. To ensure accurate comparison of quantities of mRNA, each set of primers were tested using a range of different PCR cycle numbers. This allowed a point to chose where expression was readily detectable but was still in the exponential phase of amplification.

2.6.2 PCR conditions

To ensure that the total amounts of cDNA were equal for each reaction, initial PCRs were performed using 1 µl of sample cDNA and ACTIN2 loading control primers. The volumes of cDNA used were then adjusted until bands of roughly equal intensity were seen on an agarose gel. To the appropriate volume of cDNA, a master mix was added consisting of 1 x PCR Buffer (New England Biolabs), 0.2 mM dNTPs, 0.5 µM of each primer, 0.625 Units of *Taq* DNA Polymerase (New England Biolabs) and RNase free water to a final volume of 25 µl. Tubes were gently mixed and put into a MJ Research DNA Engine PTC-200 Peltier Thermal Cycler (Genetic Research Instrumentation, Essex, UK). The basic PCR cycle used was (step 1) an incubation for 2 min 30 s at 95 °C, (Step 2) a further 45 s at 95

°C, (step 3) incubation at 55-59 °C for 1 min, (step 4) elongation at 72 °C for 1 min and a final step of a further elongation at 72 °C for 5 min (step 5). Steps 2-4 were repeated 24-28 times depending on the primers used (see Table 2.1).

2.6.3 Amplification of plasmid DNA

When PCR products were to be used in subsequent cloning experiments, *Pfu* DNA polymerase (Promega) was used to ensure high fidelity. Approximately 500 ng of DNA was used as a template. To this a master mix of 1.25 units *Pfu* DNA polymerase, 0.2 mM dNTPs, 0.6 μM of each primer and RNase free water to a total volume of 50 μl was added. The basic PCR cycle used was (step 1) an initial incubation for 5 min at 95 °C, (step 2) a further 45 s at 95 °C, (step 3) incubation at 55-59 °C for 30 s, (step 4), elongation at 72 °C for 2 min per 1000 bases of template, and a final elongation step at 72 °C for 5 min (step 5). Steps 2-4 were repeated 25 times.

2.6.4 Colony PCR

25 μl of master mix (as described in section 2.6.3) was added to each thin-walled PCR tube. Using a sterile pipette tip, one colony of transformed *E. coli* was picked from a selective LB-agar plate and placed in the PCR tube. The mix was then pipetted up and down a couple of times to release the bacteria into the liquid. This tip was then removed from the PCR mix and re-streaked onto a fresh selective plate. PCR reaction was then performed as described in section 2.6.3.

2.6.5 Electrophoresis of PCR products

The appropriate amount of agarose (1-2 % w/v) was added to TAE (40 mM Tris-acetate, 1 mM EDTA) or TBE (44 mM Tris-borate, 1mM EDTA) buffer and heated until all granules had dissolved. The liquid gel was then allowed to cool slightly (until about hand hot) before addition of 0.2 μg ml^{-1} ethidium bromide. Samples were resuspended in loading buffer (0.25 % (w/v) bromophenol blue, 0.25 % (w/v) xylene cyanol FF, 30 % (w/v) glycerol) before loading into the wells of the gel. The gel was submerged in an appropriate volume of TAE/TBE and run at 70-90 mA. Gels were visualized using a Bio-Rad Gel-Doc 2000 and the Quantity One program (Bio-Rad Laboratories).

2.6.6 Extraction of PCR products from agarose gel

DNA samples were run on an ethidium bromide stained 1-2 % agarose gel. Bands of the correct size were visualized and excised from the gel under a UV-illuminator. DNA was then extracted using the QIAquick® Gel Extraction Kit (Qiagen) according to the manufacturer's instructions. DNA was eluted off the column using 30 µl RNase free water.

2.7 Real-Time Quantitative-PCR techniques

2.7.1 qPCR primers

Similarly to section 2.6.1 qPCR primers were designed using Primer3 and obtained from VH Bio Ltd. but in this instance were purified using HPLC. Primers were designed to overlap an exon-exon junction so that cDNA could be differentiated from any contaminating genomic DNA using size.

2.7.2 Generation of standards for qPCR

qPCR primers were used to amplify up fragments of the gene of interest using RT-PCR. The resultant PCR products were then cloned into the TOPO® vector pCR®2.1-TOPO® using the TOPO TA Cloning®Kits according to the manufacturer's instructions. Colonies were screened using colony PCR (see section 2.6.4) and the plasmid extracted using the Qiagen Miniprep kit (Qiagen) according to the manufacturer's instructions (see section 2.6.6). The concentration of the final elutate was determined using a Unicam UV 500 spectrophotometer (Thermo Spectronic, WI, USA). The plasmids were then diluted down to the appropriate concentrations to act as standards for qPCR reactions.

2.7.3 qPCR reaction

In order to minimise any potential contamination of samples, preparation of all components and master mix was performed under a flow hood. In addition, all plastics and DEPC-treated water (Ambion) were treated with UV prior to use. First a master mix was prepared of 1x SYBR Green Master Mix (Stratagene), 0.2 µM of each primer and DEPC-treated water to a volume of 23 µl and added to each thin walled PCR tube. To this, 2 µl of diluted (1 in 3) cDNA or plasmid standard was added. Optically clear caps were applied to

the tubes and care was taken to ensure no liquid contained any bubbles. Samples were then loaded into the MX4000 qPCR machine (Stratagene) and run according to the manufacturer's instructions. For the primers used in this study, an annealing temperature of either 59 or 60 °C was used (see table 2.3). To obtain values of expression, the cycle numbers generated for the standards of each primer set were used to generate a standard curve. From this, amounts of cDNA for each of the samples were determined. The expression of each gene was normalised against the concentration of *ACTIN2* transcripts in each sample.

2.8 DNA cloning

2.8.1 Isolation of plasmid DNA

A Qiagen® Plasmid Mini kit was used to extract plasmid DNA. One colony containing the plasmid of interest was picked and placed in 5 ml LB medium plus the appropriate antibiotic. The culture was left to grow overnight at 37 °C with shaking. The culture was then spun at 6,000 g for 15 mins to pellet cells. Lysis of the cells and subsequent purification of the plasmid was then performed as per manufacturer's instructions. The plasmid was eluted off of the column with 50 µl sterile distilled water. The concentration of the plasmid was determined and was then stored at -20 °C.

2.8.2 Digestion

Approximately 1 µg of DNA was digested using the appropriate restriction enzymes and buffers at concentrations specified in the manufacturers instructions. Reactions were incubated for two hours at 37 °C. Products were then run on a 1 % agarose gel to ensure digestion had been successful. Bands of the appropriate size were then excised and purified using the QIAquick® Gel Extraction Kit (Qiagen) according to the manufacturer's instructions.

2.8.3 Ligation

Approximately 200 ng of vector/insert was incubated with 1x ligation buffer, 1U T4 DNA ligase (Promega) and sterile water up to a total volume of 10 µl. The reaction was left to

proceed overnight at 4 °C or for three hours at room temperature. Ten µl of this ligation was then used to transform XL1-Blue cells as per manufacturers instructions.

2.8.4 Transformation of *E. coli* cells.

XL1-Blue (Stratagene) and TOP10® (Invitrogen) cells were chemically transformed as per manufacturer's instructions.

2.9 Protein methods

2.9.1 Protein extraction from *Arabidopsis* seedlings

12-21 day old seedlings were hand ground in Micro-Extraction buffer (20 mM HEPES pH 7.8, 450 mM NaCl, 50 mM NaF, 0.2 mM EDTA, 25 % (v/v) glycerol, 0.5 mM PMSF, 1 mM DTT and 1 tablet of protease inhibitor mix (Roche Applied Science, Mannheim, Germany) per 10 ml of Micro-Extraction buffer) using a mortar and pestle on ice. Samples were then subjected to three freeze-thaw treatments (30 s on dry ice (or until sample fully frozen) followed by 30 s at 37 °C (or until sample fully thawed)). They were then spun down at 10 000 g for 10 mins at 4 °C to pull down most of the cellular debris. The supernatant was removed and transferred to a fresh tube.

2.9.2 Quantification of protein concentrations

To determine the concentrations of the protein samples obtained, the Bradford Assay was used. Bradford assay solution (Bio-Rad) was diluted five-fold with distilled water and passed through a filter to remove any particulates. 1 µl of protein sample was put into a cuvette, 999 µl of diluted Bradford solution added and the solution mixed well. The spectrophotometer was set to read at an absorbance of 550 nm and was blanked using 1 ml diluted Bradford solution. The absorbance of the samples was recorded and compared to a standard curve generated using a serial dilution of BSA standards of known concentration (1, 2, 3, 4, 6, 8 and 10 µg μl^{-1}).

2.9.3 SDS-polyacrylamide gel electrophoresis

Five µl of 4x protein loading buffer (250 mM Tris-HCl pH 6.8, 2 % (w/v) SDS, 20 % (v/v) β-mercaptoethanol, 40 % (v/v) glycerol, 0.5 % (w/v) bromophenol blue) was added to equal amounts of protein sample and the volume made up to 25 µl using Micro-extraction

buffer. Samples were then heated to 95 °C for 5 mins before being loaded onto a SDS-PAGE gel consisting of a top layer of 4 % polyacrylamide stacking gel (4 % (w/v) acrylamide, 132 mM Tris-HCl pH 6.8, 0.1 % (w/v) SDS, 0.05 % (w/v) APS, 0.15 % (v/v) TEMED) and a bottom layer of 10 % polyacrylamide separating gel (10 % (w/v) acrylamide, 0.38 M Tris-HCl pH 8.8, 0.1 % (w/v) SDS, 0.05 % (w/v) APS, 0.07 % (v/v) TEMED). Gels were run for approximately 45-50 mins (depending on separation required) at 200 V in a running buffer consisting of 25 mM Tris- HCl pH 8.5, 190 mM glycine and 1 % (w/v) SDS. To estimate the molecular weights of the proteins of interest, a pre-stained protein marker (New England Biolabs) was run alongside the samples.

2.9.4 Western Blotting

Proteins were transferred from SDS-PAGE gels onto nitrocellulose membranes at 100 V in transfer buffer (25 mM Tris-HCl pH8.5, 190 mM glycine, 20 % w/v methanol). Membranes were then stained in a solution of Ponceau (0.1 % (w/v) Ponceau S, 1 % (v/v) acetic acid) to reveal bands of Rubisco and thus determine if equal loading of protein samples had been achieved. To remove this stain, membranes were washed briefly in TBS (25 mM Tris-HCl pH 8, 150 mM sodium chloride, 2.7 mM potassium chloride) before being blocked for an hour in a milk solution (8 % w/v dried milk powder dissolved in 1 x TBS-T (25 mM Tris-HCl pH 8, 150 mM sodium chloride, 2.7 mM potassium chloride, 0.1 % (v/v) Triton X-100)).

2.9.5 Immunolabelling

Membranes were then incubated with primary antibody diluted in 8 % milk solution (see Table 2.3 for antibodies and concentrations used in this study) either for an hour at room temperature or overnight at 4 °C. They were then washed twice in TBS-TT (25 mM Tris-HCl pH 8, 150 mM sodium chloride, 2.7 mM potassium chloride, 0.2 % (v/v) Triton X-100, 0.05 % (v/v) Tween-20) for 5 mins, followed by an additional 5 min wash is TBS. Secondary antibodies (anti-rabbit or anti-mouse, Promega) conjugated to HRP were again diluted down in an 8 % milk solution and poured onto the membranes. These were left to incubate for an hour or more at room temperature. Five wash steps in TBS-TT for five minutes were then performed.

2.9.6 Immunodetection

To visualize protein bands, the ECL Plus™ Western Blotting Detection Reagents (Amersham) were used according to the manufacturer's instructions. After incubation in the detection reagents, membranes were carefully drained to remove excess liquid and placed between two sheets of clear plastic to prevent drying. This was placed in an X-ray cassette and secured using tape. Under safe light conditions, a sheet of X-ray film (Kodak) was placed over the membranes and the lid closed. Initially, film was left for 10 seconds before being developed using a X-OMAT developer. However, this time was adjusted for subsequent films according to the exposure seen on the first.

2.10 Size exclusion chromatography

2.10.1 Dialysis of protein samples

Prior to loading on the agarose column, protein samples were first dialysed to exchange the microextraction buffer in which they were extracted (see section 2.7.1) for the phosphate buffer (0.05 M sodium phosphate, 0.15 M sodium chloride, pH 7.2) used to equilibrate the column. Before being loaded into the cassette, protein samples were first microfuged again (at 10,000 g for 10 mins at 4 °C) to bring down any remaining cell debris. Approximately 0.5 ml of the supernatant was then loaded into the chamber of a Slide-a-lyzer 10K MWCO dialysis cassette (Thermo Fisher Scientific Inc.) using a syringe according to the manufacturers instructions. Cassettes were then suspended from polystyrene buoys and placed in beakers containing 500x cassette volume of phosphate buffer. The beaker and contents were then left overnight at 4 °C on a magnetic stirrer to ensure continuous gentle movement. The next morning, samples were removed from the cassettes and put on ice until ready to use.

2.10.2 Size exclusion chromatography

Approximately 600-800 μg total dialysed protein was loaded onto a Superose™ 6 HR 10/30 column (GE Healthcare, Buckinghamshire, UK) which was connected to a BioCAD 700E Workstation (Applied Biosystems, CA, USA) after the column had been equilibrated with phosphate buffer (0.05 M phosphate pH 7.2, 0.15 M NaCl). Elution was performed at a flow rate of 0.3 ml/min at room temperature. A void volume of 5 ml was allowed to pass through the column before 80 fractions of 300 μl each were collected using a FC-203B

fraction collector (Gilson, WI, USA). In order to calculate approximated sizes of eluted proteins/protein complexes, the column was calibrated using a high molecular weight standard kit (GE Healthcare).

2.10.3 Concentration of fractions

As protein samples were eluted off in relatively large volumes (300 µl), they were concentrated prior to loading onto SDS-PAGE gel using StrataClean™ resin (Stratagene). To each fraction, 3 µl of StrataClean™ resin was added. Fractions were then vortexed vigorously for 1 min before centrifugation at 2,000 g for 1 min. The supernatant was carefully removed and discarded. 5 µl protein loading buffer (see Section 2.7.3) and 10 µl phosphate buffer was added to each sample before being loaded onto 10 % SDS gel and run as described in Section 2.7.3.

2.11 Generation of stable transgenic lines

2.11.1 N-terminal deletion constructs

A series of N-terminal deletion constructs were generated to study the sub-cellular localisation and functionality of UVR8. Such deletions were made using the UVR8pro:NES-GFP-UVR8 construct in the pEZR(K)L-C vector described in Kaiserli and Jenkins (2007). Primers were designed to amplify UVR8 minus the relevant N-terminal amino acids as well as incorporate an *EcoR*1 restriction site at the 5' end of the UVR8 sequence (see table 2.3). These N-terminal primers were used in combination with a C-terminal primer which incorporates a *Sal*I restriction site at the end of the UVR8 sequence in order to amplify fragments of UVR8 from a cDNA template. The original full length fragment of the UVR8pro:NES-GFP-UVR8 vector was digested at the *EcoR*1 and *Sal*I sites (see section 2.8.2). This was then replaced with one of the amplified the N-terminal deletion fragments.

2.11.2 N-terminal addition constructs

A series of constructs whereby portions of the N-terminal of UVR8 were fused to NES-GFP was generated. A primer with a *Hind*III site at the 5' end and specific to the N-terminal part of the NES was used in combination with primers with a *Sal*1 site and

specific to the various portions of the N-terminal of UVR8 (see Table 2.4). These were then used to amplify fragments from the UVR8pro:NES-GFP-UVR8 construct in the pEZR(K)L-C vector described in Kaiserli and Jenkins (2007). The UVR8pro:NES-GFP-UVR8 vector was then digested (see Section 2.8.2) at the *Hind*III and *Sal*1 sites to remove NES-GFP-UVR8. The amplified fragments were then ligated (see Section 2.8.3) in its place.

2.11.3 NES-GFP construct

A construct was generated which consisted of a NES fused to GFP alone under the UVR8 promoter. The UVR8pro:NES-GFP-UVR8 construct was digested (see Section 2.8.2) with *EcoR*1/*Sal*1 to remove the UVR8 sequence. The DNA Polymerase I Large (Klenow) Fragment (Promega) was used to blunt the ends of the fragment according to manufacturer's instructions. The vector was then re-ligated (see section 2.8.3).

2.11.4 Transformation of *Agrobacterium tumefaciens*

One µl of relevant plasmid was added to 50 µl of *Agrobacterium tumefaciens* cells (strain GV3101) on ice and gently mixed. This was transferred to a chilled electroporation cuvette and briefly pulsed with 2.5 kV using a MicroPulser™ Electroporator (BioRad). 1 ml of ice-cold LB medium was immediately added. This was then transferred to a 15 ml Falcon® tube along with the pipette tip and allowed to recover at 28 °C with shaking for at least 3 hours. To ensure colonies with good separation were obtained, a serial dilution down to 1/1000 of the *Agrobacterium* suspension was performed. Fifty µl of these dilutions was then plated out onto LB agar plates containing 30 µg ml^{-1} gentamycin and 50 µg ml^{-1} kanamycin. Plates were left at 28 °C for two days and colonies tested using colony PCR with the appropriate primers.

2.11.5 Transformation using the floral dip method

All constructs were transformed into the *uvr8-1* background. Plants were grown under high white light conditions until each bolt had several sets of flowers on. Transformed *Agrobacterium* were grown from a single colony in 500 ml LB medium containing 30 µg ml^{-1} gentamycin and 50 µg ml^{-1} kanamycin at 28 °C until culture reached an optical density of 2.0. The culture was then spun at 2,000 g for 10 mins to pellet the cells. These were then resuspended in 1 l of infiltration medium (2.2 g l^{-1} Murashige and Skoog salts, 50 g l^{-1}

sucrose, 0.5 g l^{-1} MES, 0.044 µM benzylaminopurine and 200 µl g l^{-1} Silwet L-77). This was poured into a shallow container. Plants were turned upside down and aerial parts were submerged in the medium for 1 min. Plants were then placed in autoclave bags to maintain a humid environment and returned to high fluence rate white light conditions. The bags were removed after 2 days and plants were once again dipped in the *Agrobacterium* medium as described above. Plants were then left to set seed. This protocol was modified from Clough and Bent (1998).

2.11.6 Selection of T1, T2 and T3 generations

Transgenic seeds were grown on plates as described in Section 2.3.4. A few of the seedlings that had grown successfully on the plates were checked for expression of the construct using confocal microscopy (see Section 2.12). Approximately 30-40 T1 seedlings were transferred to individual pots of soil and allowed to set seeds. These were then grown under continuous high fluence rate white light conditions until they set seeds. T2 lines were checked for 3:1 segregation and subsequently for expression of GFP. Roughly 5 lines were then carried on. One T3 lines that showed 100 % resistance to kanamycin were then tested for localization and complementation. As there were problems finding lines with suitable levels of expression for analysis, a second T2 line was also checked for localization and complementation.

2.11.7 Transient expression in *Nicotiana benthamiana*

Agrobacteria were freshly transformed as described in Section 2.10.2. One colony was picked and added to 10 ml LB medium plus 30 µg ml^{-1} gentamycin and 50 µg ml^{-1} kanamycin. The culture was left to grow at 28 °C with shaking overnight. Cells were then spun down at 4,000 rpm in a centrifuge for 5 mins and the pellet resuspended in 10 ml of sterile 10 mM $MgCl_2$. The OD_{600} of this culture was measured and then diluted down in the appropriate volume of sterile 10 mM $MgCl_2$ until an OD_{600} of 0.2 was achieved. Acetosyringone (dissolved in DMSO) was added to the culture to a final concentration of 200 µM. The culture was then left at room temperature for a minimum of 2 hours. Small incisions were made on the underside of the leaf of a 4-6 week old *Nicotiana benthamiana* plant. A syringe was filled with the *Agrobacterium* solution and placed over these incisions. Pressure was gently applied using the fingertips on the upper-side of the leaf and the plunger carefully plunged thereby filling the intercellular space of the leaf with the

solution. Plants were left for five days to allow expression of the constructs. Leaf tissue was then taken and examined by confocal microscopy as described in Section 2.12.1.

2.12 Confocal microscopy

2.12.1 Localisation studies in *Arabidopsis*

12-14 day-old *Arabidopsis* plants or sections of tobacco leaf were infiltrated with water before being mounted on glass slides. A confocal laser scanning microscope (Zeiss LSM 510) with an argon laser set to 488 nm was used to excite GFP fluorescence. In order to prevent any overlap with chloroplast autoflourescence, GFP emission was recorded between 505-530 nm. For detection of nuclei, plants were instead infiltrated with 50 µg ml^{-1} of 4', 6'-Diamidino-2-phenylindole (DAPI) (Molecular Probes) and left for 15 mins in the dark before being mounted on slides. To visualise DAPI fluorescence, a UV laser set to 395 nm was used. All images were taken using the 40 x objective lens. In the case of *Arabidopsis* stable transgenic lines, 25 images were taken from at least 6 plants and the experiment was repeated three times. For transient expression, at least three separate tobacco plants were transformed on separate occasions and images were subsequently taken from two or more leaves. A minimum of 70 images in total were analysed. In each case, the number of nuclei exhibiting DAPI fluorescence and the number showing GFP fluorescence were compared to give a ratio of GFP/DAPI.

2.13 Computational techniques

2.13.1 Identification of UVR8-like proteins

UVR8 protein sequence was inputted into the BLASTP algorithm available at http://blast.ncbi.nlm.nih.gov/Blast. In the case of the UVR8-like sequences in *Arabidopsis*, the organism was set to *Arabidopsis thaliana* (taxid:3702). 23 UVR8-like sequences were found and retrieved for further analysis. To find potential UVR8 homologues in other plant species, the organism was set to Plants (taxid:3193). 365 Blast hits were returned and the top scoring sequence for each species listed was retrieved. The sequence for *Chlamydomonas reindhardtii* was found by setting the organism to Chlorophyta (taxid:3041) and the sequence for human RCC1 was retrieved from the Entrez database

(http://www.ncbi.nlm.nih.gov/sites/entrez). Sequences for *Physcomitrella patens* were kindly provided by Dr Andrew Cuming (University of Leeds, UK).

2.13.2 Protein alignment

Protein sequences were aligned using the ClustalX program (version 2.0, www.clustal.org). Phylogenic trees were constructed using the Bootstrap N-J Tree option with 1000 bootstrap trials. Trees were viewed using TreeView X software (http://darwin.zoology.gla.ac.uk/~rpage/treeviewx/).

2.13.3 Microarray comparison

Venn diagrams were constructed using GeneVenn software (http://mcbc.usm.edu/genevenn/genevenn.htm). Microarray comparisons across studies were performed by incorporating all data into a FileMaker Pro 10® (Filemaker Inc., CA, USA) database. Data was then exported to Excel® (Microsoft, USA) and sorted according to frequency of occurrence for each gene.

Table 2.1 Oligonucleotide primers used in RT-PCR experiments

Name	Sequence of Primer Pair	Amplified Fragment size	Locus	No. cycles
ACTIN2	5'-CTTACAATTTCCCGCTCTGC-3' 5'-GTTGGGATGAACCAGAAGGA-3'	500bp	3g18780	24
ANAC013	5'-AGCTCGTTGTTTCGGCTAGT-3' 5'-TCAGGAGACCAGAACCATCC-3'	294bp	1g32870	26*
At2g41730	5'-GTCACCAAGGCATCGTAAGG-3' 5'-ACTTGATAGCTGGCGACACG-3'	198bp	2g41730	26*
At3g12830	5'-CTAATCCGTCGTCTCTCTCG-3' 5'-ACTCCTTTTTGCTCGTAACC-3'	278bp	3g12830	30
ATBFRUCT1	5'-CCAGCTATCTTCCCATCTGC-3' 5'-AGGTTCACCAAACGAAGACG-3'	477bp	3g13790	30
CHS	5'-ATCTTTGAGATGGTGTCTGC-3' 5'-CGTCTAGTATGAAGAGAACG-3'	337bp	5g13930	26
DNAJ	5'-TCGTCGGAGAGTTTCTAGCC-3' 5'-AAGCGTCGAGTCGTAAATCG-3'	205bp	3g13310	26*
ELIP1	5'-GTAGCTTCCCTAACCTCAAG-3' 5'-GAATCCAACCATCGCTAAAC-3'	239bp	3g22840	24
HY5	5'-AGCATCTGGTTCTCGTTCTG-3' 5'-GCTGCAAGCTCTTTACCATC-3'	404bp	5g11260	28
HSP23.5M	5'-GCGGAAATGAAGAATGGTGT-3' 5'-AAGTCAAAATCCCGAACACA-3'	219bp	5g51440	26
GSTU28	5'-ACGAGACGTGGACTGATGCT-3' 5'-CGAGTGCGTAGAACCAACTGT-3'	285bp	1g53680	26
MATE4g	5'-CATGAATATCAACGGCTTGG-3' 5'-CAGCCACACCAGAAACAACC-3'	305bp	4g25640	28
MYB4	5'-TGGAACACGCATATACGAAG-3' 5'-GGAAGACTGATTCTGAGCTC-3'	299bp	5g26660	28
RPK	5'-ACAATGCGTTTCTCTTCCACA-3' 5'-GCGAGTTGAATGTTGATGGAT-3'	396bp	3g22060	26
UVR3	5'-ACCTGGCGAAGTACTAGTTC-3' 5'-CTCAAGAGATGGTACTTCTG-3'	340bp	3g15620	32
WRKY	5'-TGCACACCAGTTTGGATCAG-3' 5'-CAGCGTTCTATCAACACCAG-3'	256bp	5g24110	26

* For these primer sets, an annealing temperature of 57 °C was used instead of 55 °C to ensure that clear sharp bands were seen on an agarose gel.

Table 2.2 Oligonucleotide primers used in Q-PCR experiments.

Name	Sequence of Primer Pair	Amplified Fragment size	Origin
ACTIN2	5'-ACTAAAACGCAAAACGAAAGCGGTT-3' 5'-CTAAGCTCTCAAGATCAAAGGCTTA-3'	211	Love *et al.* 2005
CHS	5'-CTACTTCCGCATCACCAACA-3' 5'-TTAGGGACTTCGACCACCAC-3'	195	Designed using Primer3
ELIP1	5'-GTGAGATGCATGGCTGAGG-3' 5'-ACGAATCCAACCATCGCTAA-3'	203	Designed using Primer3
HY5	5'-GGCTGAAGAGGTTGTTGAGG-3' 5'-CAGCATTAGAACCACCACCA-3'	222	Designed using Primer3
WRKY	5'-TCCGATCAAGAACCACTTGTC-3' 5'-TGGCTTCACATCCTTGAGACT-3'	211	Designed using Primer3
FAH1	5'-ATGATGGGGATGTTGTCGAT-3' 5'-ACTCCGTTAAGGCCCACTCT-3'	201	Designed using Primer3
PHYB	5'-AGCAAATGGCTGATGGATTC-3' 5'-CCGTTCTGATTCTCGGATGT-3'	200	Designed using Primer3
SPA1	5'-GCCCTTGGTGTTCTTCTGTT-3' 5'-CTGAATCATCCTCGCATATCA-3'	223	Designed using Primer3
ANAC13	5'-AAGAAAGATCCGTCGGAAAAA-3' 5'-CCAATAGCCACGTTCAGTAGC-3'	187	Kasajima et al. 2007
2g41730	5'-GTCACCAAGGCATCGTAAGG-3' 5'-TCCGGTGGTATTTGAATGGT-3'	146	Kasajima et al. 2007

Table 2.3 Oligonucleotide primers used to generate UVR8 N-terminal deletion constructs

Construct	Primer sequence	Tm
UVR8PRO:NES-GFP-Δ12NUVR8	5'-TAGAATTCCCTCCTCGTAAGGTTCTTATC-3'	62
UVR8PRO:NES-GFP-Δ20NUVR8	5'-TAGAATTCTCCGCTGGTGCTAGCCACT-3'	62
UVR8PRO:NES-GFP-Δ33NUVR8	5'-TAGAATTCGACATTGTTTGTTCTTGGGGTC-3'	64
C-terminal	5'-TAGTCGACTCAAATTCGTACACGCTTGACA-3'	62

Table 2.4 Oligonucleotide primers used to generate UVR8 N-terminal constructs

Construct	Primer sequence	Tm
N-terminal	5'-AAAAGCTTATGCTTCAGAACGA-3'	60
UVR8PRO:NES-GFP-+12NUVR8	5'-TAGTCGACAGCCGTAACTTCGTCGGCA-3'	60
UVR8PRO:NES-GFP-+20NUVR8	5'-TAGTCGACGATGATAAGAACCTTACGAGG-3'	60
UVR8PRO:NES-GFP-+32NUVR8	5'-TAGTCGACAGAGAGAAGAGCGACGGAG-3'	60

.

CHAPTER 3 UVR8-INDEPENDENT SIGNALLING IN *ARABIDOPSIS*

3.1 Introduction

Previous experiments have demonstrated the vital role that UVR8 plays in UV-B response pathways in *Arabidopsis*; the *uvr8* mutant is unable to survive in sunlight (Brown *et al.* 2005). This however does not exclude the possibility that other important response pathways exist that act independently of this protein and its associated pathway. Indeed prior microarray studies performed by Brown and co-workers (2005) showed that a large number of genes, many of which appear to be UVR8 independent, exhibit a significant increase in expression under ambient levels of UV-B. The UVR8 pathway functions at low fluence rates of UV-B and is the only UV-B-specific response pathway identified to date. It is currently unknown whether additional low fluence UV-B specific pathways exist. Therefore the purpose of this study was to determine if such UVR8-independent UV-B specific pathways do indeed exist and if so, to further characterise them. To achieve this end, two main approaches were used. Firstly microarray analyses were employed to define more clearly a list of candidate genes. Subsequently, the expression of these genes was assessed in a number of mutant backgrounds using both RT-PCR and qPCR methods. The findings of this chapter demonstrate that a small number of genes exist which are induced under low fluence rates of UV-B, mostly in a manner that is independent of UVR8 as well as HY5/HYH, COP1 and known photoreceptors. Furthermore, these genes do not appear to be induced by DNA damage, are induced at very low fluences and show evidence of unique expression profiles.

3.2 Results

3.2.1 Very low fluences of UV-B induce expression of many genes

A previous microarray study performed by Brown and co-workers (2005) illustrated that a large number of genes in *Arabidopsis* are induced after illumination with UV-B (639 genes at a false discovery rate (FDR) of 5 %). Of these 639 genes, the expression of only 72 were lost in the *uvr8* mutant leaving 567 genes that are regulated by unknown mechanisms under UV-B. Hence, it seems that many other UV-B response pathways must exist. However, when looking at these results, we must take into consideration the fact that treatments were performed at a comparatively high fluence rate of 3 μmol m^{-2} s^{-1}. This

level of UV-B radiation has since been shown to trigger induction of several non-specific stress-related genes (Brown and Jenkins 2008). It may thus be supposed that a significant portion of these 567 UVR8-independent genes are induced as part of a generalised stress response and not specifically in response to the UV-B stimulus. Consequently, in order to identify only those genes that are UV-B specific, two further microarrays were performed using methods as described by Brown *et al.* (2005) at lower fluence rates of 0.3 and 1 µmol m^{-2} s^{-1} UV-B. *Arabidopsis* plants were grown for three weeks under a low fluence rate of continuous white light (LWL, 20 µmol m^{-2} s^{-1}) before treatment with four hours of UV-B at the fluence rates stated above. Control plants were taken directly from the growth rooms with LWL conditions. Leaf tissue was harvested post-treatment, RNA extracted from three independent sets of plants and submitted for microarray analysis. Lists of induced genes were compared using software available at http://mcbc.usm.edu/genevenn/genevenn.htm. Dependence on UVR8/HY5 was determined using the previous results (utilising *uvr8* and *hy5* mutants) obtained by Brown *et al.* (2005). Venn diagrams depicting the level of overlap between microarrays are shown Figure 3.1.

It was expected that treatment with low fluence rates of UV-B would induce fewer genes than higher fluence rates because, arguably, fewer stress induced genes should be expressed. However, contrary to expectations, the total number of genes that were induced by these treatments was not reduced compared with the previously performed microarray. 572 and 549 genes were up-regulated at a FDR of 5 % for 0.3 and 1 µmol m^{-2} s^{-1} microarrays respectively. Similar relationships (in terms of total number of genes induced) also held true when increasingly stringent FDRs of 2 % and 1 % were applied.

When considering the lists of genes produced from each microarray, it can be seen that a good degree of overlap exists (see Figure 3.1). As might be expected, 3 and 1 µmol m^{-2} s^{-1} and 1 and 0.3 µmol m^{-2} s^{-1} show greater degrees of overlap with each other than do 0.3 and 3 µmol m^{-2} s^{-1}. Nevertheless, a proportion of these genes (between 9.2 and 53.3 % of the total number induced) do seem to be specific to each fluence rate experiment, thereby suggesting a reasonable amount of "noise" may exist in the data.

Turning now to the UVR8/HY5 pathway, the results shown here are similar to those found in the earlier Brown study. For example, previously only 72 genes out of the total 639 could be attributed to the UVR8-regulated pathway. In the case of two lower fluence rate microarrays, the majority of these were also detected (64 and 61 for 0.3 and 1 µmol m^{-2} s^{-1} respectively). Similarly, approximately half the UVR8-dependent genes were those that have been shown to be regulated by HY5 alone (it is likely that the remaining half are regulated in a HY5/HYH redundant mechanism although this has yet to be

thoroughly tested). Interestingly, when looking at increased stringency (i.e. a FDR of 1 % compared to 5 %), UVR8-regulated genes show a greater representation at lower fluence rates than at 3 μmol m^{-2} s^{-1}. For example, when a more stringent cut-off point of 1 % FDR is selected, the two lower fluence treatments still retain most of the UVR8-dependent genes (49 and 55 genes for 0.3 and 1 μmol m^{-2} s^{-1} respectively). For the higher fluence treatment however, the number drops from 72 genes for 5 % to only 15 for 1 %.

It would therefore appear that a large number of genes are indeed induced specifically under the conditions tested here and that "stress" genes may have only accounted for a small proportion of those up-regulated in the Brown study. Furthermore, the fact that UVR8-regulated genes only account for a small proportion of the total up-regulated genes even at low fluences of UV-B suggests that at least one UVR8-independent UV-B specific signalling pathway exists.

3.2.2 Gene expression changes at a FDR of 5 % cannot be detected using qPCR

As it was planned to follow up interesting genes from the microarray results using PCR techniques, an appropriate significance cut-off point for selection of these genes was required. In several previous studies, a significance cut-off of 5 % was used (Ulm *et al.* 2004; Brown *et al.* 2005; Oravecz *et al.* 2006). Therefore to determine if this is indeed a relevant choice, expression of well-known genes that appeared around this mark across all three microarrays was assessed (see Figure 3.2 A). This includes genes encoding phytochrome B, SPA1 (a phytochrome interacting protein) and FAH1 (an enzyme involved in the synthesis of flavonoids). Primers for these genes were designed and qPCR used to assess transcript levels in the same RNA samples that were submitted for microarray analysis.

Of the three genes tested, none showed a strong increase in expression when exposed to either fluence rate of UV-B (see Figure 3.2 B). Consequently it seems that either our methods were not sensitive enough to detect the same changes that are apparent in the microarray data for this level of expression change or that a 5 % FDR cut-off is insufficiently stringent to identify true differentially expressed genes.

It was therefore decided that a more stringent FDR might be more appropriate. Accordingly, the microarray gene lists were searched for well-known UV-B induced genes. Two such examples included those that encode phenylalanine ammonia-lyase (PAL1) and cinnamate 4-hydroxylase (C4H), enzymes involved in the biosynthesis of flavonoids which absorb UV-B radiation and prevent its transmission to lower tissues. It has been previously demonstrated using either RT-PCR or mRNA hybridization methods

that their transcript levels are increased in response to a UV-B stimulus (Li *et al.* 1993; Long and Jenkins 1998; Jin *et al.* 2000). The FDR values of these genes were then determined from the microarray data. In the case of the two lower frequency microarrays, these genes appeared with FDRs between 1 and 2 % (PAL: 1.26 % for 0.3 μmol m^{-2} s^{-1}, 1.08 % for 1 μmol m^{-2} s^{-1}. C4H: 1.79 % 0.3 μmol m^{-2} s^{-1}, 1.17 % μmol m^{-2} s^{-1}). We were therefore confident that we would be able to detect transcriptional changes of other un-tested genes of similar FDRs using RT-PCR also. This was indeed found to be true when such genes were later tested (see Figure 3.8). Therefore, for future analysis, only genes that appeared with a FDR of 2 % or less were considered.

3.2.3 A 2 % FDR cut-off point produces a list of 74 genes common to all three fluence rates

A comparison between all three microarrays led to the conclusion that those genes that appeared at a FDR of 2 % or less and were common to all three microarrays would yield the most interesting results. This conferred a list of 74 genes with an apparently wide variety of functions. Of these, 23 are known to be regulated by UVR8 (half of which i.e. 11 are also dependent on functional HY5). Thus the remaining 51 genes are apparently up-regulated specifically in response to UV-B acting in as yet unknown pathways. These genes were subsequently grouped by presumed function using the TAIR web resource (www.arabidopsis.org). The final list is shown in Figure 3.4.

There are a number of genes with potentially interesting functions included in this list. For example the NAC transcription factor (from Petunia NAM and *Arabidopsis* ATAF1, ATAF2, and CUC2) ANAC13 (*Arabidopsis* NAC domain containing protein 13) was recently shown to be up-regulated by UV-B stimuli and contains a novel UV-B responsive element in its promoter (Safrany *et al.* 2008). A second transcription factor belongs to the plant specific WRKY superfamily (named after the first four amino acids in its sequence). Other members of this family have been shown to have roles in responses to both biotic and abiotic stimuli (Eulgem *et al.* 2000). Similarly to the WRKYs, heat shock proteins (HSPs) have also been shown to increase in expression under environmental stimuli and one member, HSP23.5M, is represented here (Feder and Hofmann 1999).

Unsurprisingly, several genes are associated with metabolic changes similarly to UVR8-regulated genes. For example, there are a number of enzymes including members of the UDP-glucosyl transferase family, one of which (3g21560) has been previously shown to have a role in flavonoid biosynthesis and be upregulated in response to UV-B

(Meißner *et al.* 2008). While the exact functions of other UDP-glucosyl transferases have yet to be fully elucidated, their roles could also be essential to the UV-B response.

The expression of several of these potentially interesting genes as well as several others (highlighted in red in Figure 3.4) is examined in Section 3.2.6 onwards.

3.2.4 UV-B Down-regulated genes

Identification of up-regulated genes can lead to new insights into the responses of plants to various stimuli. This however is only part of the story. While some genes are induced and some remain unchanged, a whole suit of others may be down-regulated. When considering potentially stressful conditions, it is logical that some cellular reactions etc. are turned off until such time as the 'danger' has passed or has been ameliorated. Consequently, in addition to the list of the up-regulated genes, the microarray study performed using low fluence rates of UV-B (as described in Section 3.2.1) also generated a list of genes that are down-regulated in response to these conditions. As before these were compared with those results obtained from the 3 μmol m^{-2} s^{-1} microarray to assess the level of overlap as can be seen in the Venn diagrams of Figure 3.4 A.

In Figure 3.4 B it can be seen that fewer genes are down-regulated in response to UV-B than are up-regulated although the difference is not great. In addition the total number of genes down-regulated at each cut-off point remains fairly constant across the three fluence rates, similar to the situation for up-regulated genes. Therefore changing the fluence rate does not have an apparent effect on the number of genes down-regulated.

As with the up-regulated gene lists, a list was generated which included all genes that are down-regulated at a FDR of 2 % or less across all three studies. Potential functions were assigned and the resulting list is shown in Figure 3.4 B. Again the genes show a wide variety of functions. Interestingly however, unlike those up-regulated by UV-B several of these have potential roles in cell wall architecture, cell structure and plant growth. For example the list includes genes that are responsive to hormones (auxin-responsive (2g21210) and gibberellin-responsive (1g74670)), microtubule organisation (kinesin motor protein-related (3g50240)), cell wall components ((xyloglucan endotransglucosylase/hydrolase (4g37800) and arabinogalactan protein (1g55330)), enzymes with potential roles in lipid metabolism/catabolism (fatty acid elongase, putative (2g15090) and GDSL-motif lipase/hydrolase family protein (1g29660)), an enzyme involved in cutin biosynthesis and protochlorophyllide oxidoreductase A (PORA) which is involved in chlorophyll biosynthesis (5g54190).

It has previously been shown that plants alter their morphology in response to UV-

B such as the inhibition in hypocotyl (Favory *et al.* 2009) and so it would seem that genes associated with changes in plant architecture would show changes in expression levels. Although the functions and regulation of these down-regulated genes will not be pursued in this study, it is important to remember that environmental responses involve both the promotion and inhibition of some processes.

3.2.5 Analysis of microarray data from other UV-B studies

Microarrays and the study of transcriptome changes are extremely useful tools in the analysis of responses to a number of stressful and informational stimuli in a multitude of organisms. It is therefore unsurprising that several studies have used these methods to examine UV-B responses in plants. The results of these contain a wealth of information and have each produced lists of potentially interesting genes. However, no recent analyses have been performed which compare the data from these studies. As a result, it was decided to do just this and conduct a general comparison of the up-regulated gene lists generated by various microarray experiments performed using material from UV-B treated Arabidopsis. Published gene lists from Ulm *et al.* (2004), Oravecz *et al.* (2008), Kilian *et al.* (2007), Hectors *et al.* (2007) and Brown *et al.* (2005) were obtained and input into the FileMaker database program. This allowed a spread sheet to be generated which displayed the number of times a gene was found across all datasets. Finally, as a variety of microarrays under different conditions were used in each study, the data was collated for each study. From this the number of times a gene appeared in at least one of the microarrays (i.e. the "count") within a study could be determined. The top scoring genes are shown in Figure 3.5.

Intriguingly, no one gene appeared in all microarray studies and only seven genes were common to five out of the six studies thus suggesting that UV-B responses might not be as conserved as we might expect. It should be noted that this lack in universally induced genes is not due to the effect of one particular study. The absence of expression of genes seems to be relatively evenly spread across all studies and therefore not due to one study skewing the results. Nevertheless, these top scoring seven genes do include many that have previously been shown to have major roles in UV-B responses. For example, both ELIP genes are included as well as *SigE*, all of which are UVR8-dependent genes. The remaining four genes however, a transducin family protein / WD-40 repeat family protein (5g52250), a UDP-glucoronosyl/UDP-glucosyl transferase family protein (4g15480), a GCN5-related N-acetyltransferase family protein (2g32020) and a receptor protein kinase-like (3g22060), have no defined role as yet in UV-B responses. The

expression of the last of these will be covered in following sections. However as the final three of these genes are strongly shared across microarray studies (and are only absent for the Hectors *et al.* 2007 study) this flags them as potentially interesting candidates for future studies.

Knowing the vital role that *HY5* has in UV-B responses and its apparent strong up-regulation shown in this study, it is perhaps surprising that it is not universally up-regulated in UV-B microarrays. Nevertheless, it does appear in two thirds of the studies along with two other transcription factors, *ANAC13* and *3g01970* (from the WRKY superfamily).

One final gene, 2g41730 is notable due to its extremely strong up-regulation in response to UV-B shown in this study (for fold change data see Appendix 1) and that performed by Brown *et al.* (2005). However, besides these microarrays, induction of this gene was only seen in one of the four other studies. Therefore if this unknown protein does have a role in UV-B responses, it may be highly specific to the treatment conditions.

The vast majority of genes (2802 out of a total of 3517) were unique to each study. This low degree of overlap is most likely a reflection of the wide range of conditions used; ecotype, plant ages, tissues, fluence rates, and wavelengths all differed across these experiments. Hence, this demonstrates the need for careful consideration of the treatment conditions used when undertaking such a study. These results could suggest that UV-B responses may be modified highly dependent on such factors such as those listed above. Alternatively, it may be that there is a large amount of noise inherent in the data. Indeed, by looking at the sheer number of genes that are counted as UV-B up-regulated across these studies, 3517 total, it would be surprising to find such a vast variety in responses to this one stressor.

Thus in conclusion, while a few interesting candidate genes can be identified using this approach, comparisons across studies are firstly limited due the variation in experimental methods and also due to the additive error which can potentially cloud the underlying pathways.

3.2.6 Expression profiles of UV-B specific genes

One technique that can be employed to elucidate regulatory pathways is to look for gene co-expression patterns. It was therefore decided to examine the expression of several UV-B induced genes in plants exposed to differing durations of UV-B radiation treatment. Accordingly it could then be seen whether genes regulated by the same transcription

factors had similar expression profiles, if these differed from the expression profiles of the transcription factors themselves and so forth.

It has been previously shown that *CHS* and *ELIP1* are both regulated by HY5 (Brown *et al.* 2005). Therefore the expression of these three genes, along with *WRKY30* (a gene that seems to be involved in stress pathways (Brown and Jenkins 2008)), were examined first. Three week old white light grown plants were treated with 3 μmol m^{-2} s^{-1} UV-B for times ranging between 0 hrs (white light control) and 15 hours. Gene expression was analysed using qPCR and normalised against *ACT2* transcript levels. Plots of gene expression are shown in Figure 3.6A.

As expected, expression of *HY5* showed an earlier increase than any of the other genes tested. Furthermore, this increase was very rapid, reaching 40 % of its maximum in only 30 minutes, and nearly 100 % in an hour. After this initial rapid peak, expression dropped swiftly and plataued at approximately 60 % from 6 hours onwards.

Again, as one might expect, those genes that are known to be regulated by the same factors, namely *CHS* and *ELIP1* (by both HY5 and UVR8), show remarkably similar expression profiles. Both show a slow (in comparison to *HY5*) increase in expression before reaching a peak at around 4 hours. This is followed by a slow reduction to about 60 % of maximal induction. Nevertheless, the two gene profiles are not identical; *ELIP1* seems to exhibit a second increase in expression at the tail end of the expression profile.

Transcripts of the transcription factor *WRKY30* initially accumulate and peak similarly to both *CHS* and *ELIP1*, but then shows a dramatic, rapid decrease in expression. Finally, after 12 hours expression appears to plateau at a much lower level of around 20 % of maximum.

Two UVR8 independent UV-B up-regulated genes listed in Figure 3.2 were also tested over a timecourse to determine if they followed any patterns similar to the other genes examined in Figure 3.6A. Results of these timecourses are shown in Figure 3.6B. ANAC13, like HY5 and WRKY30, is a transcription factor. However unlike *HY5*, *ANAC13* does not show an initial rapid increase in expression, instead exhibiting a more gradual one akin to that of *CHS* and *ELIP1*. Furthermore this increase remains relatively slow, with a peak in expression not being reached until approximately 9-12 hours.

Finally At2g41730, a protein of unknown function, was also chosen for analysis as it shows very large increases in expression under UV-B (fold change values of 17.08, 119.77 and 318.97 for 0.3, 1 and 3 μmol m^{-2} s^{-1} respectively). No information currently exists concerning the function of this protein nor does it have any recognisable domains.

Therefore it is of interest to see where its profile fits in compared to other UV-B induced genes. Results are shown in Figure 3.6C.

2g41730 again shows an initial increase in expression similar to that of *CHS* and *ELIP1*, but does not peak until the later point of 6 hours. Its expression then decreases to roughly 50 % although this decrease is not as rapid as that seen for *WRKY30*.

The results here demonstrate that UV-B induced genes show very similar initial increases in expression with the exception of *HY5*. After the first couple of hours the expression profiles of genes regulated by different factors appear to be quite divergent, while for those that share regulatory factors, profiles remain comparable. Therefore it seems possible that this type of analysis could be used to help untangle the regulatory pathways induced by UV-B exposure.

3.2.7 RT-PCR and qPCR timecourses give similar results.

The same samples used in qPCR expression analysis were also examined using semi-quantitative RT-PCR to assess the similarity between these methods. In the case of RT-PCR, values for gene expression were obtained by measuring the intensity of bands run on an ethidium bromide containing gel using Gel Doc software. As for qPCR, values for the genes of interest were normalised against those for *ACT2* bands. This was performed for three samples and plotted on the same graph as the data for relevant qPCR experiments. The results of these are shown in Figure 3.7.

For all four of the genes tested, there was a reasonable degree of overlap between the two methods. While the RT-PCR data are not truly quantitative, it seems that under these conditions they are representative. Therefore, as RT-PCR seemed representative and at the very least showed similar differences in maximum to basal expression, it was decided that this method would be sufficient to analyse the expression of genes of interest in different backgrounds in future experiments.

3.2.8 UVR8 independent genes that show an increase in expression specifically under low fluences of UV-B exist

In addition to the previously mentioned genes, ANAC13 and 2g41730, several other genes that fell into the UVR8-independent UV-B induced category were selected for further investigation. Both HSP23.5M (At5g51440) and a DnaJ protein (At3g13310) were chosen as they potentially act as molecular chaperones during stressful conditions where protein folding may be affected. The list also included a gene for a receptor protein kinase like

protein (RPK-L At3g22060), which is a candidate for signalling component as it contains a domain (DUF26) found in serine/threonine protein kinases. This RPK-L gene also showed up-regulation in five out of the six microarray studies compared in Figure 3.4. Finally a Multi Antimicrobial Extrusion (MATE, At4g25640) protein that functions as an antiporter was also selected.

In previous experiments performed by the Jenkins group, low fluence rate white light conditions (in which the plants were grown) were used as a control (Brown *et al.* 2005; Kaiserli and Jenkins 2007; Cloix and Jenkins 2008). That is, one control plant was left in these conditions while the others were transferred to a separate treatment room fitted with UV-B bulbs. In addition, UV-B treatments were normally conducted using these UV-B emitting tubes alone, without supplementary white light (the UV-B tubes themselves give off very little PAR). As a consequence, to ensure these experimental conditions were appropriate, a number of different light combinations were tested on wild type and *uvr8-1* plants to determine whether changing light conditions had an effect on expression patterns. Samples were obtained from plants taken directly from the white light growth conditions as well as after the standard 4 hour 1 μmol m^{-2} s^{-1} UV-B treatment. In addition to the above, plants were placed under UV-B lamps with supplementary white light, under tubes covered with a filter to remove UV-B wavelengths and finally plants were transferred to the treatment rooms for four hours in the dark. RT-PCRs were then run on these samples to look at the expression levels of the potential UV-B induced, UVR8-independent genes. Representative results are shown in Figure 3.8.

Interestingly, transferral of plants from the white light growth room to the treatment room is sufficient to induce expression of a number of the supposed UV-B induced genes independent of any light treatment. *DnaJ* and the *MATE* gene chosen both are induced under both minus UV-B and dark conditions suggesting that the conditions in the room alone are affecting gene expression. It is also of interest to note that the receptor like kinase mRNA shares this trend in the wild type plant, but appears to follow a more expected pattern (e.g. like that of *CHS* in wild type) in the *uvr8* mutant.

However, *ANAC13*, *2g41730* and *HSP23.5M* all show expression patterns similar to that of *CHS* – it is only where plants have been exposed to UV-B that we see an increase in expression levels. As a result, it would seem that for these genes at least we can be confident that they are both UV-B specific and UVR8-independent.

Consequently, for the purpose of this study, only those genes that were confirmed to be UV-B specific were taken on for further analysis.

3.2.9 UVR8 independent genes are induced by very low fluence rates of UV-B

One of the defining features of the UVR8-dependent pathway has been the fact it operates even under very low fluence rates of UV-B (as low as 0.1 μmol m^{-2} s^{-1}, Brown and Jenkins 2008). Furthermore, in the Brown study, genes that were identified as UVR8-independent did not show induction at fluence rates below 1 μmol m^{-2} s^{-1}. Therefore to demonstrate that low fluence UV-B pathways that act independently of UVR8 do indeed exist, the expression of *ANAC13, At2g41730, HSP23.5M* and *RPK-L* were analysed. RT-PCR results are shown in Figure 3.10.

For all genes tested, it seems that they are induced at sufficient levels under low fluence rates of UV-B to be detectable using RT-PCR. For most cases, the results are comparable with results for *CHS*. *HSP23.5M* is the exception to this, it seems to be expressed from 0.2 μmol m^{-2} s^{-1} onwards.

3.2.10 Induction of UVR8-independent genes mostly occurs independently of HY5 and HYH

UVR8, HY5 and HYH all seem to have an important and intimately connected role within the same UV-B responsive pathway; half the genes regulated by UVR8 are also regulated by HY5 alone and the remaining half seemingly via a HY5/HYH redundant mechanism (Brown and Jenkins 2008). We cannot however exclude the possibility that individual components such as HY5 and HYH have roles in other pathways. Section 3.2.9 demonstrates that ANAC13 and other genes act independently from UVR8 but they may still require HY5 and/or HYH.

Therefore, expression of these genes was tested in single mutants as well as the *hy5 hyh* double mutant. In almost all cases, induction under UV-B is retained in the mutants. The exception to this is again HSP23.5M which seems to have slightly reduced expression in the *hy5 hyh* double mutant relative to wild type and single mutants.

It is also interesting to note that while expression of these genes has been shown for low fluences (see Section 3.2.9), there is a greater difference in expression of these genes between 0.3 and 1 μmol m^{-2} s^{-1} than seen for *CHS*. That is, bands at 0.3 μmol m^{-2} s^{-1} are less evident when viewed next to 1 μmol m^{-2} s^{-1}.

In summary, it seems that we can rule out the involvement of either HY5 or HYH in the UV-B induction of *ANAC13* ad *At2g41730*.

3.2.11 Induction of UVR8 independent genes mostly occurs independently of COP1

CONSTITUTIVELY PHOTOMORPHOGENIC 1 (COP1), a protein involved in the negative regulation of photomorphogenesis, has also been shown to have a positive role in UV-B signalling (Oravecz *et al.* 2006). In contrast to conditions under white light alone, COP1 under UV-B acts as a positive regulator of *HY5* and hence UV-B signalling and acts with UVR8 (Favory *et al.* 2009). Consequently, the same set of genes was tested in the *cop1-4* mutant to determine if expression is retained, reduced or lost.

As can be seen in Figure 3.11, *ANAC13*, *2g41730*, and *RPK-L* all do retain expression in the *cop 1-4* mutant. *HSP23.5M* however, does not. Thus it seems this latter gene may be tied into a pathway involving COP1, HY5 and HYH. As, to date, COP1, HY5 and HYH are the only know regulatory components in the UVR8 pathway, it can be concluded that the expression of at least two genes exist entirely outside of this pathway.

3.2.12 Induction of UVR8 independent genes is not dependent on known photoreceptors

While the photoreceptors responsible for the perception of red/far red and blue/UV-A wavelengths have been well defined, the hypothesised UV-B photoreceptor remains elusive. There have been numerous theories on how the UV-B signal is perceived, none of which have been proven. One such theory is that there is no UV-B specific photoreceptor and that the plant detects UV-B via known photoreceptors. This has been disproved in the case UVR8-dependent genes (Brown and Jenkins 2007), however it cannot yet be excluded for those UVR8-independent genes. As a result, it was decided to examine the expression of *ANAC13*, *HSP23.5M*, *2g41730* and *RPK-L* in mutants that lack some of the major classes of photoreceptors. These mutants included *cry1 cry2* which lacks both cryptochromes, *phot1 phot2* which lacks both phototropins, *phyA phyB* which is deficient in the main two phytochromes, and finally *hy1-100* which is unable to make the chromophore that is incorporated in the phytochrome photoreceptor (it should be noted that *hy1-100* is somewhat "leaky").

Similarly to previous experiments, expression of the genes was analysed using RT-PCR, the results of which can be seen in Figure 3.13. All genes tested retain normal induction in response to UV-B in all mutants. Therefore it would seem that the majority of UV-B responses are not triggered via known photoreceptors.

3.2.13 Role of DNA damage in expression of *2g41730* and *ANAC13*

It has also been suggested that a single protein/family of proteins may not be responsible for UV-B perception but that instead other macromolecules may absorb UV-B radiation and pass on the signal. DNA for example shows a strong absorption at around 280 nm, as do many proteins. Such absorption of UV-B may result in DNA damage in the form of pyrimidine (6-4) pyrimidone photoproducts (6-4 PP) and cyclobutane pyrimidine dimers (CPDs). It has thus been suggested that such damage is the primary signal which initiates UV-B signalling cascades. To test this possibility it was therefore decided to assess transcript levels of both *ANAC13* and *2g41730* in mutants that are deficient in DNA repair mechanisms and as a result accumulate more dimers after UV-B exposure. The *uvr2* mutant is deficient in the photolyase that repairs CPDs and thus is incapable of repairing the predominate form of UV-B induced DNA damage. Although 6-4PP dimers form a lower percentage of the dimers induced by UV-B, the *uvr1 uvr3* mutant which is deficient in the repair of these in both light and dark conditions was also tested (Nakajima *et al.* 1998). As it is possible that under these conditions we would see an increase in expression (unlike in previous mutant analyses described here where a reduction or loss of expression was expected), qPCR was used to give quantitative results.

Mutant and wild type plants were grown in 20 μmol m^{-2} s^{-1} white light and were either immediately sampled, treated with UV-B alone, UV-B plus white light or left in the dark. A UV-B plus supplemental white light treatment was included as both photolyases require light (specifically blue/UV-A) to repair UV-B induced lesions.

No genes that show a direct induction in response to this form of DNA damage have yet been described in Arabidopsis. However, in *Phaseolus vulgaris* an increase in expression of the gene encoding the β-1,3-glucanase enzyme was found (Kucera *et al.* 2003). Consequently the equivalent of this enzyme in *Arabidopsis* was found using KEGG (EC 3.2.1.39) and the TAIR websites. Primers were designed for this gene, known as BETA-1,3-GLUCANASE 2 (BGL2), and also tested under the same conditions to see if an increase in expression in mutants relative to wild type plants was found. This would thus act as a positive control for the experiment.

The results in Figure 3.13 show that for *ANAC13* and *2g41730*, mutants and wild type have similar levels of expression under all conditions tested. There may be a slight increase in the *uvr2* mutant under LWL + UV-B conditions as opposed to LWL alone, however the difference is not particularly striking.

CHS, as expected, had higher levels under LWL + UV-B compared to UB alone, but levels between mutants and Wt were roughly equivalent. Interestingly, there seems to

be a greater variability in expression levels when LWL is introduced into the treatment conditions.

For *BGL2*, levels appear to be reduced in *uvr2* when light is absent, contrary to predictions. The levels in wild type and *uvr1 uvr3* seem roughly equivalent and even across all treatment conditions. Therefore either the conditions tested here did not produce sufficient DNA damage to induce expression of *BGL2* or alternatively, *BGL2* in *Arabidopsis* is not induced in response to this stimulus.

Therefore it seems likely that DNA damage repair is not responsible for ANAC13 and 2g41730 expression under UV-B. However, as this experiment lacks a positive control further tests would be needed to provide additional supporting evidence.

3.3 Discussion

The aim of this chapter was to investigate transcriptional changes that occur under UV-B radiation in Arabidopsis. The results of the experiments show that many genes are induced under even very low fluences of UV-B. However, it is yet unclear just what proportion of these genes might have arisen as false positives. Nevertheless, several genes are induced under UV-B and are seemingly not under the regulation of any previously known or hypothesised UV-B response and perception components.

3.3.1 Expression of genes in response to a UV-B treatment

Numerous studies have used gene expression to examine the effects of UV-B exposure on plants such as *Arabidopsis* (Christie and Jenkins 1996; Ulm *et al.* 2004; Brown *et al.* 2005). Indeed the original studies which identified the *uvr8-1* mutant identified that one feature of the mutant's inability to respond effectively to UV-B was its lack of *CHS* expression. Brown *et al.* (2005) furthered this work to show that loss in *CHS* expression is only specific to the UV-B stimulus while induction due to cold etc is retained. While these studies demonstrated the vital role that UVR8 plays in UV-B mediated responses, it does not limit all UV-B responses to the control of UVR8. One of the primary purposes of this study was therefore to determine whether such UVR8-independent responses existed and if so, to identify some of the components.

One piece of evidence which hinted at the possibility of other UV-B responsive components was the existence of a large number of genes that showed a significant increase in expression under UV-B even in the *uvr8-1* mutant. This situation however was complicated by the ambiguous treatment conditions of 3 μmol m^{-2} s^{-1} UV-B which had the

potential to act as a stressor to the plant rather than purely a mild stimulus. Additional microarray studies at lower fluence rates were therefore initiated to address this question. These also showed large numbers of induced genes thus indicating that general stress response pathways could not explain all of the changes in gene expression observed. However, further work using RT-PCR to examine the response of several selected genes (hypothesised to be UVR8-independent, low fluence rate induced) showed that transferral of plants to the treatment chambers without a UV-B source resulted in the up-regulation of a proportion of the genes tested. Three conclusions can be drawn from this part of the study. Firstly, the often-used control treatment of using plants taken directly from the growth conditions is not the optimal choice. While it seems sufficient for those UV-B responsive genes that have been well studied such as *HY5* and *CHS*, investigation into potential new candidate genes requires a stricter approach. Here a true mock treatment should be used whereby control plants are transferred to the treatment chamber where the UV-B emitting fluorescent tubes have been covered in a mylar filter. This cuts out all the radiation in the UV-B portion of the electromagnetic spectrum while leaving all other conditions constant.

This leads into the second conclusion from this study, namely that there is some factor present in the treatment chambers (and presumably absent within the growth chambers) that can give rise to significant changes in gene expression. This could be due to increased airflow, larger fluctuations in temperature or even the relatively low levels of light available to the plants when only UV-B tubes are present (an average of 4 μmol m^{-2} s^{-1} PAR for a UV-B treatment of 3 μmol m^{-2} s^{-1}, 2 for 1 and 0.8 for 0.3 μmol m^{-2} s^{-1}). Thus, an ideal experimental setup would involve growing the plants in the very same chambers where the UV-B treatment is to take place.

The final conclusion to be drawn is that despite the apparent problems inherent in the current experimental setup, some true low fluence rate UV-B induced, UVR8-independent genes do exist. Therefore other pathways associated with the specific stimulus of UV-B must also exist and have some role in the overall adjustment of the plant to UV-B conditions. The rest of this study therefore worked to further characterise this new class of genes.

3.3.2 Low fluence rate UV-B UVR8-independent gene expression

The existence of such genes having been confirmed, studies using a variety of available mutants was initiated in order to better characterise the low fluence rate UV-B UVR8-independent signalling pathway. Initial work showed that several genes retained

expression specifically in response to UV-B in the *uvr8-1* mutant. However, further work on the UVR8-mediated responses had shown the involvement of the transcription factors HY5 and HYH and also, in a more ambiguous role, COP1. For example, it has been shown that half of all UVR8-regulated genes are also under control of HY5 (Brown *et al.* 2005). Furthermore, it seems that the remaining half may be regulated in a HYH/HY5 redundant fashion (Brown and Jenkins 2008). It therefore seems that all UVR8-mediated responses are funnelled through these two vital transcription factors, indeed *hy5 hyh* mutant plants show an extreme sensitivity to UV-B exposure (Brown and Jenkins 2007). In addition to a role in UV-B responses, HY5 is also a well-known component of other light responses. This wide-ranging role suggests that HY5 may also be able to act in UV-B responses in a way that is independent of UVR8. However, the work presented here largely supports a role for HY5 and HYH under UV-B that is entirely dependent on UVR8. Work by Brown *et al.* (2005) has shown that UVR8 binds to chromatin in the region of the *HY5* promoter. It therefore seems possible that for a role in UV-B responses, the promoter region of *HY5* (and possibly also *HYH*) depends on 'activation' in some as yet cryptic manner by UVR8. As UVR8 is present at the *HY5* promoter prior to UV-B exposure, it seems activation occurs at the level of chromatin. The way in which the transcription of *HY5* is activated by UV-B through UVR8 has, to date, not been resolved. Nevertheless, it seems that we can reject the theory of a UVR8-independent HY5-dependent pathway. Thus, this leaves three major classes of genes that are initiated by UV-B: those stimulated by pathways that are not specific to UV-B (when levels exceed 1-3 μmol m^{-2} s^{-1} UV-B), UVR8/HY5/HYH dependent and UVR8/HY5/HYH independent.

Increasingly, evidence suggests a role for COP1 in UV-B mediated responses. Work by Ulm and co-workers has shown that induction of some genes is lost in the *cop1-4* mutant, that COP1 acts to positively regulate *HY5* expression under UV-B (where as under white light it acts in the opposite manner) and that it seemingly interacts with the UVR8 protein (Oravecz *et al.* 2006; Favory *et al.* 2009). The exact way in which this protein links in with the UVR8/HY5/HYH pathway has not yet been fully elucidated. By testing those UVR8-independent genes, we can determine whether COP1 may have a broad role that covers all UV-B responses and not just those attributable to the partially characterised UVR8 pathway. The results of this study show that at least one gene, *HSP23.5M* may be partially dependent on functional COP1 and HY5/HYH as it shows reduced induction under UV-B in both the *cop1-4* and *hy5 hyh* mutant. However, the methods used here, RT-PCR, are not truly quantitative. Therefore, this should be repeated using qPCR in order to resolve this more clearly. It should be noted, that as no *cop1* null mutants exist (due to

problems with lethality) the mutant allele used, *cop1-4* is somewhat leaky. It is therefore possible that we do not see a complete loss in *HSP23.5M* expression due to the presence of some residual levels of COP1.

It is interesting to note that according to Safrany *et al.* (2008), *ANAC13* expression is partially dependent on *cop1-4*. This does not seem to be particularly clear from their PCR results, however there but is a small difference when you compare relative luminescence of a ProANAC13:LUC construct. This suggests that COP1 may be having a more subtle effect on gene expression that is not readily detectable using RT-PCR methods. Therefore, it again seems that more fine-scale methods need to be employed in order to gain a higher resolution of the pathways and interactions between components that occur upon UV-B exposure.

3.3.3 Selection of candidate genes

Comparisons across both low fluence rate (0.3 and 1 μmol m^{-2} s^{-1}) microarrays as well as with data obtained from Brown *et al.* (2005) produced long lists of UV-B induced genes. Current technology however precludes the characterisation of so many genes simultaneously. Therefore a common approach is to select a number of candidate genes as representatives of the group as a whole. Clearly, in such a large mass of data it could be all too easy to lose any interesting genes amongst the general noise. Thus, in order to maximise the chances of success (i.e. find genes with interesting and relevant expression patterns) a number of filtering approaches were used. Initially, the data sets were compared in order to assess the level of overlap. Any genes that did not appear in common to all three fluence rate treatments were excluded. Subsequently, stricter significance cut-offs were used once it was demonstrated that qPCR methods failed to detect differences in genes that were deemed differentially expressed according to the microarray data. The result of these analyses was a list of 72 candidates, a significant cut-down from the original >500 candidates.

The potential functions of these genes were then determined through use of the TAIR resource. This allowed a final step whereby candidates could be selected on a *priori* knowledge on which may be the more informative. For example, there are apparent holes in our knowledge of the signalling mechanisms by which the UV-B 'message' is transmitted. Thus, investigating one of the transcription factors (ANAC13) and a potential kinase signalling component (RPK-L) may result in the filling-in of such holes.

Selection processes using personal assessment of which may prove most 'interesting' obviously has inherent problems. We might for example be introducing a

huge human bias into the investigation. Nevertheless, initial investigations using these methods can lead to interesting paths, sometimes in opposition to preconceived expectations. Fortunately, technology is fast developing new higher throughput techniques. Where once it took a decade to sequence a genome, it is now possible (albeit at some expense) to do so in a matter of days. Therefore, the ideal situation in which all of the 72 candidate genes (and possibly more) are assessed simultaneously may not be that far in the future.

3.3.4 Separating out gene pathways through timecourse analysis

While several groups have used microarray analysis to gain further insight into the mechanisms of UV-B signalling, from the results described in Section 3.2.4 it seems that there is very little overlap between the resulting gene lists. This reflects the great degree in variability in the ecotypes, tissues, treatment strength and treatment duration used by these groups. Thus, in turn, there may be many different levels, tissue specific, age specific and even ecotype specific responses. This would perhaps seem surprising considering the importance of this abiotic response. With the move from an aqueous environment, which provides sheltering from the more harmful UV-B rays, to a terrestrial one plants necessarily had to develop protective measures. We can therefore infer that the acquisition of UV-B tolerance occurred early in the evolution of land plants. Thus it is somewhat difficult to explain the apparent variety in gene responses across studies. However, this study has already highlighted the importance of selecting appropriate controls. Consequently, this diversity may in fact reflect a diversity in 'false positives' and general noise inherent in each experimental procedure. Despite this apparent problem, at the very least this comparison method should highlight more clearly those genes which are vital in the UV-B response as these are more likely to be those shared across the experiments.

An alternative solution for pulling out the most interesting UV-B responsive genes may involve the use of timecourses. Work in this study showed that there appear to be different classes of expression profile depending on how a gene is regulated. For example the transcription factor *HY5* gene shows a characteristic early peak in expression while *ELIP1* and *CHS* (both regulated by HY5) show very similar profiles to each other. This could therefore act as a basis for separating out genes according to their expression profile. Indeed this method is already used, particularly by groups working on the circadian clock. If samples were taken at a variety of different time points and submitted for analysis by microarray, it may then be possible using one of many available statistical packages to separate out, and group these UV-B responsive genes. This could subsequently be of

invaluable use in untangling the apparent multiple pathways associated with UV-B stimuli. The choice of which time points to use is an important one. Data from the timecourses of *CHS, HY5, ELIP1* and *WRKY* were analysed in order to assess which of these time points may be the most informative and separate out the different profiles. The resulting selections and the equations used to derive them are included in Appendix I.

3.3.5 Down-regulated genes under UV-B

In general, the focus of this chapter has been on those genes that show an up-regulation in response to UV-B. The other side of the coin however is those genes that show a down regulation. As important as it is to initiate protective measures in response to indications of stress, it can be of equal importance to down-regulate processes that might suffer the most under these conditions or put a halt on growth to reallocate resources. In the case of UV-B, it can be seen that altering growth in order to minimise UV-B absorption would be advantageous. Accordingly, the low fluence rate microarrays show an abundance of genes down-regulated with hormone associations as well as apparent functions in growth and development.

3.3.6 Final conclusions and future experiments

In conclusion, work described in this chapter has shown that 1) current treatment conditions can cause the up-regulation of several (possibly many) genes, 2) low fluence rate UV-B UVR8/HY5/HYH-independent genes exist, 3) that a subset of these genes may be dependent on functional COP1 4) timecourse expression profiles could potentially be used as a criterion for separation of genes into groups and 5) many genes which are down-regulated under low fluence UV-B are associated with plant growth/cell structure. While these conclusions may have filled in some of gaps in knowledge concerning plant responses to low fluence UV-B, a great deal of work remains to be done. Some potentially interesting avenues to pursue that have arisen as a result of work presented here are discussed below.

One way in which more useful data could be drawn from the microarray performed would be to submit for analysis one further set of controls. In this case it would be for plants that had been transferred to the treatment chamber where the UV-B tube had been covered in a mylar filter (which cuts out all UV-B wavelengths). This would be the true ‘mock’ treatments and would hopefully allow us to dissect out those genes induced purely in response to factors associated with placement in the treatment chambers. As discussed

above, the ideal situation would still be to repeat the experiments whereby the plants were grown in the treatment conditions from the very beginning. Nevertheless, inclusion of this control should enable elimination of at least some of the false positives seen.

While microarrays and PCR methods have proved extremely useful in the study of this area, with the rise of next generation sequencing methods such as mRNA-Seq sequencing it will soon be possible to amass and analyse much larger datasets (www.illumina.com). By collecting samples at different timepoints we could then analyse the transcriptome under each of these conditions more completely. This may help built a more robust picture of the changes in gene expression that occur. This method also has the advantage that it has a greater power to detect relatively rare transcripts. Some members of the MYB grouping for example have been shown to be involved in UV-B responses. They are however largely undetectable using the ATH chips.

Currently, the lengths of sequences that are read using this method are relatively short (~70 bp at the time of writing), but this number is continuing to increase with further optimisation of reagents and the machinery involved. It will eventually become possible to sequence much longer lengths, thus allowing identification of splice variants and the separation of close homologues.

In summary, analysis of gene expression in one of the primary areas while will benefit from new technologies, higher throughput methods and bioinformatic approaches that are becoming more prevalent. With the proper application of these methods we can hopefully build upon the knowledge gained here and fill some of the gaps both large and small in the network of low fluence UV-B response pathways.

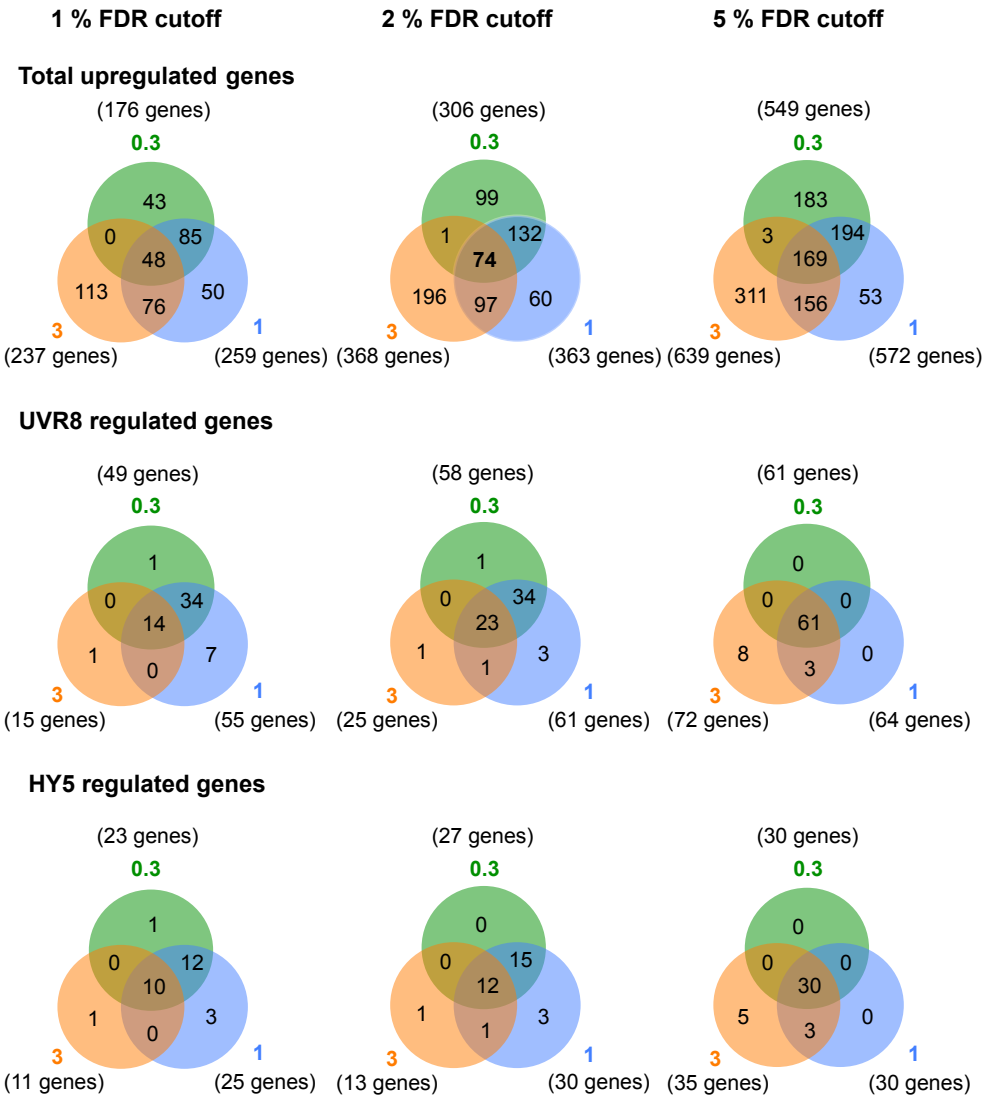

Figure 3.1 Venn diagrams depicting the overlap in gene expression between different fluence rates of UV-B. Three week old Arabidopsis plants grown in a low fluence rate of white light (20 µmol m^{-2} s^{-1}) were treated with either four hours of 0.3, 1 or 3 µmol m^{-2} s^{-1} UV-B or were left in low white light as a control. The numbers of genes which showed an increase in expression level were calculated for each of the three significance cut-off points (False Discovery Rate (FDR)). Gene lists were then compared to those published by Brown *et al.* (2005) to determine overlap and dependence on either UVR8 or HY5. Numbers in orange circle denote those obtained in the Brown *et al.* (2005) 3 µmol m^{-2} s^{-1} UV-B microarray, those in blue and green are those determined in this study to be induced by 1 and 0.3 µmol m^{-2} s^{-1} UV-B respectively.

A

	False Discovery Rate	
	0.3 µmol m^{-2} s^{-1}	1 µmol m^{-2} s^{-1}
SPA1	5.52	2.77
FAH1	4.76	3.9
PHYB	4.31	4.44

B

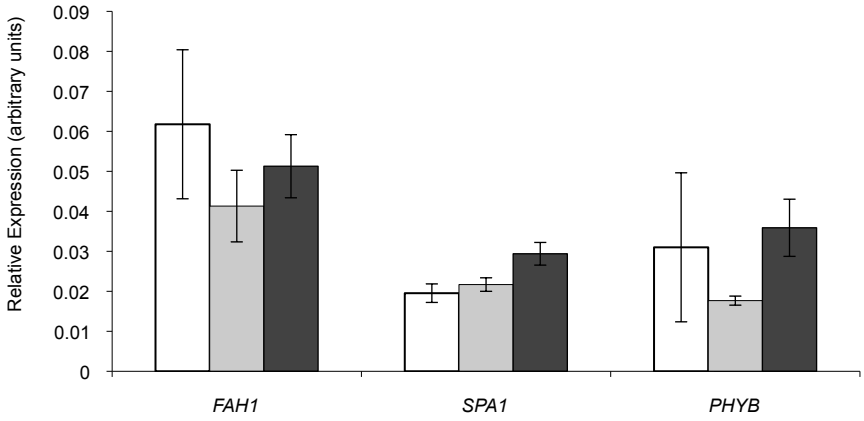

Figure 3.2. **No increase in expression in response to UV-B can be detected for genes that appear at around the 5 % FDR cut-off mark in UV-B microarrays. A** *FAH1*, *SPA1* and *PHYB* were selected for analysis as they all appear at approximately the 5 % FDR cut-off mark in both the 0.3 and 1 µmol m^{-2} s^{-1} UV-B microarrays. **B** qPCR was performed on the same samples as were submitted for microarray analysis. No significant increases in expression in response to UV-B were seen for any of the genes. White bars correspond to minus UV-B conditions, pale grey to 0.3 µmol m^{-2} s^{-1} and dark grey to 1 µmol m^{-2} s^{-1} UV-B. Error bars represent standard error for the three replicates.

UVR8 Regulated gene

		0.3			1		
Metabolism and energy		Rpscore	FDR	Fcrma	RPscore	FDR	Fcrma
At5g13930	chalcone synthase (CHS)	5.99	0	34.81	8.98	0	42.71
At3g51240	naringenin 3-dioxygenase / flavanone 3-hydroxylase (F3H)	6.2	0	32.21	9.1	0	41.91
At1g78600	zinc finger (B-box type) family protein	26.58	0	12.84	25.56	0.05	21.67
At5g56090	cytochrome oxidase assembly family protein	45.69	0	9.8	41.74	0.03	16.26
At4g15480	UDP-glucoronosyl/UDP-glucosyl transferase family protein	34.3	0	11.42	20.55	0.06	25.95
At5g08640	flavonol synthase 1 (FLS1)	58.15	0	8.48	87.36	0.12	10.28
At3g27380	succinate dehydrogenase, iron-sulphur subunit, mitochondrial (SDH2-1)	90.46	0.09	6.8	101.32	0.19	9.47
At5g17050	UDP-glucoronosyl/UDP-glucosyl transferase family protein	95.81	0.11	6.64	118.86	0.19	8.68
Stress							
At3g22840	chlorophyll A-B binding family protein / early light-induced protein (ELIP)	1.42	0	79.44	2.36	0	102.65
At4g14690	chlorophyll A-B binding family protein / early light-induced protein, putative	1.59	0	86.03	1.96	0	114.02
At4g31870	glutathione peroxidase, putative	3.82	0	50.1	5.2	0	61.1
Transcription factors							
At5g11260	bZIP protein HY5 (HY5)	27.14	0	13.09	72.79	0.11	11.45
At5g24850	cryptochrome dash (CRYD)	29.36	0	12.81	88.06	0.12	10.22
At5g24120	RNA polymerase sigma subunit SigE (sigE)	32.98	0	12.07	49.74	0.05	14.62
At3g57020	strictosidine synthase family protein	141.21	0.35	5.48	216.7	0.58	5.82
At3g17610	bZIP transcription factor family protein / HY5-like protein (HYH)	145.43	0.36	5.31	150.87	0.33	7.29
Transport							
At5g02270	ABC transporter family protein	8.14	0	26.03	10.62	0	40.04
At5g44110	ABC transporter family protein	12.21	0	20.83	15.99	0	32.01
At4g01660	ABC1 family protein	90.67	0.09	6.59	100.14	0.2	9.49
Unknown							
At5g52250	transducin family protein / WD-40 repeat family protein	55.69	0	8.59	70.87	0.11	11.65
At1g79270	expressed protein (ECT8)	112.53	0.17	6.08	163.65	0.34	6.86
At3g17800	expressed protein	186.49	0.6	4.57	264.54	0.88	4.97

UVR8 independent genes

		0.3			1		
		Rpscore	FDR	Fcrma	RPscore	FDR	Fcrma
At3g21560	UDP-glucosyltransferase, putative	6.67	0	29.44	10.53	0	42.45
At3g04000	short-chain dehydrogenase/reductase (SDR) family protein	15.92	0	18.33	34.71	0.03	18.99
At1g05680	UDP-glucoronosyl/UDP-glucosyl transferase family protein	16.3	0	18.54	9.95	0	40.95
At2g36750	UDP-glucoronosyl/UDP-glucosyl transferase family protein	19.56	0	15.41	11.82	0	37.38
At5g22300	nitrilase 4 (NIT4) /// nitrilase 4 (NIT4)	20.49	0	15.3	19.94	0.06	25.54
At5g53970	aminotransferase, putative	25.81	0	13.78	58.97	0.08	13.2
At5g39050	transferase family protein	30.55	0	12.76	23.52	0.05	24.35
At2g36790	UDP-glucoronosyl/UDP-glucosyl transferase family protein	32.41	0	12.57	23.55	0.05	24.34
At2g25450	2-oxoglutarate-dependent dioxygenase, putative	32.98	0	11.7	32.49	0.04	18.52
At5g43450	2-oxoglutarate-dependent dioxygenase, putative	43.22	0	10.1	43.14	0.03	15.84
At3g57520	alkaline alpha galactosidase, putative	49.18	0	9.43	137.22	0.25	7.73
At1g72680	cinnamyl-alcohol dehydrogenase, putative	50.12	0	9.42	56.42	0.09	13.86
At2g29490	glutathione S-transferase, putative ATGSTU1	66.19	0.03	8.02	64.63	0.11	12.53
At2g43820	UDP-glucoronosyl/UDP-glucosyl transferase family protein	70.52	0.03	8.02	88.7	0.11	10.29
At2g29460	glutathione S-transferase, putative ATGSTU4	94.77	0.11	6.58	30.85	0.04	19.57
At1g17170	glutathione S-transferase, putative ATGSTU24	95.38	0.11	6.78	5.04	0	72.49
At1g05560	UDP-glucose transferase (UGT75B2)	110.88	0.17	6.26	97.98	0.19	9.64
At4g34135	UDP-glucoronosyl/UDP-glucosyl transferase family protein	144.03	0.36	5.44	95.5	0.14	9.89
At4g15550	UDP-glucose:indole-3-acetate beta-D-glucosyltransferase (IAGLU)	157.65	0.45	5.28	199.75	0.49	6.24
At2g30140	UDP-glucoronosyl/UDP-glucosyl transferase family protein	161.42	0.45	5.09	93.5	0.15	10.16
At5g07440	glutamate dehydrogenase 2 (GDH2)	200.78	0.71	4.45	167.98	0.35	6.86
At1g32940	subtilase family protein	203.01	0.73	4.41	38.03	0.03	17.18
At3g54420	class IV chitinase (CHIV)	246.8	1.04	3.95	13.57	0	31.57
At1g50380	prolyl oligopeptidase family protein	265.96	1.16	3.85	284.44	1	4.82
At2g43620	chitinase, putative	267.98	1.17	3.79	136.92	0.24	7.62
At3g22370	alternative oxidase 1a, mitochondrial (AOX1A)	287.88	1.24	3.76	151.66	0.34	7.29
At4g22530	embryo-abundant protein-related	293.3	1.28	3.67	45.51	0.03	15.8
At1g09500	cinnamyl-alcohol dehydrogenase family / CAD family	295.87	1.29	3.63	68.27	0.11	12.02
At4g20860	FAD-binding domain-containing protein	302.88	1.3	3.64	121.57	0.2	8.46
At2g37760	aldo/keto reductase family protein	330.68	1.52	3.51	250.98	0.79	5.28
At1g22400	UDP-glucoronosyl/UDP-glucosyl transferase family protein	359.91	1.85	3.27	57.35	0.08	13.26
Signalling							
At3g22060	**receptor protein kinase-related**	**64**	**0.02**	**8.15**	**60.7**	**0.08**	**13.11**
Stress							
At3g13310	**DNAJ heat shock N-terminal domain-containing protein**	**8.14**	**0**	**26.86**	**29.4**	**0.04**	**20.92**
At3g50970	dehydrin xero2 (XERO2) / low-temperature-induced protein LTI30 (LTI30)	37.86	0	11.33	47.04	0.03	14
At5g51440	**23.5 kDa mitochondrial small heat shock protein (HSP23.5-M)**	**326.29**	**1.47**	**3.54**	**10.93**	**0**	**36.07**
Transcription factors							
At3g01970	WRKY family transcription factor	41.75	0	10.42	68.66	0.11	11.86
At1g32870	**no apical meristem (NAM) family protein**	**73.15**	**0.03**	**7.59**	**38.84**	**0.03**	**16.67**
Transport							
At4g25640	**MATE efflux family protein**	**22.51**	**0**	**14.76**	**41.4**	**0.03**	**16.33**
At3g21690	MATE efflux family protein	88.95	0.08	6.87	102.84	0.18	9.42
At1g79410	transporter-related	171.4	0.49	5.01	94.72	0.14	9.68
At4g01870	tolB protein-related	199.28	0.7	4.55	176.49	0.38	6.59
At1g61800	glucose-6-phosphate/phosphate translocator, putative	290.14	1.26	3.64	47.66	0.02	14.35
Unknown							
At2g41730	**expressed protein**	**16.88**	**0**	**17.08**	**2.05**	**0**	**119.77**
At1g10140	expressed protein	20.12	0	15.25	59.86	0.08	12.74
At5g13360	auxin-responsive GH3 family protein	35.14	0	12	54.32	0.09	14.84
At1g68620	expressed protein	53.57	0	9.13	38.72	0.03	16.91
At2g31945	expressed protein	113.32	0.17	5.97	39.85	0.03	16.55
At2g36630	expressed protein	119.74	0.21	5.87	192.8	0.44	6.21
At1g21550	calcium-binding protein, putative	154.22	0.44	5.07	93.07	0.14	9.76
At5g54100	band 7 family protein	202.69	0.73	4.4	66.55	0.1	12.47
At5g42150	expressed protein	226.68	0.95	4.17	86.45	0.12	10.29
At1g63840	zinc finger (C3HC4-type RING finger) family protein	237.55	1.03	4.05	196.28	0.45	6.07

Figure 3.3. **74 genes that are induced by low fluence rates of UV-B.** List shows all genes that are induced in all three microarrays at a cutoff point of 2 % FDR. RPscore is a measure of differential expression FCrma gives the fold change in expression. Those genes highlighted in red were taken on for further study.

A **Down-regulated genes**

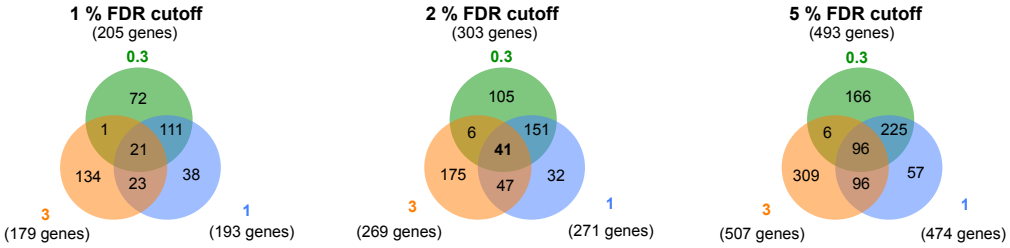

B

		0.3			1		
		Rpscore	FDR	Fcrma	RPscore	FDR	Fcrma
Cell associated							
At1g55330	arabinogalactan-protein (AGP21)	335.29	1.57	-3.36	214.43	0.71	-4.41
Hormone responsive							
At2g21210	auxin-responsive protein, putative	76.86	0.07	-7.45	122.99	0.27	-6.64
At1g74670	gibberellin-responsive protein, putative	173.19	0.46	-4.68	77.35	0.19	-7.63
Metabolism and energy							
At5g23020	2-isopropylmalate synthase 2 (IMS2)	236.69	0.86	-4.06	187.78	0.55	-4.74
At4g03050	2-oxoglutarate-dependent dioxygenase, putative (AOP3)	39.63	0.04	-9.28	43.04	0.03	-9.85
At5g44020	acid phosphatase class B family protein	199.48	0.61	-4.28	52.17	0.13	-8.51
At1g04040	acid phosphatase class B family protein	41.25	0.03	-9.59	50.39	0.11	-9.22
At3g02020	aspartate kinase, lysine-sensitive, putative	341.17	1.64	-3.17	195.19	0.59	-4.53
At2g15090	fatty acid elongase, putative	33.59	0	-9.62	24.05	0	-12.63
At1g29660	GDSL-motif lipase/hydrolase family protein	24.5	0	-10.64	29.42	0	-10.82
At1g26560	glycosyl hydrolase family 1 protein	295.56	1.31	-3.36	267.03	1.17	-3.74
At5g03760	glycosyl transferase family 2 protein	178.61	0.47	-4.22	182.67	0.51	-4.52
At1g03310	isoamylase, putative / starch debranching enzyme, putative	267.73	1.08	-3.56	288.1	1.32	-3.64
At3g14210	myrosinase-associated protein, putative	93.66	0.11	-6	138.8	0.36	-5.25
At5g63180	pectate lyase family protein	319.68	1.49	-3.31	200.72	0.63	-4.44
At3g07010	pectate lyase family protein	251.81	0.97	-3.85	263.38	1.15	-3.96
At3g18000	phosphoethanolamine N-methyltransferase 1/PEAMT 1 (NMT1)	317.4	1.48	-3.31	347.82	1.95	-3.34
At4g00400	phospholipid/glycerol acyltransferase family protein	377.87	1.99	-2.98	310.09	1.59	-3.5
At5g54190	NADPH-protochlorophyllide oxidoreductase A (PORA)	108.47	0.11	-5.42	84.77	0.19	-6.61
At4g30020	subtilase family protein	221.49	0.74	-3.92	293.87	1.39	-3.64
At4g37800	xyloglucan:xyloglucosyl/endo-xyloglucan transferase, putative	117.14	0.14	-5.57	199.53	0.62	-4.46
Signalling							
At3g25500	formin homology 2 domain-containing protein	366.77	1.93	-3.02	354.58	1.99	-3.28
At3g19850	phototropic-responsive NPH3 family protein	211.33	0.68	-4	67.21	0.16	-7.49
At1g54820	protein kinase family protein	177.44	0.48	-4.22	150.19	0.44	-4.93
At1g51940	protein kinase family/peptidoglycan-binding LysM domain-containing protein	327.2	1.54	-3.35	127.92	0.32	-5.72
At3g05490	rapid alkalinization factor (RALF) family protein	153.82	0.38	-5.09	104.51	0.21	-6.57
Stress							
At3g12610	DNA-damage-repair/toleration protein, putative (DRT100)	147.18	0.34	-4.88	114.87	0.25	-5.85
At4g30660	Hydrophobic/low temperature and salt responsive protein, putative	219.78	0.73	-4.39	209.94	0.69	-4.63
Transcription factors							
At2g34620	mitochondrial transcription termination factor-relate /mTERF-related	369.15	1.92	-2.98	77.08	0.17	-7
At5g08330	TCP family transcription factor, putative	176.15	0.48	-4.6	23.42	0	-12.79
Transport							
At3g50240	kinesin motor protein-related	343.38	1.65	-3.2	143.43	0.38	-5.3
At3g10520	non-symbiotic hemoglobin 2 (HB2) (GLB2)	116.78	0.14	-5.69	178.64	0.5	-4.71
At1g55260	protease inhibitor/seed storage/lipid transfer protein (LTP) family protein	134.42	0.26	-4.95	71.75	0.17	-7.12
Unknown							
At1g13650	expressed protein	121.14	0.21	-5.28	170.64	0.48	-4.88
At5g03120	expressed protein	164.69	0.39	-4.85	168.83	0.49	-5.17
At2g30930	expressed protein	182.29	0.49	-4.51	64.59	0.15	-8.19
At5g11070	expressed protein	331.18	1.55	-3.37	55.44	0.12	-8.86
At1g49500	expressed protein	60.47	0.02	-8.37	109.35	0.24	-6.8
At3g60320	expressed protein	317.74	1.48	-3.26	127.4	0.31	-5.47
At2g34510	expressed protein	79.19	0.07	-6.83	48.75	0.11	-9.08
At2g42320	nucleolar protein gar2-related	363.96	1.92	-3.13	342.38	1.92	-3.46

Figure 3.4 Genes that are down-regulated by low fluence rates of UV-B. Three week old *Arabidopsis* plants grown in a low fluence rate of white light (20 µmol m^{-2} s^{-1}) were treated with either four hours of 0.3, 1 or 3 µmol m^{-2} s^{-1} UV-B or were left in low white light as a control. **A** Venn diagrams depicting the overlap in gene repression between different fluence rates of UV-B. The numbers of genes which showed an decrease in expression level were calculated for each of the three significance cut-off points (False Discovery Rate (FDR)). **B** List shows genes that are down-regulated in all three microarrays at a cutoff point of 2 % FDR. RPscore is a measure of differential expression FCrma gives the fold change in expression.

A

		Brown	Headland		Ulm		Hectors		Kilian						Safrany			Count
Gene	**Title**	**3uE**	**1uE**	**0.3uE**	**1hr**	**6hr**	**Low**	**Mid**	**.25hr**	**.5hr**	**1hr**	**3hr**	**6hr**	**24hr**	**1hr**	**6hr**	**96hr**	
AT4G14690	chlorophyll A-B binding family protein / early light-induced protein, putative	Y	Y	Y	N	N	N	Y	N	Y	Y	Y	N	N	Y	Y	Y	5
AT3G22840	chlorophyll A-B binding family protein / early light-induced protein (ELIP)	Y	Y	Y	N	N	N	Y	N	Y	Y	N	N	N	Y	Y	Y	5
AT5G52250	transducin family protein / WD-40 repeat family protein	Y	Y	Y	N	Y	N	N	N	Y	Y	N	N	N	Y	Y	Y	5
AT4G15480	UDP-glucoronosyl/UDP-glucosyl transferase family protein	Y	Y	Y	N	Y	N	N	N	N	Y	Y	N	N	Y	Y	N	5
AT2G32020	GCN5-related N-acetyltransferase (GNAT) family protein	Y	Y	N	N	Y	N	N	N	Y	Y	Y	N	N	N	N	Y	5
AT5G24120	RNA polymerase sigma subunit SigE (sigE) / sigma-like factor (SIG5)	Y	Y	Y	N	Y	N	N	N	N	Y	N	N	N	Y	Y	N	5
AT3G22060	receptor protein kinase-related	Y	Y	Y	N	Y	N	Y	N	N	N	N	N	N	N	Y	N	5
AT3G51240	naringenin 3-dioxygenase / flavanone 3-hydroxylase (F3H)	Y	Y	Y	N	N	N	N	N	N	Y	Y	N	N	Y	Y	Y	4
AT3G52740	expressed protein	Y	Y	Y	N	N	N	N	N	Y	Y	N	N	N	Y	Y	Y	4
AT5G17050	UDP-glucoronosyl/UDP-glucosyl transferase family protein	Y	Y	Y	N	N	N	N	N	Y	Y	N	N	N	Y	Y	Y	4
AT3G21560	UDP-glucosyltransferase, putative	Y	Y	Y	N	N	N	Y	N	N	N	N	N	N	Y	Y	Y	4
AT3G54420	class IV chitinase (CHIV)	Y	Y	Y	N	Y	N	N	N	N	N	N	N	N	Y	Y	Y	4
AT4G01660	ABC1 family protein	Y	Y	Y	N	Y	N	N	N	N	N	N	N	N	Y	Y	Y	4
AT4G37150	esterase, putative	N	Y	Y	N	Y	N	N	N	N	N	Y	N	N	Y	Y	Y	4
AT5G08640	flavonol synthase 1 (FLS1)	Y	Y	Y	N	N	N	Y	N	N	N	N	N	N	Y	Y	Y	4
AT1G05560	UDP-glucose transferase (UGT75B2)	Y	Y	Y	Y	Y	N	N	N	N	N	N	N	N	N	N	Y	4
AT1G32870	no apical meristem (NAM) family protein	Y	Y	Y	N	N	N	N	N	N	N	Y	N	N	Y	Y	N	4
AT1G32940	subtilase family protein	Y	Y	Y	N	N	N	N	N	N	N	Y	Y	N	N	N	Y	4
AT1G68620	expressed protein	Y	Y	Y	N	Y	N	N	N	N	N	N	N	N	Y	N	Y	4
AT1G78600	zinc finger (B-box type) family protein	Y	Y	Y	N	Y	N	N	N	N	N	N	N	N	Y	Y	N	4
AT2G17270	mitochondrial substrate carrier family protein	N	Y	Y	N	Y	N	N	N	N	Y	N	N	N	Y	Y	N	4
AT4G25640	MATE efflux family protein	Y	Y	Y	N	N	N	N	N	N	Y	N	N	N	Y	Y	N	4
AT4G37290	expressed protein	Y	Y	N	N	Y	N	N	N	Y	Y	Y	N	N	N	N	N	4
AT5G02270	ABC transporter family protein	Y	Y	Y	N	N	N	N	N	N	Y	N	N	N	Y	Y	N	4
AT5G11260	bZIP protein HY5 (HY5)	Y	Y	Y	N	N	N	N	N	N	Y	N	N	N	Y	Y	N	4
AT5G44110	ABC transporter family protein	Y	Y	Y	N	N	N	N	N	N	Y	N	N	N	Y	Y	N	4
AT1G05680	UDP-glucoronosyl/UDP-glucosyl transferase family protein	Y	Y	Y	N	N	N	N	N	N	N	Y	N	N	N	N	Y	4
AT1G32350	alternative oxidase, putative	Y	Y	N	Y	Y	N	N	N	N	N	Y	N	N	N	N	N	4
AT1G72680	cinnamyl-alcohol dehydrogenase, putative	Y	Y	Y	N	Y	Y	N	N	N	N	N	N	N	N	N	N	4
AT2G04050	MATE efflux family protein	Y	Y	N	N	Y	N	N	N	N	N	Y	Y	N	N	N	N	4
AT2G04070	MATE efflux family protein	Y	Y	N	N	Y	N	N	N	N	N	Y	Y	N	N	N	N	4
AT2G21640	expressed protein	Y	Y	N	N	N	N	N	N	N	N	Y	Y	N	N	N	Y	4
AT2G22880	VQ motif-containing protein	Y	N	N	N	Y	N	N	Y	Y	N	N	N	N	Y	N	N	4
AT2G29460	glutathione S-transferase, putative	Y	Y	Y	N	Y	N	N	N	N	N	N	N	N	N	Y	N	4
AT2G31945	expressed protein	Y	Y	Y	N	N	N	N	N	Y	N	N	N	N	N	Y	N	4
AT2G32030	GCN5-related N-acetyltransferase (GNAT) family protein	Y	Y	N	N	Y	N	N	Y	Y	N	N	N	N	N	N	N	4
AT2G37970	SOUL heme-binding family protein	Y	N	N	N	Y	N	N	N	N	Y	N	N	N	Y	Y	N	4
AT2G38465	expressed protein	N	N	N	Y	Y	Y	N	N	N	N	Y	N	N	N	Y	N	4
AT3G01970	WRKY family transcription factor	Y	Y	Y	N	Y	N	N	N	N	N	N	N	N	N	Y	N	4
AT3G17800	expressed protein	Y	Y	Y	N	Y	N	N	N	N	N	N	N	N	Y	N	N	4
AT3G27380	succinate dehydrogenase, iron-sulphur subunit, mitochondrial (SDH2-1)	Y	Y	Y	N	Y	N	N	N	N	N	N	N	N	N	Y	N	4
AT3G56710	sigA-binding protein	Y	Y	N	N	Y	N	N	N	Y	Y	N	N	N	N	N	N	4
AT4G15550	UDP-glucose:indole-3-acetate beta-D-glucosyltransferase (IAGLU)	Y	Y	Y	N	Y	N	N	N	N	N	N	N	N	Y	N	N	4
AT4G28460	hypothetical protein	Y	Y	N	N	Y	N	N	N	Y	Y	N	N	N	N	N	N	4
AT5G24110	WRKY family transcription factor	Y	Y	N	N	Y	N	N	N	Y	Y	N	N	N	N	N	N	4
AT5G53970	aminotransferase, putative	Y	Y	Y	N	Y	N	N	N	N	N	N	N	N	Y	N	N	4
AT1G08050	zinc finger (C3HC4-type RING finger) family protein	Y	Y	N	N	Y	N	N	N	N	Y	N	N	N	N	N	N	4
AT1G10170	NF-X1 type zinc finger family protein	Y	Y	N	N	Y	N	N	N	N	N	Y	N	N	N	N	N	4
AT1G71530	protein kinase family protein	Y	Y	N	N	Y	N	N	N	N	N	Y	N	N	N	N	N	4
AT1G75040	pathogenesis-related protein 5 (PR-5)	Y	Y	N	N	N	Y	N	N	N	N	N	N	N	Y	N	N	4
AT1G78410	VQ motif-containing protein	Y	Y	N	N	Y	N	N	N	Y	N	N	N	N	N	N	N	4
AT2G04040	MATE efflux family protein	Y	Y	N	N	N	N	N	N	N	N	Y	N	N	N	N	Y	4
AT2G15480	UDP-glucoronosyl/UDP-glucosyl transferase family protein	Y	Y	N	N	Y	N	N	N	N	N	N	N	N	N	N	Y	4
AT2G23270	expressed protein	Y	Y	N	N	Y	N	N	N	N	N	Y	N	N	N	N	N	4
AT3G15352	cytochrome c oxidase copper chaperone-related	Y	Y	N	N	Y	N	N	N	N	N	N	N	N	N	Y	N	4
AT3G25250	protein kinase family protein	Y	Y	N	N	Y	N	N	N	Y	N	N	N	N	N	N	N	4
AT3G49160	pyruvate kinase family protein	Y	Y	N	N	Y	N	N	N	N	N	N	N	N	N	Y	N	4
AT3G50930	AAA-type ATPase family protein	Y	Y	N	N	Y	N	N	N	N	Y	N	N	N	N	N	N	4
AT3G60420	expressed protein	Y	Y	N	N	Y	N	N	N	N	Y	N	N	N	N	N	N	4
AT3G62150	multidrug resistant (MDR) ABC transporter, putative	Y	Y	N	N	Y	N	N	N	N	N	N	N	N	N	N	Y	4
AT4G11370	zinc finger (C3HC4-type RING finger) family protein	Y	Y	N	N	Y	Y	N	N	N	N	N	N	N	N	N	N	4
AT4G22980	expressed protein	Y	Y	N	N	Y	N	N	N	N	Y	N	N	N	N	N	N	4
AT4G38540	monooxygenase, putative (MO2)	Y	Y	N	N	Y	Y	N	N	N	N	N	N	N	N	N	N	4
AT5G40690	expressed protein	Y	Y	N	N	Y	N	N	N	N	N	Y	N	N	N	N	N	4
AT5G62480	glutathione S-transferase, putative	Y	Y	N	N	Y	N	N	N	N	N	Y	N	N	N	N	N	4

B

Count	No. genes
6	0
5	7
4	58
3	167
2	483
1	2802
Total	3517

Figure 3.5 Overlap of genes between different microarray studies. Lists of genes up-regulated under UV-B treatment were collated and assessed for overlap. **A** Those genes most commonly up-regulated by UV-B treatment i.e. occur in at least 4 out of the 6 microarray studies. Studies: Brown *et al.* (2005), microarray data shown in Fig 3.1 (Headland), Ulm *et al*. (2004), Hectors *et al*. (2007), Kilian *et al.* (2007) and Safrany *et a*l. (2008). Fluence rates of UV-B shown for Brown and Headland in μmol m^{-2} s^{-1} (μE). **B** Summary of the number of genes that appear across gene lists.

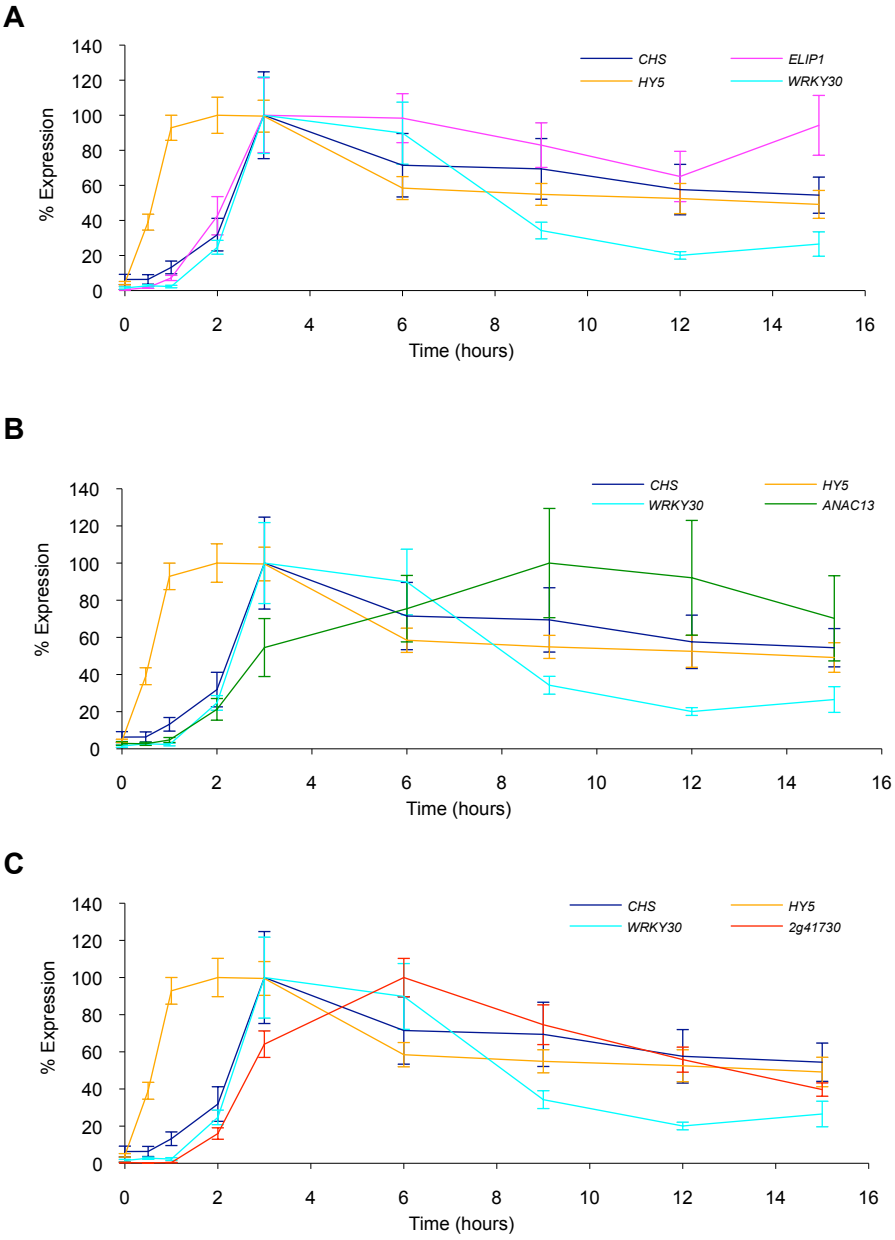

Figure 3.6 Timecourse of expression of UV-B induced genes. Three week old wild type plants were grown under 20 µmol m^{-2} s^{-1} white light and treated with 3 µmol^{-2} s^{-1} UV-B for the times shown above before tissue was harvested and RNA extracted. Values for relative expression (adjusted to *ACT2* transcript levels) were determined using qPCR. Graphs show changes in gene expression over time. Y-axis depicts percentage of maximal expression and x-axis gives the length of treatment. Bars represent standard error, n=6. *HY5*, *CHS* and *WRKY30* profiles used as reference for *ELIP1*(**A**), *ANAC13* (**B**) and *2g41730* (**C**) levels respectively.

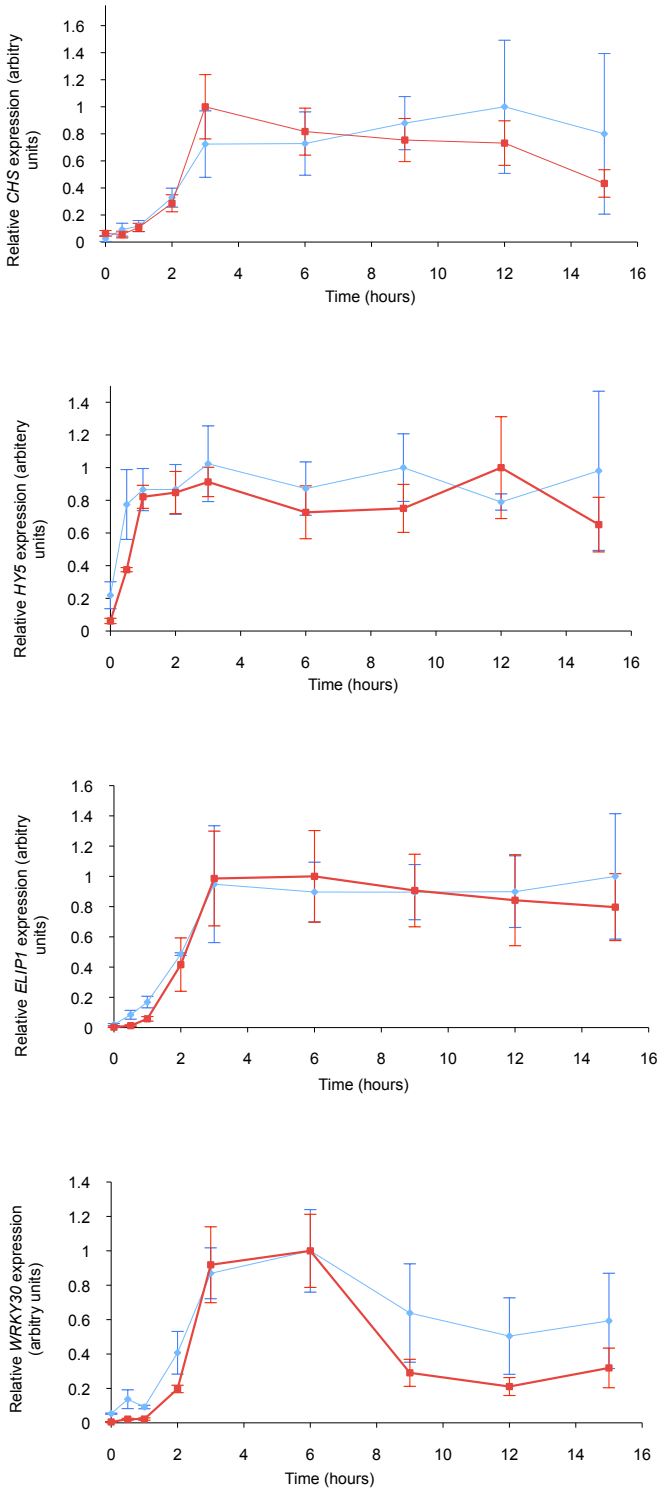

Figure 3.7 Comparison between RT-PCR and qPCR timecourses. Three of the samples analysed by qPCR in figure 3.6 were also analysed with RT-PCR. Gene expression values were normalised to control *ACT2* transcripts. Q-PCR profiles shown in red, RT-PCR shown in blue. Bars represent standard error, n=3.

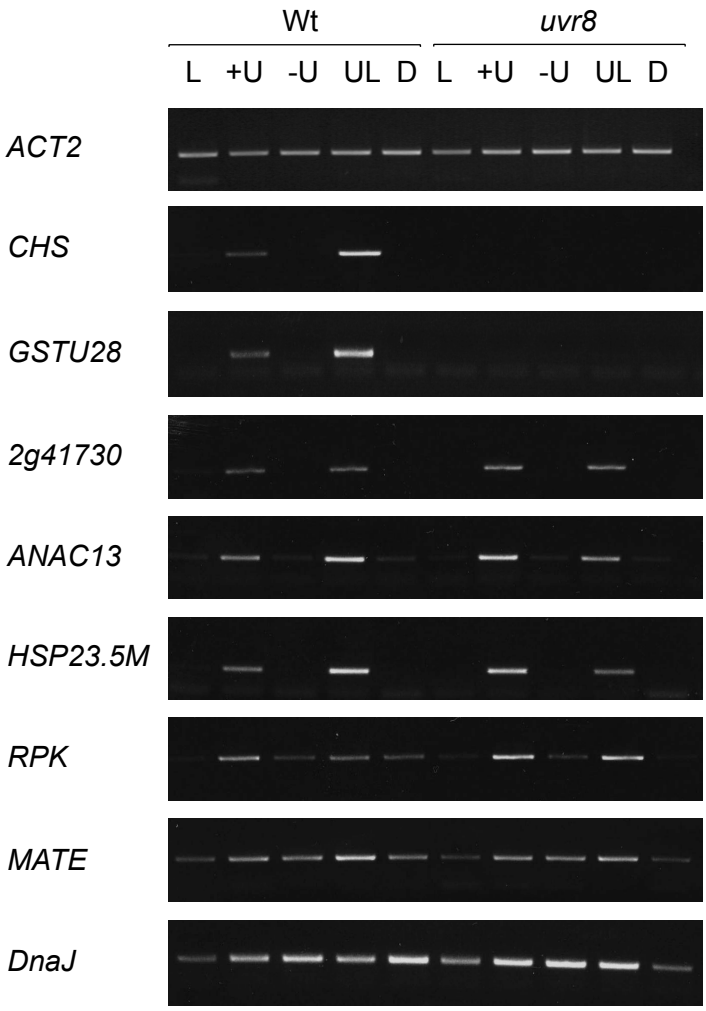

Figure 3.8 Expression of genes under different light conditions. Three week old wild type or *uvr8-1* plants were grown in a low fluence rate of fluorescent white light (20 µmol m^{-2} s^{-1}) were either given no further treatment (L) or treated for four hours under 1 µmol m^{-2} s^{-1} UV-B (+U), UV-B tubes wrapped in –UV-B filter (-U), 1 µmol m^{-2} s^{-1} UV-B with supplemental 20 µmol m^{-2} s^{-1} white light (UL) or transferred to darkness for four hours (D). Transcript levels were assayed using RT-PCR and compared with control *ACT2* transcripts. For PCR conditions used refer to Table 2.1.

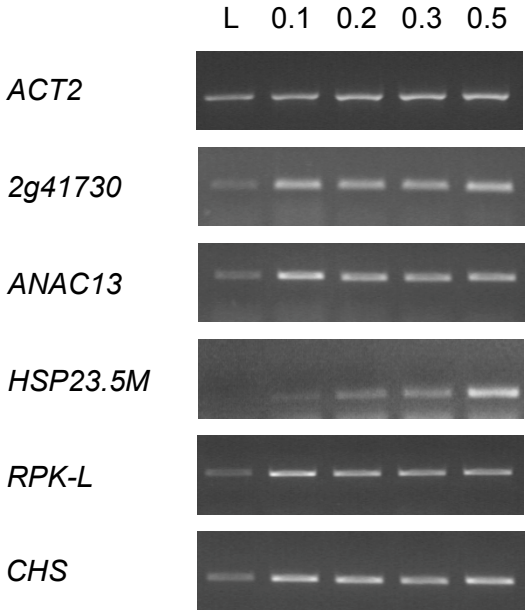

Figure 3.9 Expression of genes under very low fluence rates of UV-B. Three week old wild type plants were grown in a low fluence rate of white light (20 μmol m^{-2} s^{-1}) were treated for either four hours of 0.1, 0.2, 0.3, or 0.5 μmol m^{-2} s^{-1} UV-B or were left in low white light as a control. Transcript levels were assayed using RT-PCR and compared with control *ACT2* transcripts. For PCR conditions used refer to Table 2.1.

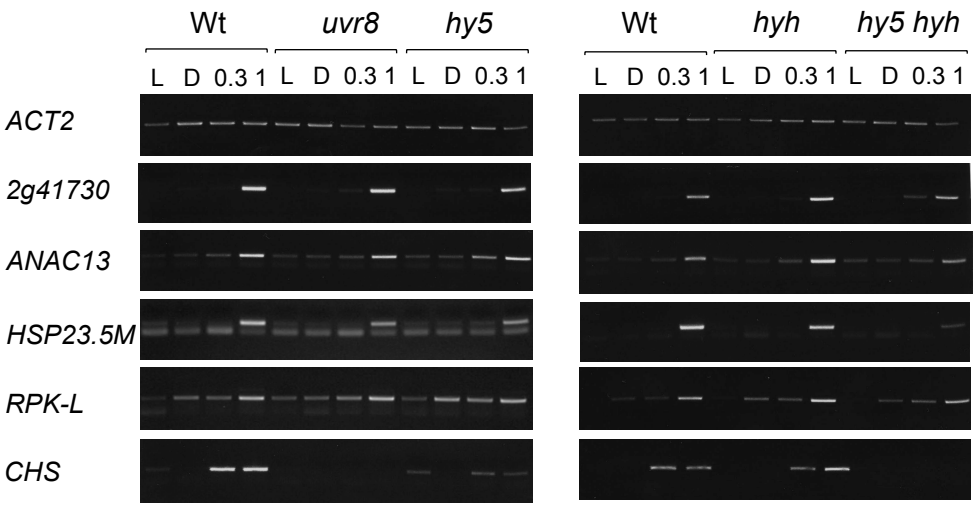

Figure 3.10 Expression of genes in wild type and in mutant backgrounds deficient in UV-B signalling components. Three week old wild type or mutant plants were grown in a low fluence rate of fluorecent white light (20 µmol m^{-2} s^{-1}) were either given no further treatment (L) or treated for four hours with 0.3 µmol m^{-2} s^{-1} UV-B (0.3) 1 µmol m^{-2} s^{-1} UV-B (1), or transferred to darkness for four hours (D). Transcript levels were assayed using RT-PCR and compared with control *ACT2* transcripts. For PCR conditions used refer to Table 2.1.

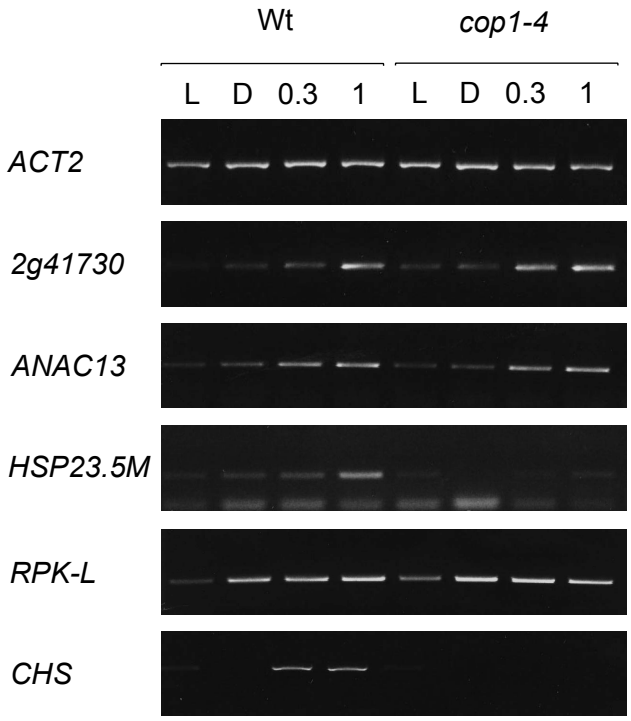

Figure 3.11 Expression of genes in wild type and in mutant backgrounds deficient in COP1. Three week old wild type or *cop1-4* mutant plants were grown in a low fluence rate of fluorescent white light (20 µmol m^{-2} s^{-1}) and either given no further treatment (L) or treated for four hours with 0.3 µmol m^{-2} s^{-1} UV-B (0.3), 1 µmol m^{-2} s^{-1} UV-B (1) or transferred to darkness for four hours (D). Transcript levels were assayed using RT-PCR and compared with control *ACT2* transcripts. For PCR conditions used refer to Table 2.1.

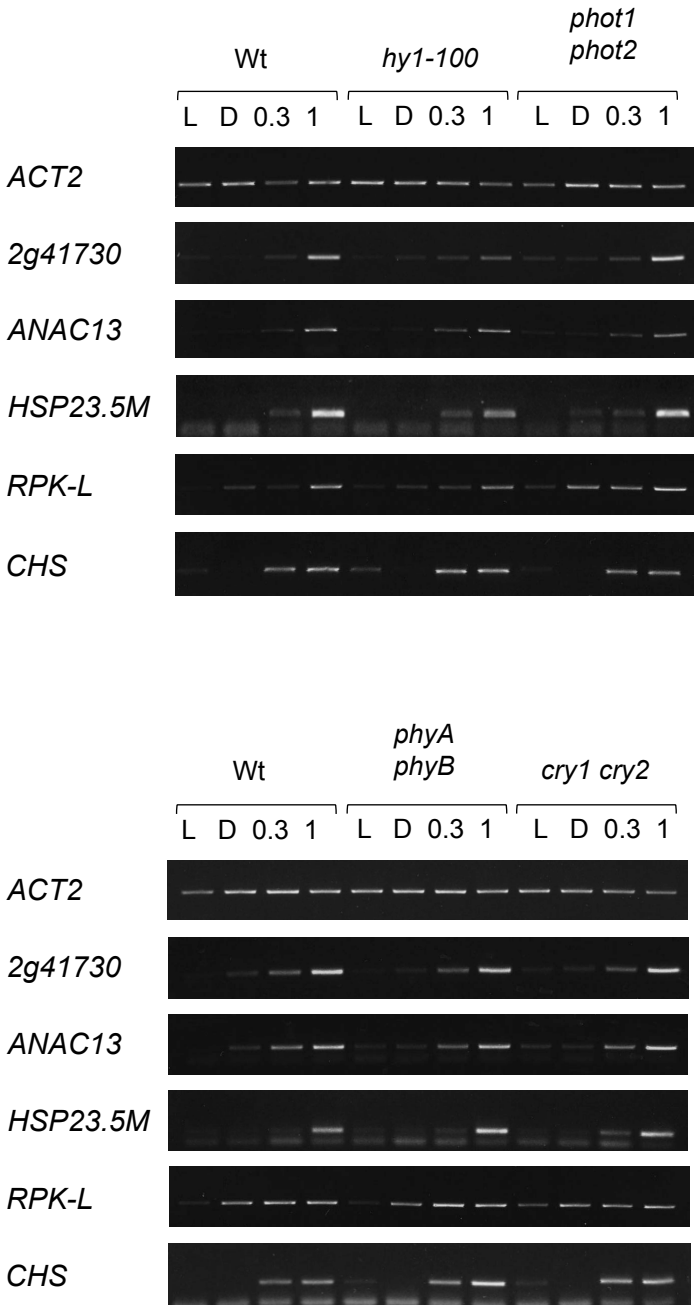

Figure 3.12 Expression of genes in wild type and in mutant backgrounds deficient in photoreceptors. Wild type and mutant plants were grown for three weeks (except for *phyA phyB* and *hy1-100* mutants which were grown for four weeks) in a low fluence rate of fluorescent white light (20 µmol m^{-2} s^{-1}) and were either given no further treatment (L) or treated for four hours with 0.3 µmol m^{-2} s^{-1} UV-B (0.3) 1 µmol m^{-2} s^{-1} UV-B (1), or transferred to darkness for four hours (D). Transcript levels were assayed using RT-PCR and compared with control *ACT2* transcripts. For PCR conditions used refer to Table 2.1.

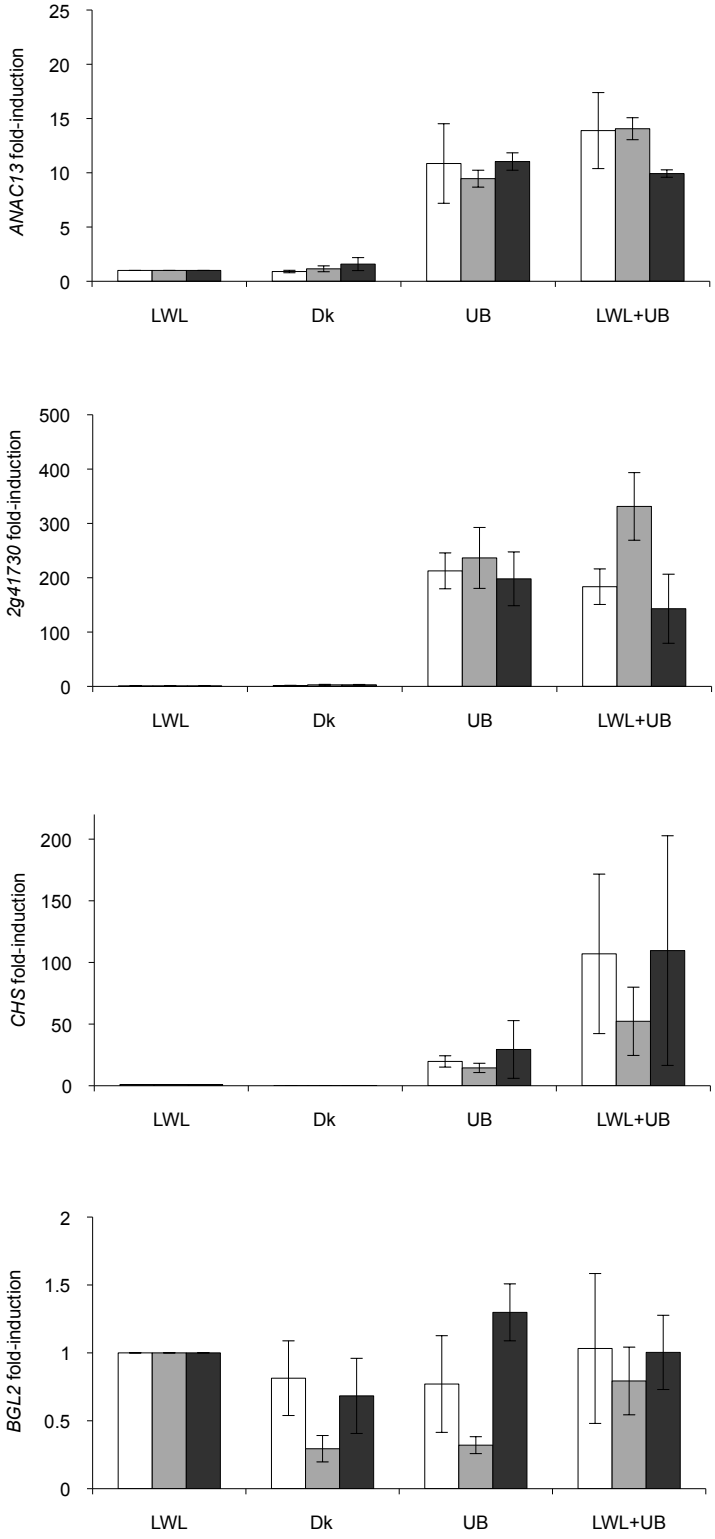

Figure. 3.13 DNA damage signaling does not appear to have a role in expression of *ANAC13* and *2g41730* under UV-B. Expression of low fluence rate UV-B induced genes in DNA repair mutants. Plants were grown in a low fluence rate of fluorescent white light (20 µmol m^{-2} s^{-1}) and either given no further treatment (L) or treated for four hour with 1 µmol m^{-2} s^{-1} UV-B (UB), UV-B supplemented with 20 µmol m^{-2} s^{-1} white light (LWL+UB) or transferred to darkness for four hours (Dk). Expression levels of each gene were first normalised to *ACT2* levels before fold change was calculated compared to control minus UV-B levels. White bars represent Wt, pale grey bars *uvr2* and dark grey *uvr1 uvr3*. Error bars depict standard error, n=3.

CHAPTER 4 UVR8-LIKE PROTEINS AND ROLE OF THE N-TERMINAL IN UVR8 LOCALISATION

4.1 Introduction

Although the known function of UVR8, namely chromatin binding, occurs in the nucleus a GFP tagged version of the protein has been shown to be mainly localised in the cytoplasm under minus UV-B conditions (Kaiserli and Jenkins 2007). Upon exposure to UV-B however, the same protein rapidly accumulates in the nucleus. Previous work has demonstrated that the N-terminal tail of UVR8 may be responsible for this 'accumulation', as deletion of the first 23 amino acids impairs the nuclear accumulation. The exact reasons and the mechanisms for this apparent change in localisation have yet to be determined. The purpose of this chapter is to further investigate this phenomenon and to further pin down the region of the UVR8 protein that is responsible. To this end a number of constructs were generated which either removed parts of the N-terminal or added segments of the same region to a GFP tag. In order to indentify possible interesting regions, the sequences of UVR8-like proteins in Arabidopsis and its homologues in other plant species are examined.

From the work presented here it can be deduced that the N-terminal region does indeed have an important role in the protein's localisation with different segments having different effects. Specifically the first 12 amino acids are sufficient for nuclear accumulation while the first 20 are necessary. Finally the first 32 residues can result in the nuclear localisation of NES-GFP irrespective of light treatment.

4.2 Results

4.2.1 UVR8-like proteins in *Arabidopsis thaliana*

The severity of the mutant phenotype of *uvr8* under ambient levels of UV-B as well as a failure to identify any other UV-B-specific regulatory genes in a mutant screen implies that UVR8 is not acting in a redundant fashion with another element. Nonetheless there are a number of proteins in Arabidopsis that show strong similarity to UVR8 and it is therefore interesting to see if any of these UVR8-like proteins share some of the same features.

A BLAST search was performed using UVR8 as the query sequence and *Arabidopsis thaliana* as the search organism. This resulted in a list of 23 proteins that showed significant sequence alignment to UVR8. Protein names and ATG numbers are shown in Figure 4.1. As of yet the UVR8-like proteins have not been subject to much investigation. Therefore most do not have recognised names or have been assigned functions. Nonetheless, the great advantage of working in a model species with a complete genome sequence allows us to examine protein sequences and determine if there are any shared motifs with our protein of interest.

UVR8 itself has been shown to be closely related to the human REGULATOR OF CHROMATIN CONDENSATION1 (RCC1) protein (Kliebenstein *et al.* 2002). Through comparison with other RCC1 proteins in hamsters, Drosophila and yeast, 41 conserved residues were identified which reside in the RCC1 repeat regions. Furthermore Renault *et al.* (1998) suggest that these have a structural role in maintaining the seven bladed propeller structure of the protein. UVR8 also possesses RCC1 repeat regions and retains 31 of these 41 conserved structural residues. Consequently it has been shown to have a similar structure to RCC1 (Kaiserli PhD thesis, 2008). Therefore it is of interest to see whether any of the UVR8-like proteins have similar numbers of conserved residues and hence likely also have a similar structure to both RCC1 and UVR8.

The 23 UVR8-like proteins along with UVR8 and RCC1 were first aligned to each other using ClustalX software. Using the residues listed in Renault *et al* (1998) as reference, the numbers of structurally important residues that are conserved for each of the UVR8-like proteins were calculated. The values obtained are shown in Figure 4.1.

While some of these proteins do retain similar number of residues to UVR8 (e.g. At3g53830 (31) and At3g55580 (30)), others have relatively few (e.g. At3g03790 (16)). Generally, it can be seen that the values cover a wide spectrum. Therefore it would seem that there may be a number of variations on the structural theme and this may be correlated with a diversity of functions.

The UVR8-like sequences were also compared with RCC1 to see whether there was a good degree of conservation in residues essential for Ran binding/GEF activity. Overall it seemed that relatively few of these were actually conserved (data not shown). Out of 23 of the residues deemed necessary for Ran Binding/GEF activity, the maximum number conserved was five for 5g42140, less even than UVR8 which has eight (Kaiserli PhD thesis, 2008). Three UVR8-likes had none of the residues in common.

In particular nine of the UVR8-like sequences seem to be particularly closely related. Not only do they show a strong degree of sequence similarity, they also share

several 'insertions' at either the beginning or end of certain blade sequences (for the full alignment of UVR8-like sequences see Appendix III). These include insertions at the beginning of blade 3, and ends of blades 5 and 7, with each of these being roughly 50 amino acids long. Furthermore, again the sequences of these insertions are remarkably similar between the proteins. Finally, the aforementioned proteins have a C-terminal tail that extends roughly 200-400 residues longer than that of both UVR8 and RCC1. In total, these sequence similarities and shared insertions suggest that these proteins fall into a group. In addition this implies that they may have similar and perhaps even redundant functions distinct from that of UVR8.

Therefore, although it seems that some of the residues considered important for structure and Ran binding/GEF activity are not conserved in many of the UVR8-like proteins, it is interesting to determine whether they share similar regions to those that are vital for UVR8 functionality.

4.2.2 N- and C-terminal regions of the UVR8-like proteins

Besides from the structurally important amino acids there are a number of other regions that are important for UVR8 function. Work performed by Kaiserli and Jenkins (2007) has shown that regions within the extreme N and C-termini of UVR8 have important functions. The N-terminus seems to have a role in protein localisation while a region within the C-terminal tail has an unknown but nevertheless essential role in protein function.

Concentrating first on the N-terminal, if we look at the corresponding region in RCC1, a bipartite Nuclear Localisation Signal (NLS) can be found. While there are no similar regions in UVR8, deletion of the first 23 amino acids of UVR8 results in impaired nuclear accumulation in response to UV-B (Kaiserli and Jenkins 2007). This is in contrast to the full length GFP tagged version which shows near complete localisation of the GFP signal in nuclei post-UV-B illumination.

Figure 4.2 A shows part of the ClustalX alignment of the UVR8-like proteins around the N-terminal region of UVR8 (for the full alignment see Appendix III). None of the UVR8-like proteins seem to show similarity to UVR8 in this region, the sequences in fact are quite diverse. Most of the N-terminal tails prior to the start of the predicted structurally important sequence are a maximum of 90 residues long. However At4g14370 appears to have a large extension – its N-terminal sequence is 998 residues longer than that of UVR8. This may indicate a specialised function for this particular UVR8-like protein. Indeed, TAIR describes this protein as a disease resistance protein unlike the other UVR8-likes which are mostly described by their similarity to RCC1 or UVR8.

At the C-terminal, UVR8 contains a 27 amino acid insertion that bares no similarity to any portion of the RCC1 sequence. Like the N-terminal deletion, removal of this region results in a non-functional protein. Neither are able to rescue *CHS* and *HY5* expression in response to UV-B. The deletion protein however is still able to bind to chromatin. Therefore this region appears to be key although its function remains elusive.

None of the UVR8-like proteins show similarity to UVR8 in the C-terminal region regions. The 27 amino acids of the C-terminal insertion alone was also aligned to all of the UVR8-like sequences to determine if any similar regions could be found in other parts of the sequences. None however showed any similarity. Therefore it seems that this region within UVR8 may be associated with an unique function in UVR8.

It is interesting to note that the first nine UVR8-like proteins again show remarkable similarity to each other in both the N and C terminal regions. Furthermore, nor are these regions similar to that of RCC1 (data not shown). This supports the hypothesis that the shared sequences of this grouping may indicate shared functions.

In summary, as no UVR8-like protein shows significant similarity in both the N and C-terminal regions it is unlikely that any of these would have similar roles to UVR8 in UV-B responses. It would be interesting however to test null mutants for each of these 23 UVR8-like genes under a variety of biotic and abiotic stresses to evaluate whether they may have important roles in other stress-acclimation responses.

4.2.3 UVR8 homologues in other plant species

With advancing technology, more and more genome sequences from plants are becoming available. It is therefore possible to search more comprehensively for potential homologues in other model species. Given the apparently vital role UVR8 plays in the response of *Arabidopsis thaliana* to low levels of UV-B, it is to be expected that some form of this protein may be present in other plant species. Consequently it was decided to perform additional BLAST searches with the search narrowed to Viridiplantae (green plants). This resulted in a long list of similar sequences (over 100) in a wide variety of species with some species having multiple UVR8-like sequences. Several of these species were selected for further analysis. For those with multiple UVR8-like sequences only the closest to UVR8 was obtained. In addition two sequences from *Physcomitrella patens* which were kindly provided by Dr Andrew Cuming (Leeds) were also included. Finally, as collaborative work with a group in China was being conducted, two potential UVR8-like sequences from rice (*Oryza sativa*) were obtained and analysed along with other selected sequences.

With this large number of sequences in hand, a ClustalX alignment was performed. A distance tree was then generated using neighbour joining methods and is shown in Figure 4.3.

When looking at the distance tree generated there appear to be a split into different portions. First looking at the bottom portion of the tree, the grouping is as we might expect. The *Arabidopsis* sequence is most closely related to that of its fellow brassica field mustard (*Brassica rapa*). Three other eudicots are grouped together and are close to the brassica grouping. Next the two rice and one maize sequence form a monocot grouping. The two physcomitrella sequences meanwhile seem to be more closely related to each other than to any other species. It is therefore unclear which is the likeliest true UVR8 homologue for this group.

The upper part of the tree appears to have a pattern which mirrors that of the lower part with a similar monocot/dicot grouping. There is however one exception to this, the sequence for *Chlamydomonas* is nested within the eudicots. One might expect that the single representatives of the gymnosperms, chlorophyta and especially the animal RCC1 sequence would form outgroups separate from the rest of the tree. Most surprisingly, this is not the case for RCC1 which can be found nested within various plant species. Instead pine (*Picea sitchensis*), the only gymnosperm representative, takes this position, its sequence is seemingly more divergent.

It would therefore seem that it is relatively simple to identify potential homologues of UVR8 in other species. However, in order to help determine whether these may indeed be acting in the same manner as *Arabidopsis* UVR8 we need to look more closely at their sequences. For example, do they have similar regions at the extreme termini. In particular, as the focus of this chapter is on the localisation of UVR8, do these potential homologues have similar N-terminal regions to UVR8. If so, then this would firstly help identify which regions are most highly conserved and therefore have an important role in regulating protein localisation. Secondly, we could also be more confident that these proteins that we have found might be true UVR8 homologues and thus the UV-B response in alternate species may be investigated further. It would be particularly interesting if the UVR8s for other species were able to compliment the *uvr8-1* phenotype.

4.2.4 Conserved regions in the N-terminal of UVR8

In order to answer the questions posed by the results from the previous section a ClustalX alignment was performed for the proteins which comprised the lower part of the distance tree. This included representatives from the main plant groups; eudicots, monocots,

gymnosperms and bryophytes. Figure 4.4 A shows the alignment around the N-terminal regions of the proteins.

When comparing these N-terminal sequences, it can be seen that there is a good degree of conservation, certainly far more than seen in the comparison of the 23 UVR8-like proteins in Arabidopsis. Moreover it is evident there is an area of strong conservation between amino acids 20-33. This is interesting as previous work by Kaiserli and Jenkins (2007) showed that the first 23 amino acids at the N-terminus of UVR8 are essential for protein functionality. Furthermore, a fusion protein consisting of this N-terminal deletion fused to GFP showed impaired accumulation under UV-B in comparison the full-length version. As these amino acids are highly conserved across a variety of plant species it suggests that this impaired nuclear accumulation in the deletion plants may be explained by the loss of some of these conserved residues. It is thus likely that a motif responsible for protein localisation resides in or around this region. Consequently, it would be interesting to examine whether the loss of all 33 amino acids would result in a complete removal of nuclear accumulation. This therefore could give a potential model on which to propose a mechanism for the nuclear accumulation of UVR8 when exposed to UV-B.

Furthermore, by again referring to the sequence alignment we can see that there is a reasonable amount of similarity in sequences between residues 12-20, but that prior to residue 12, the regions show very little conservation. Therefore, this seems to delineate three regions that may have varying effects on the localisation and function of UVR8; the first 12 residues, residues up to number 20, and all residues (33) prior to the start of the predicted structurally important sequence. This latter region was defined as finishing at point 33 as comparisons between RCC1 and UVR8 sequences determined that the blade structure in UVR8 is likely to start at position 34. Thus, in order to pin down more accurately the region/s responsible for nuclear accumulation of UVR8 under UV-B as well as its functionality, a series of deletion constructs were generated. These included both a GFP tag so that protein location could be detected and also a Nuclear Exclusion Signal (NES) derived from mammalian PKI protein (Matsushita *et al.* 2003). NES peptides were added as this results in almost complete nuclear exclusion under minus UV-B conditions as opposed to a higher proportion without (Kaiserli and Jenkins, 2007). This allows a more clearly defined difference between minus UV-B and plus UV-B conditions, thereby allowing an ease of determination whether the localisation of UVR8 has been affected. Schematics of the constructs generated are shown in Figure 4.4A

To make these constructs primers were generated to amplify the sequence of UVR8 from the point desired until the end. This was then ligated into the vectors previously

generated by Kaiserli and Jenkins (2007) containing a NES fused to GFP driven under the native UVR8 promoter. Hereafter the various constructs will be referred to as Δ12N, Δ20N and Δ33N.

All three constructs were then transformed into *uvr8-1* plants as described in Chapter 3. However, due to inability to find Arabidopsis lines with detectable expression for the Δ33N, this construct was instead transiently expressed in tobacco as described in Sections 4.2.8 and 4.2.9.

4.2.5 Protein expression in deletion constructs

uvr8-1 plants were transformed with the deletion constructs described in Section 4.2.4 using the floral dip method (modified protocol from Clough and Bent, 1998) and T3 lines selected as described in Chapter 3. Due to the nature of *Agrobacterium* mediated transformation, the expression levels of constructs can be variable. In order to conduct further experiments, lines need to be selected which show expression levels as close as possible to that of native levels.

Although a large number of T3 lines were screened for each of the deletion constructs, when protein levels were analysed using Western blotting methods, nearly all showed barely detectable or undetectable levels. As the previously studied 23 amino acid deletion (Δ23N) showed good levels of expression (Kaiserli and Jenkins 2007), it is unlikely that this problem was due to the deletion of amino acids from UVR8 impacting on expression. It is more likely that this was simply a problem of transgene locations and possible post-transcriptional silencing. Further screening on an even larger scale may remedy this and reveal better lines.

Consequently, for both Δ12N and Δ20N, only one T3 line each was found that had reasonable levels of expression at both the protein level and when examined under the microscope for GFP fluorescence. Figure 4.5 shows western blots of proteins extracted from Δ12N line 4.3 and Δ20N line 8.3.

Δ12N line 4.3 seems to have protein levels comparable to native UVR8. Therefore as such we can expect that changes in the behaviour of this protein are due to changes in its sequence and not artefacts due to inappropriate levels of expression.

Δ20N however has a reduced protein level but is still detectable in 20 μg total protein extract. Unfortunately, this was the maximally expressing line of all that were tested. Therefore due to time constraints this was the line selected for further analysis. Ideally, at least three lines would be selected and tested for each construct. This eliminates the possibility that the effects seen are due to the positional insertion. Thus to help add

weight to the experiments using these deletions, for each, one additional T2 line which showed reasonable GFP fluorescence under the microscope was also tested to determine if results were replicable. Functionality and localisation of these constructs is described in the following sections.

4.2.6 Δ12N is functional and accumulates in the nucleus under UV-B

As the deletion constructs were transformed into a *uvr8-1* background, functionality of the construct could be determined by examining expression of UVR8-regulated genes under UV-B. Two such genes are *CHS* and *HY5* which both show a strong induction under even very low levels of UV-B. Therefore transformed plants, along with *uvr8-1* and wild type controls, were grown in low fluence rate white light (20 μmol m^{-2} s^{-1}) for three weeks. Plants were then exposed to 1 μmol m^{-2} s^{-1} UV-B or left in low white light conditions for four hours. RNA was extracted and RT-PCRs performed using *ACTIN2*, *CHS* and *HY5* primers. The results of this can be seen in Figure 4.6A.

In Δ12N plants it does seem that *CHS* and *HY5* expression is rescued. Interestingly though the levels of expression under UV-B for both genes appear to be lower than that for wild type plants. This is somewhat surprising considering that the levels of protein expression of the Δ12N construct appear to be roughly equivalent to those of native UVR8 (see Figure 4.5). However, neither western blotting nor RT-PCR are truly quantitative so this may account for the discrepancy.

One further observation that can be made from Figure 4.6 A is that the levels of *CHS* expression under white light in the Δ12N construct seem to be higher than for wild-type. Furthermore, this also seems to be the case for the Δ20N construct (as can be seen in Figure 4.7 A). As this is not apparent in the *uvr8-1* mutant it would suggest that the addition of the construct might subtly affect the reaction of the plants to low white light conditions.

While the functionality of this construct does not seem to be impaired the possibility remained that its localisation may have been altered. Therefore, Δ12N plants were examined under a confocal microscope in order to test this. Plants were either taken directly from low white light conditions where they had been grown for 12-14 days or were treated with 2 hours of 3 μmol m^{-2} s^{-1} of UV-B. This UV-B treatment had been previously shown to be sufficient to induce a strong nuclear accumulation in NES-GFP-UVR8 plants (Kaiserli and Jenkins 2007). In order to facilitate the identification of nuclei, plants were infiltrated with DAPI stain and incubated for 15 minutes prior to mounting and

examination under the microscope. For each treatment 25 images were taken. The numbers of nuclei exhibiting GFP fluorescence and/or DAPI staining were counted. Subsequently, from this count data, the percentages of co-localisation of GFP and DAPI could be calculated. The experiment was repeated a total of three times and the graph in Figure 4.6 C shows the averaged results from these repeats. A t-test was performed on the data and the p-value is shown in the figure legend. Figure 4.6 B shows images that are representative of the three experiments.

Similarly to the full length NES-GFP-UVR8 fusion protein, Δ12N shows almost complete nuclear exclusion under low white light conditions. The GFP signal is localised in the cytoplasm and can be clearly seen in the perinuclear region. When plants are exposed to UV-B there is a shift in localisation, here large numbers of nuclei exhibit GFP fluorescence (73.1 %). Indeed, the t-test shows that the differences in co-localisation between the two treatments are highly significant with a p-value of just 0.0003.

The experiment was also repeated with T2 plants (line 1) and very similar results were found with co-localisation under low white light and UV-B being 1 % and 80.8 % respectively (data not shown). As these results correlate strongly with those found for NES tagged full-length UVR8, it would seem that the loss of the first 12 amino acids of UVR8 do not adversely affect either its function or its ability to accumulate in the nucleus under UV-B.

4.2.7 Δ20N is non-functional and does not accumulate in the nucleus under UV-B

To understand the role of the first 20 amino acids of UVR8, the Δ20N construct was tested for functionality using RT-PCR similarly to Δ12N. From the results in Figure 4.7 A it can be seen that unlike in Δ12N plants, the Δ20N construct is unable to rescue the UV-B response phenotype in an *uvr8-1* background. No detectable expression can be seen in response to UV-B for either *CHS* or *HY5*. This result is similar to that found for the Δ23N deletion tested by Kaiserli and Jenkins (2007). It would thus appear that the removal of eight further amino acids downstream of residue number 12 in UVR8 results in a loss of functionality. Therefore it is in this region that the start of a region essential for the correct function of UVR8 lies. This is despite the fact that this N-terminal tail it is 1) supposedly unnecessary for the seven-bladed propeller structure of the protein and 2) not required for chromatin binding (Kaiserli and Jenkins 2007).

Once again, to expand the study and look at subcellular localisation of the fusion protein, Δ20N plants were tested via confocal microscopy. The methods used were as described in Section 4.2.6. Representative images and graph depicting the average

percentages of co-localisation across the three experiments are shown in Figures 4.7 B and C.

Under low fluence rate white light conditions, we again see very little GFP signal in the nuclei while it is evident in the region surrounding the nuclei as well as the cytoplasm bordering the cell. This however also holds true in plants that have been treated with UV-B. The images of the two treatments have similar appearances and the levels of co-locations are roughly equal. This is supported by the t-test results which yield a p-value of 0.3, thus indicating there is no significant difference in protein localisation between conditions with and without UV-B.

The experiment was also repeated with T2 plants (line 28) with similar results. The differences between the two treatments however were more pronounced with values for low white light and UV-B being 0.5 and 20.8 % respectively. While this seems to indicate some movement into the nucleus, the value of 20.8 % is much lower than for the full-length version. It would therefore appear that removal of the first 20 amino acid either completely or severely impairs nuclear accumulation under UV-B.

4.2.8 Transient expression in tobacco as a means to assess UVR8 accumulation

As mentioned above, no Δ33N T3 lines could be found that expressed to a sufficient level. Taking into account the results from the Δ20N study, it seemed likely that a loss of a further 33 amino acids from the N-terminus of UVR8 would have a similar effect - namely a loss in functionality. It was therefore decided that in this case, transient expression in tobacco would be sufficient to demonstrate whether the protein indeed showed a severe impairment in nuclear accumulation or not. However, as this method had not been used before to assess to the localisation of an NES tagged version of UVR8 it was decided to test the system using the NES-GFP-UVR8 construct generated by Kaiserli and Jenkins (2007). Tobacco leaves were infiltrated with a suspension of *Agrobacterium* cells carrying the pEZR vector with NES-GFP-UVR8 driven by the native promoter. Plants were left for 5 days to allow the infection to take hold before being sampled directly or after a 2 hour treatment with 3 ± 1 μmol m^{-2} s^{-1} UV-B. Similar to experiments using *Arabidopsis*, sections of leaf were stained with DAPI before mounting on glass slides. Over 70 images were taken across three separate experiments for each treatment. Representative images of this are shown in Figure 4.8 A while Figure 4.8 B shows the average percentage co-localisation of DAPI and GFP for each treatment. Unlike for experiments using *Arabidopsis*, it was decided to combine data across all three experiments. This was due to

the fact that uptake of the construct is not uniform across the leaf tissue, instead good expression often appears in small patches. As a result, the total number of images generated per experiment varied depending on the efficiency of the transfection. Furthermore, as the cells of tobacco leaves are larger, fewer cells can be covered in the one screen, in most cases only 3 or 4 nuclei could be seen at any one time. Therefore, the total numbers of nuclei counted were generally lower than that for the stable transformation experiments. Consequently, the data from a minimum of 70 images across the experiments was combined before analysis.

Nonetheless, the larger cells of tobacco and the infiltration method used do have their advantages. Firstly we can get a finer look at the localisation of the signal. For example, it could be seen that when the signal was present in the nucleus, it appeared to be excluded from the nucleolus. Also, the variability in signal strength across the leaf meant that small regions with very good expression could be found. This facilitated the assessment of the signal localisation, it was therefore easier to call whether the GFP co-localised with DAPI fluorescence.

Looking at the results from the NES-GFP-UVR8 experiment shown in Figure 4.8 it can be seen that they closely parallel that for stably transformed *Arabidopsis* as seen in Kaiserli and Jenkins (2007). As expected we see strong nuclear exclusion under white light conditions and a high degree of signal co-localisation after UV-B exposure. In particular, the average values for this experiment are very close to those for Δ12N where is was determined that the protein behaves similarly to the full length version (1.2 %/74.7 % and 3.9 %/73.1 % for NES-GFP-UVR8 and Δ12N respectively in LWL/UB). Therefore it was determined that this would likely be a very useful tool to examine the location of various UVR8 constructs rapidly and effectively.

4.2.9 Δ33N does not accumulate in the nucleus under UV-B

As using the NES system in transiently expressed Tobacco was deemed effective, the localisation of Δ33N was assessed using the same methods as described in the previous section. The results of this are presented in Figure 4.9.

As for Δ20N, the percentage co-localisation under low white light and UV-B for Δ33N appear to be equal. This is reflected in the p-value of 0.9 showing virtually no difference between the values. Thus, as expected, Δ33N does not accumulate in the nucleus more strongly under UV-B. Loss of these amino acids results in abolition of nuclear accumulation.

Interestingly however, the percentage co-localisation under low white light and UV-B appear to be higher for Δ33N than for the full-length protein in low white light, ~20 % and 1.2 % respectively. By removing some residues from the N-terminus, we see more of the fusion protein 'leaking' into the nucleus under white light conditions. In addition, looking back at the results for the previous deletion constructs, we see a gradual increase in the percentage co-localisation in white light with levels for NES-GFP-UVR8, Δ12N, Δ20N and Δ33N being 1.2 %, 3.9 %, 7.7 % and 22.5 % respectively. This suggests that there may be some feature of the whole UVR8 protein that enhances nuclear exclusion under low white light conditions. This may simply be the size of the protein, its conformation or alternatively through some specific means coded in the amino acid sequence.

4.2.10 UVR8 N-terminal addition constructs

The previous series of experiments showed that deletion of several regions in the N-terminal of UVR8 results in the loss of nuclear accumulation of the protein under UV-B. Furthermore it seems that at least the first 20 amino acids of the UVR8 sequence are necessary for nuclear accumulation under UV-B. It is therefore interesting to examine whether these same regions are sufficient for nuclear accumulation under UV-B. It was thus decided to generate such constructs with NES tagged GFP fused to short pieces of the N-terminal sequence. Firstly however, the localisation of NES-GFP alone was to be tested to ensure that it behaved as we would predict. That is it should be present in the cytoplasm under both white light and UV-B conditions due to the strong NES signal. Without any UVR8 sequence present, we would expect there to be no UV-B response unless other factors were at work that were not yet known.

Figure 4.10 shows a schematic of the constructs that were generated and then tested for sufficiency in the transient tobacco expression system. As work by Kaiserli and Jenkins (2007) had shown that deletion of a 27 amino acid region in the C-terminal tail also resulted in non-functionality, it seemed highly unlikely that short N-terminal regions would, by themselves, confer functionality. Consequently, the transient expression in tobacco system was chosen so that localisation could be determined rapidly with relative ease.

The N-terminal sections to be tested included the same regions that had been deleted in the experiments described above. Firstly the $UVR8_{PRO}$::NES-GFP construct was generated by digesting the $UVR8_{PRO}$::NES-GFP-UVR8 plasmid at *Eco*R1 and *Sal*1 sites, thereby removing the UVR8 fragment. The overhang ends were then filled in using Klenow and the plasmid blunt ligated. $UVR8_{PRO}$::NES-GFP12NUVR8, $UVR8_{PRO}$::NES-

GFP20NUVR8 and $UVR8_{PRO}$::NES-GFP32NUVR8 constructs were generated first by amplification of the desired regions (from the NES onwards) using primers which also added a *Hind*III site to the 5' end and *Sal*I to the 3'. Then the UVR8PRO::NES-GFP-UVR8 plasmid was digested with *Hind*III/*Sal*I to remove the whole NES-GFP-UVR8 sequence and replaced with the small amplified fragments.

From here forwards the addition constructs will be referred to as NES-GFP, +12N, +20N and +32N. It should be noted that here the first 32 amino acids are used in contrast to previous experiments where 33 were used. This was subsequently decided that because it was unclear in alignments whether the 33rd residue, a glycine, may constitute one of the important structural residues. As the Δ20N and Δ23N both show a loss in functionality, is unlikely that the loss of this residue in the Δ33N would have any further detrimental effects. However, as a precaution it was decided that from this point onwards 32 residues may be a more appropriate choice.

Having successfully prepared these constructs, they were subsequently tested for localisation as described in the following sections.

4.2.11 NES tagged GFP remains in the cytoplasm under both white light and UV-B

Figure 4.11 shows representative images and percentage localisation of the NES-GFP construct in tobacco using the transient system. As expected, the NES-GFP protein is mainly localised in the cytoplasm under both white light and also UV-B conditions. Interestingly, here it seems that the protein actually shows a stronger nuclear exclusion under UV-B than for white light (15.6 % and 34.7 %) respectively. The seemingly high levels under white light are perhaps to be expected considering previous results. Indeed they seem to fit the pattern of increasingly short NES and GFP tagged fusions exhibiting a greater degree of nuclear co-localisation in white light than longer fusion proteins. Consequently, it would seem that the levels under UV-B are unexpectedly low. Furthermore, the differences between the two treatments are very significant with a p-value of 0.0007. Thus, although it is possible that this is an artefact occurring in just this particular experiment, it is more likely that there is a biologically relevant reason behind this. Perhaps a UV-B treatment affects the physiology of the cell and nuclear trafficking in general in a way that we do not yet understand. For example, it may be the case that post UV-B treatment, nuclear import is decreased and/or nuclear export is increased. Further experiments using both this protein as well as NES-GFP fused to other proteins (unrelated to UV-B responses) are needed to clarify this issue.

Nevertheless, if there is some factor reducing the nuclear accumulation of the NES-GFP protein under UV-B and addition of sections of UVR8 are able to overcome this, then this demonstrates the strength of the cryptic nuclear accumulation signal within the N-terminal region of UVR8.

4.2.12 +12N accumulates in the nucleus under UV-B

Work using deletion constructs has shown that removal of the first 12 amino acids in the sequence of UVR8 had no effect on the nuclear accumulation of the protein. We might therefore expect that addition of these same residues to the NES-GFP construct likewise would have no effect. By examining the results shown if Figure 4.12, this however does not seem to be the case. +12N transformed plants show similar levels of GFP signal in the nucleus under low white light to NES-GFP plants. When exposed to UV-B though, the levels of co-localisation in the +12N plants increase to 79.4 %, close to values seen for the full length UVR8 construct. Thus, although the loss of the 12 most N-terminal amino acids of UVR8 does not impact on its nuclear accumulation, addition of the very same residues is sufficient to cause a UV-B induced nuclear accumulation of NES-GFP. Consequently it seems that in this portion of the UVR8 sequence a UV-B responsive localisation signal lies. Alternatively this region could act as the site for interaction with another yet unknown protein which regulates the localisation of the resulting complex. However, as this region does not appear to be necessary for either localisation or function, then the remaining N-terminal region must be able to compensate for any losses in the first residues perhaps in a redundant fashion.

4.2.13 +20N accumulates in the nucleus under UV-B

As it had already been determined that loss of the 20 most N-terminal amino acids of UVR8 resulted in a loss in nuclear accumulation in response to UV-B, and taking into account the results for the +12N construct, it was expected that the +20N construct would also accumulate in response to UV-B. As Figure 4.13 shows, this does indeed seem to be the case. However, while the differences between the two treatments remain significant ($p = 0.004$), the accumulation under UV-B is not as great as in the previous case. +20N, unlike +12N, does not reach a level of approximately 80 % after UV-B exposure, instead only achieving 54.7 % co-localisation.

It is not clear why this particular construct does not show a nuclear accumulation that is as strong as +12N. Further repeat experiments, those involving stably transformed

Arabidopsis lines or generation of additional plus constructs may help to resolve this. Nonetheless, we can conclude that the first 20 amino acids are both necessary and sufficient for nuclear accumulation specifically in response to a UV-B treatment.

4.2.14 +32N is constitutively in the nucleus

Again, in line with the previous addition constructs, it was expected that +32N would show similar patterns of localisation. However, as shown in Figure 4.14 it can be seen that plants that have not been exposed to UV-B exhibit similar high levels of co-localisation to those that had been irradiated. When comparing mean a p-value of 0.5157 is obtained thereby demonstrating that the differences between the two treatments are not significant. It would thus seem that by including 12 more amino acids of the UVR8 sequence on top of the +20N construct allows the protein to overcome its NES signal and localise in the nucleus irrespective of the light treatment. That is, by adding further amino acids onto the construct we have lost the UV-B responsiveness that it seemingly provided by inclusion of the first 12 residues alone.

In conclusion it seems that within the first 12 amino acids of UVR8 a UV-B responsive NAS exists that appears to be acting redundantly with a second found in the upstream 8 residues. In the first 20 residues, meanwhile a necessary and sufficient UV-B responsive NAS element is present. Finally, within the region between residues 20-32 lies a strong NAS which is insensitive to light treatment.

4.2.15 +32N in a *uvr8-1* background exists primarily in the nucleus irrespective of light treatment

The previous result, that addition of the first 32 amino acids of UVR8 onto a NES-GFP tag resulted in constitutive nuclear localisation was a surprising one. It was therefore decided that this would be an interesting avenue to pursue. Although it seems highly unlikely that the first few 32 amino acids alone would be functional, the NES-GFP-32NUVR8 construct was transformed into a *uvr8-1* background in *Arabidopsis*. We could therefore determine whether the localisation in both systems was the same. This would lend weight to both the conclusions from the previous section and also that the two methods were analogous.

Due to time constraints, it was not possible to carry the lines through to homozygosity. Therefore T1 plants that exhibited kanamycin resistance were examined under the microscope in order to assess patterns of localisation. At least six plants were

examined and 20 or more images taken per experiment. The experiment was repeated 3 times and the results shown in Figure 4.15 are averaged across the three experiments.

It can be seen that the patterns of co-localisation in *Arabidopsis* do seem to closely mirror those for Tobacco. Therefore it does indeed seem that the first 32 amino acids of UVR8 are able to confer constitutive nuclear accumulation irrespective of light treatment and despite the presence of a NES tag.

It should be noted however that although the patterns between the two systems are consistent, the absolute levels of co-localisation in the *Arabidopsis* plants are lower than that for their tobacco counterparts. This may result from lower expression levels in the T1 generation making it harder to detect nuclei with GFP fluorescence. It is likely that with subsequent generations the signal would improve thus enabling clearer determination of localisation.. However, the observation that in the two systems (tobacco and *Arabidopsis*) the results for this construct are highly comparable with similarly sized error bars is encouraging and confirms the transient system to be an appropriate one for initial investigations into protein localisation

4.3 Discussion

Previous work on the UVR8 protein had already shown that it binds to chromatin in the promoter region of UV-B induced genes, accumulates in the nucleus under UV-B and has very little Ran GEF activity unlike its close homologue, human RCC1 (Kliebenstein *et al.* 2002; Brown *et al.* 2005; Cloix and Jenkins 2008). Furthermore, we know that regions in the N and C-terminal of the protein are essential to its function. However, we do not yet fully understand the roles of these two regions nor do we have a clear mechanism for how UVR8 acts. Work in this chapter therefore attempted to shed further light onto these issues by first examining potential homologues both within Arabidopsis and also between different plant species. Subsequently, focus was turned to the N-terminal region of the protein in order to more clearly define its role in UVR8 localisation and functionality. It has been shown here that a number of UVR8-like proteins exist in Arabidopsis, none of which appear to share the unique N and C-terminal regions found in UVR8. The protein itself does appear to have homologues in a wide range of plant species from different groups. Finally, the accumulation behaviour of a GFP tagged protein is strongly dependent on which portions of the N-terminal are either added onto or deleted from the UVR8 protein. While the latter result can be somewhat confusing due to the complex range of

phenotypes we see, it nevertheless highlights the importance of this region in the appropriate localisation of UVR8.

4.3.1 UVR8-like genes in Arabidopsis

A simple BLAST search using UVR8 as a query sequence reveals 23 similar proteins in *Arabidopsis*. As none of these had well described functions, their sequences were analysed in order to determine whether any were particularly closely related to UVR8 and as such might share similar functions. It was immediately apparent that there is a great deal of variation in these UVR8-like proteins. For example in the degree of structural conservation (in terms of conserved residues that maintain the blade structure) seems to be somewhat reduced compared to UVR8. However, when we consider that the yeast (*Sacchromyces cerevisiae*) homologue to RCC1 is also missing about 10 of these structural residues, it is possible that there is some degree of flexibility in the overall structure.

Further differences between UVR8 and similar proteins in Arabidopsis include a lack in regions similar to those found to be of key importance in UVR8. In addition to comparisons using the ClustalX software, the N-terminal 32 amino acids and the 27 residues found towards the C-terminal were also submitted for analysis using the BLAST alignment tool. This failed to find any homologous regions in any other proteins in the Arabidopsis proteome. It therefore seems that these regions are indeed unique to UVR8 and provides further evidence that it is these regions which may confer the UV-B specific functions of this protein.

As it seems that none of the UVR8-like proteins are likely to have a redundant function to UVR8, we can consider what roles they may actually have. For example, when performing the ClustalX analyses, it was clear that nine seemed to show marked similarity in sequence. Furthermore, these same proteins also had several insertions compared to UVR8. Interestingly, all of these occurred in regions predicted to be between blades. Thus it may be that the overall 7-bladed structure is indeed retained in these proteins, suggesting that this structure may have an important role in their overall function.

It should be noted that the apparent failure to identify other proteins that are likely to act in a redundant fashion to UVR8 is perhaps to be expected. Early mutant screens performed by the Jenkins group which identified several *uvr8* alleles only produced mutations in this gene and no other. This evidence highlights the vital role which UVR8 plays in UV-B responses. Nonetheless, work in the previous chapter has shown that other UV-B induced genes exist which are independent of the identified UVR8 pathway. The regulatory mechanisms behind these however have yet to be determined. Therefore it is

still possible that one/several of these UVR8-like proteins may be involved in this separate UV-B responsive pathway(s).

In summary, it seems that further investigation into the N and C-terminal regions of UVR8 may be key in the determination of its exact mode of action and hold the key to its function.

4.3.2 UVR8 homologues in other plant species

It can be hypothesised that UVR8 may have arisen relatively early in land plant evolution with the colonisation of land and hence the loss of the filtering properties of water, plants may have needed to rapidly evolve mechanisms to survive UV-B stress. This would have had to include the up-regulation in pathways that would lead to increased repair mechanisms and ultimately the production of compounds or structures that would have the ability to reflect or absorb this potentially harmful radiation. It would seem that UVR8 would fulfil the role of a molecule which, upon 'activation' by UV-B, could trigger downstream signalling resulting in such protection and curative measures. In addition, it would be of clear advantage to plants to respond to low, as of yet undamaging, levels of UV-B and trigger acclimation responses in order to offset any potentially harmful subsequent stresses. A role which again in *Arabidopsis* seems to be fulfilled by UVR8.

Consequently, it is no great step to theorise that if UVR8 is indeed such a vital component of UV-B responsiveness, homologues should exist across a large range of plant groups, possibly stretching back to the chlorophytes. Therefore a search for potential homologues in species with completed or partially completed genome sequences was undertaken. It was found that a number of possible homologues could indeed be found in a wide range of species some of which bear remarkable similarity to the *Arabidopsis* UVR8 sequence and have been annotated as likely homologues. When these protein sequences were assembled into a distance tree two large clades appear. The upper clade as depicted in Figure 4.3 includes Human RCC1. As of yet, no homologue of RCC1 has been found in plants which shares its Ran GEF activity. It is possible that those proteins in the upper clade are actually such examples of functional homologues to RCC1. In turn, we can suppose that those proteins found in the lower clade along with Arabidopsis UVR8 are true UVR8 homologues. Consequently, this sharp split into two clades may be explained by the presence of two distinct types of proteins. As some of these genome sequences are not yet complete and fully annotated, and due to the close similarity in the protein sequences, this may have resulted in proteins that are more closely related to UVR8 or to RCC1.

Once these proteomes are completed further searches can be performed in order to test this theory.

Taking into consideration the structure of this tree, it was decided to focus only on those sequences which made up the lower clade. Both N and C-terminal sequences were analysed in order to assess similarity to UVR8. As none of the UVR8-likes identified seemed to posses either region (which have been shown to have an essential role in UVR8 function) this would seem to be good criteria to identify potential UVR8 homologues. BLAST searches were therefore also performed using just these N or C-terminal regions (see Appendix 2). Interestingly, for those species in the upper clade, no similarities could be found for either region in these proteins. For the lower clade there was a more diverse mix. Unsurprisingly, those species (i.e. the dicots) which are shown to be very close to the *Arabidopsis* UVR8 sequence have very significant values of similarity in both regions. Outside of the dicots however, we have a split between the two regions. For the C-terminal region, most of the potential homologues had relatively strong significance values. However, there is seemingly greater diversity in the N-terminal region. For example, proteins from *Picea sitchensis*, one of the rice sequences and both *Physcomitrella patens* sequences have values >0.05. Despite this, when N-terminal sequences were aligned using ClustalX (see Figure 4.4) it is clear that at least between residues 20-33 there is a very strong degree of similarity. It therefore would seem that it is these residues which are most strongly conserved and hence likely to be responsible for the essential function of the N-terminal. It was on this basis that N-terminal deletions were constructed as discussed below and in Sections 4.2.4-15.

When the N-terminal regions of those species in the upper clade are examined, it is interesting to note that almost all have no apparent similarity to *Arabidopsis* UVR8 when they are aligned. The one exception to this is for *Chlamydomonas reinhardtii* which, similar to the lower clade sequences, shows a strong similarity in residues 20-33 (data not shown). However, this is not true for the C-terminal region. Even when the sequences for *Chlamydomonas* and *Arabidopsis* are aligned, no region that corresponds to the 27 amino acid segment in the C-terminal can be found. This apparent natural split makes the *Chlamydomonas* protein a potential subject of interest as it could potentially both untangle the functions of the two essential regions in, and also give clues as to the evolution of the UVR8 protein.

The close relationship between the N and C-terminal sequences in the lower clade species does suggest that UVR8 homologues have the potential to be readily found in other species. Furthermore, their apparent presence in a wide variety of groups including mosses

and gymnosperms suggests a relatively ancient origin. However, as it is not clear whether the protein sequence from *Chlamydomonas* is indeed an UVR8 homologue we cannot yet determine how far back the origin of UVR8 can be traced to.

4.3.3 The role of the N-terminal of UVR8 in protein localisation

The results described in Sections 4.2.5-15 suggest that different parts of the N-terminal region may be responsible for different effects. In summary, loss of the first 12 amino acids has no effect on protein localisation while loss of 20-33 prohibits nuclear accumulation after UV-B. Addition of the first 12 or 20 amino acids to a GFP tag causes a UV-B induced nuclear accumulation while addition of 32 amino acids gives rise to a constitutive nuclear localisation.

Considering first the results using 12 amino acids of UVR8, it is somewhat confusing as to why the removal or addition of these residues results in such contrary localisation patterns. That is, if removal of this region seemingly has no effect, then we might not expect that addition of the same region to have similar effects to the full length protein. Therefore, we can conclude that this region is sufficient but not necessary for UV-B induced nuclear accumulation. This can also be considered contrary to expectations as the first 12 amino acids show little conservation between various UVR8 like sequences in other plant species (see Figure 4.4). Furthermore, that such a short region of protein is sufficient to confer UV-B responsiveness is also something of a surprise.

Perhaps this region forms part of a binding site for an interacting protein. Deletion of this segment may not be sufficient to abolish binding thus allowing normal localisation patterns. When only this region is used, it may provide sufficient anchorage for an interacting partner, which may be involved in UV-B sensing, to bind thereby promoting nuclear accumulation under these conditions. Alternatively, it may be that there are redundant signals within the N-terminal sequence that are important in nuclear accumulation. Thus, removal of one of these in the first 12 residues may not be sufficient to affect localisation due to the remaining signal within the next 20. This may explain why the removal of all the N-terminal of UVR8 is required for definitive loss in nuclear accumulation under UV-B.

Results from the microscopy studies described here suggest that removal of the first 20 amino acids of UVR8 gives rise to a complete loss in nuclear accumulation of UVR8 post UV-B treatment. It would hence seem that within this region lies a motif necessary for mediating UV-B induced nuclear accumulation. Initially it may seem that this result may be at odds with that found by Kaiserli and Jenkins (2007) whereby removal of 23 N-

terminal amino acids resulted in reduced nuclear accumulation. This study however did not use a NES tag and therefore had higher levels (about 50 % colocalisation) of protein in the nucleus under white light. Upon UV-B exposure, this rose to approximately 60 % colocalisation of GFP and DAPI signals. It can thus be seen that the differences between the two light treatments in the Δ23 study (~10% increase with UV-B) are not large. Therefore both this result and the Δ20 data shown here are consistent with the hypothesis that this N-terminal region is necessary for UV-B induced nuclear accumulation.

As the Δ23 deletion construct is still localised to the nucleus under white light as levels similar to that of GFP-tagged full-length UVR8, it would thus appear that the loss of this region does not completely abolish nuclear localisation. Instead it would seem that the strong nuclear accumulation (at the expense of cytoplasmic UVR8 levels) in response to a UV-B stimulus has been lost. It has yet to be conclusively determined whether the nuclear accumulation of UVR8 seen under UV-B is as a result of increased nuclear import or decreased nuclear export. Therefore this ~20 amino acid N-terminal of UVR8 is apparently necessary for either enhanced nuclear import or for increased nuclear retention under UV-B conditions depending upon which of these processes is the underlying cause of changes in UVR8 distribution in the cell.

Finally, while either 12 or 20 amino acids seem to be sufficient to cause UV-B induced nuclear accumulation, 32 gives rise to constitutive nuclear localisation under minus as well as plus UV-B conditions. Therefore, by addition of a further 12 residues we lose UV-B responsiveness and retain an ability to accumulate in the nucleus. Interestingly, this is despite the presence of an NES tag which ordinarily strongly promotes export of proteins into the cytoplasm. This suggests two possibilities. Firstly that the overall effect of this 32 amino acid region is a strong NAS which is insensitive to light treatment. Alternatively, that within these extra amino acids (i.e. on top of the first 20) lies a cryptic NLS. As the first 12-20 amino acids alone are sufficient to cause UV-B responsive nuclear accumulation, it is not clear why a NLS would be needed. Nor is it clear why increasing the length of the fragment would result in such a strong NAS that is no longer responsive to the UV-B stimulus. Perhaps, the addition of these extra amino acids in isolation from the rest of the UVR8 protein gives rise to inappropriate binding that causes the apparent mis-localisation under minus UV-B conditions.

Nevertheless, it is obvious that no concrete conclusions can be drawn until such time that additional experiments, which dissect this N-terminal region further, are performed.

It should be noted that the exact mechanisms behind this nuclear 'accumulation' are not yet clear. Two distinct possibilities exist which can explain the phenomenon seen. Firstly, the UVR8 protein could be actively imported into the nucleus after a UV-B treatment. Alternatively, it may be that it is the rates of nuclear export which are altered. In this latter scenario, under minus UV-B conditions, UVR8 is continually exported from the nucleus so that the bulk of the protein remains in the cytoplasm. After a UV-B pulse, the export process of this particular protein may be blocked so that larger concentrations accumulate. Preliminary work by Eirini Kaiserli (unpublished data) using Leptomycin B, an inhibitor of nuclear export, favours the latter explanation. Addition of this inhibitor resulted in nuclear accumulation of the NES construct in the absence of UV-B.

If it is indeed the active export of UVR8 that is altered under different light conditions, then this suggests that the initial N-terminal amino acids are essential for the retention of the UVR8 protein. This is consistent with the observation that solely the 32 N-terminal amino acids of UVR8 bound to a GFP tag are constitutively within the nucleus. It would appear that within this short sequence lies a nuclear retention signal (also known as a nuclear localisation signal) that is insensitive to light conditions.

The work presented in this chapter has promoted our understanding of the role of the N-terminal region in the localisation of UVR8. The picture however is far from complete and while the experiments described here form a good foundation, additional work is needed so that the seemingly various effects of different parts of this region can be tied down more thoroughly.

4.3.4 Future experiments

While work described in this Chapter has shown that sequences similar to UVR8 exist in both Arabidopsis and a variety of species, and in addition to further pinning down the important residues within the N-terminal, it has also revealed areas which would benefit from additional investigation. This next section will suggest experiments which may help to build a more complete picture of UVR8 action and the role of proteins similar to UVR8.

A number of sequences were identified in *Arabidopsis* that show similarity to UVR8. As of yet, none of these have concrete functions. A number of experiments could be performed which would provide an insight into their functions. For example, ChIP assays could be performed in order to determine whether, similarly to RCC1 and UVR8, these proteins also have the ability to bind to chromatin. It is possible that while having a role independent from UV-B, they may be involved in response to other abiotic or even

biotic stimuli. Further analysis into their expression patterns, localisation as well as response of knock-out mutants under a variety of conditions could help clarify this.

Turning next to the potential UVR8 homologues in other plant species, it would be interesting to see whether whole proteins and also N or C-terminal segments are able to rescue the null mutant or deletion constructs respectively. As there seems to be strong conservation in the N-terminal region even between *Arabidopsis* and *Chlamydomonas*, there is a good possibility of functional complementation but it would still be interesting to see whether any of the amino acids substitutions that have take place have subtle effects on the protein localisation and its ability to accumulate under UV-B. Furthermore, if these identified proteins are indeed true UVR8 homologues, they should have the ability to rescue the UV-B hypersensitivity phenotype of *uvr8-1*. Therefore transformation with full length versions of the protein also would be of interest. In the case of rice and *Physcomitrella* this may help resolve which of the two very similar proteins are the true homologues or even if they are redundant copies.

In order to confirm that it is the presence of specific UV-B responsive components in UVR8 that are responsible for its accumulation under UV-B, one final control experiment should be performed. While is was shown that UVR8 promoter driven GFP is unable to accumulate in the nucleus, it should also be determined whether this is also true for a cytoplasmically localised protein of a similar size to UVR8. It is possible that the accumulation of UVR8 under UV-B that we see is not a specific effect but a general reduction in nuclear export due to this particular treatment. By GFP tagging an alternate protein, this should resolve the issue and allow us to suggest whether UV-B responsiveness is an inherent feature of UVR8.

While, unlike RCC1 which contains a bipartite NLS, no recognisable NLSs could be detected in the N-terminal region of UVR8 (Kaiserli, 2008), this does not exclude the possibility that a novel as yet unidentified NLS is present. It would therefore be interesting to take the 12 amino acid segment which lies between residues 20-32 and determine whether this is sufficient to act as an NLS. Not only could this segment be fused to GFP to assess its localisation, it could also be tagged to NES-GFP to determine whether it is indeed strong enough to overcome the export signal.

Finally, it is somewhat ambiguous whether G33 is one of structural importance, therefore when the plus constructs were generated +32N was chosen instead of taking the first 33 residues. Consequently the deletion study using Δ33N should be repeated to ensure that loss in nuclear accumulation is not dues to a compromised structure. Evidence that plus constructs are sufficient for nuclear accumulation/localisation would suggest that

loss of the first 32 amino acids would still result in severely compromised nuclear accumulation. In addition, as the Δ20 construct was non-functional this in total suggests that the results for Δ32N are unlikely to differ greatly from that seen for Δ33N.

Gene	Description	No. conserved structural residues
RCC1	REGULATOR OF CHROMOSOME CONDENSATION1	41
UVR8	UV RESISTANCE LOCUS8	31
At5g12350	Ran GTPase binding / chromatin binding / zinc ion binding	21
At5g19420	Ran GTPase binding / chromatin binding / zinc ion binding	26
At5g42140	zinc finger protein, putative / regulator of chromosome condensation (RCC1) family protein	26
At1g76950	PRAF1	25
At1g69710	zinc finger protein, putative / regulator of chromosome condensation (RCC1) family protein	23
At3g47660	regulator of chromosome condensation (RCC1) family protein	19
At3g23270	regulator of chromosome condensation (RCC1) family protein	17
At4g14370	disease resistance protein (TIR-NBS-LRR class), putative	18
At1g65920	regulator of chromosome condensation (RCC1) family protein / zinc finger protein-related	19
At3g53830	regulator of chromosome condensation (RCC1) family protein / UVB-resistance protein-related	31
At3g55580	regulator of chromosome condensation (RCC1) family protein;	30
At3g02510	regulator of chromosome condensation (RCC1) family protein	28
At5g16040	regulator of chromosome condensation (RCC1) family protein	28
At1g27060	regulator of chromosome condensation (RCC1) family protein	26
At5g08710	regulator of chromosome condensation (RCC1) family protein / UVB-resistance protein-related	27
At5g48330	regulator of chromosome condensation (RCC1) family protein	26
At5g11580	UVB-resistance protein-related / regulator of chromosome condensation (RCC1) family protein	22
At5g60870	regulator of chromosome condensation (RCC1) family protein;	19
At3g26100	regulator of chromosome condensation (RCC1) family protein	29
At3g15430	regulator of chromosome condensation (RCC1) family protein	25
At3g02300	regulator of chromosome condensation (RCC1) family protein	25
At3g03790	ankyrin repeat family protein / regulator of chromosome condensation (RCC1) family protein	16
At1g19880	regulator of chromosome condensation (RCC1) family protein	24

Figure 4.1 23 UVR8-like proteins in *Arabidopsis thaliana*. Table shows UVR8/RCC1 related genes in *Arabidopsis thaliana*. Protein sequence for UVR8 was submitted to NCBI BLAST and 23 similar sequences were returned. Sequences were aligned and scored for the number of conserved structural residues in RCC1 as determined by Renault *et al.* (1998).

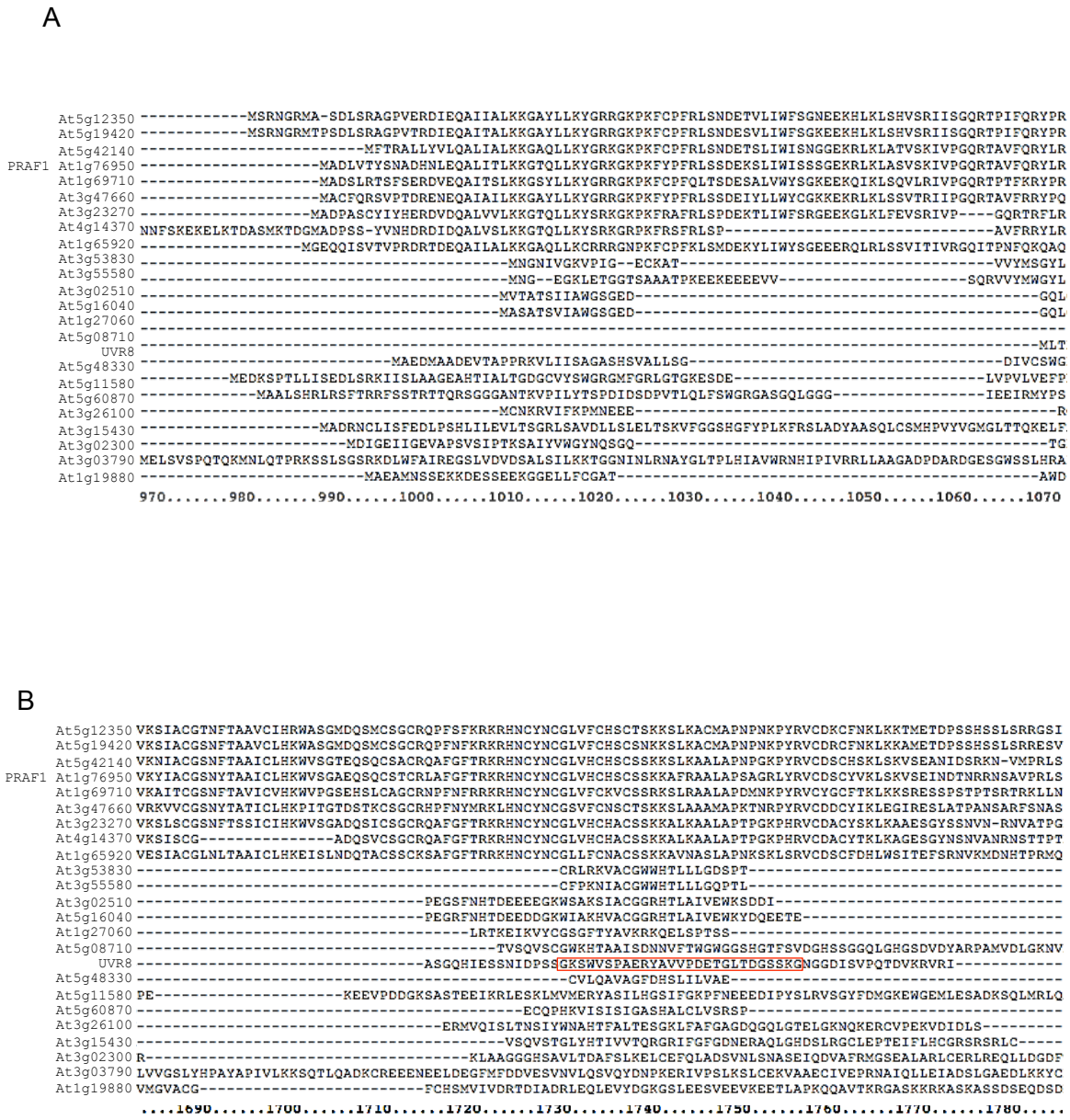

Figure 4.2 Multiple sequence alignment of UVR8 and 23 UVR8-like proteins in *Arabidopsis thaliana*. Protein sequences were aligned in ClustalX. **A** Section of the alignment showing the conservation around N-terminal regions of the proteins. At4g14370 extends approximately 980 amino acids prior to the start of the UVR8 sequence. **B** Section of the alignment showing the degree of conservation around the C-terminal end of UVR8. C-terminal insertion (relative to RCC1) shown in red box.

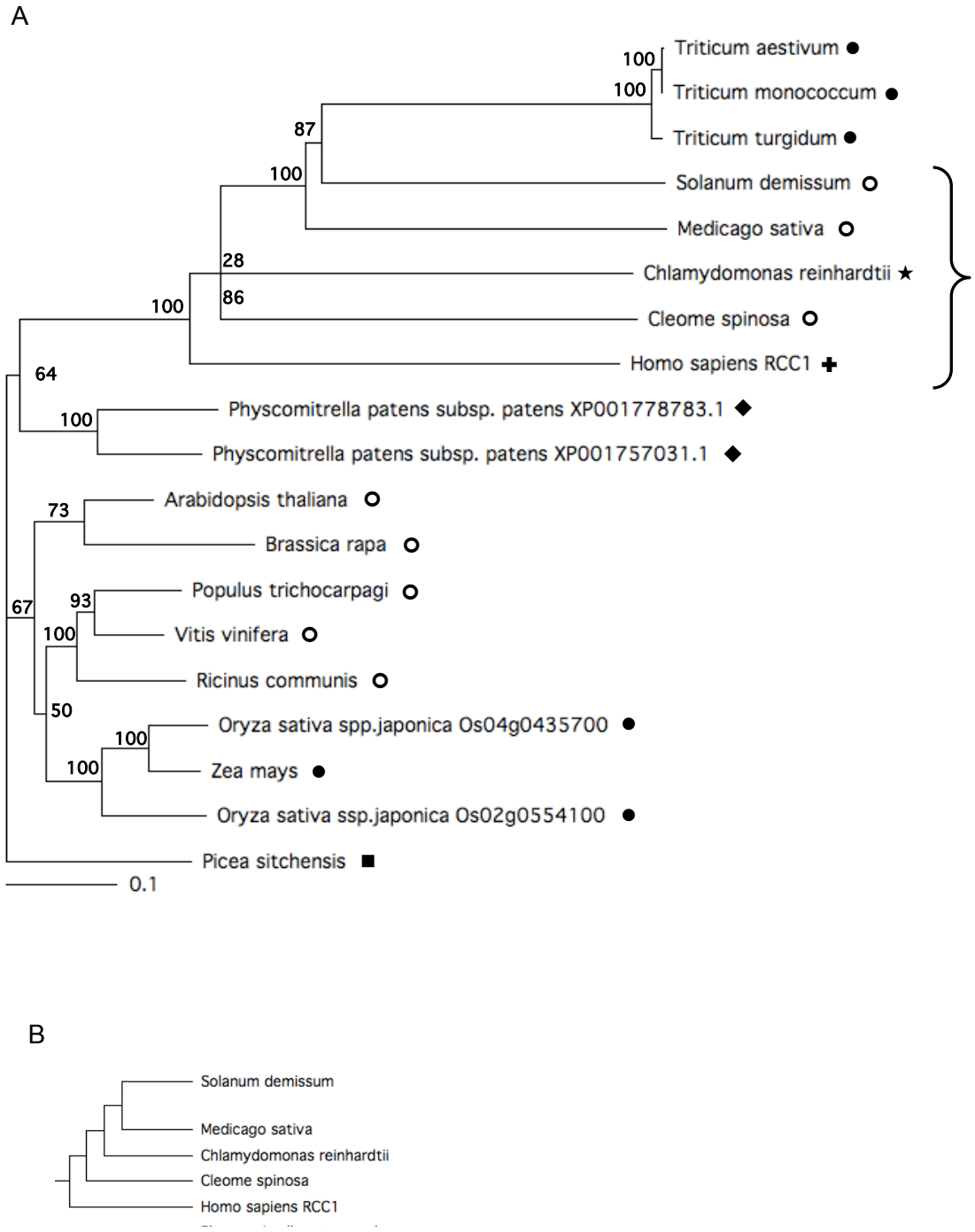

Figure 4.3 Phylogenetic tree showing the predicted evolutionary relationships between UVR8 in *Arabidopsis* and similar proteins in other species. A Distance tree showing the similarity between the UVR8 and potential homologues in other species. ○ = eudicots, ● = monocots, ■ = gymnosperms, ◆ = bryophytes, ★ = chlorophyta, ✚ = animal. **B** Depiction of the relationships of the branches shown in the brackets in A.

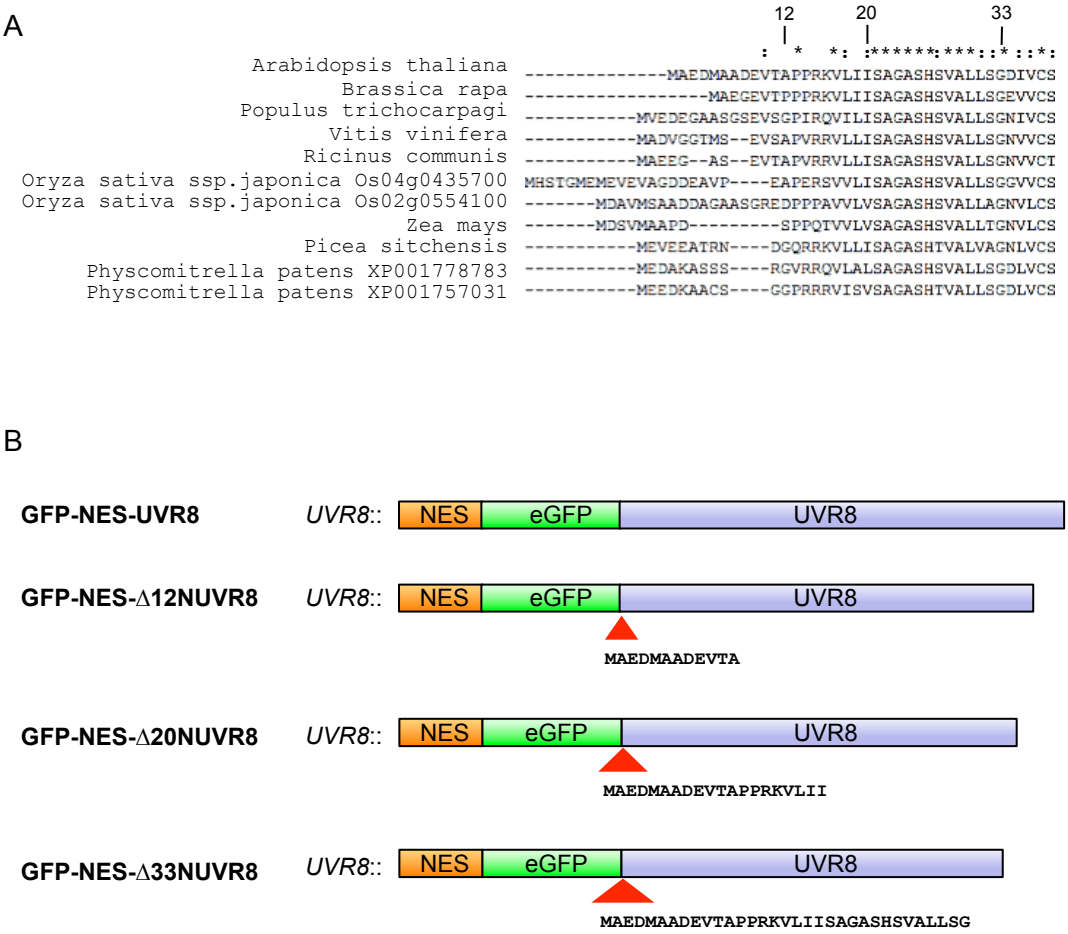

Figure 4.4 N-terminal UVR8 constructs. A Alignment of *Arabidopsis* UVR8 and similar proteins from other plant species. **B** N-terminal deletions generated with GFP tag and a nuclear exclusion signal (NES). Deleted amino acids are shown below the red triangles.

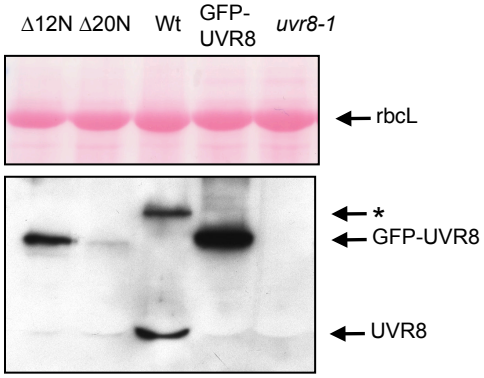

Figure 4.5 Expression levels of constructs *in planta*. Western blots showing the protein levels of Δ12N (line 4.3) and Δ20N (line 8.3) in comparison to Wt and GFP-UVR8 levels. Plants were grown for three weeks in 20 μmol m^{-2} s^{-1} white light. 20 μg total protein extract loaded for each lane. UVR8 was detected using a specific antibody raised against a C-terminal region of the protein. Asterisk marks the unknown upper band sometime seen in Wt samples.

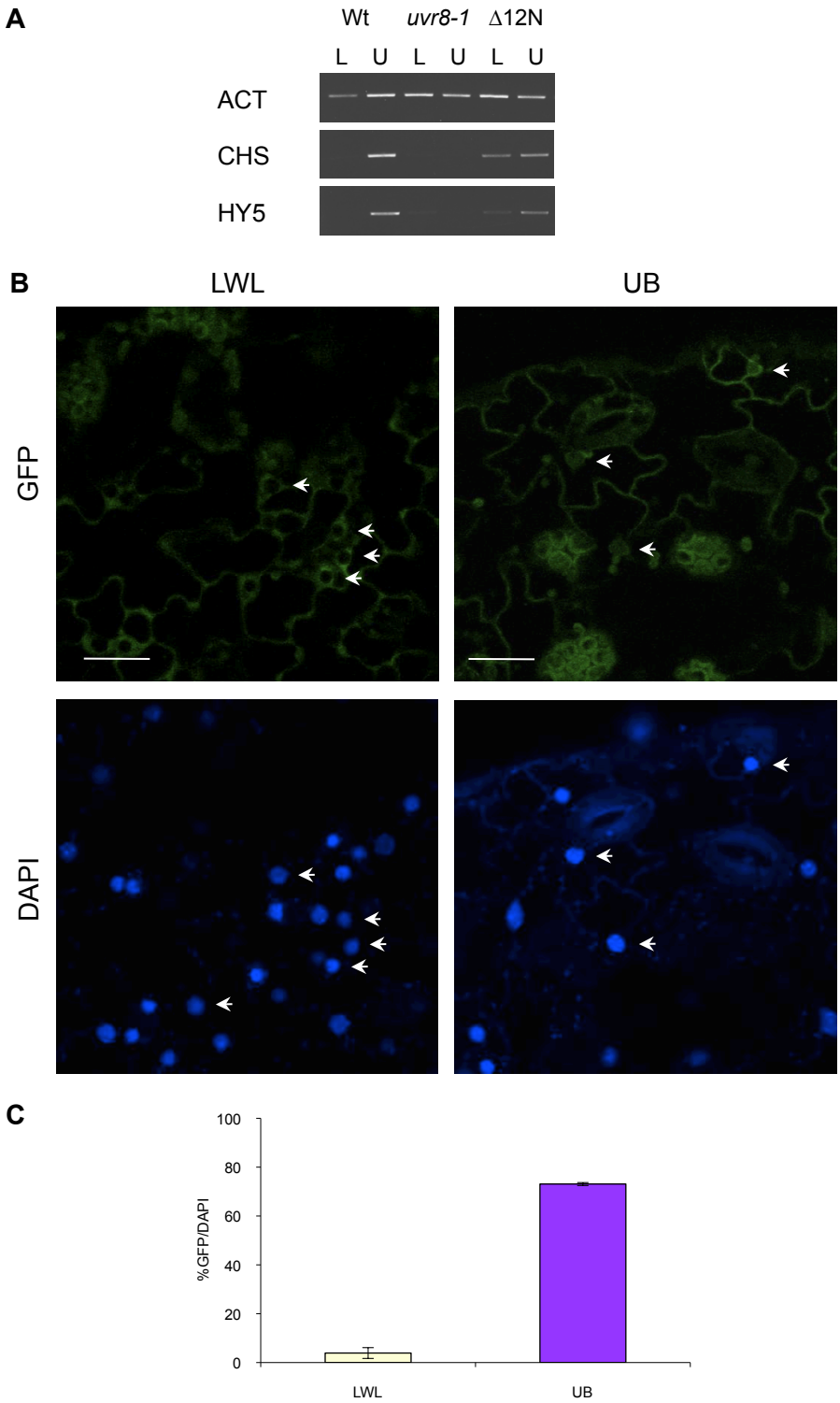

Figure 4.6 NES-GFP-Δ12NUVR8 rescues the phenotype of *uvr8-1* and accumulates in the nucleus in response to UV-B in *Arabidopsis*. Three week old Arabidopsis plants grown in a low fluence rate of white light (20 µmol m^{-2} s^{-1}) were treated with either four hours of 1 µmol m^{-2} s^{-1} UV-B (UB) or were left in low white light as a control (LWL). **A** RT-PCR showing that expression of *CHS* and *HY5* upon UV-B exposure is rescued. Δ12N plants ($UVR8_{PRO}$::NES-GFP-Δ12NUVR8) were from T3 line 4.3; similar results also seen in the T2 line 1 (data not shown) . **B** Confocal images of leaf tissue taken from plants expressing $UVR8_{PRO}$::NES-GFP-Δ12NUVR8. DAPI was used to stain nuclei. Scale bar represents 20 μm **C** Graph depicts the percentage of nuclei that show co-localisation of DAPI stain as well as GFP fluorescence in 20 μmol m^{-2} s^{-1} white light (LWL) and 2 hours 3 μmol m^{-2} s^{-1} UV-B (UB). Above results show data obtained from T3 line 4.3 averaged over three experiments, bars show standard error. p = 0.0003. Similar results were also found for the T2 line 1 (data not shown).

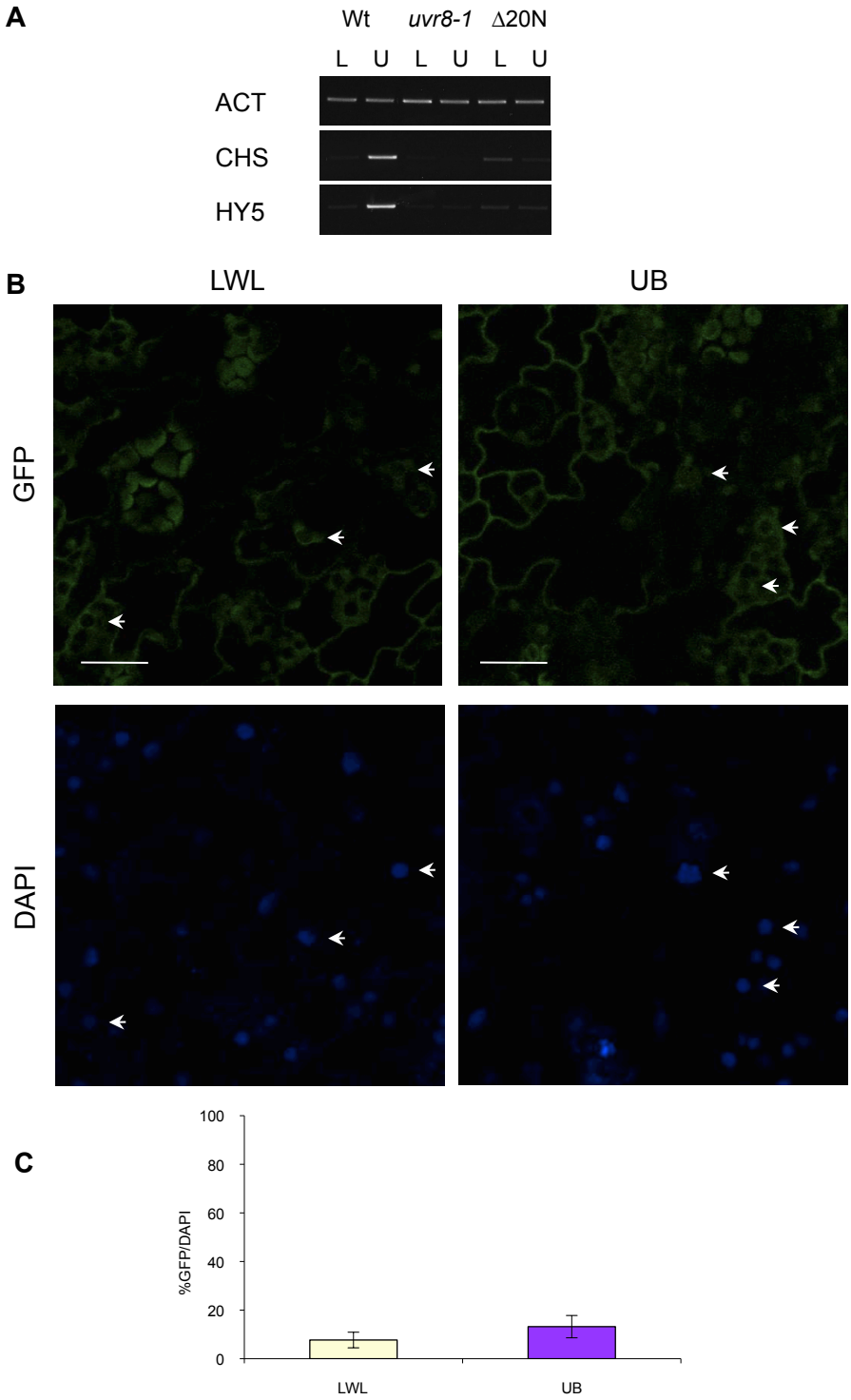

Figure 4.7 NES-GFP-Δ20NUVR8 is unable to rescue the phenotype of *uvr8-1* plants and is localised mainly in the cytoplasm in both low white light and UV-B in *Arabidopsis*. Three week old Arabidopsis plants grown in a low fluence rate of white light (20 µmol m^{-2} s^{-1}) were treated with either four hours of 1 µmol m^{-2} s^{-1} UV-B (UB) or were left in low white light as a control (LWL). **A** RT-PCR showing that expression of *CHS* and *HY5* upon UV-B exposure is not rescued. Δ20N ($UVR8_{PRO}$::NES-GFP-Δ20NUVR8) results shown for T3 line 8.3; similar result also seen for T2 line 28 (data not shown). **B** Confocal images of leaf tissue taken from plants expressing $UVR8_{PRO}$::NES-GFP-Δ20NUVR8. DAPI was used to stain nuclei. Scale bar represents 20 μm. **C** Graph depicts the percentage of nuclei that show co-localisation of DAPI stain as well as GFP fluorescence in 20 μmol m^{-2} s^{-1} white light (LWL) and 2 hours 3 μmol m^{-2} s^{-1} UV-B (UB). Above results show data obtained from T3 line 8.3 averaged over three experiments, bars show standard error. p = 0.3. Similar results were also found for T2 line 28 (data not shown).

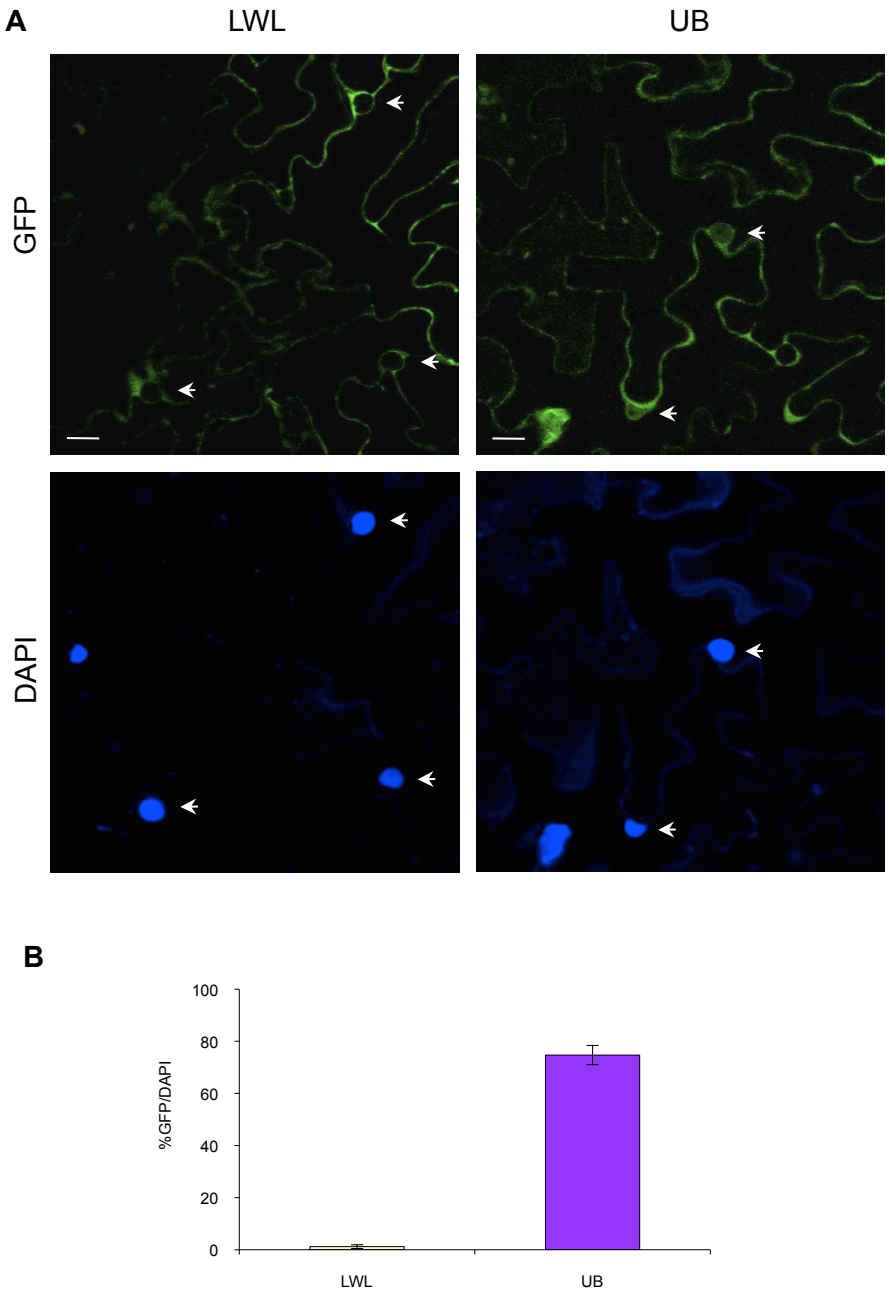

Figure 4.8 NES-GFP-UVR8 is localised in the cytoplasm under low fluence rate white light but accumulates in the nucleus under UV-B in tobacco. A Confocal images of leaf tissue taken from tobacco plants (*Nicotiana benthamiana*) transiently expressing $UVR8_{PRO}$::NES-GFP-UVR8 construct. DAPI was used to stain nuclei. Scale bar represents 20 μM **B** Graph depicts the percentage of nuclei that show co-localisation of DAPI stain as well as GFP fluorescence in 20 μmol m^{-2} s^{-1} white light (LWL) and 2 hours 3 ± 1 μmol m^{-2} s^{-1} UV-B (UB). Graph depicts results from a minimum of 70 images, bars show standard error. $p < 2.2x10^{-16}$.

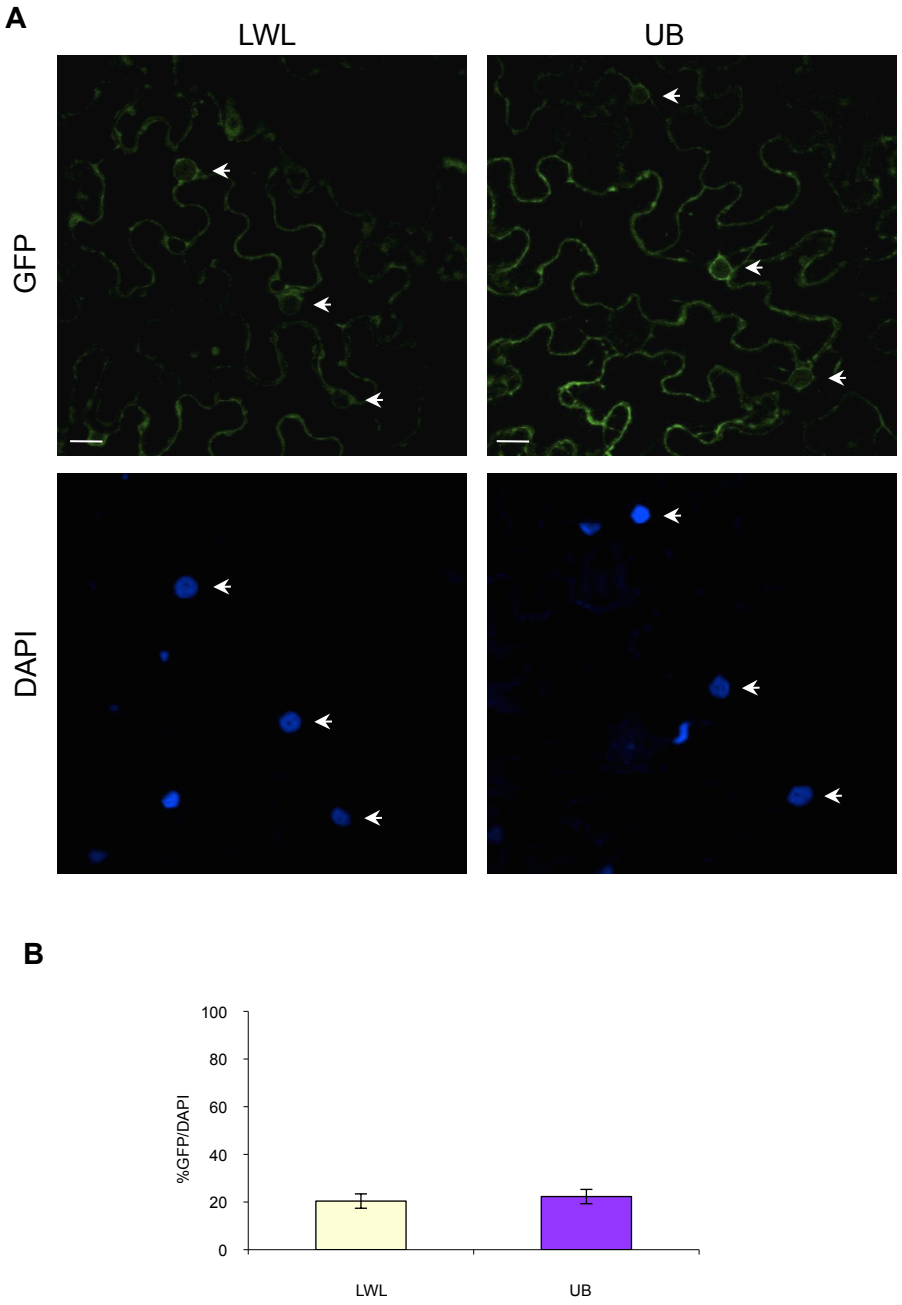

Figure 4.9 NES-GFP-Δ33N is localised in the cytoplasm under both low white light and UV-B in tobacco. A Confocal images of leaf tissue taken from tobacco plants (*Nicotiana benthamiana*) transiently expressing $UVR8_{PRO}$::NES-GFP-Δ33N construct. DAPI was used to stain nuclei. Scale bar represents 20 μm. **B** Graph depicts the percentage of nuclei that show co-localisation of DAPI stain as well as GFP fluorescence in 20 μmol m^{-2} s^{-1} white light (LWL) and 2 hours 3 ± 1 μmol m^{-2} s^{-1} UV-B (UB). Graph depicts results from a minimum of 70 images, bars show standard error. p = 0.9.

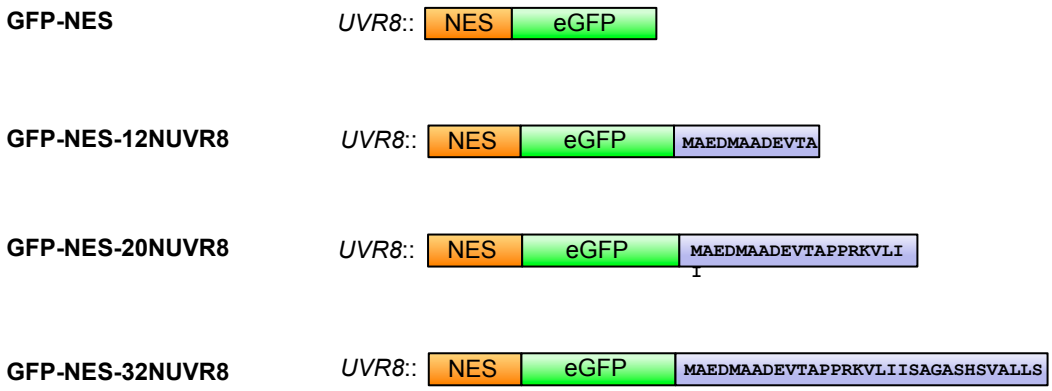

Figure 4.10 N-terminal UVR8 constructs. Constructs generated with either the GFP tag and NES signal only, or with the addition of portions of the N-terminal region of UVR8.

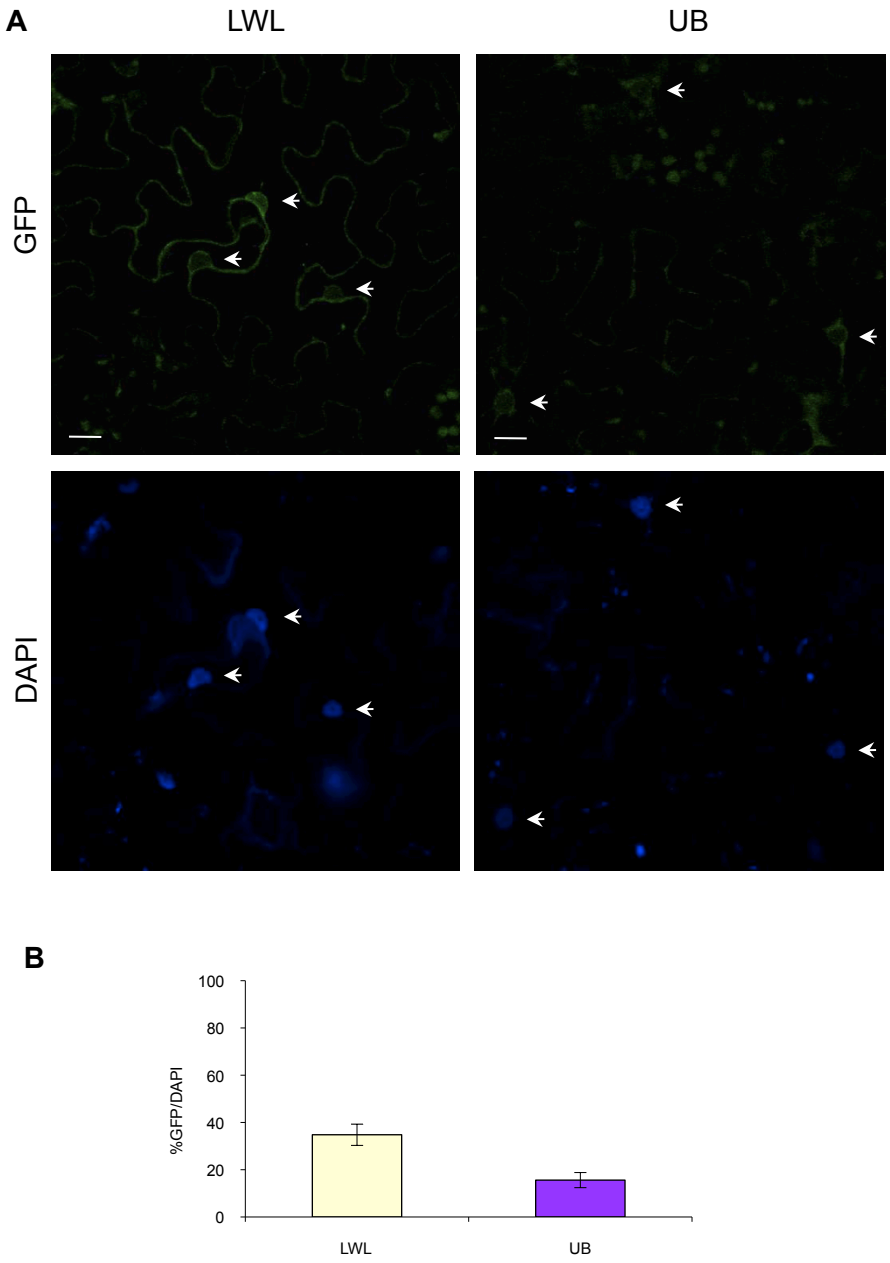

Figure 4.11 NES-GFP is mainly localised in the cytoplasm under both low fluence rate white light and UV-B in tobacco. A Confocal images of leaf tissue taken from tobacco (*Nicotiana benthamiana*) plants transiently expressing $UVR8_{PRO}$::NES-GFP construct. DAPI was used to stain nuclei. Scale bar represents 20 μM. **B** Graph depicts the percentage of nuclei that show co-localisation of DAPI stain as well as GFP fluorescence in 20 μmol m^{-2} s^{-1} white light (LWL) and 2 hours 3 ± 1 μmol m^{-2} s^{-1} UV-B (UB). Graph depicts results from a minimum of 70 images, bars show standard error. p = 0.0007.

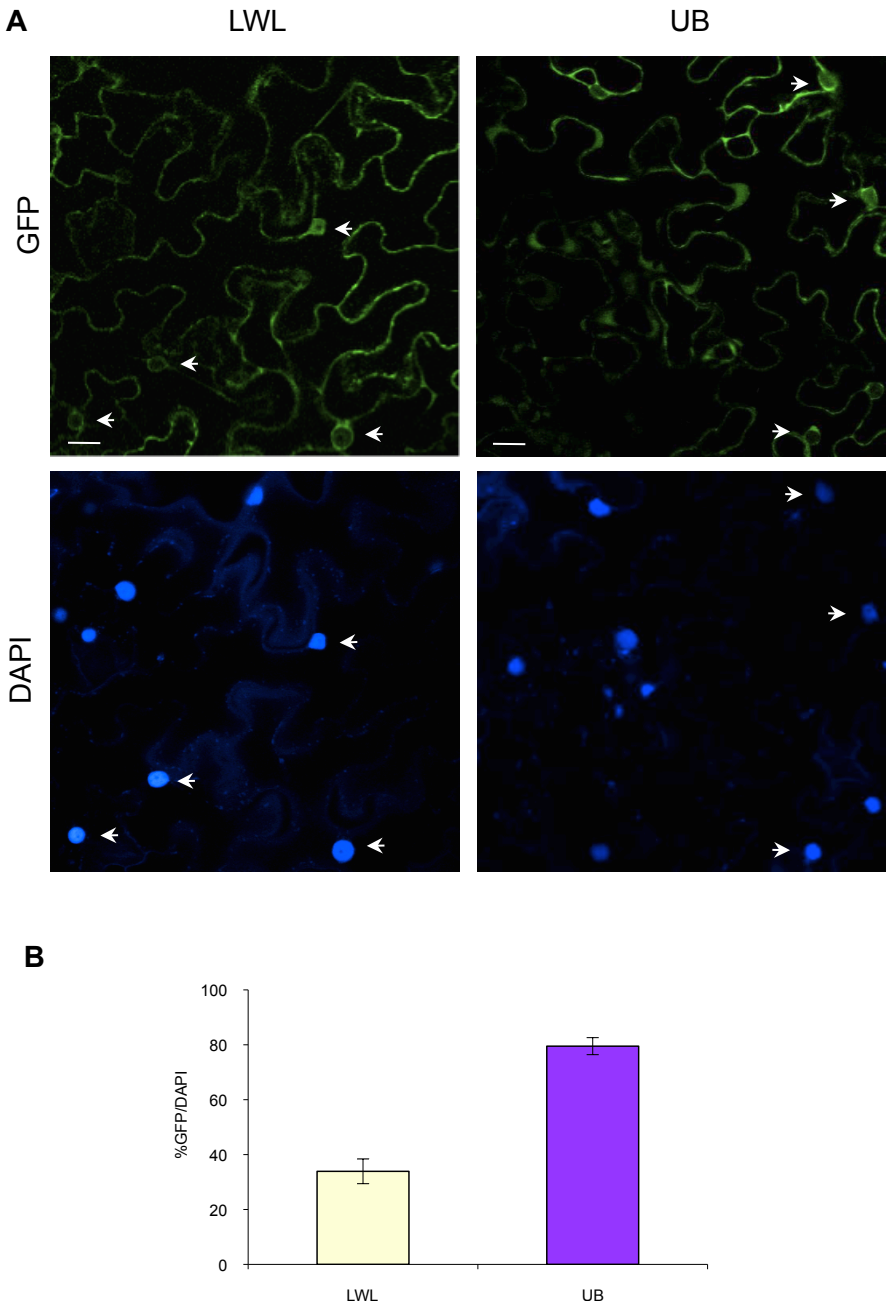

Figure 4.12 NES-GFP-12NUVR8 is localised mainly in the cytoplasm in low fluence rate white light and accumulates in the nucleus in response to UV-B in tobacco. A Confocal images of leaf tissue taken from tobacco plants (*Nicotiana benthamiana*) transiently expressing the $UVR8_{PRO}$::NES-GFP-12NUVR8 construct. DAPI was used to stain nuclei. Scale bar represents 20 μM. **B** Graph depicts the percentage of nuclei that show co-localisation of DAPI stain as well as GFP fluorescence in 20 μmol m^{-2} s^{-1} white light (LWL) and 2 hours 3 ± 1 μmol m^{-2} s^{-1} UV-B (UB). Graph depicts results from a minimum of 70 images, bars show standard error. $p = 4.7 \times 10^{-14}$.

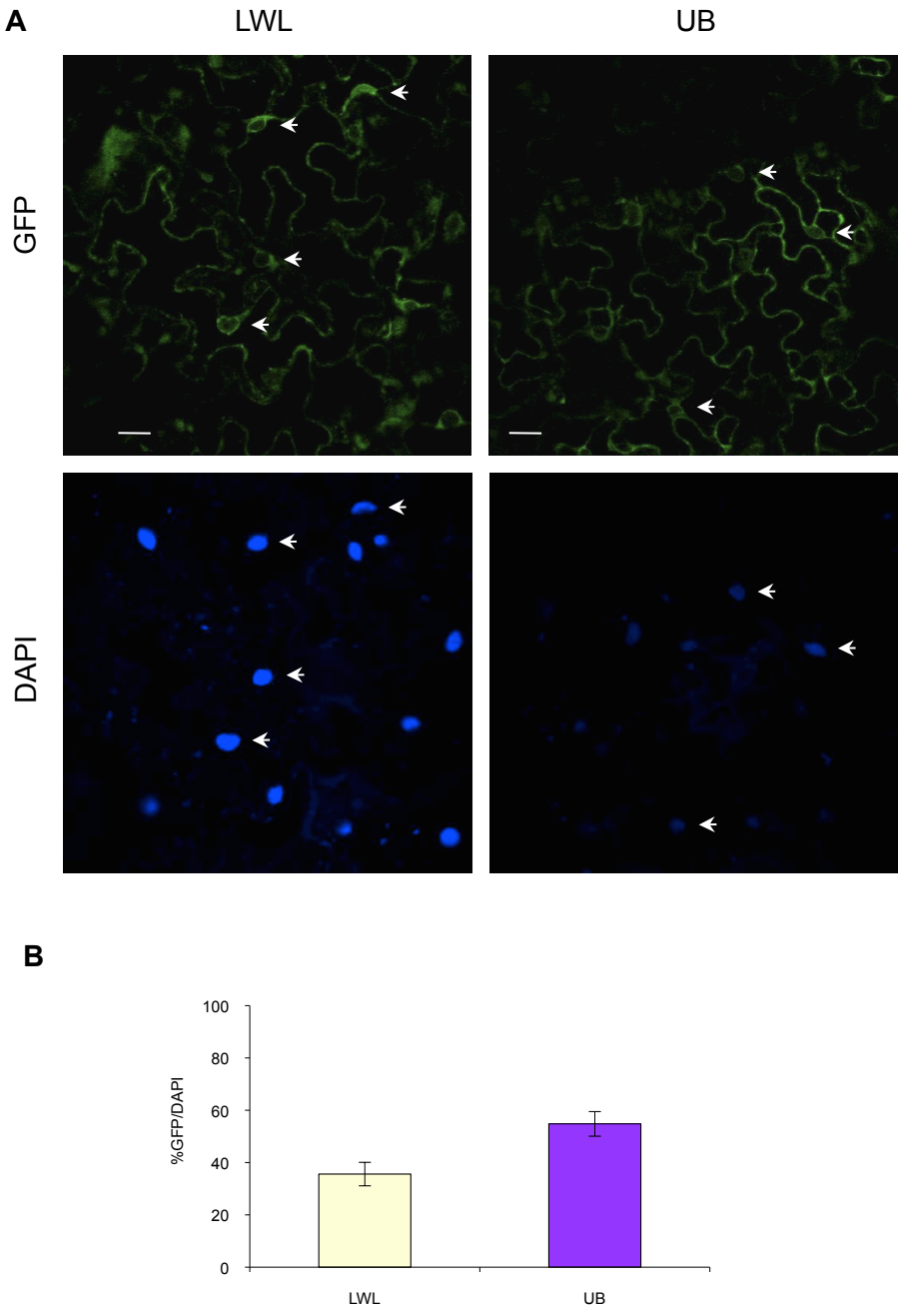

Figure 4.13 NES-GFP-20NUVR8 is localised mainly in the cytoplasm under low fluence rate white light and in the nucleus under UV-B in tobacco. A Confocal images of leaf tissue taken from tobacco plants transiently expressing the $UVR8_{PRO}$::NES-GFP-20NUVR8 construct. DAPI was used to stain nuclei. Scale bar represents 20 μM. **B** Graph depicts the percentage of nuclei that show co-localisation of DAPI stain as well as GFP fluorescence in 20 μmol m^{-2} s^{-1} white light (LWL) and 2 hours 3 ± 1 μmol m^{-2} s^{-1} UV-B (UB). Graph depicts results from a minimum of 70 images bars show standard error. p = 0.004.

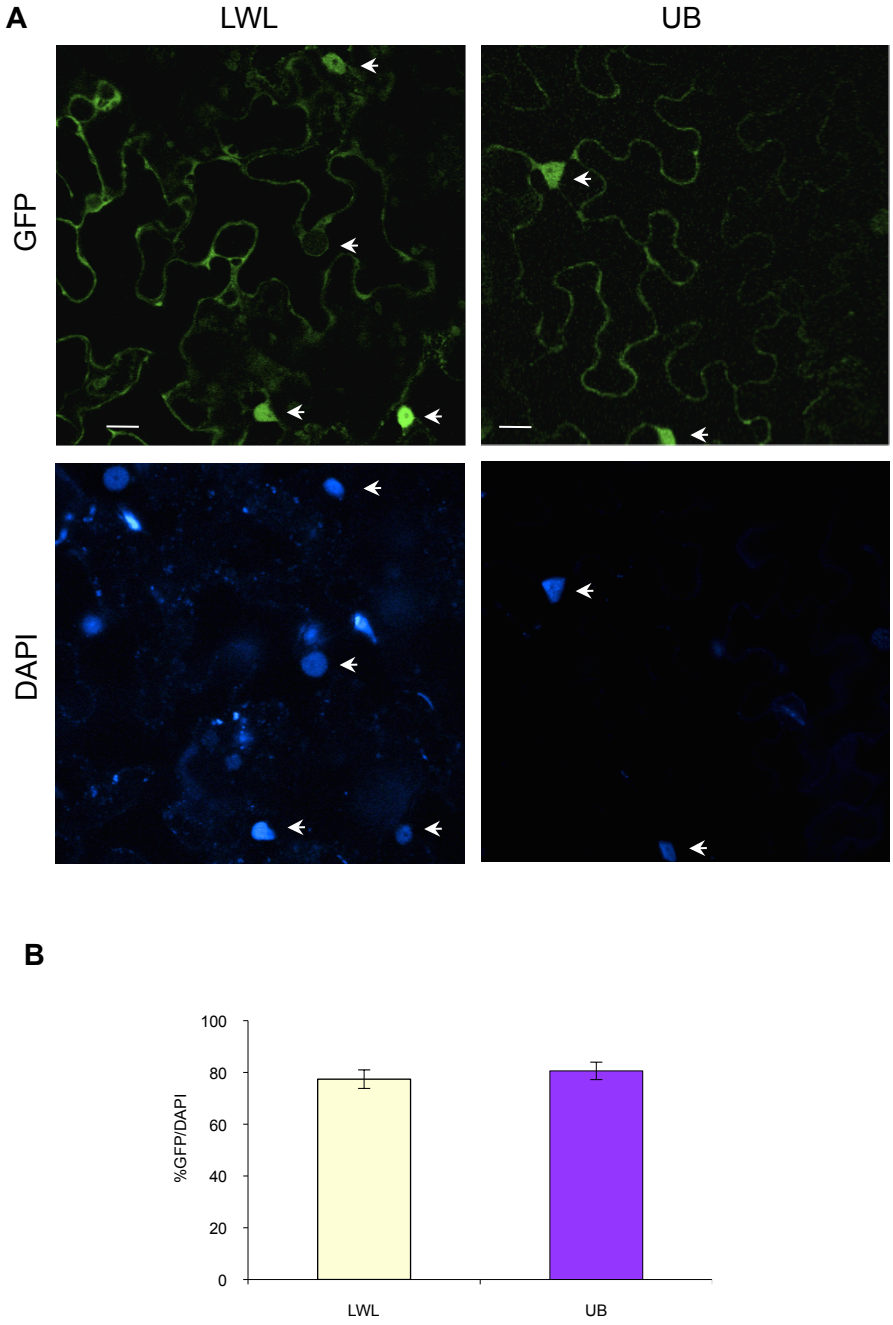

Figure 4.14 NES-GFP-32NUVR8 is localised in the nucleus under both low fluence rate white light and UV-B in tobacco. A Confocal images of leaf tissue taken from tobacco plants (*Nicotiana benthamiana*) transiently expressing the $UVR8_{PRO}$::NES-GFP-32NUVR8 construct. DAPI was used to stain nuclei. Scale bar represents 20 μM. **B** Graph depicts the percentage of nuclei that show co-localisation of DAPI stain as well as GFP fluorescence in 20 μmol m^{-2} s^{-1} white light (LWL) and 2 hours 3 ± 1 μmol m^{-2} s^{-1} UV-B (UB). Graph depicts results from a minimum of 70 images, bars show standard error. p = 0.5.

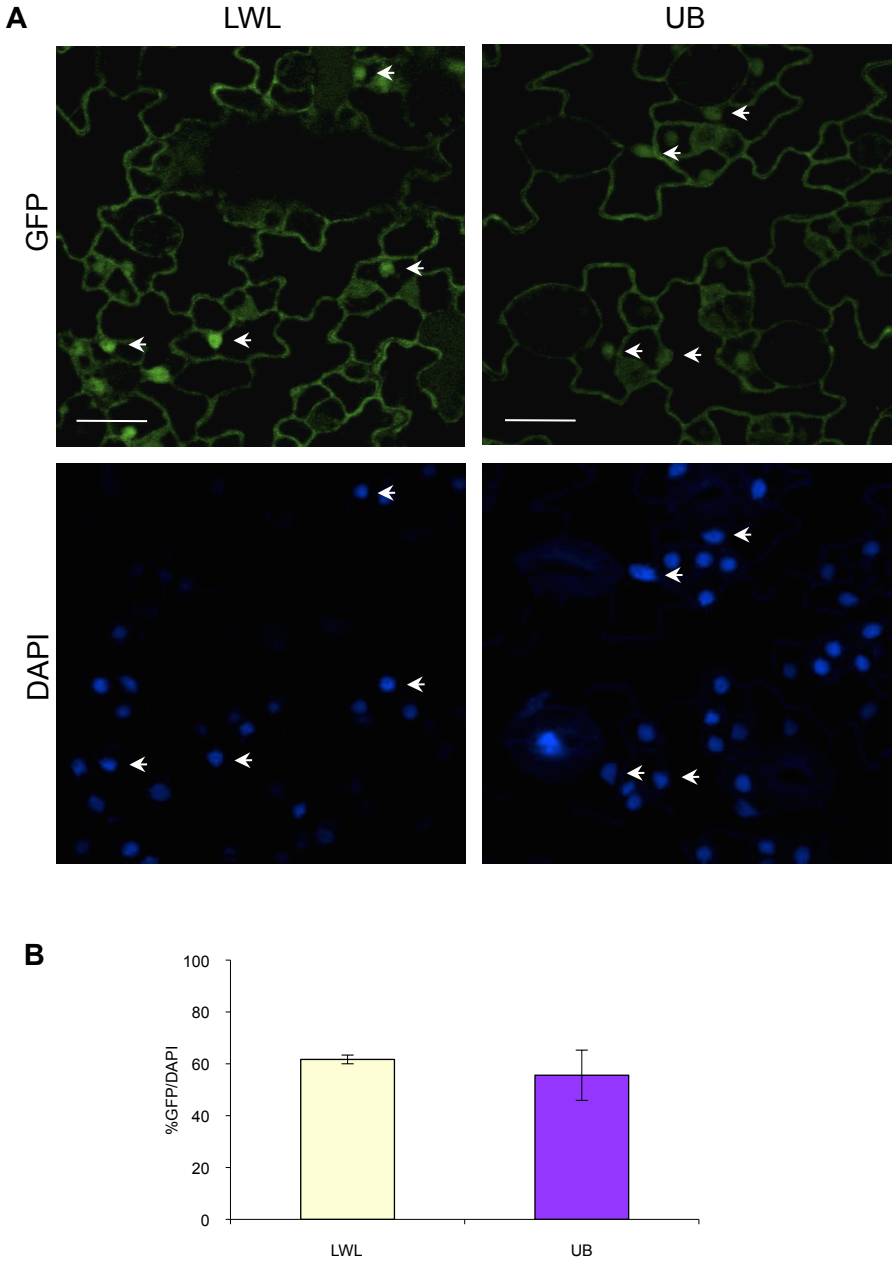

Figure 4.15 NES-GFP-32NUVR8 is mainly localised in the nucleus under both low fluence rate white light and UV-B in *Arabidopsis*. A Confocal images of leaf tissue taken from stably transformed T1 *Arabidopsis* plants expressing the $UVR8_{PRO}$::NES-GFP-+32N construct. DAPI was used to stain nuclei. Scale bar represents 20 μM. **B** Graph depicts the percentage of nuclei that show co-localisation of DAPI stain as well as GFP fluorescence in 20 μmol m^{-2} s^{-1} white light (LWL) and 2 hours 3 UV-B (UB). Bars show standard error. Results averaged over three experiments. $p = 0.5$.

CHAPTER 5 THE UVR8 COMPLEX

5.1 Introduction

In many situations, cellular proteins do not work in isolation but instead as part of a complex either through binding to additional monomers or via interaction with one or more other proteins. It is therefore a very real possibility that the UVR8 protein may also be acting as part of complex. This complex, for example, may be necessary for the nuclear accumulation/cytoplasmic retention under different light conditions, for recruitment of transcription factors at promoter sites or a number of other processes. Indeed the discovery of interacting partners could give rise to vital insights into the function of this protein and its mechanisms of action. Currently several techniques exist which can identify such interactions, for example mass spectrometry and yeast-two hybrid assays. Both of these methods have been utilised by members of the Jenkins lab to identify proteins interacting with UVR8, but without a great deal of success. For the former, obtaining sufficient protein amounts proved difficult while for the latter, no candidates were identified. As a consequence, this chapter describes further attempts to identify potential UVR8-interacting proteins. First, efforts to boost protein concentration levels for use with mass spectrometry are described. Secondly, an alternative method, Size Exclusion Chromatography (SEC), was used and the results obtained are detailed.

While the first of these approaches proved unfruitful, results from SEC experiments show that UVR8 does indeed appear to exist as part of a complex that is of a constant size under different light conditions. Furthermore, the size of this complex alters disproportionally with the addition of a GFP tag and shows a dramatic reduction in size with the deletion of the first 23 N-terminal amino acids.

5.2 Results

5.2.1 Extraction of proteins from pea, cabbage and cauliflower tissue

As previous attempts to analyse the UVR8 protein using mass spectrometry had failed, partly due to low protein concentration, it was decided to turn to other plant tissues that may be processed in bulk. These had the potential to yield much larger amounts of the protein to submit for analysis. Pea was selected as there were already plants being grown for use within the department. It is also suitable as this species has been used in many

previous biochemical studies and produces a relatively large amount of leaf tissue (in comparison to *Arabidopsis*) per plant. In addition to pea tissue, cabbage leaves and cauliflower florets were also both analysed. As members of the Brassicacea family these species are relatively close to *Arabidopsis* thus increasing the chance of detection using the *Arabidopsis* UVR8 antibodies. A further advantage to using the latter two species is that tissues selected for extraction contain relatively little rubisco. This protein is highly abundant in photosynthetically active tissues. Its size (in monomer form) is quite close to that of UVR8 and thus the sheer abundance of this protein can complicate protein analysis. Hence using rubisco-poor tissues should decrease the noise in samples. This is especially true of cauliflower floret samples which have extremely low levels of rubisco (relative to green leafy tissue). It should be noted that previous work (Kaiserli PhD thesis, 2008) has shown that the UVR8 protein is present in almost all tissues including flowers. We can therefore expect that reasonable amounts should be present in cauliflower florets.

For each of the three species described above, 1g of tissue was harvested and protein extracted using standard *Arabidopsis* protein extraction methods (see Section 2.9.1). Ten, 20 and 40 μg total protein extract were loaded onto 10 % SDS gels along with 20 μg extract from wild type *Arabidopsis* as a positive control. A variety of protein concentrations (as determined by Bradford assay) were used to ensure that clear bands were detected for each plant species (i.e. not too feint or strong). Protein blots were performed and probed with N and C-terminal UVR8 antibodies as described in Section 2.9.4. Both antibodies were tested to try to maximise identification of UVR8 homologues in these species. As we do not have sequences for UVR8-homologues in these plants it was uncertain if the antibodies would bind appropriately. The experiment was repeated three times and representative blots are shown in Figure 5.1.

In most examples presented here, no bands were detected for either antibody whether of a size similar to that of *Arabidopsis* UVR8 or not. The exception to this was for C-terminal antibody probed pea blots. These showed evidence of bands, albeit much higher and more faint than for *Arabidopsis*. It is therefore apparent that the sequences of UVR8 homologues in these species are not sufficiently similar to be detected using antibodies generated specifically for *Arabidopsis* UVR8. Consequently, in vitro pull-down methods using immobilised UVR8 antibodies (in order to enrich samples for the UVR8 protein and its potential interactors) would also be unsuccessful.

It would therefore seem that this strategy is not an appropriate one to search for potential interacting proteins unless a new antibody is produced, and other avenues should be pursued.

5.2.2 UVR8 protein extraction and stability

Once the previous results had been taken into consideration, it was reasoned that use of other plant species to extract UVR8 would not be suitable for analysis via mass spectrometry. It was therefore decided to return to *Arabidopsis* and try an alternate method for protein analysis, namely Size Exclusion Chromatography (SEC). This technique involves the separation of proteins and protein complexes according to size by passage through a Superose™ column. In summary the process involves loading a protein sample onto the top of the column and collection of the resulting fractions. The columns have been designed so that there is a strong relationship between the elution volume of a protein and the size of the complex it exists in (if any). Before these experiments were performed, as this was a new technique, it was decided to first optimise the process of protein extraction so that the greatest concentration of UVR8 could be obtained. In addition, it was necessary to ensure that this protein would remain stable throughout the fractionation process.

To address the first of these questions, the extraction buffer commonly used in the Jenkins lab was tested against a SDS buffer to see whether the former was really extracting the maximum amounts of UVR8 protein possible. It was hypothesised that an alternative buffer which contained SDS, in addition to a boiling treatment, might further break up cellular membranes and thus release more UVR8 into solution. First, protein was extracted using the standard microextract buffer as described in Section 2.9.1. Next a second sample of leaf tissue was ground in a 2 % SDS buffer and boiled for 5 mins. Both of these protein samples were then tested for total protein concentration using the Bradford Assay. 20 µg total protein extract for each was loaded onto a 10 % SDS gel and a standard western blot performed. Membranes were probed with the C-terminal UVR8 antibody. This was repeated three times to ensure consistent results.

The results presented in Figure 5.2 A show that, contrary to predictions, microextraction buffer out-performs the SDS buffer in terms of UVR8 protein levels. Therefore, not only does the former procedure seem to release reasonable amounts of UVR8 protein but also appears to be a generally better method of extraction than a stronger SDS buffer. Consequently it was decided to continue to use this buffer in all subsequent protein extractions.

Although an appropriate buffer had been selected, it was still a possibility that the disruption of cellular membranes is not as thorough as possible. Furthermore, UVR8 binds strongly to chromatin. It is thus possible that this binding may prevent full solubilisation

and movement of UVR8 into native protein gels and also the Superose™ column. In order to determine whether this may indeed be the case, a protein sample extract was subjected to a brief sonication to break up the chromatin and cell membranes, thereby potentially releasing yet more UVR8. This sonicated sample, along with an untreated one, were again run on a protein gel, a blot performed and probed with a UVR8 specific antibody.

As can be seen from the blots in Figure 5.2 B, the relative protein concentrations of samples pre and post-sonication are roughly equal. It is therefore unlikely that the chromatin binding properties of UVR8 are limiting its availability in protein gels. Therefore, inclusion of a sonication step in the protein extraction process was deemed unnecessary.

While the microextraction buffer has many advantages and was found to extract good amounts of UVR8, it was established during initial runs through the Superose™ column that it gave rise to build-up in pressure and a slow running column. This is most likely due to the relatively high concentration of glycerol in this buffer. Generally for this type of column a phosphate buffer is recommended. Therefore it was decided to test the stability of the UVR8 protein in this alternate buffer solution. As the microextraction buffer proved the most efficient for extraction, the decision was made to continue to extract using this method but then subsequently exchange buffers using dialysis. This process involves loading protein samples into Slide-a-lyzer dialysis cassettes which are then suspended in the desired phosphate buffer solution overnight at 4 ºC with gentle stirring. While previous handling of the UVR8 protein had found it to be stable at 4 ºC for periods of approximately 24 hours, it is possible that the protein would not be as stable in this particular buffer. In addition, after this dialysis, protein samples would be run on the column for several hours at room temperature, potentially also resulting in degradation. Thus, to investigate this, an experiment was performed whereby samples were incubated at a variety of different temperatures. This included samples taken directly after dialysis as well as after 6 hours at standard room temperature and also at 27 ºC (on a particularly hot few days over the summer). These samples were then run on protein gels and blots performed to determine whether any degradation had occurred.

Figure 5.2 C shows that the bands pre and post dialysis, as well as across all incubation temperatures, are sharp and show no signs of the blurring indicative of protein degradation. It therefore seems that neither dialysis of the protein at 4 ºC nor running the column at room temperature will adversely affect the stability of the UVR8 protein itself.

Interestingly however, it appears that a difference in the band patterns arises in dialysed samples. Occasionally when blots are probed with the UVR8 antibody two other

bands can be seen; one appears as a band just above/below that of UVR8 and sometimes a much larger upper band can be seen at roughly the 80 kDa mark. Until this time, neither were consistently produced nor any particular treatment or condition identified which reliably gives rise to this phenomenon. It should be noted that a similar pattern was observed when this experiment was repeated. It would therefore appear that either the dialysis process or the incubation overnight at 4 ºC might cause this.

Nevertheless, it appeared that preparation of protein samples was optimised to the best of our knowledge. Therefore the next stages in the preparation of the experiment were undertaken. Focus was turned to producing a standard curve for the column so that protein complex sizes could be determined.

5.2.3 Generation of standard curves for Size Exclusion Chromatography

In order to calculate protein/protein complex sizes, a series of standards first has to be run on the column so that a standard curve can be generated. Each of the protein standards (ovalbumin, conalbumon, aldolase and ferretin) and the column were prepared as per manufacturers instructions. Each of the standards was then run separately on the column. A chromatogram is thus produced for each protein, the peak of which can be used to read off the elution volume for that particular sample. This elution volume in combination with the void volume and column volume, can be used to calculate a value for Ka (for equation see Figure 5.3). This was then plotted for each of the standards against the log of their respective molecular weights (logMr). A line of best fit was drawn thus giving the equation ($y = -0.010x + 0.085$) as can be seen in Figure 5.3. By using these equations in reverse the sizes of unknown samples can be inferred.

To determine whether this system worked effectively, sizes were calculated for a protein of known size, rubisco (approximately 540 kDa). For preliminary experiments, blots were stained for presence of protein by ponceau staining. Similar to the method used for UVR8 whereby membranes are probed with antibody, this reveals which fractions have high levels of the protein of interest. In the case of rubisco, bands resulting from a ponceau stain can be easily identified and are often used as evidence for equal loading. Therefore, which fraction shows the greatest amount of rubisco (i.e. thickest band) can be identified. For example, in the representative blot shown in Figure 5.3 B, it can be seen that the peak fraction is number 26. With the knowledge that each fraction contains 300 µl, we can determine the elution volume and hence approximate complex size. In this example this gave a value of ~500 kDa for rubisco, quite close to the reported size of approximately 540 kDa.

This process was repeated for the 60 kDa aspecific band which appears when samples are probed using the anti-GFP antibody. The resulting banding pattern implied a size of about 50 kDa for this protein. This suggests that the protein responsible for the bands seen on such blots exists as a monomer.

While both these values are somewhat smaller than we might expect, they are nevertheless quite close. To get this close to the apparent size of the protein is encouraging. It does however highlight the fact that this technique has comparatively less power in detecting small difference in size.

It should be noted that bands here (particularly for rubisco stains) are particularly large as a total of ~600-800 μg total protein extract was loaded onto the column. Such large protein amounts are needed to reduce the effects due to dilution in the 24 ml column.

Consequently as it appeared that this method did indeed seem to detect different protein sizes with reasonable accuracy over a wide range of sizes, it was decided to continue and test a number of mutants and transgenic lines available within the Jenkins group.

5.2.4 UVR8 protein levels across mutants and transgenic lines to be studied.

Prior to performing the size exclusion experiments, it was decided to run protein blots to determine comparative protein expression levels in transgenic lines expressing each of the constructs. In particular, work on some of the constructs had shown decreasing protein levels in comparison to the original T3 lines described by Kaiserli and Jenkins (2007). If appropriate bands could be detected to reasonable levels, this should mean that sufficient complex would be present to detect using SEC methods.

For each construct to be tested protein was extracted either directly from white light grown 3 week-old seedlings or after a 4 hour treatment with 1 μmol m^{-2} s^{-1} UV-B. 20 μg total protein extract from these plants was then run on 10 % SDS gels, western blots performed and membranes probed with either the C-terminal or GFP antibody. Wild type or GFP samples were included in each run for comparison. Representative blots of these can be seen in Figure 5.4.

Firstly wild type, the GFP-UVR8 and the NLS or NES tagged versions of UVR8 were tested. As can be seen in Figure 5.4 the expression levels vary considerably. Relative to wild type levels, there is a greater concentration of GFP-UVR8, in line with results shown by Kaiserli (2008). The same blot however shows a low concentration of NLS and very little NES at all. Initial work with the original NLS and NES lines had shown higher levels of expression (Kaiserli PhD thesis, 2008). However, later generations

of these plants are currently being used in the lab and it would seem that expression levels have been reduced perhaps due to silencing effect. Nevertheless, as much larger total protein amounts were to be loaded onto the column (600-800 µg), it was decided that there would be sufficient levels to detect in the fractions when loaded onto a protein gel.

Next Δ23N samples were run alongside GFP-UVR8. In Figure 5.4 B it can be seen that levels appear to be roughly equal to that of GFP-UVR8. On this particular gel, samples were run for longer than usual. The result of this is the appearance of two bands of very close size. Similarly to the large upper band, the cause of this double band remains elusive and unpredictable. While it is not entirely clear which of these, or alternatively both, are UVR8, they appear to have roughly even levels both within a sample and across all samples shown here.

Finally Figure 5.4 C shows sample extracted from wild type tissue and from the *cop1-4* mutant. Here, as we would expect, the protein levels of UVR8 are not altered by the loss of functional COP1. Interestingly, these samples show the large upper band only in the wild type samples. The meaning behind this is not clear and warrants further investigation.

In summary, it seemed that all constructs would produce sufficient UVR8 levels for analysis using SEC and therefore detailed investigation into the sizes of this potential complex was initiated.

5.2.5 UVR8 exists in a 70-90 kDa complex size in wild type tissue

When Western blotting is performed on protein samples extracted form *uvr8-1* tissue and probed with either UVR8 antibody (C or N-terminal), no bands can be seen. However, to be certain that the methods used here in combination with the huge increase in the amount of protein analysed do not alter this fact, it was decided first to look at resulting fractions when samples collected from *uvr8-1* plants are loaded onto the column. *uvr8-1* plants were grown for three weeks in low fluence rate white light conditions (20 µmol m^{-2} s^{-1}) and tissue harvested. Protein was extracted and sample dialysed as detailed above and in Chapter 3. Approximately 600-800 µg total protein extract was loaded onto the column and 80 fractions of 300 µl were collected. As these fractions were of a relatively large volume they were first concentrated using StrataClear™ resin prior to loading onto a 10 % SDS protein gel. A western blot was performed and the membrane probed with the C-terminal UVR8 antibody. In Figure 5.5 A a broad range of fractions are shown in order to determine whether any bands can be seen.

As for previous studies, this UVR8 Ct terminal antibody (generally the more sensitive of the two UVR8 antibodies) does not detect any UVR8 protein in this sample. We are therefore confident that bands in these, and subsequent samples only arise as a result of UVR8 presence.

The next questions to address were whether native UVR8 exists in a complex and if so, whether the complex size would differ between plus and minus UV-B conditions. Therefore, wild type plants were grown for three weeks in low fluence rate white light. Half of these where then harvested for protein extraction directly, while the second half were first exposed to a 4 hour 1 μmol m^{-2} s^{-1} UV-B treatment. The SEC process was then performed as described above. For each treatment the procedure was repeated three times, the approximate complex sizes calculated which were then averaged to give the values show in Figure 5.5. Only the blots of select fractions (19-44) are shown here as preliminary experiments had shown that bands were only present in this range of samples.

On first examining the blots shown in Figure 5.5, it can be seen that the band pattern under UV-B and low white light are very similar. The peak fraction for each appears between number 31-32. Calculations from this and for the two other repeat experiments gave average protein sizes of approximately 90 and 70 kDa for white light and UV-B respectively. This is noticeably larger than the size of a UVR8 monomer (42 kDa). It thus seems that UVR8 may indeed be interacting with a protein or proteins with a size/cumulative size of 50 and 30 kDa respectively. The size difference between the two light treatments however is not large; therefore taking into account the relatively low resolution of the column, we cannot exclude the possibility that these two complexes are indeed the same size. Consequently, we cannot yet determine whether the complex components are the same or different (but of a similar size) under both or either light treatments. An interesting possibility, derived from the fact that the interacting protein appears to be roughly the same size as UVR8, is that UVR8 is naturally present as a dimer.

Looking at the blots again, it can be seen that the input lanes are quite faint. This shows that the fractions contain relatively large concentrations of the UVR8 protein. This is to be expected considering that 800 μg total protein extract was loaded onto the column and is spread over relatively few fractions. It is therefore possible that this method could be a means of enriching for UVR8 in samples to submit for mass spectrometry.

In summary, these results show that UVR8 exists in a complex. Consequently, it is of interest to try to investigate this further by use of different transgenics or mutants available to determine whether any of these show an alteration in protein size.

5.2.6 Addition of a GFP tag to UVR8 causes a large increase in complex size

The result from the previous section suggested the possibility that UVR8 might be present as a dimer. In order to test this theory as well as to assess the effect that the addition of a GFP tag would have (if any), it was decided to repeat the experiment using samples from GFP-UVR8 transformed plants. If the complex is a dimer of UVR8, then the resulting complex size from GFP-UVR8 samples should be approximately 144 kDa (42 kDa UVR8 plus the 30 kDa GFP tag gives rise to about a 72 kDa monomer). Alternatively, if UVR8 is interacting with something other than itself, the resulting complex should equate to roughly 100-120 kDa.

Before testing the GFP-UVR8 construct however, it was decided to determine the banding pattern resulting from use of the GFP antibody. Similarly to that described in the previous section, *uvr8-1* samples were run on the column and then probed with the GFP antibody. As expected, as can be seen in Figure 5.6A, the only bands present were the 60 kDa non-specific bands seen in all blots probed using this antibody. Therefore it looked as if this antibody could be used in subsequent experiments using GFP-tagged versions of proteins.

Subsequently, protein extracts from untreated and UV-B treated GFP-UVR8 plants were run on the column and analysed as described in previous sections. Figure 5.6 B shows the representative blots and the average (n = 3) calculated sizes for these samples.

Contrary to either prediction, protein blots from these samples showed a large shift towards fractions containing much larger proteins and protein complexes; the resulting average complex size from these is about 300 kDa and thus much larger than that attributable to formation of a dimer. It therefore seems that, by the addition of the GFP tag, we have introduced other elements to the complex. This therefore raises a number of possible explanations. One such possibility is that other unknown proteins are interacting with GFP and thereby artificially increasing the size of the overall complex.

It is however interesting to note that now the complex seemingly has a size that is roughly equivalent to a tetramer of GFP-UVR8. The reason for this may lie in the properties of the GFP protein itself. Previous literature has reported that GFP has a tendency to form dimers/multimers (Yang *et al.* 1996). The multimerization of GFP may therefore block UVR8 interacting with any other proteins. Alternatively, it may be that UVR8 naturally dimerizes, but the presence of the GFP tag causes and additional binding between GFP modules therefore resulting in a tetramer.

Whatever the underlying truth behind these observations is, we can conclude that the addition of a GFP tag to UVR8 is having a large impact on the size of the complex. As

all of the variations in UVR8 generated so far (i.e. addition of localisation signals and deletions) also have GFP tags, then this may cloud the results. Nevertheless, we can still glean some vital information on the effects of changing the properties of UVR8 even with this complication. For example, if any of the alterations results in a large change in this complex, then we can conclude that UVR8 is still exerting an effect on some of the components. Further studies using some of these constructs were therefore initiated, the results of which are described below.

5.2.7 GFP-UVR8 complex size shows differences across cellular compartments

Under minus UV-B conditions UVR8 is present mainly in the cytoplasm and but is also present to a low degree in the nucleus. After UV-B there is a strong accumulation in the nucleus and relative decrease in cytoplasmic presence. Localisation and light treatment are therefore tightly linked and thus this might be true for the complex i.e. that there are different complex sizes according to the different compartments. However, the spread of both native and GFP tagged UVR8 across these compartments under both light conditions may be impacting on our ability to separate out the complexes according to treatment. We therefore decided to look at the localisation of the proteins when they are entirely restricted to different compartments. This can be achieved using the NLS and NES tagged versions of the proteins described in the previous results chapter. Under low white light conditions these tags restrict the protein to the nucleus and cytoplasm respectively. Therefore protein extracts from both untreated and UV-B treated NLS and NES plants were run on the column as described in previous sections. Representative blots and average complex sizes (n = 3 for NLS; n = 2 for NES samples) are shown in Figure 5.7.

For samples derived from NLS tagged plants, we again see an average complex size of about 300 kDa for both light conditions. We can therefore conclude that the complex size for nuclear localised UVR8 (when tagged to GFP) is roughly 300 kDa and also that it is unchanged by UV-B treatment. Thus, in this case it seems that either the complex remains unchanged by UV-B treatment or that the components exchanged after treatment are of equivalent size to those before treatment. However, the potential complications introduced by the presence of the GFP tag prevent firm conclusions from being drawn.

For NES samples under white light conditions, we see a similar banding pattern to NLS tagged samples while the average complex size is calculated to be approximately 340 kDa. It thus does seems that the complex within the cytoplasm may slightly larger than that in the nucleus (by about 50-60 kDa). This may suggest different components to the

complex with different compartments however as the difference is not very large and as there are issues with resolution in this method, this precludes concrete conclusions from being drawn.

As GFP-UVR8 protein tagged with the NES moves strongly into the nucleus, we would expect to see a similar average complex size to that found for NLS plants. Here however, this does not appear to be the case; the calculated complex is roughly 100 kDa larger than we would expect. The most likely reason for this lies in problems encountered with this particular set of samples. Firstly, as there were only two replicates for NES samples due to problems with adequate expression, it is possible that an outlying value is artificially increasing the average value. In addition, the comparatively fainter bands from these samples increased the difficulty in identifying the peak fractions, thereby skewing the data. It seems that additional repeats, preferably using lines that show increased levels of expression, are needed to clarify this issue.

Despite these difficulties, the results so far show that the complex sizes under UV-B conditions and when UVR8 is restricted to the nucleus are consistently smaller (albeit only slightly so) than that for untreated and cytoplasmic samples.

5.2.8 Deletion of 23 N-terminal amino acids of UVR8 results in a reduction in complex size

Work covered in the previous chapter had shown that loss of the N-terminal region of UVR8 results in the loss in function of the protein. Furthermore, the protein shows reduced or complete loss of nuclear accumulation depending on which amino acids are removed. The reasons for this loss in functionality are not yet known. One possibility is that this loss in function and impaired nuclear accumulation direct results from the loss of a protein binding region. Therefore, to test this theory it was decided to run one of these deletion constructs on the column and assess the complex size. As the deletion constructs generated here showed very low protein levels, it was decided to use the Δ23N construct generated by Kaiserli and Jenkins (2007). Plants were grown and protein extracted as described in the previous sections. Resulting blots and average complex sizes (n = 3) are shown in Figure 5.8.

The complex size calculations for this construct gave values of about 160-170 kDa under both low white light and under UV-B. It is immediately apparent that the loss of only a few amino acids of UVR8 has resulted in a huge reduction in the average complex size. The size of the complex has halved in comparison to those values for GFP-UVR8 samples. Interestingly, this complex now appears to be the size expected for a GFP-UVR8

dimer as discussed in Section 5.2.5. Therefore, if the hypothesis that the complex may be a tetramer is true, we seem to have lost two units of the complex. The loss of the first 23 amino acids may have blocked a UVR8-UVR8 dimerization, leaving only that attributable to the GFP.

This result does seem to negate the hypothesis that it is GFP alone that is causing an artificial multimerization or recruiting other unknown proteins. It appears that UVR8 is still having an effect on the overall complex size and a seemingly important one. Furthermore, it seems that both the UV-B and non UV-B complex are dependent on these key amino acids.

It is interesting to note that the UV-B treated Δ23N samples have and extended 'tail' of bands in the protein blot. This may suggest that more that one complex is present with so that the second smaller complex causes the bands to extend into fractions 35-39. However, as Western blotting methods are not truly quantitative and exposure time of films to the blots can strongly influence band strength, this would need to be tested further in order to confirm presence of multiple complexes.

In conclusion, it seems that in addition to a vital role in UVR8's function and localisation, the N-terminal amino acids are potentially important in the formation of an appropriate complex. However, again due to the presence of the GFP tag, we cannot yet be certain that the loss of these amino acids is affecting complex formation. Nevertheless, this result offers a potential insight into the role of these N-terminal residues in the function of the protein.

5.2.9 UVR8 complex size changes in the *cop1-4* mutant under low white light

Recent work by Ulm and co-workers has suggested that UVR8 might be interacting with COP1 (Favory *et al.* 2009). COP1 monomers are 76 kDa in size, therefore the expected complex size for an interaction with one COP1 monomer would be in the region of 115 kDa. Hence, it does not seem that the data presented here supports this. Nevertheless, it was decided to examine the complex size of UVR8 in the *cop1-4* mutant to determine whether there is in fact a change in the complex size. Plants were grown, treated and SEC was performed as described in the preceding sections. Resulting blots and average complex sizes (n = 2) are shown in Figure 5.9.

The calculated sizes of the complex give values of 125 and 70 kDa for untreated and UV-B treated samples respectively. While the value of 70 kDa for UV-B is consistent with previous values for wild type plants, that for low white light seems to be larger than expected. This result suggests that COP1 may indeed be having an effect on the UVR8

complex under white light conditions. However, instead of a decrease in average complex size, we see an increase. One possibility is that COP1 has a role in preventing the formation of this larger complex under minus UV-B conditions. We do however have to take into account that the *cop1-4* mutant is not a null mutant. Complete loss in functional COP1 results in lethality and thus all mutant alleles are somewhat leaky. Although the *cop1-4* is a relatively strong mutant, some protein will remain and it is thus hard to assess what impact these residual protein levels may have.

5.3 Discussion

The aim of the work described in this chapter was to determine whether UVR8 acted in a complex. Mass spectrometry has previously been attempted by the Jenkins lab to identify proteins associated with UVR8, but with little success. As attempts to extract and identify UVR8-like proteins in other plant species were unsuccessful concentration was instead turned to SEC. Use of this method did indeed answer the question of whether UVR8 existed in a complex and furthermore showed that the complex size decreased with the removal of the N-terminal. However, due to the relatively low resolution of the method and the added complication of the presence of the GFP tag, questions as to compartment specificity and the effect of light could not be answered as clearly. Finally, the results using *cop1-4* seem to be contrary to our expectations based on data from Favory *et al.* (2009). Therefore, while SEC has answered our initial question and given a tantalising glimpse into the UVR8 complex, it is clear that this groundwork will need to built upon in order to fully resolve the UVR8 complex and its components.

5.3.1 Optimisation of UVR8 protein extraction

When considering the peptide used to generate the N-terminal antibody, namely the first 14 amino acids of the UVR8 sequence, it is perhaps unsurprising that no bands were seen using protein extracts from other plant species. This region covered the least conserved region of the N-terminal as can be seen in Figure 4.4. Even the relatively closely related *Brassica rapa* shows little conservation in this region with *Arabidopsis* UVR8. It would therefore seem that this particular antibody is too specific for the *Arabidopsis* sequence and thus cannot bind to any proteins in other plant species.

The C-terminal antibody however was raised against a peptide found in the 27 amino acid region found by Kaiserli and Jenkins (2007) to be essential for UVR8 function and, as discussed in Chapter 4, is seemingly conserved across potential UVR8 homologues

in other plant species. We might therefore expect that this antibody is more likely to produce bands on a western blot. Indeed, when examining Figure 5.1 the clearest bands seem to arise when the C-terminal antibody was used. Interestingly however, these did not appear for the more closely related Brassicas, but for the pea extracts instead. Intriguingly, a faint band of a roughly equivalent size is also seen for the N-terminal antibody blot, thus raising the possibility that both antibodies are detecting the same protein.

Of all the samples and antibodies, C-terminal pea yielded the best results. However, even these bands are quite feint compared to that of *Arabidopsis* indicating that either the potential homologue in pea is found at lower concentrations or that the antibody isn't binding as efficiently. It would therefore seem that this approach, that is using tissue from other plants to bulk up the amounts of UVR8 extracted, is not a feasible one unless an antibody that cross-reacts widely can be produced. Consequently, continued use to the well-characterised model species *Arabidopsis* seems to be the best method in the short term to further investigate the protein-based mechanisms of UV-B signalling.

It was therefore decided to undertake a series of experiments using SEC. To ensure that as much protein was extracted as possible, various aspects of the protein purification process were assessed. It was shown that the extraction buffer previously used by the Jenkins group worked the best and that overall protein concentrations could not be improved by the addition of a sonication step. It therefore seems that the relatively low concentration of UVR8 in samples previously submitted for mass spec analysis was not the result of ineffectual protein extraction. For *Arabidopsis* leaf tissue at the very least, this method does indeed seem to be the optimal one. As these experiments were only performed using this particular tissue, we cannot extend this to all plant species or even to other tissue types. It is therefore possible that the failure to identify strong bands in the protein extractions shown in Figure 5.1 may be due to the lack of optimisation to other sample sources. Nevertheless, the relatively strong rubisco bands seen in the ponceau stained membranes of pea would suggest that the extraction of soluble proteins could not have been too adversely affected.

Figure 5.2 also showed that the UVR8 protein appears to be stable overnight at 4 ºC and after additional incubations of several hours at room temperature. While we can conclude that the protein itself is resistant to degradation in different buffers and at different temperatures, we cannot exclude the possibility that the protein complex itself is either disrupted or that artificial aggregations occur. Indeed it is interesting to note that the large non-specific band that sometimes appears on UVR8 blots is present strongly in those samples that had been subjected to dialysis overnight at 4 ºC. While this phenomenon was

not pursued here, it would be of interest to determine whether it is the incubation, phosphate buffer or dialysis process itself that causes an enrichment of this band.

It is also of interest to note that the increased enrichment in the upper band is not accompanied by a decrease in the UVR8 band. Due to the semi-quantitative nature of Western blots, it is difficult to say this with a great degree of certainty. However, as equal amounts of total protein extract were loaded onto the gel and taking into account the evenness of the rubisco bands, it is unlikely that the total amounts of protein present are significantly different.

It is of course by no means certain that this upper band does contain some proportion of UVR8. As the N-terminal antibody performs with greater efficiency than the C-terminal antibody, it is the former that is used most often. Comparatively fewer blots are probed with the C-terminal antibody. However, by looking at the samples from *Arabidopsis* in Figure 5.1, we can see that faint bands of roughly equivalent size can be found around the 83 kDa marker. This suggests that two antibodies raised to two distinct regions may be producing the same banding pattern and hence binding to the same protein. Although this evidence is somewhat circumstantial, it does hint that some UVR8-specific process results in the presence of an upper band in some blots. In addition, this blot (and some others presented in this thesis) shows that this upper band is present in multiple blots, even those where the protein has not been incubated overnight at 4 ºC or had its buffer exchanged via dialysis. We can therefore conclude that although this process seems to strongly enrich this band, it is not entirely responsible for its formation.

One final observation on this upper band is that in the blots shown in Figure 5.4 A and C, this upper band shows a reduced intensity in UV-B treated samples. Again, Western blotting techniques prohibit accurate quantification so we are unable to draw concrete conclusions. Nevertheless, this implies that there may be a UV-B responsive component to this phenomenon.

5.3.2 Effects of GFP on UVR8 complex size

The results presented in Figure 5.6 show that UVR8 does indeed exist in a complex. It was hoped that by looking at the elution volume of a GFP tagged construct, the difference in size between this and that of native UVR8 would determine whether UVR8 was forming a dimer or interacting with a similarly sized protein. Contrary to expectations, it was found that the GFP construct was considerably larger than native UVR8. So large in fact that it now equated to a tetramer of GFP-UVR8. It is therefore clear that the GFP tag is having a large impact on the overall size of the complex and is seemingly recruiting other elements

into the complex size. This immediately raises the question of whether this may be affecting the function of UVR8. As the introduction of the GFP-UVR8 construct into the *uvr8-1* background rescues functionality, it would appear that the function could not be too adversely affected. It is possible that this aggregation does not occur in vivo and that it is some component of the extraction process or the dialysis that results in this effect.

Furthermore it is known that GFP can dimerize (Yang *et al.* 1996). This could explain the effect seen here. Thus, the presence of the GFP may be causing a tetramerisation thereby blocking the native UVR8 interactions. If this is the case, it suggests that the formation of a complex is not essential for function otherwise we would expect that GFP-UVR8 could not rescue *uvr8-1* which again is not the case. Alternatively, and possibly more attractively, the GFP could be causing an additional dimerisation on top of that due to the presence of UVR8 alone. That is, if UVR8 was interacting with protein X and that the GFP tag was dimerising, we would see an overall complex size that is smaller than that seen i.e. ~220 kDa rather than closer to ~280.

One potential means to clarify this issue would be to overexpress GFP alongside GFP-UVR8 to disrupt the formation of multimers of UVR8. Alternatively, if it seems that the complex is formed in vitro, free GFP could be added to the sample prior to loading on the Sepharose® column. The fractions could then be probed with the UVR8 antibody and hopefully if GFP is in excess only a GFP-UVR8/GFP complex would be seen.

Obviously and ideally, all of the above experiments would be repeated using the same constructs but with the removal of the GFP tag. This should give a better resolution and hopefully confirm the above results. While GFP has been an extremely useful tool in molecular biology, particularly in the field of microscopy, it is evident that it is not without its flaws. As the protein sequence is further modified and with the arrival of new tags such as iLOV, these flaws may be reduced or eliminated (Chapman *et al.* 2008).

5.3.3 The UVR8 complex

Despite the apparent problems associated with working with GFP-tagged constructs we can draw several conclusions from work using the SEC method. Firstly, that native UVR8 does indeed exist in a complex (and a relatively strong one capable of withstanding 12 hours or more at 4 ºC plus 4 hours more at room temperature). This complex seems to be slightly smaller post UV-B treatment and this may be associated with a change in localisation. That is NLS tagged protein given rise to a slightly smaller average complex size than cytoplasmic which correlated with the localisation of the protein under UV-B and white light respectively. Second, deletion of the N-terminal 23 amino acids causes a huge

reduction in protein size. Third, loss in functional COP1 gives rise to a larger calculated complex size but only under low white light conditions.

With the exception of NES and Δ23N samples, the calculated complex size of UV-B treated samples seems to be slightly smaller than for those in LWL. In general, this correlated with the differences in compartments. That is, both NLS samples are smaller than for NES under low white light where the compartments are the nucleus and cytoplasm respectively. Therefore UVR8 seems to exist in a smaller complex whenever localised in the nucleus (i.e. where the majority of the protein is localised after UV-B exposure) and larger when in the cytoplasm (i.e. where the majority of the protein is localised under minus UV-B conditions). However, under this premise, we would expect NES UV-B samples to be of equivalent size to NLS. This does not seem to be the case here; the sample in question is actually ~100kDa larger when exposed to UV-B (and therefore mainly in the nucleus). As this apparent complex is so much larger this may indicate that either this is an unrepresentative result and therefore requires additional repeats or alternatively that there are other mechanisms at play in this particular case. Due to the extremely low protein expression of this construct, the former of these hypotheses seems to be the more likely. As the bands are comparatively fainter than seen for other constructs it is increasingly more difficult to identify the peak fraction. This introduces additional error and thereby can give rise to less accurate results. It would therefore seem that these experiments should be repeated, ideally using a transgenic line which shows increased levels of the construct.

Nevertheless, it does seem that there are subtle differences in average complex sizes between the different compartments. As the average complex size appears to be strongly similar in both NLS samples, this suggests that it is the localisation that is responsible for the complex composition and not the light treatment. If the complex size were responsive to UV-B, then we might expect to see a shift towards a smaller complex size in the NLS minus UV-B samples. As this appears not to be the case, we can infer that it is localisation that is having the larger effect on the UVR8 complex. It may be that the components of the complex are in fact responsible for UVR8's localisation; one may lead to retention in the nucleus while the other encourages restriction to the cytoplasm.

As the differences in average complex size between the compartments are not large, and due to the relatively low resolution of SEC, it could be that these differences in size are coincidental. For example identification of different fractions as the peak can lead to large differences in the calculated complex size. Perhaps then these differences, especially those for the larger fractions as the range of sizes that each fraction represents

increases with complex size, are too subtle to separate confidently. Working under this hypothesis, the size of the complex in fact does not differ across light conditions in native UVR8, GFP-UVR8 or NLS samples. In this case, we can return to the theory that the UVR8 protein may be dimerizing. Although this second hypothesis seems to fit with data for the 23ΔN samples better, we cannot link different complexes with different light conditions and compartments. One of the weaknesses of this technique is that brief transient complexes cannot be detected. That is, UVR8 may exist mostly as a dimer, except under a change in conditions, e.g. after UV-B, when a transient complex enhances UVR8 accumulation in the nucleus or blocks its export. Of course, the situation might be that the localisation of the UVR8 complex is regulated by means that are not dependent on a direct protein-protein interaction with UVR8. For example the nuclear pores may undergo a change post-UV-B that significantly reduces the export of all proteins including UVR8 from the nucleus.

So far it would seem that the two main hypotheses for the composition of the UVR8 complex, i.e. a UVR8 dimer or UVR8 plus unknown components, would seem to have equal merit. If however we include the results from the *cop1-4* samples, the latter of these becomes the more likely. While samples from *cop1-4* plants that had been exposed to UV-B showed a calculated complex similar to that of native UVR8, samples under minus UV-B conditions show a fraction pattern shifted towards a larger size complex. Thus, while the nuclear complex has remained unchanged, a loss in functional COP1 has resulted in an apparent increase in the size of un-exposed complex. It is not immediately clear why loss of COP1 might lead to formation of a larger complex size. Indeed, more recent work has shown that COP1 and UVR8 interact so we might expect a decrease in size in the *cop1-4* mutant rather than the contrary. One possibility is that COP1 degrades some protein or proteins bound to UVR8 under minus UV-B conditions thereby allowing an alternative protein to bind in its place. Thus when COP1 is removed, the larger protein or proteins are able to preferentially bind to UVR8.

The results presented here interestingly seem to be the very opposite of those presented by Favory *et al*. (2009). These authors show that the interaction between UVR8 and COP1 is UV-B dependent. We would therefore expect a complex size of ~115 kDa after UV-B. This however is not seen in the wild type samples and the closest calculated complex size to this occurring in the *cop1-4* mutant under low white light. Consequently, it seems that while both UVR8 and COP1 are known to have important roles in UV-B responses, the exact way in which these proteins interact and their immediate downstream

effects are still elusive. No doubt further work on both of these proteins will help clarify and crystallise the networks involved.

5.3.4 The role of the N-terminal region in the UVR8 complex

Work presented in the previous chapter has already demonstrated the important role that the N-terminal of UVR8 plays in its function and localisation. Calculations of complex size in the Δ23N construct shown in Figure 5.8 show that this small region also appears to have a vital role in correct complex assembly. Unfortunately, due to the presence of the confounding GFP tag, we cannot have an accurate representation of the complex size when this region is absent. Nevertheless, loss of this region results in a halving of the complex size relative to GFP-UVR8. We can thus hypothesise that the key to this region may be the existence of a binding site whereby the interacting partners (be it an unidentified protein or a second UVR8 molecule) can attach to UVR8. These interacting partners may in turn regulate the localisation of the complex causing it to accumulate in the nucleus upon exposure to UV-B. Furthermore, it has been shown that this localisation is necessary but not sufficient for UVR8 function thus implying an additional functional role for the N-terminal. This also could be as a result of the appropriate binding of interacting proteins. Thus, it may be that either or both of these effects are the result of interacting proteins. If it is possible to more accurately record the complex sizes of the various constructs under different light conditions it may be possible to start separating out these effects. It may be the case that the nuclear accumulation is dependent on one form of the complex while the addition, removal or exchange of components regulates the activity.

Before taking these conclusions too far however, we have to consider the possibility that by removal of this N-terminal region we have in some way interrupted the GFP dimerisation. Again this issue is one that may be remedied by repeating the experiment in the absence of a GFP tag.

5.3.5 Future experiments

Aside from the aforementioned repeats with the removal of the GFP tag, there are a number of other experiments that would both complement and enhance the results described here. For example, returning again to the N-terminal, it would be interesting to apply the plus constructs described in the previous chapter to the column. If the loss of the N-terminal 23 amino acids results in an apparent large reduction in the complex size, then accordingly by use of the addition constructs we would expect to again see complexes

larger that the size of the GFP construct alone. Furthermore, this may help clarify the situation regarding the roles of the first 12, 20 and 32 amino acids. If there is sufficient sequence in the first 12 residues for binding with interactors (thus allowing nuclear accumulation under UV-B) then this should be apparent from the complex size. While these experiments determine that the N-terminal region is necessary for complex formation, we have not yet determined whether it is sufficient. Use of the plus constructions should allow us to resolve this.

As the N-terminal appears to be an important region for complex formation, the pull-down experiments published by Favory *et al.* (2009) should be repeated using the N-terminal constructs. If the main complex binding site is lost with the N-terminal, then it should no longer be possible to pull-down Δ23N-UVR8 with COP1.

For example, if it is solely the N-terminal region that is necessary for complex formation, then application of samples from ΔC plants should yield similar results to GFP-UVR8. If there is again a reduction in complex size, then this would lead us to the conclusion that multiple regions are necessary and also that protein interactions may be tied to the functions of both regions. If there is no apparent change in size, it would seem that the vital, if elusive, function of the C-terminal is independent of any protein interactions.

The results obtained from use of the *cop1-4* mutant seem to contradict the results obtained by Favory *et al.* (2009). Additional SEC experiments may help clarify the issue. Firstly, the blots obtained from use of wild type tissue on the column could be probed with a COP1 antibody to see whether the pattern of bands is similar. In particular if, as stated by Favory et al, the COP1-UVR8 interaction is UV-B dependent, then we would expect the patterns seen from using either antibody to be similar only in UV-B treated samples.

An alternate use for the SEC method would be to use it to concentrate samples for mass spectrometry. However, the fraction size, 300 µl, that the protein elutes in is quite large and UVR8 is spread over many fractions. Here, the large fraction size problem is overcome by use of Strataclear™ resin which binds to proteins allowing them to be spun down and resuspended in a smaller volume. This works well when loading buffer is added and the sample can be loaded directly on a gel. For the more sensitive mass spectrometry analysis however, this could cause a huge problem. If the proteins could be washed from the resin, then this would seem like an attractive method. In addition to concentration of the sample, this fractionation method should have removed the majority of the rubisco protein (which elutes from the column much earlier). This should dramatically reduce noise in the readings and improve the data acquired.

Finally, in order to obtain more accurate values for the complex size smaller fractions could be taken so that the elution volume could be determined with greater precision. Alternatively, columns with better separation in the 40-400 kDa size range could also be used. For example, while the Sepharose 6HR 30/100 column has a separation range of 50-50,000 kDa, a Superdex 75 column has a range of 30-700 kDa (also available from GE Healthcare).

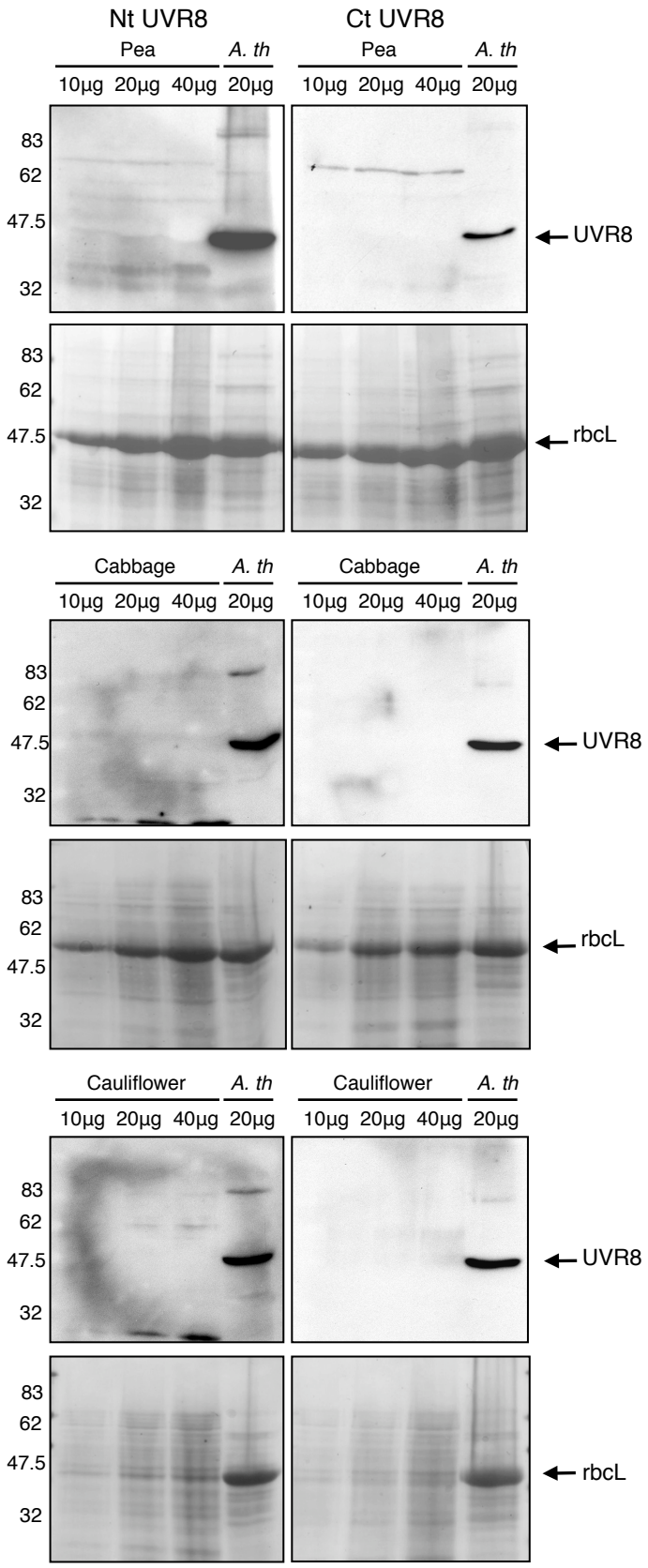

Figure 5.1 UVR8 is not detectable in pea (*Pisum sativum*), cabbage (*Brassica oleracea cv Capitata*) or cauliflower (*Brassica oleracea cv Botrytis*) tissue. Leaf tissue was extracted in micro-extraction buffer and run on a 10 % SDS-Page gel. Proteins were transferred to nitrocellulose membrane and stained with ponceau. Membranes were then probed with N-terminal or C-terminal anti-UVR8 antibody. No protein of the predicted size was detected. Protein extracted from *Arabidopsis thaliana* (*A. th*) was used as a control. Rubisco large subunit (rbcL) shown as a loading control.

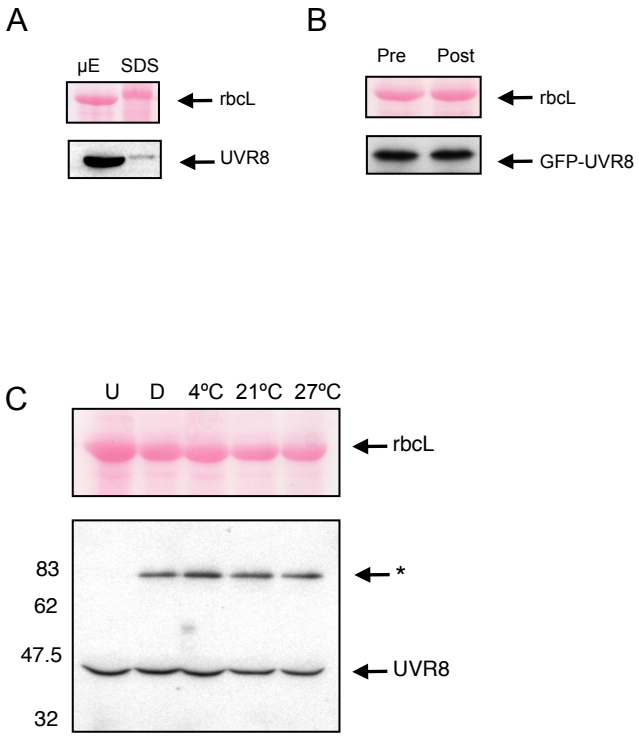

Figure 5.2. **Optimisation of UVR8 protein extraction and assessment of its stability under different temperatures.** Leaf tissue from three week old *Arabidopsis* seedlings was used for all experiments and protein extracted as described. All blots were probed with the C-terminal UVR8 antibody. **A** microextraction buffer is more efficient means of extracting UVR8 protein than a 2 % SDS buffer. Western blot showing UVR8 protein levels after extraction using microextraction buffer (μE) or a 2 % SDS buffer with a subsequent boiling treatment for 5 mins (SDS). **B** Sonication of protein extracts does not improve UVR8 yield. Protein was extracted using microextraction buffer then either directly spun down (Pre) or given three short pulses of sonication before centrifugation (Post). **C** UVR8 protein is stable at room temperature. Western blot showing whole cell extract prior to dialysis (U), extract post-dialysis (D), dialysed extract that had been left at 4 ºC, 21 ºC or 27 ºC for four hours. Rubisco large subunit (rbcL) shown as a loading control. Asterisk denotes the unknown upper band sometimes seen in Wt samples.

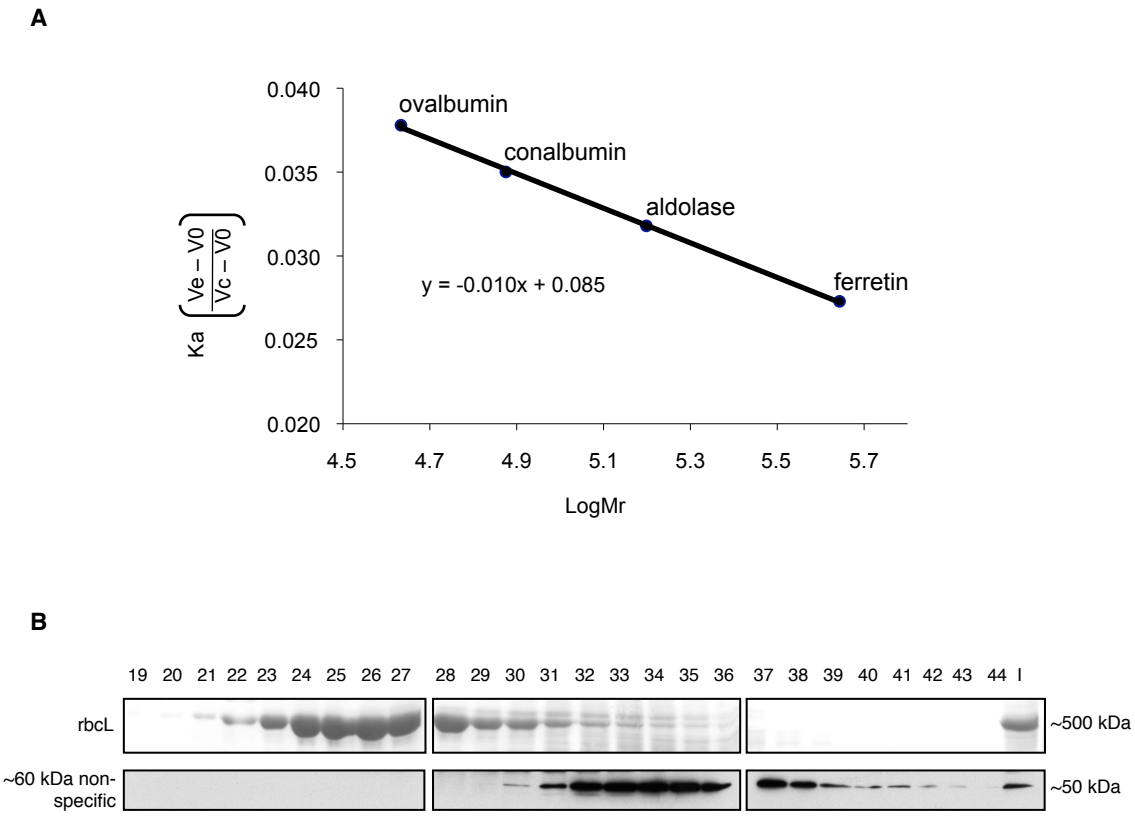

Figure 5.3 Calibration curve for Size Exclusion Chromotography column. **A** Ferretin, aldolase, conalbumin and ovalbumin protein standards were run on Superose® 6 hr column and fractions collected. K_a (where V_e = volume at which protein eluted, V_0 = void volume and V_C = column volume) was plotted against the log of the molecular weight of the protein standard. **A** standard curve was generated and an equation to describe this line was produced. This equation was subsequently used to determine the approximate molecular weights of the UVR8 complexes. **B** Calculations on fractions showing rubisco large subunit (rbcL) and a 60 kDa non- specific band (as seen when using the GFP antibody) result in good estimates of protein sizes. Numbers to the right of figure indicate calculated size of protein/complex. Blots was probed with a GFP antibody.

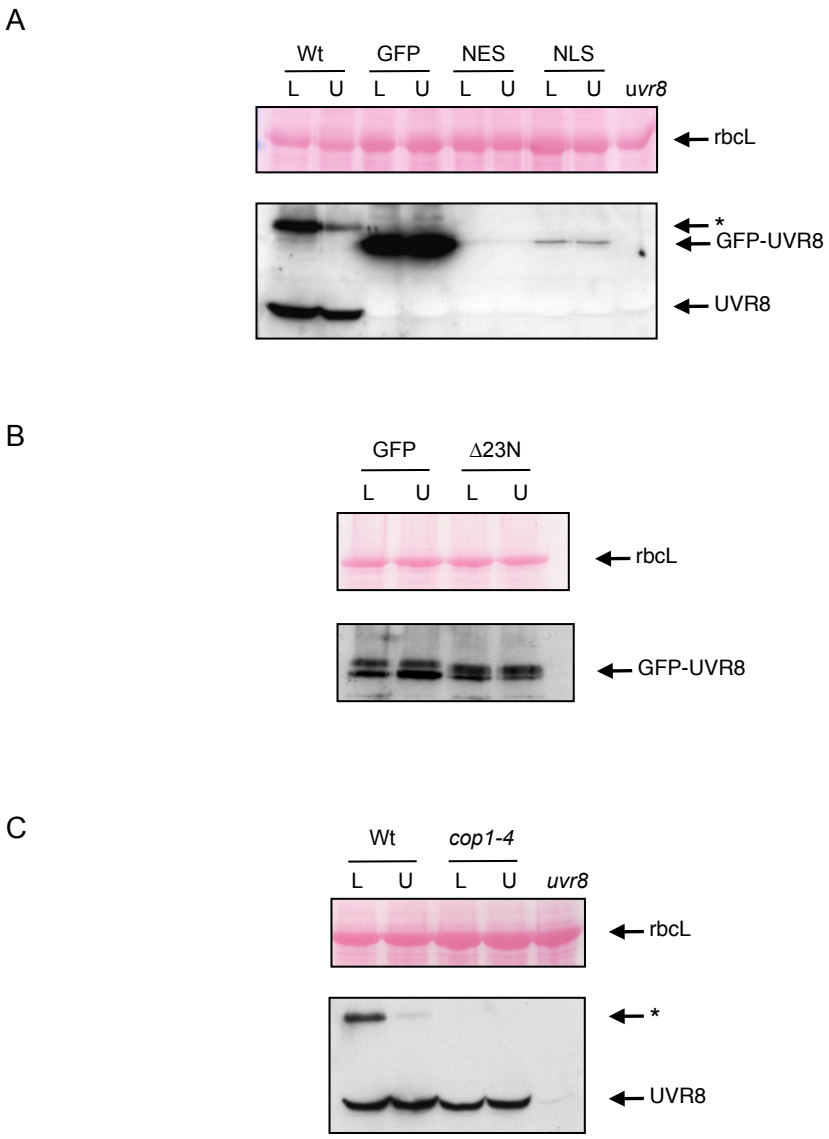

Figure 5.4 Western Blots showing the relative protein amounts in the constructs used for SEC. All plants were grown for three weeks in 20 µmol m^{-2} s^{-1} white light. Protein was extracted from leaves of untreated (LWL) and UV-B treated (UB, 4 hrs 1 µmol m^{-2} s^{-1}) plants. In all blots, 20 µg total protein extract was loaded onto 10 % SDS gels and were probed with the C-terminal UVR8 antibody. Rubisco large subunit (rbcL) shown as a loading control. Asterisk denotes the unknown upper band sometimes seen in Wt samples.

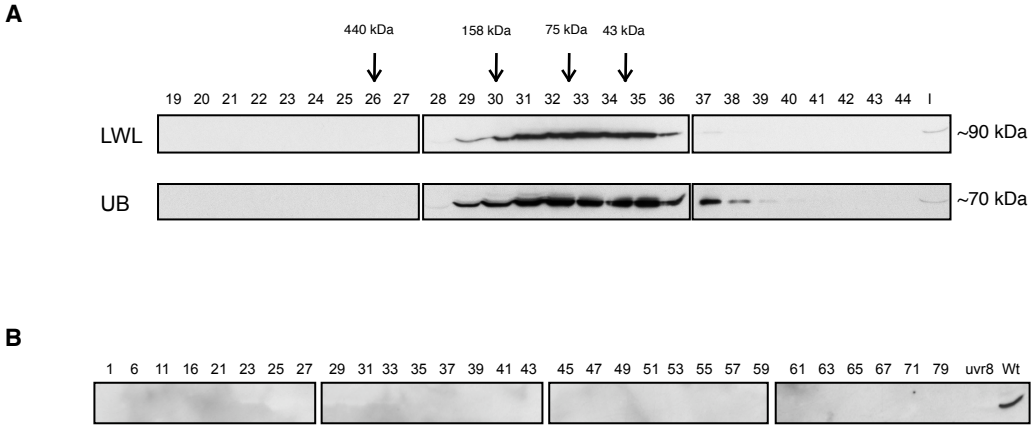

Figure 5.5 UVR8 exists in a complex whose size is unaffected by UV-B treatment. **A** Wild type plants were grown for three weeks in 20 μmol m^{-2} s^{-1} white light. Whole cell extract from leaves of untreated (LWL) and UV-B treated (UB, 4 hrs 1 μmol m^{-2} s^{-1}) plants was run on a Superose® 6 hr column and fractions collected. Fractions 19 to 44 were run on a 10 % SDS-acrylamide gel and transferred to nitrocellulose membrane. Membranes were tested for presence of UVR8 by probing using anti-UVR8 antibody. Fraction numbers are shown above the blots, I = Input (20 μg total protein). Approximate sizes of complexes were determined using the calibration curve generated from standard samples (see Figure 5.3). **B** No bands could be detected in any fractions taken from samples extracted from *uvr8-1* plants and probed with the C-terminal UVR8 antibody.

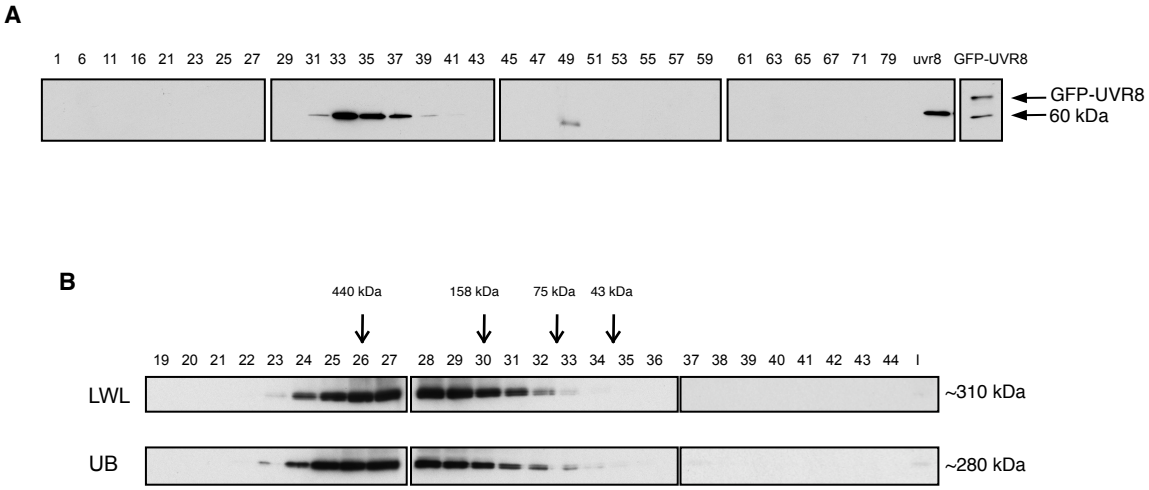

Figure 5.6 GFP-tagged UVR8 exists in a much larger complex size than wild type UVR8. Plants were grown for three weeks in 20 μmol m^{-2} s^{-1} white light. Whole cell extract from leaves of untreated (LWL) and UV-B treated (UB, 4 hrs 1 μmol m^{-2} s^{-1}) plants was run on a Superose® 6 hr column and fractions collected. Fractions were then run on a 10 % SDS-acrylamide gel and transferred to nitrocellulose membrane. Membranes were tested for presence of UVR8 by probing using anti-GFP antibody. **A** Only the ~60 kDa non-specific band could be detected in any fractions taken from samples extracted from *uvr8-1* plants and probed using the GFP Monoclonal antibody. **B** Blot showing fractions 19 to 44 from GFP-UVR8 samples. Fraction numbers are shown above the blots, I = Input (20 μg total protein). Approximate sizes of complexes were determined using the calibration curve generated from standard samples (see Figure 5.3).

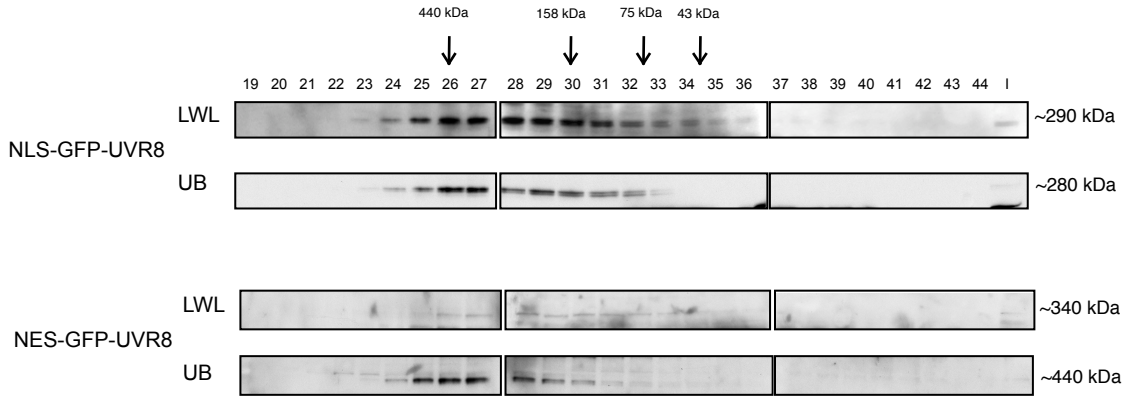

Figure 5.7 The effects of addition of NLS or NES tag to distribution of GFP-UVR8 in SEC fractions. NLS-GFP-UVR8 and NES-GFP-UVR8 plants were grown for three weeks in 20 µmol m^{-2} s^{-1} white light. Whole cell extract from leaves of untreated (LWL) and UV-B treated (UB, 4 hrs 1 µmol m^{-2} s^{-1}) plants were run on a Superose® 6 hr column and fractions collected. Fractions 19 to 44 were run on a 10 % SDS-acrylamide gel and transferred to nitrocellulose membrane. Membranes were tested for presence of UVR8 by probing using anti-GFP antibody. Fraction numbers are shown above the blots, I = Input (20 µg total protein). Approximate sizes of complexes were determined using the calibration curve generated from standard samples (see Figure 5.3).

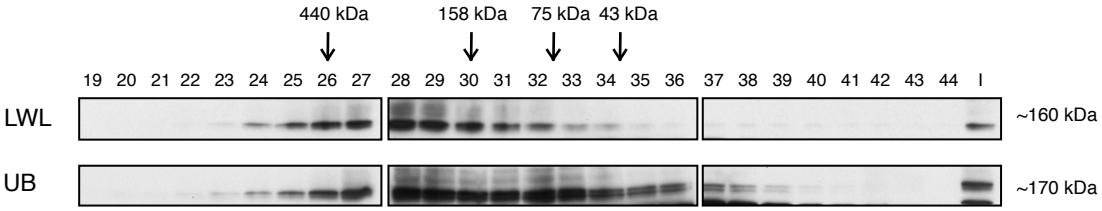

Figure 5.8 The effect of deletion of portions of the N-terminal of UVR8 on the distribution of UVR8 in SEC fractions. GFP-Δ23NUVR8 plants were grown for three weeks in 20 μmol m^{-2} s^{-1} white light. Whole cell extract from leaves of untreated (LWL) and UV-B treated (UB, 4 hrs 1 μmol m^{-2} s^{-1}) plants was run on a Superose® 6 hr column and fractions collected. Fractions 19 to 44 were run on a 10 % SDS-acrylamide gel and transferred to nitrocellulose membrane. Membranes were tested for presence of UVR8 by probing using anti-GFP antibody. Fraction numbers are shown above the blots, I = Input (20 μg total protein). Approximate sizes of complexes were determined using the calibration curve generated from standard samples (see Figure 5.3).

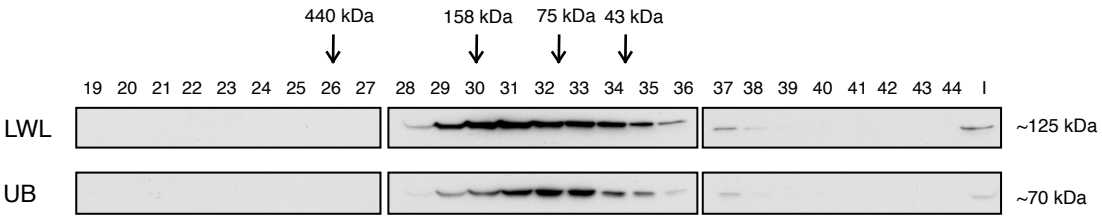

Figure 5.9 Loss of functional COP1 results in an apparent change in complex size *in vivo* only under white light conditions. *cop1-4* plants were grown for three weeks in 20 µmol m^{-2} s^{-1} white light. Whole cell extract from leaves of untreated (LWL) and UV-B treated (UB, 4 hrs 1 µmol m^{-2} s^{-1}) plants mutant plants was run on a Superose® 6 hr column and fractions collected. Fractions 19 to 44 were run on a 10 % SDS-acrylamide gel and transferred to nitrocellulose membrane. Membranes were tested for presence of UVR8 by probing using the anti-UVR8 antibody. Fraction numbers are shown above the blots, I = Input (20 µg total protein). Approximate sizes of complexes were determined using the calibration curve generated from standard samples (see Figure 5.3).

CHAPTER 6 FINAL DISCUSSION

6.1 Introduction

With the transition from an aqueous habitat to a terrestrial one, early land plants had to acquire tolerance to one more stress in addition to the myriad that they were already accustomed too, namely exposure to increased levels of UV-B. This radiation, which is mostly filtered out by a short column of water, has the potential to act as a major factor of damage to cellular components (Rozema *et al.* 2002; Frohnmeyer 2003; Tedetti and Sempéré 2006). Therefore, plants have evolved a series of responses in order to attenuate this stressor and cope with some of the inevitable damage. While the receptor responsible for perceiving this stimulus remains elusive, the first UV-B specific component was recently identified. UVR8 is known to have a vital role in the up-regulation of two transcription factors, HY5 and HYH, which in turn up-regulate a whole suit of protective genes (Brown *et al.* 2005; Brown and Jenkins 2007). The exact mechanisms by which UVR8 causes the up-regulation of these transcription factors is as yet still unknown. Nevertheless progress is being made in solving this mystery and we have already identified a number of defining characteristics for this vital protein. UVR8 is mainly localised in the cytoplasm in the absence of UV-B, but upon exposure both GFP-tagged and native UVR8 strongly accumulate in the nucleus (Kaiserli and Jenkins, 2007). UVR8 has the ability to bind to chromatin, but lacks the Ran-GEF activity seen in the related protein, human RCC1. Specifically, UVR8 has been found to be enriched in the chromatin regions around the promoter of *HY5*, suggesting a potential means by which it may facilitate the up-regulation of this gene (Brown *et al.* 2005). Finally, it has been shown that two regions at the termini of the protein are essential for its function: a 27 amino acid insertion (relative to RCC1) at the C-terminus and part of the N-terminal, the loss of which has the effect of impaired nuclear accumulation (Kaiserli *et al.* 2007).

The aim of this study was to answer a number of questions surrounding UV-B responses in *Arabidopsis*. The first of these was whether other response pathways that are induced by non-damaging, low fluence rate UV-B but are not dependent on UVR8 exist. Secondly, to expand the search for proteins similar to UVR8 in both *Arabidopsis* and also in other plant species to determine whether any homologues might be identified. Thirdly, to further investigate the role of the N-terminal region in the localisation of UVR8. Finally, we wanted to answer the question of whether UVR8 was acting alone or if it instead acted as part of a complex or complexes.

While many questions do still remain, the work presented here has shown that other UVR8-independent pathways exist but that we have to take care when performing microarrays as the existence of a number of false positive results can severely hinder the identification of candidate genes. BLAST searches identified a number of UVR8-like proteins in *Arabidopsis*, none of which seem to possess the N or C-terminal regions deemed necessary for function, as well as several candidate homologues in other plant species. Construction of a phylogenetic tree showed that these candidates may be roughly split into two groups, one that bears more similarity to human RCC1 and one that appears closer to UVR8. Closer examination of the N-terminal region showed that removal of different regions and the addition of these same regions to a GFP tag resulted in a variety of different localisation phenotypes. The most striking of these was that the first 32-33 amino acids are both necessary and sufficient to cause nuclear accumulation which, in the case of the latter, is not dependent on a UV-B stimulus. Finally, it seems that UVR8 does indeed exist in a complex, although the exact sizes and changes due to treatment or localisation are not fully clear due to the confusing presence of the GFP tag. Despite this it appears that the N-terminal may, in addition to having a role in localisation, be necessary for complex formation.

In this next chapter, these results and their implications will be discussed further and the advances in our knowledge of UV-B responses outlined.

6.2 UV-B transcriptional studies

Examination of transcriptional differences has been one tool that has been widely used in the analysis of UV-B responses, as changes in gene expression appear to be one of the major means by which plants moderate their responses to this stimulus (Casati and Walbot 2003; Ulm *et al.* 2004; Brown *et al.* 2005; Hectors 2007; Kilian *et al.* 2007; Brown and Jenkins 2008; Safrany *et al.* 2008). However, it can be difficult to untangle these transcriptional changes as huge numbers of genes are involved, for example >500 in this study and that performed by Brown *et al.* (2005). When all genes which show induction under UV-B across a variety of studies are grouped, this gives >3000 genes to consider (see Figure 3.5). Application of threshold limits and identification of commonality both within and between studies can help to initially narrow down this search. In this study for example, microarray data was validated using the methods that were to be used in subsequent analysis. That is, several genes were checked using qPCR and RT-PCR methods to ensure that differential expression could still be detected. As the RNA samples

used for these confirmation studies were the very same samples that were submitted for microarray analysis, we can then define clear thresholds (such as an appropriate False Discovery Rate) to use when cutting down these gene lists into a more manageable size. Once such filtering methods have been used, candidate genes with potentially interesting functions can be selected for initial analysis. However, with current technology for generating large sequencing data sets, the potential exists to generate even more data thus potentially exacerbating the problem of handling such quantities of information (Mortazavi *et al.* 2008). This may include information on groups of genes that are expressed at levels not normally detectable using microarray chips. One example of this, in the case of UV-B signalling, is the MYB family of transcription factors. While these have been shown to be involved in UV-B responses (Jin *et al.* 2000; Zhao *et al.* 2007; Cloix and Jenkins 2008), they have yet to appear in any microarray data sets generated by the Jenkins group. Thus there exists the potential for whole new groups of genes to investigate. Even so, with the advent of new technology, new bioinformatic tools to process these data sets will follow shortly thereby opening up novel ways by which this information can be mined.

Returning to the microarray datasets produced in this study, one of the issues we wanted to examine was the classification of low fluence and high fluence responses. Currently the line between low and high fluence is not clear and it is not even clear if such a definitive line exists. Previous experiments performed by the Jenkins group had used plants which had never been subjected to UV-B exposure before treatment with a 3 μmol m^{-2} s^{-1} fluence rate of this radiation. There was the worry that this, although only 75 % of the dose plants can receive in daylight (Jenkins 2009), might be a significant stressor to the plant. Indeed a later Brown and Jenkins study (2008) showed that at a fluence rate of approximately 3 μmol m^{-2} s^{-1}, genes associated with stress are expressed. It was for this reason we decided to investigate lower fluence rate treatments to determine whether a significant portion of the genes up-regulated in the first microarray were due to more generalised stress responses and not specific UV-B responses. The results presented here showed that contrary to predictions that lower fluence treatments would reduce the number of more general stress-response genes induced and thus reduced the total number of genes induced, that there was not a significant drop in the total number of genes that are induced. It therefore appears that regardless of the fluence rate used, similar numbers of genes show significant increases in expression.

Despite these similar numbers however, when the gene lists are examined it can be seen that differences between the three datasets are present. Interestingly, of the three genes identified by Brown and Jenkins (2008) to be induced as part of a general stress-

response, two (*WRKY30* (5g24110) and *FAD oxidored* (1g2630)) also appear in the 1 µmol m^{-2} s^{-1} microarray but not the 0.3 µmol m^{-2} s^{-1}. This would seem to suggest that at a fluence rate of 1 µmol m^{-2} s^{-1} for four hours that this treatment might still be inducing more general stress responses in non-acclimated plants. Nevertheless, the final member of this general stress response group, *UDP gtfp* (1g05680), does show a significant induction in the 0.3 µmol m^{-2} s^{-1} microarray. Thus, it may be that although this latter treatment is too low to cause significant damage to the plant, that due to a lack of prior exposure, it is still sufficient to induce expression of genes classed as general stress responses.

Another study has attempted to characterise genes on the basis of severity of treatment (Brosche and Strid 2003). Of the highest category neither of the example genes (*PR-1* (2g14610) and *PDF1.2* (5g44420)) appeared in any of the microarrays compared in Figure 3.5. One gene classed as an intermediate induced gene however, *PR-5* (1g75030) was similarly to *WRKY30* and *FAD oxidored* seen in both the 3 and 1, but not the 0.3 µmol m^{-2} s^{-1} microarrays. This does seem to support the evidence that the 0.3 µmol m^{-2} s^{-1} fluence rate treatment removes the majority of genes previously classed as more general stress responses and as such is the most appropriate treatment level for this length of exposure.

An alternative explanation to the observation of pathogenesis-related genes such as *PR-1* and *PR-5* showing induction in low fluence rate microarrays lies in the observation that UV-B can induce tolerance to other abiotic and biotic stresses such as drought (Gitz and Liu-Gitz 2003), cold (Chalker-Scott and Scott 2004) or insect herbivory (Izaguirre *et al.* 2003). It could therefore be the case that a certain degree of cross-tolerance is built into the low fluence UV-B responses. That is, exposure to low levels of UV-B actually enhances the plants overall fitness and ability to withstand the stresses found in the natural environment.

Another consideration we have to make is that the conditions in which we grow and treat plants are very artificial; amount and duration of light as well as temperature, humidity and other factors are usually kept unnaturally constant. This can be helpful when examining the effects of stresses as is allows us to reduce the variation in a population of plants due to fluctuations in these parameters. We do however have to consider that in the natural environment, huge fluctuations in these effects will indeed take place. UV-B fluence rate for example can be altered by altitude, cloud cover, overhead vegetation and many other factors (McKenzie *et al.* 2003; Paul and Gwynn-Jones 2003). Thus, the ways in which a plant is able to acclimatise to biotic and abiotic stresses will be correspondingly complex. While some studies have endeavoured to asses the degree of overlap in several

stimuli in their experiments (Kilian *et al.* 2007) it is clear that to gain a more complete picture of plant environmental responses, we will need to incorporate many factors into our model.

It is also interesting to note that experiments performed here and elsewhere often use highly inbred plant lines. This has the advantage of reducing the genetic diversity in the population, again conferring the advantage that we can focus on variation due to the treatment. However, a recent study looking into plant responses to red light via the phytochromes, examined natural variation in the phyB photoreceptor (Filiault *et al.* 2008). This is also an interesting approach for investigation of UV-B responses. For example, from work shown in Chapter 4, it can be seen that while there are regions of strong conservation in the UVR8 protein sequence between plant species, it does not apply to the whole sequence. It would therefore be interesting to examine further both these differences between species and also within *Arabidopsis thaliana*. There are a wide range of ecotypes available for this species which in turn come from a wide range of different habitats. These different ecotypes could be examined in their tolerance to UV-B to see if this can be linked to polymorphisms in *UVR8*, *ANAC13* or other UV-B response components. Indeed, similar studies using maize ware undertaken by both Casati *et al.* (2006) and Correia *et a*l. (1999). The former of these showed that maize accessions derived from higher altitudes (and thus exposed to greater natural levels of UV-B) have an increase in transcripts associated with chromatin remodelling. This in turn has been linked with UV-B responses; for example, UVR8 has been shown to associate with histones and that upon UV-B exposure in *Arabidopsis* there is an increased association of some UV-B responsive gene promoters with diacetlylated H3 (K9/K14) (Brown *et al.* 2005; Cloix and Jenkins 2008). The second of these studies showed variations in maize accessions in carotenoid content and differing reductions in photosynthetically associated components when exposed to UV-B.

Another study which has used *Arabidopsis* ecotypes showed that C4 exhibits greater oxidative stress and Ws a lower biomass after UV-B exposure when they are compared to Col-0 (Kalbina and Strid 2006). These differences may in turn help to explain the variation seen in transcriptome changes across the microarray studies compared in Figure 3.5. For example, Brown *et al.* (2005), Headland and Hectors, *et al.* (2007) studies used L*er*, Ulm, *et al.* (2004) and Safrany, *et al* (2008) studies used Ws, while Kilian, *et al* (2007) used Col-0. This, in addition to the different growth conditions, growth media and treatment length could cause a great variation in the UV-B transcriptome. As mentioned above however, by comparing these studies, we have a method for flagging interesting

candidate genes. That is, those genes that are common across these microarrays, regardless of the wide variety of experimental procedures may be those with highly important functions. Although no genes do appear across all six of the studies compared here, there are a number that are shared across four of five of them. Of this group of seven common genes, two belong to the EARLY LIGHT INDUCED (ELIP) family. Currently, there is somewhat conflicting evidence for the roles of the ELIP proteins in plants. Hutin *et al.* (2003) reported that the *chaos* mutant, which is unable to rapidly accumulate ELIP proteins, is more sensitive to photooxidative stress under high light or chilling. This in combination with localisation of ELIPs in the thylakoids and their hypothesised chlorophyll binding properties would suggest a photoprotective role. However, Rossini *et al.* (2006) report that a *elip1 elip2* double mutant does not show increased photoinhibition or photooxidative stress relative to wild type. Therefore, while the exact role and function of these proteins remains elusive, it seems that they do have an important role in UV-B responses. From the results of these studies and the observation that genes for these proteins show strong up-regulation in the majority of UV-B microarrays, we would predict that both *chaos* and *elip1 elip2* plants may have a reduced sensitivity to UV-B. It would be interesting to compare the phenotypes of these mutants to that of *uvr8* and *hy5* mutants to determine whether they show similar hypersensitivity.

One other chloroplast-associated gene was also shown to have strong up-regulation in the majority of the studies compared. SigE/Sig5 is involved in the regulation of plastid genes (Yao *et al.* 2003). Again this highlights that one of the key responses to UV-B may be to modify photosynthetic processes in order to prevent or repair damage that may occur to these extremely photosensitive components.

Of the remaining four genes common to most of the microarray studies, one is annotated as a receptor-like protein kinase (RPK-L). Receptor like protein kinases (RPKs) are a large family (>400) in *Arabidopsis* that are usually made up of an extracellular domain, a transmembrane domain and an intracellular domain in which lies the kinase part of the protein (Tichtinsky *et al.* 2003; Afzal *et al.* 2008). A good example of this family is the brassinosteroid receptor (BRASSINOSTEROID INSENSITIVE 1(BRI1)) which also has a hypothesised role in UV-B signalling (Savenstrand *et al.* 2004; Li 2005). Mutants defective in this gene were shown to have reduced induction of *CHS* under UV-B conditions (Savenstrand *et al.* 2004). Little is known however about the gene in question here, RKP-L. It has a domain of unknown function (DUF26) and interestingly lacks the kinase domain. To date it has been annotated as having a role in ABA responses and has been suggested to be subject to rapid evolution (Barrier *et al.* 2003; Xin *et al.* 2005;

Casasoli *et al.* 2008). Generally, this group of receptor like kinases have not yet been well studied and it is unclear what role (given the absence of a kinase domain) that they may have in signalling cascades.

Interestingly, the same study that linked RPK-L to ABA responses (Xin *et al.* 2005) also identified GCN5-related N-acetyltransferase (GNAT) family protein (2g32020) as being responsive to this hormone. This gene is included in the group of seven which are common to five of the six UV-B studies compared (see Figure 3.5). ABA is known to have a role in response to abiotic stresses such as salt and drought stress (Seki *et al.* 2007). It is possible that this versatile hormone may have an additional role in plant responses to UV-B.

Similarly to RPK-L, 2g32020 is UVR8/HY5/HYH independent, which combined with their association with ABA responses suggests they may be implicated in the same pathway. Interestingly, these two genes are the only ones of the seven that are seemingly independent of the UVR8 pathway.

The remaining two genes in this grouping both seem to be part of the UVR8 signalling pathway. Currently there is very little information, apart from its dependence on UVR8 and HY5, on the transducin / WD-40 repeat family protein (5g52250) (Brown and Jenkins 2007). The UDP-glucoronosyl/UDP-glucosyl transferase family protein (UGT84A1 (4g15480)), on the other hand is hypothesised to have a role in accumulation of sinapate esters (UV-B screening compounds) and is dependent on UVR8 but not HY5 (Brown *et al.* 2005; Meißner *et al.* 2008). It is possible that this gene may belong to the HYH/HY5 redundant class described by Brown and Jenkins (2008).

6.3 UVR8-independent UV-B responsive genes

Early work into UV-B responses often studied the expression *CHS* as this gene was known to be one of the best responders to UV-B. (Li *et al.* 1993; Christie and Jenkins 1996; Long and Jenkins 1998). For this reason it was used in the Brown *et al.* (2005) study to show that *uvr8* mutants were specifically impaired in their UV-B responses. From such work we now have a clearer picture of how this occurs. UVR8 acts upstream of two transcription factors HY5 and HYH. Half of UVR8 dependent genes are also dependent on functional HY5, and evidence suggests the remaining half may be regulated in a HY5/HYH redundant mechanism (Brown *et al.* 2005; Brown and Jenkins 2008). In this study, the

same tools were used to examine the UVR8-independent pathway, that is examination of gene expression under different light conditions in a variety of different mutants.

Interestingly, initial work showed that several genes hypothesised from the microarray data to be low fluence induced UVR8-independent showed increases in expression in minus UV-B conditions. Thus, some condition other than UV-B treatment within the chamber is sufficient to induce significant levels of gene expression. Of the small subset of genes that were further analysed by PCR methods here, a third were shown to be clear false positives (*MATE* and *DnaJ*) while another gene was somewhat more ambiguous (*RPK-L*). This suggests a significant proportion of the ~500 genes induced by UV-B in the Brown study as well as those presented here may also be false positives. This perhaps goes someway to explaining the sheer numbers of genes that are apparently induced by low levels of UV-B. One way in which these apparent false positives could be eliminated would be to perform an additional microarray in true minus UV-B conditions. Those genes that showed induction (presumably including *MATE* and *DnaJ*) in these conditions could then be identified and removed from the list of UV-B induced genes.

Despite this apparent problem, four genes were identified which were seemingly truly UV-B responsive. The more ambiguous gene, RPK-L (3g22060) seems to have variable results; in Figure 3.8 it appears to have more pronounced expression in the absence of UVR8 but this pattern is not continued in Figure 3.10. It is therefore difficult to interpret results from this gene especially seeing as there seem to be issues with some up-regulation in minus UV-B conditions. If the conditions in the treatment chamber are in some way affecting the levels of hormones such as ABA, this could explain the increased expression of this gene. Interestingly, the situation in which UV-B specific induction is seen most clearly occurs in the Ws ecotype as well as mutants in the Ws background (See Figure 3.10). It could therefore be that there are ecotypic differences in the expression of this gene. Nevertheless, its presence in the majority of the microarray studies compared in Figure 3.5 suggests that while the exact circumstances around its expression are ambiguous, there is good evidence that its UV-B induction is not an artefact.

While expression of *RPK-L* seems to be clearly HY5/HYH independent, this appears not to be the case for *HSP23.5M*. This gene was not identified in the Brown *et al* (2005) study as one which either UVR8 or HY5 dependent. Expression however in the *hy5 hyh* mutant seems to be somewhat reduced in comparison to the other genes examined, but is retained as normal in the *uvr8-1* mutant. In addition, this was the only gene to show a reduction in expression in the *cop1-4* mutant. From these results we can infer that a separate UV-B response pathway involving these three components but not UVR8 exists.

It is possible that this pathway may only be acting at relatively higher fluence rates; unlike for the other genes examined, *HSP23.5M* expression is not clearly induced at fluences up to 0.5 μmol m^{-2} s^{-1}. In conclusion these results suggest another whole class of UV-B responsive genes may exist; mid-high fluence rate induced UVR8-independent, that are dependent on functional COP1 as well as the presence of either HY5 or HYH.

Heat-shock proteins (HSPs) are present in all cells and are used to ensure appropriate folding as well as to restrict unfolding of proteins in a variety of different stress conditions (Feder and Hofmann 1999). While this particular small heat-shock protein has an unknown function, there is evidence of a role for these molecular chaperones in ameliorating UV-B stress. In cyanobacteria, it has been shown that mutation of a small heat-shock protein confers increased resistance to UV-B. This is thought to occur through enhanced repair to the PSII (Balogi *et al.* 2008). This *HSP23.5M* is predicted to be localised in the mitochondria rather than the chloroplasts (Waters 2008). Nevertheless, HSPs have an important role in protection from UV-B stress as well at the well characterised protection from heat stress for which they are named.

In addition to the results for *HSP23.5M* and *RPK-L*, work presented here has also conclusively shown that true low-fluence UVR8/HY5/HYH independent genes do exist. Two such examples are ANAC13 and 2g41730. 2g41730 encodes a small (119 amino acid) protein of unknown function and with no recognisable domains. A BLAST search using the protein sequence only brings back similar sequences (of which very few) in plants so it would seem that this may be a plant specific component. The feature that tagged this transcript as being of interest was its very high levels of induction in both the microarrays presented here as well as that in the Brown *et al* (2005) study. This can also be seen when looking at the fold change values of the timecourse data (see Appendix I). As there is so little data on this gene, we are not able to infer what role it may be having in UV-B responses. Nevertheless, it warrants further investigation and may be a representative of an entirely new family of proteins.

In contrast to 2g41730, much more information is known about the transcription factor ANAC13. Data presented here seems to support recent work that has been looking at ANAC13 more closely. Safrany *et al.* (2008) also demonstrated that *ANAC13* expression is UV-B responsive and independent of both COP1 and UVR8. In addition, they identified a novel UV responsive element in the promoter region of this gene, termed $UVBox^{ANAC13}$ which is necessary and sufficient for UV-B induction.

ANAC13 comes from a very large family of transcription factors that are specific to plants and which are named for their NAC (NAM, ATAF1,2, CUC2) domain (Ooka *et*

al. 2003; Olsen *et al.* 2005). This conserved NAC domain resides at the N-terminal and includes a DNA binding domain, while the highly diverse C-terminal possesses a transcriptional activation domain (Ooka *et al.* 2003). This family has a diverse range of roles in development as well as both abiotic and biotic stresses. So far no downstream targets nor any upstream factors controlling ANAC13 up-regulation have been found. Interestingly, it is also up-regulated by red light, thereby suggesting a possible diversity of roles in light signalling. It should be noted however that this red-light induction uses a separate domain in its promoter (Safrany *et al.* 2008).

For those genes shown to be UVR8-dependent, has been shown that their UV-B induction occurs independently of known photoreceptors (Brown and Jenkins 2007). This seems also to be true for the UVR8-independent genes shown here as none exhibited reduced expression under UV-B in any of the photoreceptor mutants examined (see Figure 3.12). It has been suggested in past that DNA damage could in fact be acting as an initial signal in UV-B reception. For example, in bean UV-B induced expression of β-1,3-glucanase (βGlu) is reversed by exposure to blue light that would activate DNA photolyase, suggesting its expression is induced by DNA damage (Kucera *et al.* 2003). Work presented in Figure 3.13 attempted to test whether this may also be true for UVR8 independent genes. It was found that levels of *ANAC13* and *2g41730* expression were relatively equal in wild type plants in both the absence and presence of supplemental light concurrent with UV-B treatment. As the predominant form of UV-B induced DNA damage, the formation cylcopyrimidine dimers (CPDs) is repaired in the presence of blue light, we might expect that fewer dimers (as they are rapidly repaired) would result in reduced expression of the genes under consideration if presence of this damage were indeed the initiating signal in this cascade. This apparent separation of gene induction from DNA damage is also supported by the result that no large change in expression occurred in mutants that are unable to repair UV-B induced lesions. However, as the results from the positive control were not clear we cannot be entirely confident that the conditions used were sufficient to actually induce dimer formation. In spite of this, the conditions used were sufficient to see large increases in the expression of the genes of interest. Thus even if the treatment was too mild to induce DNA damage, changes in expression are seen thereby implying that these effects are not linked. Consequently it seems unlikely that this mechanism of UV-B perception is responsible for the up-regulation of either *ANAC13* or *2g41730*.

In summary, it seems that in addition to the low fluence UVR8/HY5/HYH dependent and high-fluence UVR8-independent pathways as described by Brown and

Jenkins (2008), two additional pathways exist. Firstly a low fluence UVR8/HY5/HYH/COP1 independent pathway seems to regulate expression of *ANAC13*, *2g41730* and a receptor-like kinase gene (3g22060). Secondly a mid fluence UVR8-independent COP1/HY5/HYH dependent pathway regulates expression of the *HSP23.5M* gene. Neither of these pathways is dependent on functional blue or red-light photoreceptors nor is the former dependent on UV-B induced damage to initiate the signalling cascade. It is likely that more genes will be identified as part of these groups and that the groupings themselves will become further sub-divided once the regulatory mechanisms of each are more clearly defined.

6.3 UVR8-like proteins

Considering that UV-B would have been a relatively novel abiotic stress to plants as they colonised land, it might be expected that the roots of this response in plants are ancient. If UVR8 is one of the major players in the UV-B response, it is possible that this too is relatively ancient, thus suggesting the existence of homologues in a wide variety of terrestrially adapted plants. Homologues do indeed seem to be present in a wide range of plant species. However, on the basis of a phylogenetic tree (see Figure 4.3) they group into either ones that appear closer to RCC1 or ones closer to UVR8. This is also reflected in the presence or absence of N and C-terminal regions similar to those found in UVR8. Besides this split, the two parts of the groups each have predictable associations. That is, the eudicots form a cluster as do monocots and so forth.

At the time of writing, for these various plants species we only have complete genome sequences for *Arabidopsis* and *Oryza sativa ssp japonica*. No doubt this will rapidly change with maize, potato and tomato genomes well on the way to being fully sequenced and annotated. Of the species compared in Figure 4.3 there is a mix of genomes listed as being in progress, under assembly or for which there is no known concerted effort to sequence. It is therefore a very real possibility that we may be missing the true UVR8 homologue in several cases. Indeed if the number of UVR8-like proteins found in *Arabidopsis* is considered, the sequences compared may in fact include homologues of some of these UVR8-likes. Nevertheless, the development of new sequencing technologies should rapidly increase the rate at which any organism's genome sequence is determined therefore providing greater knowledge concerning potential homologues of this protein.

Similarity with RCC1 itself can be a confounding factor, especially seeing as no true RCC1 homologue has been found in *Arabidopsis* yet. Although none of the UVR8-like sequences in *Arabidopsis* shown here show strong conservation in the residues predicted to be vital for Ran binding or GEF activity, such activity should be tested in order to rule out the possibility that the RCC1-homologue is residing within this group (Kaiserli PhD thesis, 2009). Indeed, currently, many of these proteins are only annotated according to their similarity to RCC1.

Only one member of the UVR8-like group in *Arabidopsis* has been functionally annotated. PRAF1 (named for PH, RCC1 and FYVE) has phospholipid binding properties in vitro and is thus predicted to be membrane localised. The PRAF1 transcript itself meanwhile is a target for CaMV derived siRNA suggesting a role in pathogen defence (Moissard and Voinnet 2006). Interestingly, work on this protein has shown that the isolated RCC1-like region of the protein has the ability to catalyze guanine nucleotide exchange on a subset of the Rab proteins (Jensen *et al.* 2001). Thus, although it did not show significant similarity in the hypothesised functional residues for GEF activity, PRAF1 nonetheless exhibits some of this activity. It is possible that these important residues did not align correctly when the original comparison was performed. Alternatively, it seems that the lack in similarity does not prohibited Ran GEF activity. While UVR8 has been shown to lack significant Ran-GEF activity, this provides further grounds for testing the other UVR8 homologues in order to determine whether they share this feature with PRAF1.

While the functions of these UVR8-like proteins are yet to be determined, it does seem that they are unlikely to be functional homologues to UVR8 itself. None of the proteins examined possess regions similar to the N and C-terminal regions shown to be vital for UVR8 function. Furthermore, the evidence that *uvr8-1* mutants show extreme UV-B sensitivity combined with an inability to find other vital UV-B protective genes in a mutant screen, suggests that if they do indeed have a role in UV-B responses, it is a more minor one and as such are not acting in a redundant fashion with UVR8 (Brown *et al.* 2005).

6.4 The UVR8 complex

Many proteins act as part of a complex, be it through interactions with one or several other different components or by the incorporation of several monomers to form a multimer. The addition or removal of complex components can have an impact on the activity or

localisation of the protein in question. Therefore, one of the important areas of investigation into a newly identified protein is to determine whether it is acting alone. This can give a valuable insight into its function, for example by linking it with a well characterised pathway. For these reasons, with the identification of UVR8 as the first known UV-B specific element, searches were undertaken in order to identify any potential interacting partners. As both mass spectrometry and yeast-two-hybrid (discussed below) approaches proved problematic, it was decided to turn to SEC as an alternative means of complex identification.

This study has shown that UVR8 does indeed exist in a complex. This having been determined, opens up a new avenues for investigation; for example, giving rise to questions such as how this complex changes under different light conditions and whether it is necessary for protein function. Work presented here also demonstrated that the size of this complex can be reduced with the removal of the first 23 amino acids and a change in the size distribution of UVR8 protein altered with the removal of functional COP1. However, the question of whether this complex size differs in low fluence rate white light versus UV-B conditions and cytoplasm versus nucleus is not so clear-cut. Problems associated with the presence of a GFP tag as well as column resolution prevent clear determination. Despite these pitfalls, which should be easily remedied by using constructs without the GFP tag and a narrower resolution column respectively, we now have a better groundwork on which to base our hypotheses on UVR8 mechanism. The role of the N-terminal amino acids will be discussed more in the following section, while below conclusions stemming from work with the other constructs and the problems encountered will be covered.

One such difficulty that was encountered early on in this study was the observation that when a GFP tag was present in a construct, this hugely inflated the size of the complex. More specifically, in the experiments presented here the complex size doubled. GFP is commonly known to dimerize and it would thus seem that the presence of this tag resulted in a UVR8 complex dimer. GFP has been an extremely useful tool in molecular and microscopic analyses but it is not without its limitation. For example, it exhibits pH sensitivity, undergoes photobleaching when exposed to continuous irradiation and is relatively large with a size of ~30 kDa (White and Stelzer 1999; Shaner *et al.* 2007). Recent work by Chapman and colleagues (2008) has shown that a modified version of the LOV2 (light, oxygen or voltage sensing) domain of PHOTOTROPIN 2 (PHOT2), termed iLOV, can act as a fluorescent protein tag. This has the advantage that it is smaller (~10 kDa), stable over a large pH range, photoreversible and does not dimerize. Therefore, use

of iLOV as a tag would allow use of the construct in localisation studies without having a negative impact on use in SEC experiments.

One of the main down-falls of using western blotting to look at fractions from SEC is that it is not truly quantitative. This can make it difficult to judge which fraction appears to have the peak concentration of the protein of interest. Also, if there is a mix of complex sizes, for example there is an equilibrium between two forms, then if the difference in size is not extreme, separate fraction peaks will be difficult to identify and the blot will appear extended. However, as band intensity is dependent on the exposure time of the film to the chemiluminescent substance (as well as several other factors), then this can alter the range of bands seen. In the experiments performed in this study, several films were exposed for varying durations of time in order to attempt to combat this problem. Nevertheless, the risk remains that the non-quantitative nature of this experiment may be masking interesting results. This difference in spread of protein bands can be seen in Figure 5.8. The blot for UV-B treated Δ23N samples seems more extended than that for the untreated sample. It thus may be in this case that more than one complex exists, but this is difficult to determine with certainty using this method.

Another difficulty with this method is that it is not sensitive enough to detect small modifications in the protein such as phosphorylation or ubiquitination. While no current work has tested whether ubiquitination may have a role in UVR8 function, previous work using *Arabidopsis* cell culture has shown that both phosphorylation and de-phosphorylation are necessary for inductions of *CHS* under UV-B (Christie and Jenkins 1996). While this might imply that modification of the UVR8 protein might be necessary, subsequent analysis performed by Kaiserli showed that protein phosphatase inhibitors were neither able to remove the double band sometimes seen on protein gels, nor did they affect the nuclear accumulation of NES-GFP-UVR8 under UV-B conditions (Kaiserli PhD thesis, 2008). Thus it seems unlikely that phosphorlyation plays a role in UVR8 accumulation under UV-B, although it remains possible that downstream events may be affected by this form of post-translational modification.

A yeast-two-hybrid approach had been previously utilised by the Jenkins group in order to identify potential UVR8 interacting proteins. Despite screening two different libraries, no potential interacting partners were identified. Subsequently, several candidate interacting partners were tested using a direct approach. Again, no interaction was found for UVR8 with either HY5 or for any of the other candidates (Kaiserli PhD thesis, 2008). This included tests using COP1 which appears contrary to work performed by Favory *et al.* (2009). However, the Favory study showed that the COP1-UVR8 interaction is UV-B

dependent possibly explaining why Kaiserli and co-workers found no interaction. The work presented here though is nevertheless still at odds with that published by Favory and co-workers. No reduction in size of the complex was seen in the *cop1-4* mutant under UV-B and instead an increase was seen for untreated samples (see Figure 5.9). While the former result suggests that in this study at least, we were unable to detect this interaction, the reason behind the latter observation is more difficult to interpret. Therefore in conclusion, while it is clear that COP1 and UVR8 are both acting in UV-B responses, the precise way in which their associated dependent responses link together and the nature of the UVR8-COP1 complex is yet to be determined.

6.5 Role of the N-terminal of UVR8 in its function, localisation and complex formation

The UVR8 protein is known to have significant sequence similarity to human RCC1 with the exception of two regions at the termini (Kliebenstein *et al.* 2002; Brown *et al.* 2005; Kaiserli and Jenkins 2007). Within the C-terminus resides a 27 amino acids insert in UVR8 relative to RCC1 that has been shown to be essential for UVR8 function although the exact nature of the function of this region has yet to be determined (Kaiserli and Jenkins 2007). At the N-terminal, where RCC1 has a bi-partate NLS, no equivalent could be found in UVR8. Instead, particularly between residues 20-32 lies a region that is strongly conserved in proteins from other plant species bearing similarity to *Arabidopsis* UVR8 (see Figure 4.3). When a portion of this region was deleted (up to residue 23), a strong reduction in the nuclear accumulation of the protein was seen (Kaiserli and Jenkins, 2007). This suggests that the functional importance of this region may be tied to the protein localisation. Consequently, an extension of this work was performed here where 12, 20 and 33/32 amino acids were removed from UVR8 as well as added on to a GFP tag. The results of the localisation studies described here demonstrated a clear link between this region and appropriate localisation. The first 12 residues are not necessary for either appropriate localisation or function, but are sufficient for UV-B induced nuclear accumulation. The first 20 meanwhile are both necessary and sufficient for the same UV-B induced nuclear localisation. In line with work by Kaiserli and Jenkins using the Δ23N construct, these same residues are also necessary for UVR8 function. Finally, the 33 N-terminal amino acids are clearly necessary for UV-B induced nuclear accumulation while the first 32 confer constitutive nuclear accumulation of GFP under both plus and minus UV-B conditions.

If we incorporate the results from SEC experiments, we can potentially link localisation with complex formation as the Δ23N construct, in addition to mis-localisation, appears to have a strongly reduced complex size relative to full length GFP-UVR8. However, it would seem that the story may be quite complex. For example if complex formation is necessary for nuclear accumulation, then we would expect the Δ23N construct to completely lose nuclear accumulation under UV-B. Nevertheless, the increase in nuclear accumulation seen for the Δ23N construct is only a difference of ~10 % relative to white light levels. Thus is seems only residual levels of nuclear accumulation are seen and the first 20-23 amino acids of UVR8 can be considered to have a major role in protein localisation. However, it has yet to be tested whether the apparent dual roles for this region in localisation and complex formation are in fact linked.

A second interesting observation is that while +12N and +20N retain UV-B mediated nuclear accumulation, +32N is nuclear localised. This suggests first, that some signal spread across the first 20 amino acids is able to cause cytoplasmic retention under minus UV-B conditions and second, that some feature of residues 21-32 is able to overcome this retention signal. While this latter region has no obvious NLS signal, it may be acting as such and is strong enough to overcome the NES signals adjoined to the most N-terminal portion of the sequence. However, as the full length version, NES-GFP-UVR8 regains cytoplasmic localisation under minus UV-B, it would appear that this NLS signal is masked in some way the remainder of the sequence is present. Under this hypothesis, the Δ20 an Δ23 constructs may show impaired nuclear accumulation due to the loss in signals present in the 1-20/23 amino acid region, but are still able to accumulate slowly due to a few remaining signals upstream of this region.

It would therefore appear that in addition to some cytoplasmic retention signals within the first 20 amino acids region, there also lies a segment essential for complex formation. Also, as the Δ23N construct is able to accumulate (albeit to a very small degree) under UV-B but is not able to rescue to the *uvr8-1* phenotype, this implies the loss in functionality of this protein may be more closely linked with the reduction in complex size than the protein localisation. If these two effects (complex formation and functionality) are linked, it would be especially interesting to determine what the interacting partner is as it would appear that appropriate binding may be essential for protein function, perhaps even involved in the activation of the UVR8 and the subsequent initiation of gene expression after UV-B. Under this assumption, if this interacting partner were to be knocked out, then we would expect a lack of induction of the UVR8-mediated pathway and its downstream effects. As mentioned previously, mutant screens previously

performed by the Jenkins group to indentify essential UV-B components resulted in the identification of four mutant alleles of UVR8, but no other genes were flagged. It is possible that this unknown interacting partner is essential for other aspects of a plant's normal cellular processes so that severe mutations in this gene result in lethality. This may explain its absence in the mutant screen. Alternatively, as the complex size of native UVR8 appears to be ~70-90 kDa, roughly double the size of UVR8 (43 kDa), then it may be that UVR8 is acting as a dimer. Under this theory, the nature if the interaction would have to be dependent on direct UVR8-UVR8 contact as the presumed artificial dimerization seen in Δ23N is not sufficient to restore function (Kaiserli and Jenkins 2007). This theory may help explain why the relatively short 12 amino acid N-terminal region of UVR8 fused to GFP is able in the tobacco system to retain UV-B induced nuclear accumulation. That is, the +12N construct could be interacting with the UVR8 homologue in tobacco (NtUVR8) thus conferring a normal localisation phenotype. The full length NtUVR8 interactor may ensure cytoplasmic localisation under minus and nuclear accumulation under plus UV-B conditions. However, this could only hold true if the hypothesised NLS region in the 20-32 amino acid region is a strong signal. When the +32N construct was examined in the transient tobacco system (with the presence of a UVR8 homologue) and also in T1 *uvr8-1* transformed seedlings (lacking any functional UVR8), very similar results were seen. Therefore, if +32N in tobacco is interacting with NtUVR8 then the NLS signal exposed on +32N must be strong enough to overcome any effects of binding to NtUVR8 otherwise we would expect to see different results in the two systems.

While the work performed as part of this study has revealed several interesting aspects of the UVR8 protein, especially in the region of the N-terminal, there is significant scope for further work building on the conclusions drawn here. With this additional work (some suggestions for which are included in Section 6.7) we can hope to fully resolve the roles of the different regions of UVR8, understand its mechanisms of action and how this is associated with both complex formation and localisation.

6.6 Conclusions

The list below is a summary of the major conclusion that can be drawn form this study.

a. A large number of genes are induced under low fluence rate UV-B.
b. However, a significant proportion of these may be false positives.

c. There is relatively little overlap between microarray studies performed by other groups. This most likely reflects the differences in experimental procedures.
d. A group of low fluence rate UV-B induced genes that are not dependent on functional UVR8, HY5 or HYH do exist. Nor are these genes dependent on known photoreceptors or are induced by DNA damage.
e. Genes that form parts of different pathways exhibit different expression profiles under UV-B treatment.
f. 23 proteins that show similarity to UVR8 exist in *Arabidopsis*. None of these however possess recognisable N or C-terminal domains associated with UVR8 functionality.
g. A number of proteins exist in other plant species which can be split into groups based on greater similarity to either UVR8 or human RCC1.
h. The first 12 amino acids of UVR8 are not necessary but are sufficient for UV-B induced nuclear accumulation. They are not necessary for UVR8 function.
i. Meanwhile the first 20 appear to be both necessary and sufficient for UV-B induced nuclear accumulation. They are also necessary for UVR8 function.
j. The initial 33 residues are necessary for nuclear accumulation and the first 32 are sufficient to cause constitutive nuclear localisation of GFP.
k. Native UVR8 exists in a complex ~70-90 kDa in size.
l. The presence of a GFP tag appears to cause artificial dimerization of the complex.
m. Loss of the 23 most N-terminal residues results in a reduction in complex size.
n. Removal of functional COP1 leads to an increased complex size in minus UV-B conditions.

Despite the progress made in this study, our knowledge of UV-B responses in plants includes a number of gaps. Some further work which should be initiated in order to fill these is outlined below.

6.7 Future work

Work performed as part of this study has revealed several new aspects of UV-B responses in *Arabidopsis thaliana*. Research into the UVR8-independent UV-B induced transcriptome changes was undertaken which showed the existence of UVR8/HY5/HYH independent pathways and identified interesting candidate genes for further study. In addition, we now have additional information into the role of the N-terminal of UVR8 as

well as evidence that the protein exists as part of a complex. Nevertheless, our picture of UV-B responses is far from complete, especially when compared to those of other light qualities.

Work presented here as well as that performed by Safrany *et al.* (2008) has shown that UV-B mediated UVR8-independent pathways do indeed exist. While the role that UVR8 plays in UV-B responses is obviously of vital importance, it is nonetheless interesting to investigate these other pathways further and determine why the induction of these genes is seen under UV-B. The huge number of genes induced under these conditions makes it difficult to know where best to focus. Perhaps the expression profiling suggested here would help crystalise the different sets of components involved and possibly untangle the many pathways. In addition, a mutant screen approach similar to that which identified UVR8 as a UV-B specific component could be utilised to find crucial up-stream signalling components (Brown *et al.* 2005). In this case, instead of using a ProCHS:LUC construct, the promoter region could be replaced with that for *ANAC13* or one of the other UVR8-independent genes. This may lead to the identification of novel components and possibly even a UV-B photoreceptor.

While it appears that COP1 is involved in both UVR8 dependent and independent UV-B responses, it is still unclear the exact way in which these pathways intermix (Favory *et al.* 2009). Recent work has found that COP1 acts differently under UV-B compared to its role as a negative regulator of photomorphogenesis; in the latter case it acts as a repressor of HY5 activity whereas in the former it appears to promote expression (Favory *et al.* 2009)). This therefore appears to be a key area for further work, especially with the observation that UVR8 interacts with COP1 under UV-B (Favory *et al.* 2009). It is important to understand how UV-B promotes interaction between UVR8 and COP1 and how this interaction leads to the regulation of transcription.

For the purposes of this work, only those genes that were common to microarrays at the three fluence levels were considered in order to maximise the likelihood of pursuing genuine UV-B responsive genes. However, it could also be interesting to look at only those genes that appear in 0.3 and 1 μmol m^{-2} s^{-1} fluence rate microarrays. This grouping could include genes that are specific to low fluence and get shut off at high. UVR8 responses have been shown to persist at higher more damaging UV-B levels (Brown and Jenkins 2008) but this does not necessarily exclude the possibility that a low fluence pathway exists.

The collective evidence from all the microarrays examined here seems to suggest that many UV-B signalling pathways may exist involving a multitude of different genes.

One way in which to untangle these may be to perform timecourse studies such as that shown in Figure 3.6. From these results it would seem that *CHS* and *ELIP1* share very similar expression profiles, while the transcription factor that regulates them both, *HY5*, shows a drastically different pattern of expression. Furthermore, a second transcription factor *ANAC13*, the stress-related *WRKY30* and *2g41730* all show different profiles from each other as well as to the UVR8 dependent components. Thus, this situation could be taken advantage of. Submission of samples taken from different time-points for microarray would allow the construction of a large number of expression profiles. These in turn could be compared and, using mathematical modelling, grouped according to similarity. Similar approaches have already been used in circadian clock studies (Covington *et al.* 2008; James *et al.* 2008) and in yeast to untangle transcriptional networks (Qian *et al.* 2003; Kudlicki *et al.* 2007). This approach was considered for this study. To that end, a number of calculations were made using the timecourse data in Figure 3.6 as a basis, in order to determine the best time-points to use for such a study. That is, which timepoints would give the maximal possible difference between the various profiles, thus ensuring more accurate allocation into groups. These calculations can be found in Appendix I along with suggestions for timepoints for a future experiment.

If we next turn to the UVR8 protein itself, one hypothesis is that UVR8 may be dimerizing. One way in which to test this theory is to use the directed yeast-two-hybrid approach used before with UVR8 as both the bait and prey. Alternatively, both native and tagged versions could be expressed in the same plant and analysed by SEC. This would allow us to determine if a range in complex sizes is seen which would correspond to the three types of complex formed (untagged homodimers, tagged homodimers and heterodimers of tagged and untagged monomers).

Work here has further supported the observation that the N-terminal region of UVR8 is of key importance in the appropriate localisation of the protein as well as its interaction with an as yet unidentified protein partner. However, the roles of sub-sections of this region are not yet fully clear. Thus to resolve some of the issues mentioned above, it would seem that we need to cut down the N-terminal further. For example, tag a fluorescent protein (e.g. iLOV so that the same plants could be used in microscopy and SEC) with just the 20-32 amino acid region to see if this still confers constitutive nuclear localisation of whether the N-terminal as a whole is needed. A series of experiments with each separate region or in different combinations may help to separate out the three components seen. That is 1) UV-B responsive nuclear accumulation 2) constitutive

nuclear localisation 3) complex formation. We could subsequently link these in turn to protein functionality in order to determine the exact role of this important region.

Further study of the N-terminal region may also lead to further insights into the exact mechanisms by which UVR8 localisation occurs. Evidence from work performed by Eirini Kaiserli (unpublished data) suggests that it is UVR8 export from the nucleus that is being controlled; treatment with a nuclear export inhibitor leptomycin B results in a strong nuclear accumulation of NES-GFP-UVR8. This inhibitor acts by binding to the recognition site of Exportin 1, thus preventing it from associating with other proteins (Fukuda *et al.* 1997). It would therefore seem that Exportin 1 may be involved in the localisation phenotype of UVR8 under UV-B conditions. Nevertheless, more work is required in order to determine the exact means by which UVR8 moves to or is excluded from cellular compartments.

Finally, while the N-terminal region of UVR8 appears to be vital in protein localisation and complex formation, it is not yet clear whether these two effects are linked or are separate features. Further investigation into the components of the UVR8 complex is required. It is possible that once these interacting partners have been confirmed, they may prove to have roles in protein localisation or the ability to activate UVR8 once the UV-B signal has been perceived. That is, nuclear localisation and presence of UVR8 on the promoter region of *HY*5 are not sufficient to induce the UVR8-mediated UV-B pathway (Kaiserli and Jenkins 2007). Some other, yet unknown event has to occur before transcription is initiated and this may turn out to be attributable to the interacting partners of UVR8. Thus knowledge of the exact components of the UVR8 complex under various conditions may give the required insight needed to determine the exact mechanisms of UVR8's sub-cellular localisation and activity.

APPENDIX IA
UV-B TIMECOURSES

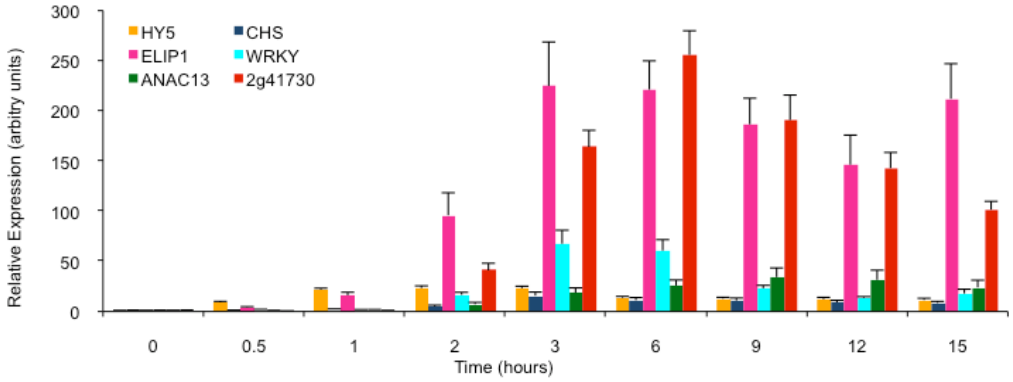

Figure 7.1 Timecourse of fold change values of UV-B induced genes. Three week old wild type plants were grown under 20-25 µmol m^{-2} s^{-1} white light and treated with 3 µmol^{-2} s^{-1} UV-B for the times shown above before tissue was harvested and RNA extracted. Values for relative expression (adjusted to *ACT2* transcript levels) were determined using qPCR. Graphs show changes in gene expression over time. Y-axis depicts fold change in expression and x-axis gives the length of treatment. Bars represent standard error, n=6.

APPENDIX IB
TIMEPOINT SELECTION

Using the data generated by qPCR analysis described in Section 3.2.6 a series of equations were drawn up in order to determine the optimal time-points for a microarray analysis using three timepoints. . The genes considered included HY5, ELIP1, CHS and WRKY.

In order to obtain the best separation of different expression profile, timepoints should reflect the maximum difference between each of the genes To calculate the difference between genes **'i'** and **'j'** over three time points t_1, t_2 and t_3, where $g\bar{e}_i\ (t_1)$ equals the mean gene expression of gene 'i' at timepoint 1.

$$\delta_{ij} = \left| g\bar{e}_i\ (t_1) - g\bar{e}_j\ (t_1) \right|^2 + \left| g\bar{e}_i\ (t_2) - g\bar{e}_j\ (t_2) \right|^2 + \left| g\bar{e}_i\ (t_3) - g\bar{e}_j\ (t_3) \right|^2$$

To determine the total difference between all four genes where δ_{ij} equals the difference between genes 'i' and 'j' at timepoints 1, 2 and 3.

$$\Sigma\ \delta_{ijkl} = \delta_{ij} + \delta_{ik} + \delta_{il} + \delta_{jk} + \delta_{jl} + \delta_{kl}$$

To determine the variance for gene 'i' at timepoint 1 where $ge_i\ (t_1\ r_1)$ equals the gene expression of gene 'i' at timepoint 1 in replicate 1.

$$\text{var (i)} = \left| ge_i\ (t_1\ r_1) - g\bar{e}_i\ (t_1) \right|^2 + \left| ge_i\ (t_1\ r_2) - g\bar{e}_i\ (t_1) \right|^2 + \left| ge_i\ (t_1\ r_3) - g\bar{e}_i\ (t_1) \right|^2 + \left| ge_i\ (t_1\ r_4) - g\bar{e}_i\ (t_1) \right|^2 + \left| ge_i\ (t_1\ r_5) - g\bar{e}_i\ (t_1) \right|^2 + \left| ge_i\ (t_1\ r_6) - g\bar{e}_i\ (t_1) \right|^2 \times 1/6$$

To calculate the score for each combination of three time points

$$\text{SCORE } (t_1, t_2, t_3) = \frac{\text{Sum of the difference between genes 'i' 'j' 'k' and 'l' for } (t_1, t_2, t_3)}{\text{Sum of the variance for genes 'i' 'j' 'k' and 'l' for } (t_1, t_2, t_3)}$$

$$\frac{\Sigma\ \delta_{ijkl}}{\Sigma\ var_{ijkl}}$$

The score was calculated for each of the 84 possible combinations of three timepoints (from original qPCR analysis which looked at expression levels for nine timepoints).

To determine which timepoints would be the best to use for subsequent microarrays, the combination of three timepoints which yeilded the highest score (i.e. the timepoints which show the greatest difference between genes, but the smallest variance within genes) was selected.

Code	t1	t2	t3	dCH	dCE	dCW	dHE	dHW	dEW	d all	varC	varH	varE	varW	var all	SCORE
S5	0	0.5	9	0.007	0.077	0.006	0.131	0.000	0.125	0.346	0.003	0.000	0.012	0.000	0.015	22.867
S23	0	6	9	0.013	0.192	0.006	0.304	0.003	0.253	0.771	0.006	0.000	0.027	0.001	0.034	22.781
S44	0.5	6	9	0.013	0.192	0.006	0.304	0.004	0.253	0.771	0.006	0.000	0.027	0.001	0.034	22.772
S11	0	1	9	0.008	0.077	0.006	0.131	0.001	0.125	0.349	0.003	0.000	0.012	0.000	0.015	22.700
S59	1	6	9	0.013	0.192	0.006	0.304	0.005	0.254	0.774	0.006	0.000	0.027	0.001	0.034	22.698
S32	0.5	1	9	0.008	0.077	0.006	0.131	0.001	0.126	0.349	0.003	0.000	0.012	0.000	0.015	22.683
S4	0	0.5	6	0.006	0.115	0.000	0.172	0.003	0.128	0.426	0.003	0.000	0.015	0.001	0.019	22.417
S10	0	1	6	0.006	0.115	0.001	0.172	0.004	0.129	0.428	0.003	0.000	0.015	0.001	0.019	22.289
S31	0.5	1	6	0.006	0.115	0.001	0.173	0.005	0.129	0.428	0.003	0.000	0.015	0.001	0.019	22.275

Table 7.1 Results from score calculations. Table shows the resulting values from the equations described above. T1, t2 and t3 = timepoints (in hours). d = difference, C = *CHS*, H = *HY5*, E= *ELIP1* and W = *WRKY* so dCH = difference between expression of *CHS* and *HY5*.

APPENDIX II
ALIGNMENT OF UVR8-LIKE PROTEINS IN *ARABIDOPSIS*

Figure 7.2 The following pages show the full multiple sequence alignment of UVR8 with the 23 UVR8-like proteins in *Arabidopsis thaliana*. Protein sequences were aligned in ClustalX as described in Chapter 2.13.2.

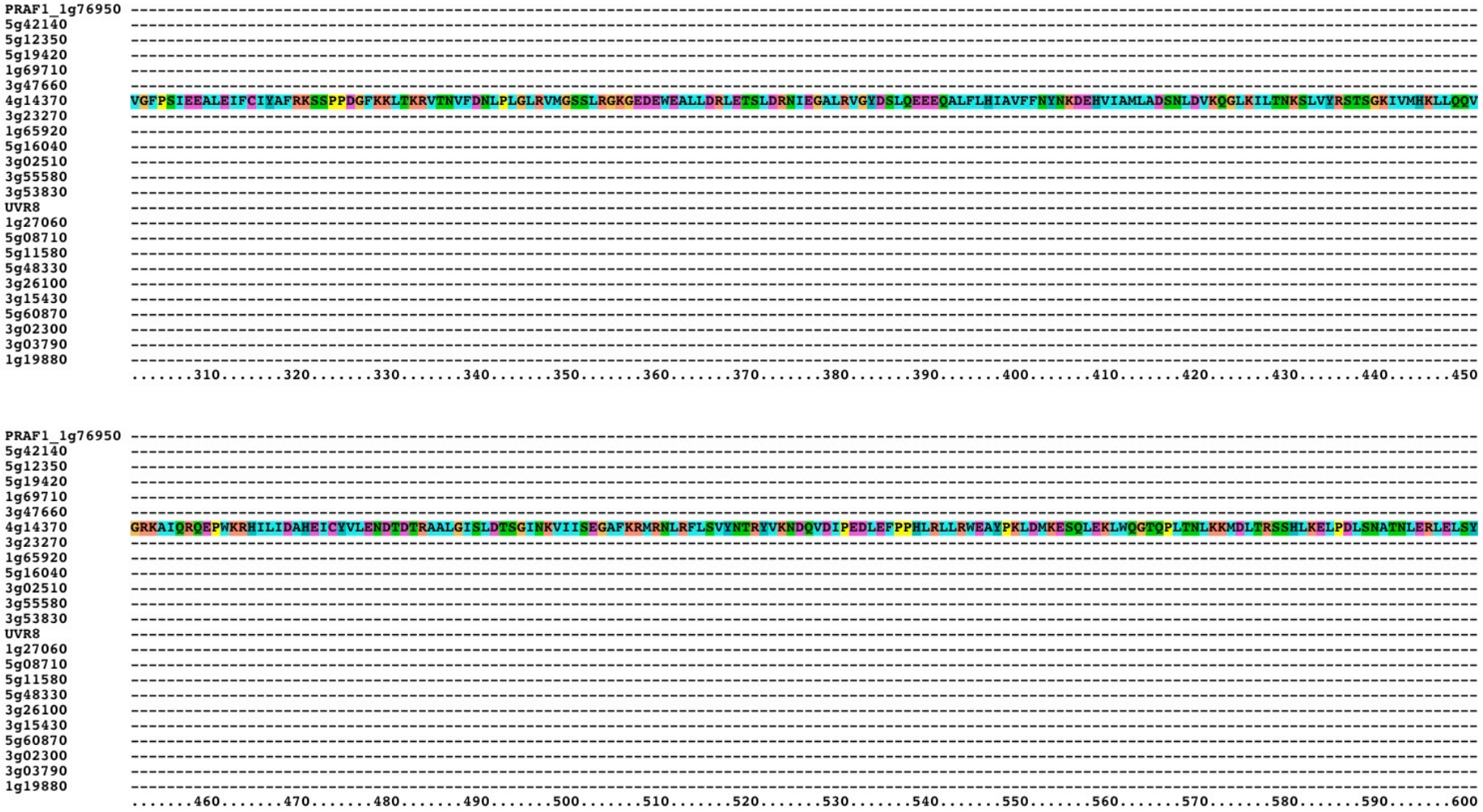
PRAF1_1g76950
5g42140
5g12350
5g19420
1g69710
3g47660
4g14370
3g23270
1g65920
5g16040
3g02510
3g55580
3g53830
UVR8
1g27060
5g08710
5g11580
5g48330
3g26100
3g15430
5g60870
3g02300
3g03790
1g19880
VGFPSIEEALEIFCIYAFRKSSPPDGFKKLTKRVTNVFDNLPLGLRVMGSSLRGKGEDEWEALLDRLETSLDRNIEGALRVGYDSLQEEEQALFLHIAVFFNYNKDEHVIAMLADSNLDVKQGLKILTNKSLVYRSTSGKIVMHKLLQQV
450
.....310.....320.....330.....340.....350.....360.....370.....380.....390.....400.....410.....420.....430.....440.....450
GRKAIQRQEPWKRHILIDAHEICYVLENDTDTRAALGISLDTSGINKVIISEGAFKRMRNLRFLSVYNTRYVKNDQVDIPEDLEFPPHLRLLRWEAYPKLDMKESQLEKLWQGTQPLTNLKKMDLTRSSHLKELPDLSNATNLERLELSY
600
.....460.....470.....480.....490.....500.....510.....520.....530.....540.....550.....560.....570.....580.....590.....600

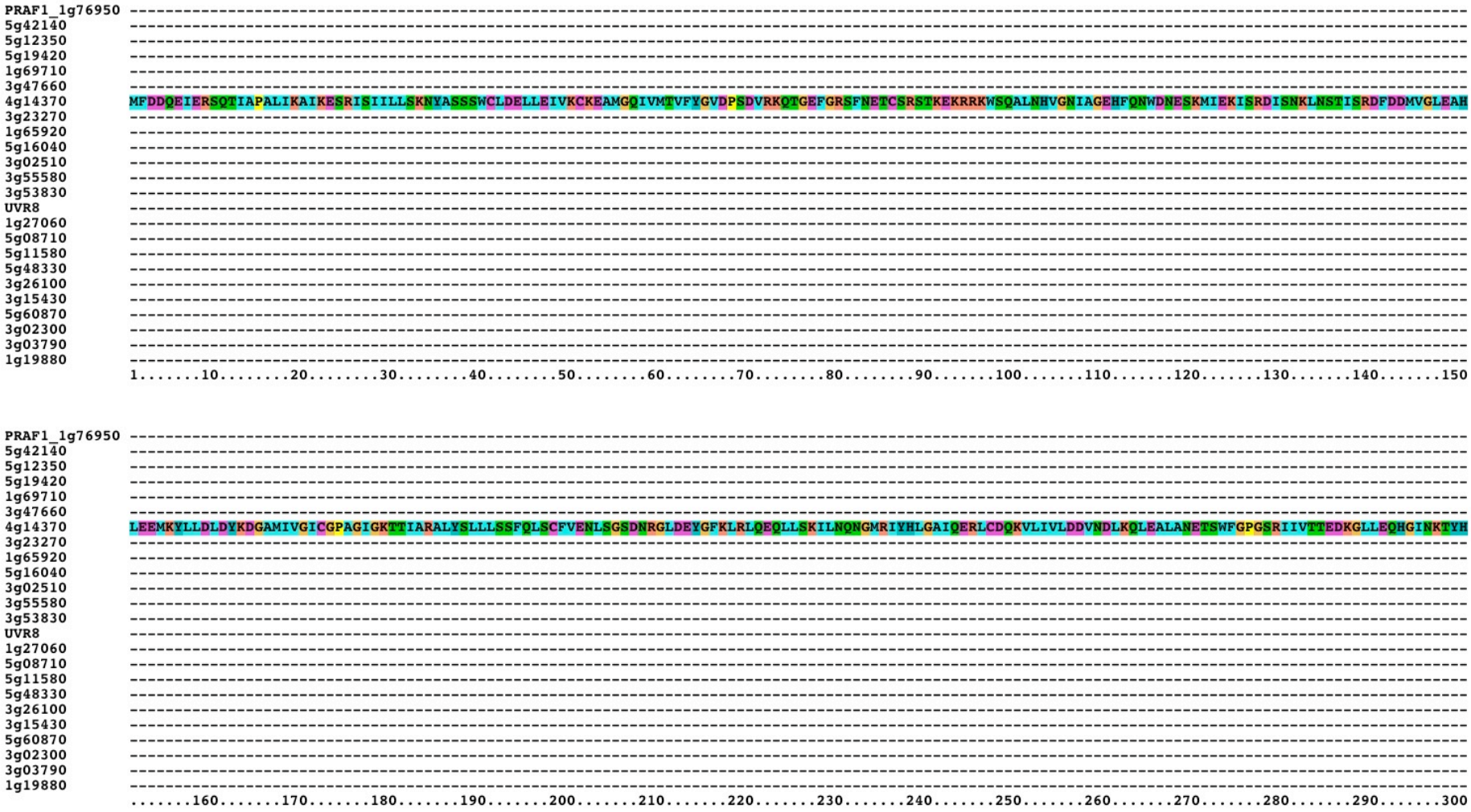
PRAF1_1g76950
5g42140
5g12350
5g19420
1g69710
3g47660
4g14370
3g23270
1g65920
5g16040
3g02510
3g55580
3g53830
UVR8
1g27060
5g08710
5g11580
5g48330
3g26100
3g15430
5g60870
3g02300
3g03790
1g19880
MFDDQEIERSQTIAPALIKAIKESRISIILLSKNYASSSWCLDELLEIVKCKEAMGQIVMTVFYGVDPSDVRKQTGEFGRSFNETCSRSTKEKRRKWSQALNHVGNIAGEHFQNWDNESKMIEKISRDISNKLNSTISRDFDDMVGLEAH
150
1.....10.....20.....30.....40.....50.....60.....70.....80.....90.....100.....110.....120.....130.....140.....150
LEEMKYLLDLDYKDGAMIVGICGPAGIGKTTIARALYSLLLSSFQLSCFVENLSGSDNRGLDEYGFKLRLQEQLLSKILNQNGMRIYHLGAIQERLCDQKVLIVLDDVNDLKQLEALANETSWFGPGSRIIVTTEDKGLLEQHGINKTYH
300
.....160.....170.....180.....190.....200.....210.....220.....230.....240.....250.....260.....270.....280.....290.....300

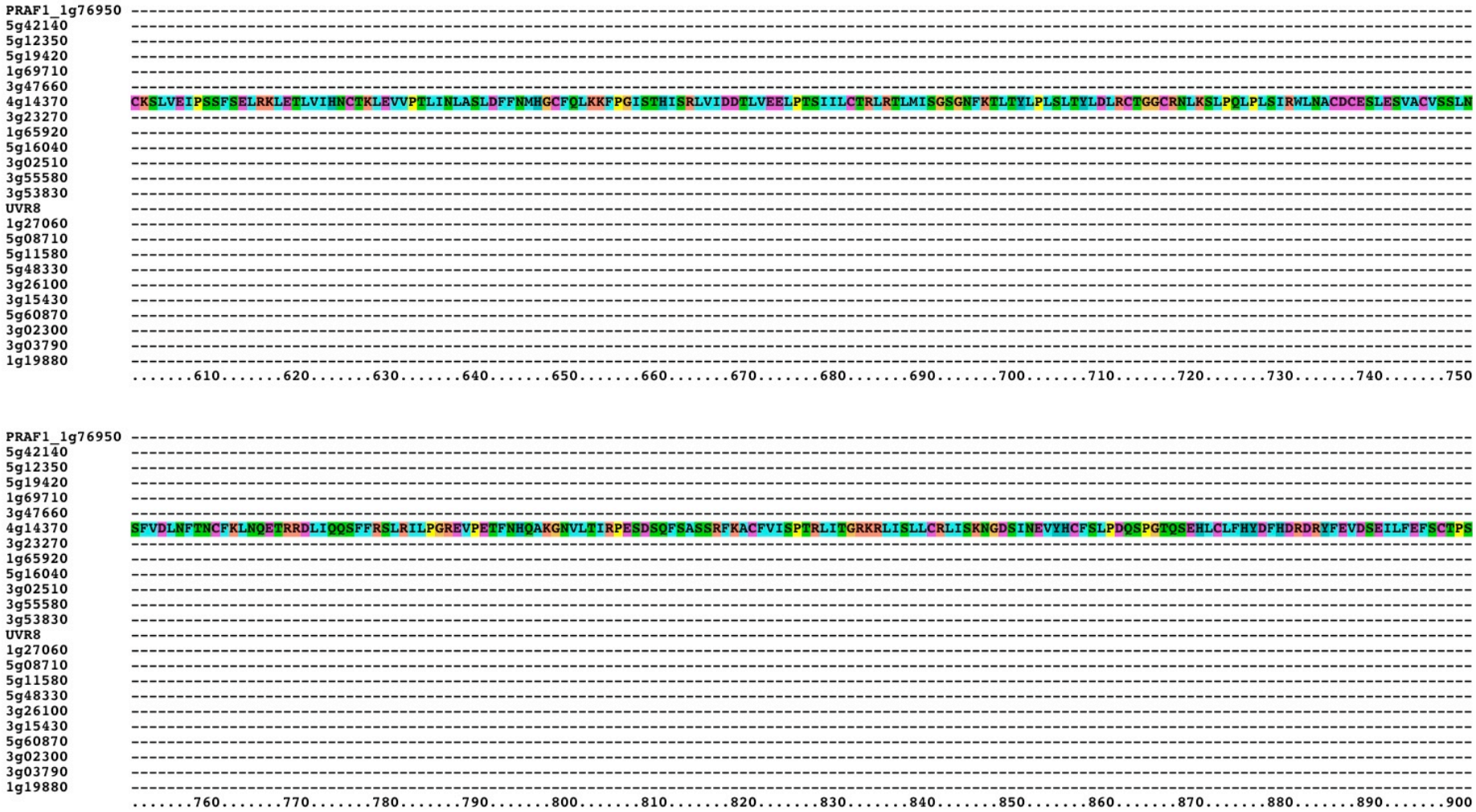
PRAF1_1g76950
5g42140
5g12350
5g19420
1g69710
3g47660
4g14370
3g23270
1g65920
5g16040
3g02510
3g55580
3g53830
UVR8
1g27060
5g08710
5g11580
5g48330
3g26100
3g15430
5g60870
3g02300
3g03790
1g19880
CKSLVEIPSSFSELRKLETLVIHNCTKLEVVPTLINLASLDFFNMHGCFQLKKFPGISTHISRLVIDDTLVEELPTSIILCTRLRTLMISGSGNFKTLTYLPLSLTYLDLRCTGGCRNLKSLPQLPLSIRWLNACDCESLESVACVSSLN
750
.....610.....620.....630.....640.....650.....660.....670.....680.....690.....700.....710.....720.....730.....740.....750
SFVDLNFTNCFKLNQETRRDLIQQSFFRSLRILPGREVPETFNHQAKGNVLTIRPESDSQFSASSRFKACFVISPTRLITGRKRLISLLCRLISKNGDSINEVYHCFSLPDQSPGTQSEHLCLFHYDFHDRDRYFEVDSEILFEFSCTPS
900
.....760.....770.....780.....790.....800.....810.....820.....830.....840.....850.....860.....870.....880.....890.....900

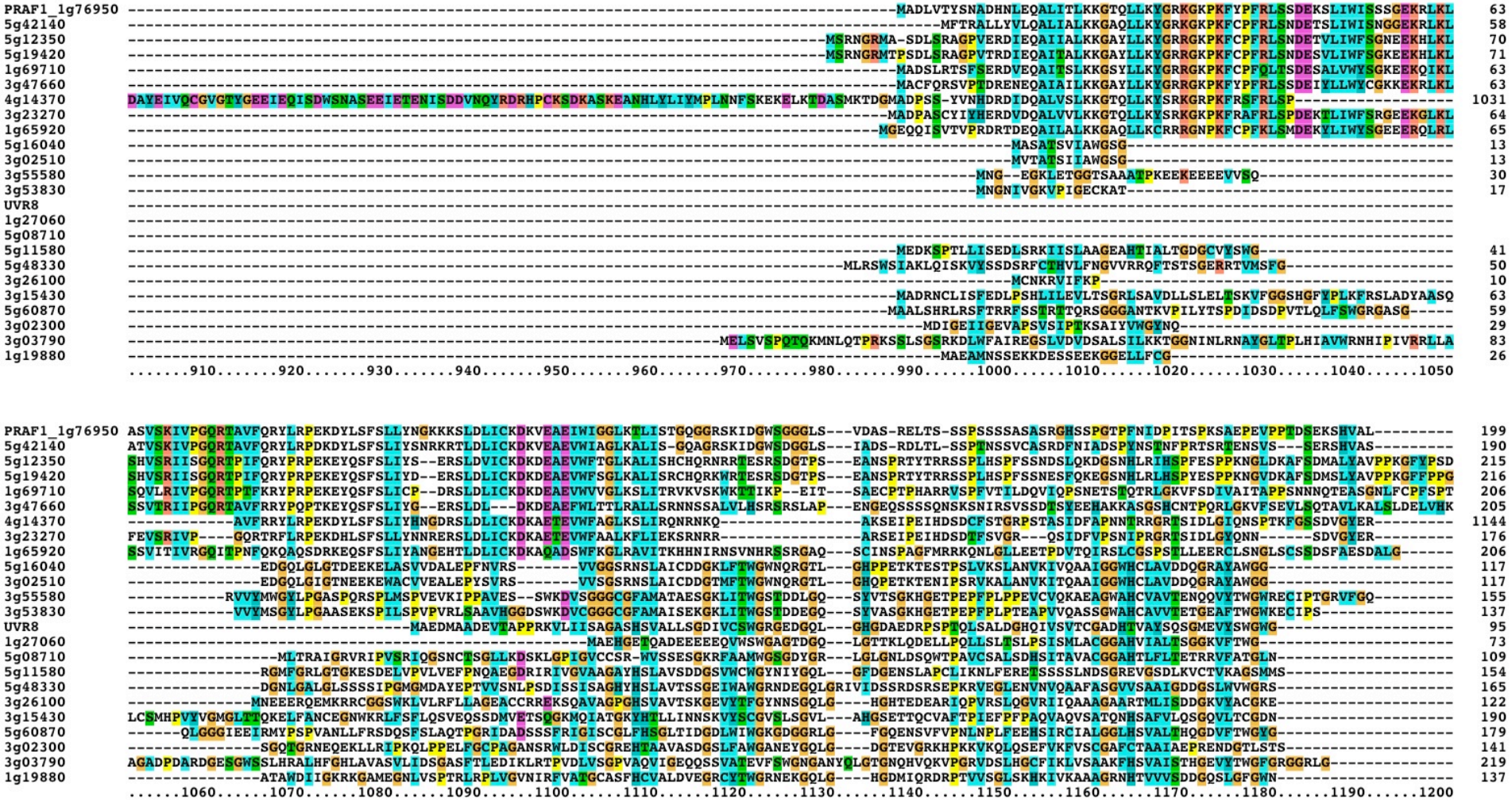
PRAF1_1g76950
5g42140
5g12350
5g19420
1g69710
3g47660
4g14370
3g23270
1g65920
5g16040
3g02510
3g55580
3g53830
UVR8
1g27060
5g08710
5g11580
5g48330
3g26100
3g15430
5g60870
3g02300
3g03790
1g19880
.....910.....920.....930.....940.....950.....960.....970.....980.....990.....1000.....1010.....1020.....1030.....1040.....1050
PRAF1_1g76950
5g42140
5g12350
5g19420
1g69710
3g47660
4g14370
3g23270
1g65920
5g16040
3g02510
3g55580
3g53830
UVR8
1g27060
5g08710
5g11580
5g48330
3g26100
3g15430
5g60870
3g02300
3g03790
1g19880
.....1060.....1070.....1080.....1090.....1100.....1110.....1120.....1130.....1140.....1150.....1160.....1170.....1180.....1190.....1200

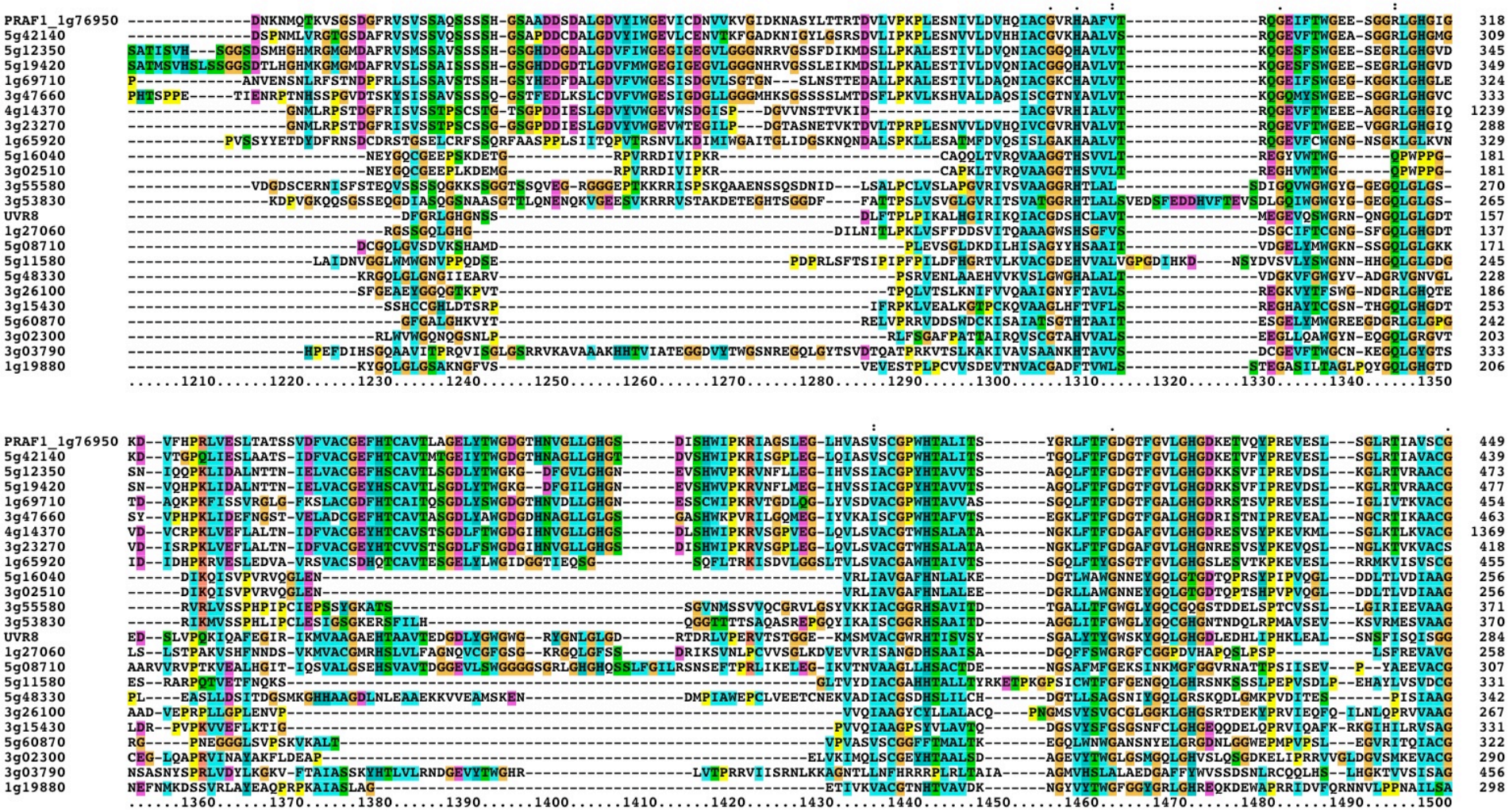
PRAF1_1g76950
5g42140
5g12350
5g19420
1g69710
3g47660
4g14370
3g23270
1g65920
5g16040
3g02510
3g55580
3g53830
UVR8
1g27060
5g08710
5g11580
5g48330
3g26100
3g15430
5g60870
3g02300
3g03790
1g19880
.....1210.....1220.....1230.....1240.....1250.....1260.....1270.....1280.....1290.....1300.....1310.....1320.....1330.....1340.....1350
.....1360.....1370.....1380.....1390.....1400.....1410.....1420.....1430.....1440.....1450.....1460.....1470.....1480.....1490.....1500

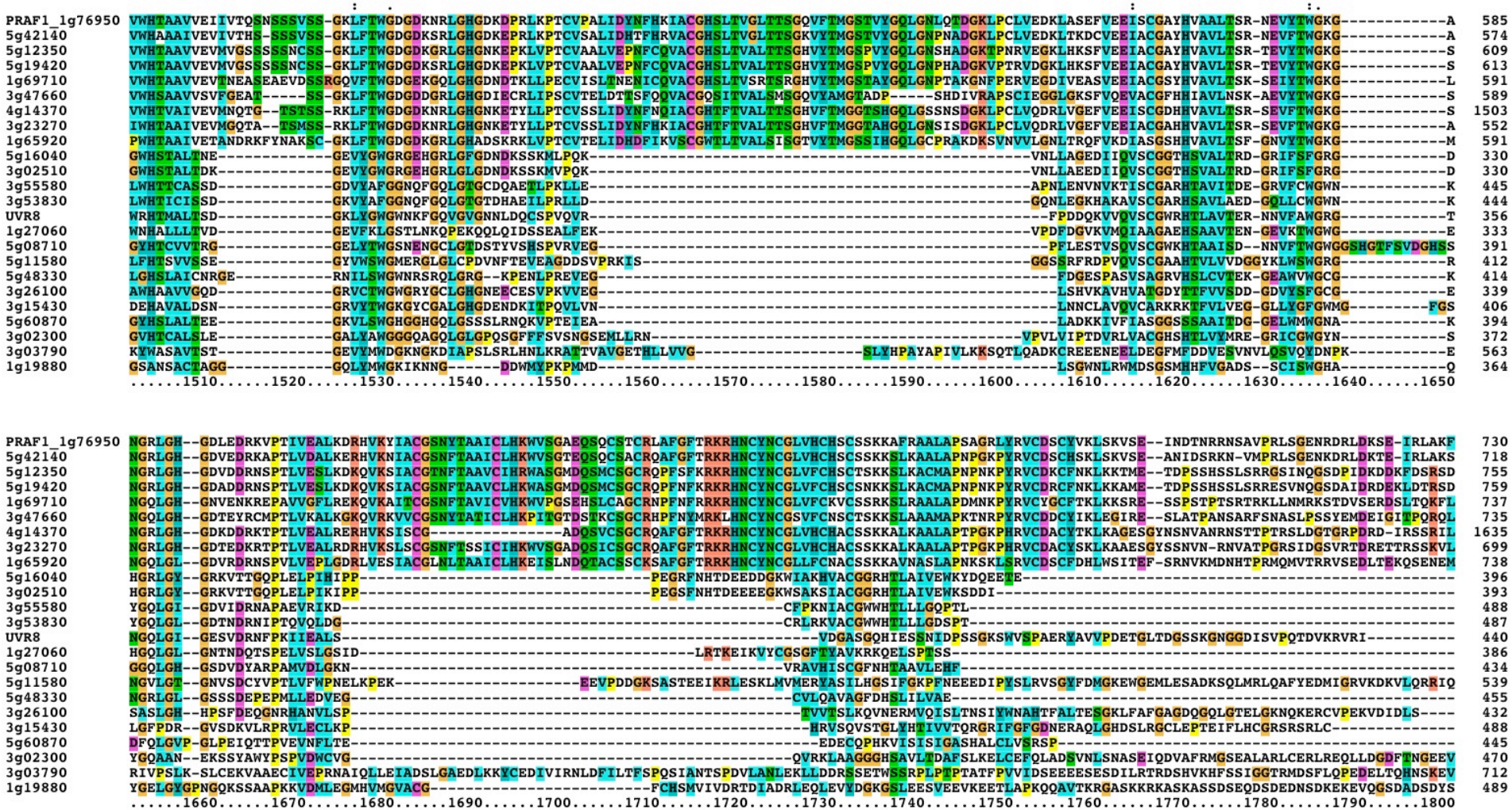
PRAF1_1g76950
5g42140
5g12350
5g19420
1g69710
3g47660
4g14370
3g23270
1g65920
5g16040
3g02510
3g55580
3g53830
UVR8
1g27060
5g08710
5g11580
5g48330
3g26100
3g15430
5g60870
3g02300
3g03790
1g19880

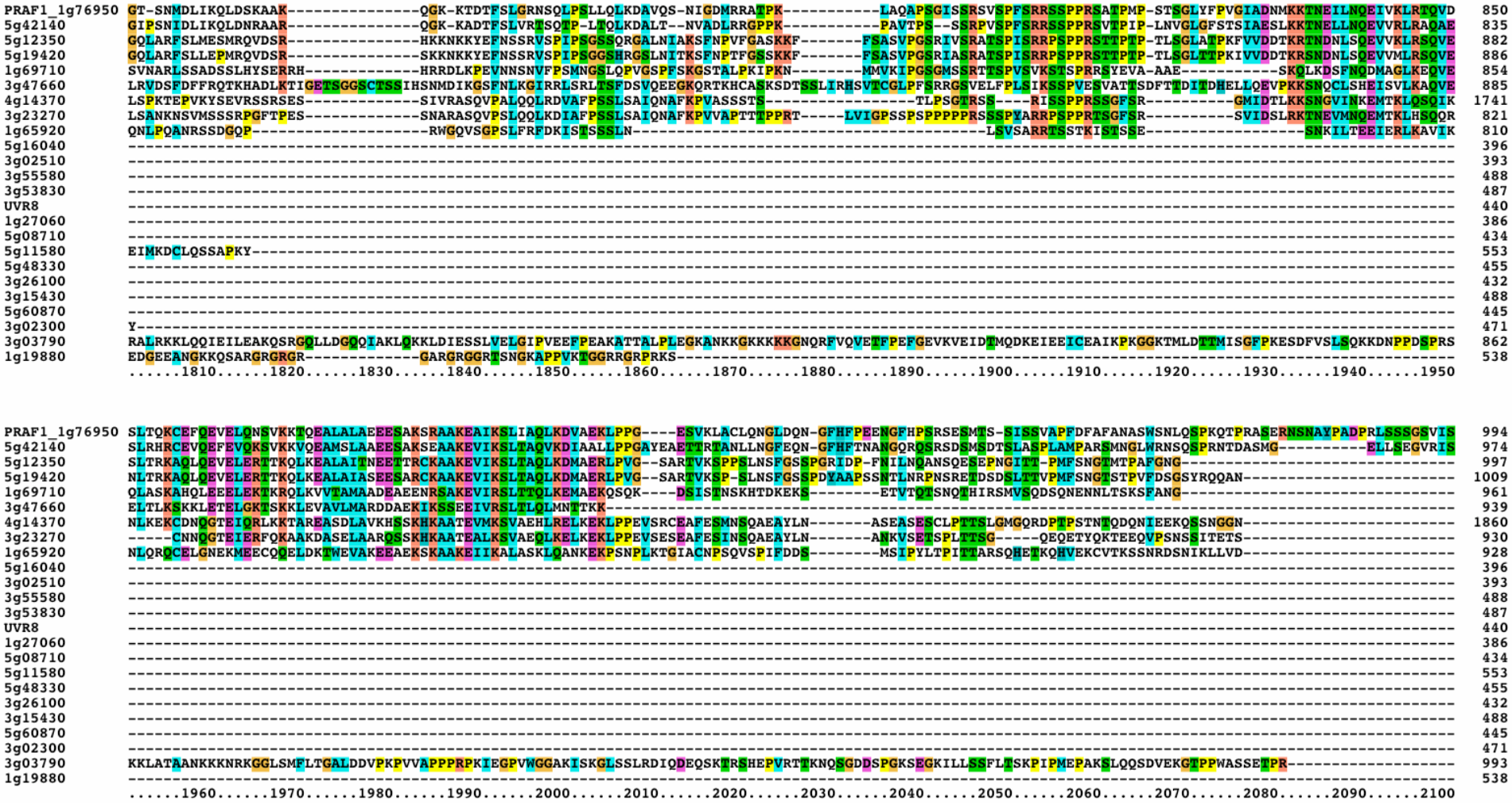
PRAF1_1g76950 GT-SNMDLIKQLDSKAAK----------QGK-KTDTFSLGRNSQLPSLLQLKDAVQS-NIGDMRRATPK----------LAQAPSGISSRSVSPFSRRSSPPRSATPMP-STSGLYFPVGIADNMKKTNEILNQEIVKLRTQVD 850
5g42140 GIPSNIDLIKQLDNRAAR----------QGK-KADTFSLVRTSQTP-LTQLKDALT--NVADLRRGPPK----------PAVTPS--SSRPVSPFSRRSSPPRSVTPIP-LNVGLGFSTSIAESLKKTNELLNQEVVRLRAQAE 835
5g12350 GQLARFSLMESMRQVDSR----------HKKNKKYEFNSSRVSPIPSGSSQRGALNIAKSFNPVFGASKKF-------FSASVPGSRIVSRATSPISRRPSPPRSTTPTP-TLSGLATPKFVVDDTKRTNDNLSQEVVKLRSQVE 882
5g19420 GQLARFSLLEPMRQVDSR----------SKKNKKYEFNSSRVSPIPSGGSHRGSLNITKSFNPTFGSSKKF-------FSASVPGSRIASRATSPISRRPSPPRSTTPTP-TLSGLTTPKIVVDDTKRSNDNLSQEVVMLRSQVE 886
1g69710 SVNARLSSADSSLHYSERRH----------HRRDLKPEVNNSNVFPSMNGSLQPVGSPFSKGSTALPKIPKN--------MMVKIPGSGMSSRTTSPVSVKSTSPRRSYEVA-AAE----------SKQLKDSFNQDMAGLKEQVE 854
3g47660 LRVDSFDFFRQTKHADLKTIGETSGGSCTSSIHSNMDIKGSFNLKGIRRLSRLTSFDSVQEEGKQRTKHCASKSDTSSLIRHSVTCGLPFSRRGSVELFPLSIKSSPVESVATTSDFTTDITDHELLQEVPKKSNQCLSHEISVLKAQVE 885
4g14370 LSPKTEPVKYSEVRSSRSES----------SIVRASQVPALQQLRDVAFPSSLSAIQNAFKPVASSSTS----------TLPSGTRSS----RISSPPRSSGFSR----------GMIDTLKKSNGVINKEMTKLQSQIK 1741
3g23270 LSANKNSVMSSSRPGFTPES----------SNARASQVPSLQQLKDIAFPSSLSAIQNAFKPVVAPTTTPPRT-----LVIGPSSPSPPPPPRSSSPYARRPSPPRTSGFSR----------SVIDSLRKTNEVMNQEMTKLHSQQR 821
1g65920 QNLPQANRSSDGQP----------RWGQVSGPSLFRFDKISTSSSLN----------LSVSARRTSSTKISTSSE----------SNKILTEEIERLKAVIK 810
5g16040 396
3g02510 393
3g55580 488
3g53830 487
UVR8 440
1g27060 386
5g08710 434
5g11580 EIMKDCLQSSAPKY---------- 553
5g48330 455
3g26100 432
3g15430 488
5g60870 445
3g02300 Y---------- 471
3g03790 RALRKKLQQIEILEAKQSRGQLLDGQQIAKLQKKLDIESSLVELGIPVEEFPEAKATTALPLEGKANKKGKKKKKGNQRFVQVETFPEFGEVKVEIDTMQDKEIEEICEAIKPKGGKTMLDTTMISGFPKESDFVSLSQKKDNPPDSPRS 862
1g19880 EDGEEANGKKQSARGRGRGR----------GARGRGGRTSNGKAPPVKTGGRRGRPRKS---------- 538
.....1810.....1820.....1830.....1840.....1850.....1860.....1870.....1880.....1890.....1900.....1910.....1920.....1930.....1940.....1950
PRAF1_1g76950 SLTQKCEFQEVELQNSVKKTQEALALAEEESAKSRAAKEAIKSLIAQLKDVAEKLPPG----ESVKLACLQNGLDQN-GFHFPEENGFHPSRSESMTS-SISSVAPFDFAFANASWSNLQSPKQTPRASERNSNAYPADPRLSSSGSVIS 994
5g42140 SLRHRCEVQEFEVQKSVKKVQEAMSLAAEESAKSEAAKEVIKSLTAQVKDIAALLPPGAYEAETTRTANLLNGFEQN-GFHFTNANGQRQSRSDSMSDTSLASPLAMPARSMNGLWRNSQSPRNTDASMG----------ELLSEGVRIS 974
5g12350 SLTRKAQLQEVELERTTKQLKEALAITNEETTRCKAAKEVIKSLTAQLKDMAERLPVG--SARTVKSPPSLNSFGSSPGRIDP-FNILNQANSQESEPNGITT-PMFSNGTMTPAFGNG---------- 997
5g19420 NLTRKAQLQEVELERTTKQLKEALAIASEESARCKAAKEVIKSLTAQLKDMAERLPVG--SARTVKSP-SLNSFGSSPDYAAPSSNTLNRPNSRETDSDSLTTVPMFSNGTSTPVFDSGSYRQQAN---------- 1009
1g69710 QLASKAHQLEEELEKTKRQLKVVTAMAADEAEENRSAKEVIRSLTTQLKEMAEKQSQK----DSISTNSKHTDKEKS--------ETVTQTSNQTHIRSMVSQDSQNENNLTSKSFANG---------- 961
3g47660 ELTLKSKKLETELGKTSKKLEVAVLMARDDAEKIKSSEEIVRSLTLQLMNTTKK---------- 939
4g14370 NLKEKCDNQGTEIQRLKKTAREASDLAVKHSSKHKAATEVMKSVAEHLRELKEKLPPEVSRCEAFESMNSQAEAYLN-------ASEASESCLPTTSLGMGQRDPTPSTNTQDQNIEEKQSSNGGN---------- 1860
3g23270 -----CNNQGTEIERFQKAAKDASELAARQSSKHKAATEALKSVAEQLKELKEKLPPEVSESEAFESINSQAEAYLN-------ANKVSETSPLTTSG-----QEQETYQKTEEQVPSNSSITETS---------- 930
1g65920 NLQRQCELGNEKMEECQQELDKTWEVAKEEAEKSKAAKEIIKALASKLQANKEKPSNPLKTGIACNPSQVSPIFDDS--------MSIPYLTPITTARSQHETKQHVEKCVTKSSNRDSNIKLLVD---------- 928
5g16040 396
3g02510 393
3g55580 488
3g53830 487
UVR8 440
1g27060 386
5g08710 434
5g11580 553
5g48330 455
3g26100 432
3g15430 488
5g60870 445
3g02300 471
3g03790 KKLATAANKKKNRKGGLSMFLTGALDDVPKPVVAPPPRPKIEGPVWGGAKISKGLSSLRDIQDEQSKTRSHEPVRTTKNQSGDDSPGKSEGKILLSSFLTSKPIPMEPAKSLQQSDVEKGTPPWASSETPR---------- 993
1g19880 538
.....1960.....1970.....1980.....1990.....2000.....2010.....2020.....2030.....2040.....2050.....2060.....2070.....2080.....2090.....2100

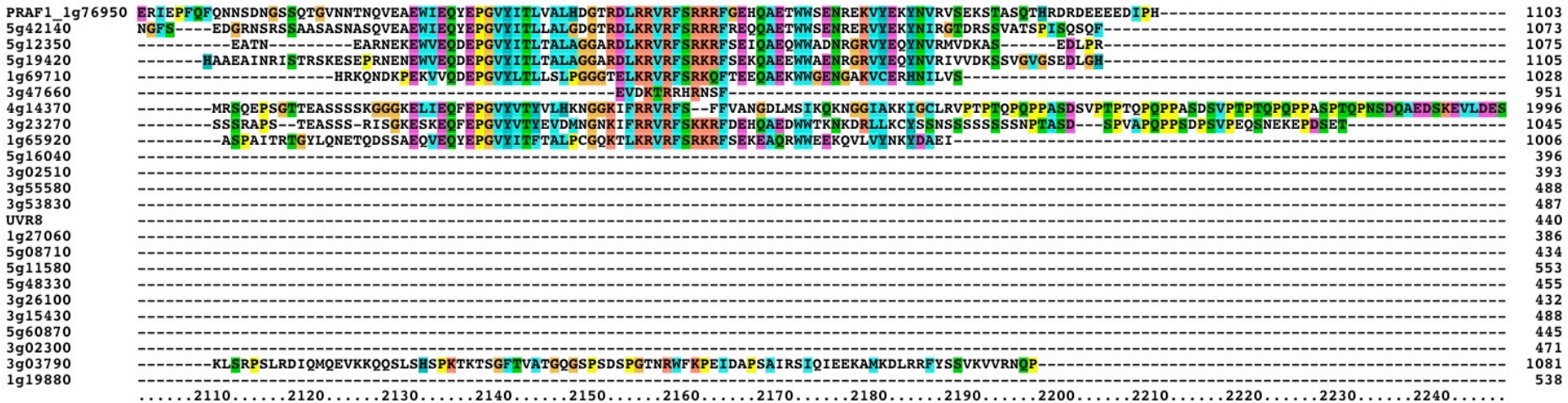
PRAF1_1g76950 ERIEPFQFQNNSDNGSSQTGVNNTNQVEAEWIEQYEPGVYITLVALHDGTRDLRRVRFSRRRFGEHQAETWWSENREKVYEKYNVRVSEKSTASQTHRDRDEEEEDIPH 1103
5g42140 NGFS----EDGRNSRSSAASASNASQVEAEWIEQYEPGVYITLLALGDGTRDLKRVRFSRRRFREQQAETWWSENRERVYEKYNIRGTDRSSVATSPISQSQF 1073
5g12350 ----------EATN---------EARNEKEWVEQDEPGVYITLTALAGGARDLKRVRFSRKRFSEIQAEQWWADNRGRVYEQYNVRMVDKAS-------EDLPR 1075
5g19420 -------HAAEAINRISTRSKESEPRNENEWVEQDEPGVYITLTALAGGARDLKRVRFSRKRFSEKQAEEWWAENRGRVYEQYNVRIVVDKSSVGVGSEDLGH 1105
1g69710 --------------------HRKQNDKPEKVVQDEPGVYLTLLSLPGGGTELKRVRFSRKQFTEEQAEKWWGENGAKVCERHNILVS 1028
3g47660 --EVDKTRRHRNSF 951
4g14370 --------MRSQEPSGTTEASSSSKGGGKELIEQFEPGVYVTYVLHKNGGKIFRRVRFS--FFVANGDLMSIKQKNGGIAKKIGCLRVPTPTQPQPPASDSVPTPTQPQPPASDSVPTPTQPQPPASPTQPNSDQAEDSKEVLDES 1996
3g23270 --------SSSRAPS--TEASSS-RISGKESKEQFEPGVYVTYEVDMNGNKIFRRVRFSKKRFDEHQAEDWWTKNKDRLLKCYSSNSSSSSSSNPTASD---SPVAPQPPSDPSVPEQSNEKEPDSET 1045
1g65920 ---------ASPAITRTGYLQNETQDSSAEQVEQYEPGVYITFTALPCGQKTLKRVRFSRKRFSEKEAQRWWEEKQVLVYNKYDAEI 1006
5g16040 396
3g02510 393
3g55580 488
3g53830 487
UVR8 440
1g27060 386
5g08710 434
5g11580 553
5g48330 455
3g26100 432
3g15430 488
5g60870 445
3g02300 471
3g03790 --------KLSRPSLRDIQMQEVKKQQSLSHSPKTKTSGFTVATGQGSPSDSPGTNRWFKPEIDAPSAIRSIQIEEKAMKDLRRFYSSVKVVRNQP 1081
1g19880 538
.....2110.....2120.....2130.....2140.....2150.....2160.....2170.....2180.....2190.....2200.....2210.....2220.....2230.....2240.....

APPENDIX III
POTENTIAL UVR8 HOMOLOGUES

		Value		
Protein	**Species**	**Whole UVR8**	**C-terminal only**	**N-terminal only**
ref|NP_201191.1| UVR8 (UVB-RESISTANCE 8); chromatin binding /...	*Arabidopsis thaliana*	0	3E-17	6E-11
gb|AAD43920.1|AF130441_1 UVB-resistance protein UVR8 [Arabido...	*Arabidopsis thaliana*	0	3E-17	7E-11
ref|XP_002274569.1| PREDICTED: hypothetical protein [Vitis vi...	***Vitis vinifera***	**0**	**0.0000003**	**0.0003**
ref|XP_002309939.1| predicted protein [Populus trichocarpa] >...	***Populus trichocarpa***	**0**	**0.0000002**	**0.001**
ref|XP_002522929.1| uvb-resistance protein uvr8, putative [Ri...	***Ricinus communis***	**0**	**0.000000002**	**0.00001**
emb|CAN67581.1| hypothetical protein [Vitis vinifera]	*Vitis vinifera*	0	0.0000003	0.004
ref|XP_002446509.1| hypothetical protein SORBIDRAFT_06g017130...	*Sorghum bicolor*	0	0.00004	0.056
gb|ACU19352.1| unknown [Glycine max]	*Glycene max*	0	0.006	0.003
ref|NP_001141147.1| hypothetical protein LOC100273233 [Zea ma...	***Zea mays***	**0**	**0.00004**	**0.057**
ref|NP_001052849.1| Os04g0435700 [Oryza sativa (japonica cult...	***Oryza sativa***	**0**	**0.00004**	**0.22**
ref|NP_001047115.1| Os02g0554100 [Oryza sativa (japonica cult...	***Oryza sativa***	**0**	**0.00004**	**0.033**
gb|EEC73389.1| hypothetical protein OsI_07634 [Oryza sativa I...	*Oryza sativa*	0	0.00004	0.032
gb|EEE57180.1| hypothetical protein OsJ_07117 [Oryza sativa J...	*Oryza sativa*	0	0.00004	0.028
XP_001702277.1 hypothetical protein CHLREDRAFT_122886 []	***Chlamydomonas reinhardtii***	**0**	#N/A	#N/A
ref|XP_001778783.1| predicted protein [Physcomitrella patens ...	***Physcomitrella patens***	**2.00E-170**	**0.000001**	**0.079**
ref|XP_001757031.1| predicted protein [Physcomitrella patens ...	***Physcomitrella patens***	**5.00E-168**	**0.000001**	**0.051**
gb|ACG32833.1| HECT domain and RCC1-like domain-containing pr...	*Zea mays*	2.00E-151	#N/A	0.038
gb|ABV89648.1| UVB-resistance 8 [Brassica rapa]	***Brassica rapa***	**7.00E-148**	**1E-11**	**0.0000006**
emb|CAD41017.1| OSJNBb0086G13.15 [Oryza sativa (japonica cult...	*Oryza sativa*	2.00E-96	#N/A	0.52
gb|ACN35037.1| unknown [Zea mays]	*Zea mays*	4.00E-87	0.00004	#N/A
gb|ABR17254.1| unknown [Picea sitchensis]	***Picea sitchensis***	**2.00E-73**	**0.0000001**	**0.63**
ref|XP_001777928.1| predicted protein [Physcomitrella patens ...		1.00E-55	#N/A	#N/A
ref|XP_002273073.1| PREDICTED: hypothetical protein [Vitis vi...		3.00E-50	#N/A	#N/A
ref|NP_568268.3| Ran GTPase binding / chromatin binding / zin...		3.00E-49	#N/A	#N/A
emb|CAC42896.1| putative protein [Arabidopsis thaliana]		3.00E-49	#N/A	#N/A
ref|XP_002527043.1| Ran GTPase binding protein, putative [Ric...		3.00E-49	#N/A	#N/A
ref|NP_197443.3| Ran GTPase binding / chromatin binding / zin...		4.00E-49	#N/A	#N/A
gb|EEE63569.1| hypothetical protein OsJ_18386 [Oryza sativa J...		5.00E-49	#N/A	#N/A
gb|AAT77332.1| unknown prtein [Oryza sativa Japonica Group]		6.00E-49	#N/A	#N/A
ref|NP_001055416.1| Os05g0384800 [Oryza sativa (japonica cult...		6.00E-49	#N/A	#N/A
gb|ABO93003.1| putative regulator of chromosome condensation ...		8.00E-49	#N/A	#N/A
gb|AAU93591.2| Zinc finger protein, putative [Solanum demissum]	***Solanum demissum***	**1.00E-48**	**#N/A**	**#N/A**
gb|EEC79138.1| hypothetical protein OsI_19792 [Oryza sativa I...		1.00E-48	#N/A	#N/A
ref|XP_002459109.1| hypothetical protein SORBIDRAFT_03g046020...		3.00E-48	#N/A	#N/A
ref|XP_002297742.1| predicted protein [Populus trichocarpa] >...		9.00E-48	#N/A	#N/A
ref|XP_002273996.1| PREDICTED: hypothetical protein [Vitis vi...		1.00E-47	#N/A	#N/A
ref|XP_002513064.1| Ran GTPase binding protein, putative [Ric...		2.00E-47	#N/A	#N/A
ref|NP_199029.1| zinc finger protein, putative / regulator of...		2.00E-47	#N/A	#N/A
dbj|BAF07333.2| Os01g0952300 [Oryza sativa Japonica Group]		6.00E-47	#N/A	#N/A
ref|XP_002313993.1| predicted protein [Populus trichocarpa] >...		7.00E-47	#N/A	#N/A
ref|NP_001045419.1| Os01g0952300 [Oryza sativa (japonica cult...		8.00E-47	#N/A	#N/A
gb|EEC72175.1| hypothetical protein OsI_05225 [Oryza sativa I...		8.00E-47	#N/A	#N/A
dbj|BAD87854.1| putative ZR1 protein [Oryza sativa Japonica G...		8.00E-47	#N/A	#N/A
gb|EEE56014.1| hypothetical protein OsJ_04782 [Oryza sativa J...		8.00E-47	#N/A	#N/A
emb|CAO16844.1| unnamed protein product [Vitis vinifera]		8.00E-47	#N/A	#N/A
ref|XP_002279847.1| PREDICTED: hypothetical protein isoform 1...		9.00E-47	#N/A	#N/A
ref|XP_002279913.1| PREDICTED: hypothetical protein isoform 2...		9.00E-47	#N/A	#N/A
ref|XP_002522401.1| Ran GTPase binding protein, putative [Ric...		2.00E-46	#N/A	#N/A
ref|XP_002298476.1| predicted protein [Populus trichocarpa] >...		2.00E-46	#N/A	#N/A
gb|AAM61698.1| UVB-resistance protein-like [Arabidopsis thali...		3.00E-46	#N/A	#N/A
ref|XP_002304793.1| predicted protein [Populus trichocarpa] >...		3.00E-46	#N/A	#N/A
ref|XP_002516745.1| Ran GTPase binding protein, putative [Ric...		3.00E-46	#N/A	#N/A
ref|NP_197108.1| regulator of chromosome condensation (RCC1) ...		4.00E-46	#N/A	#N/A
gb|EEC83614.1| hypothetical protein OsI_29322 [Oryza sativa I...		5.00E-46	#N/A	#N/A
ref|XP_002511559.1| Ran GTPase binding protein, putative [Ric...		6.00E-46	#N/A	#N/A
ref|NP_001140994.1| hypothetical protein LOC100273073 [Zea ma...		7.00E-46	#N/A	#N/A
emb|CAO42840.1| unnamed protein product [Vitis vinifera]		7.00E-46	#N/A	#N/A
ref|XP_002283479.1| PREDICTED: hypothetical protein [Vitis vi...		1.00E-45	#N/A	#N/A
ref|XP_002311672.1| predicted protein [Populus trichocarpa] >...		1.00E-45	#N/A	#N/A
ref|NP_001061858.1| Os08g0430700 [Oryza sativa (japonica cult...		1.00E-45	#N/A	#N/A
ref|NP_001045490.1| Os01g0964800 [Oryza sativa (japonica cult...		1.00E-45	#N/A	#N/A
dbj|BAF07404.2| Os01g0964800 [Oryza sativa Japonica Group]		1.00E-45	#N/A	#N/A
ref|XP_002329325.1| predicted protein [Populus trichocarpa] >...		1.00E-45	#N/A	#N/A
ref|XP_001770494.1| predicted protein [Physcomitrella patens ...		2.00E-45	#N/A	#N/A
ref|NP_001141854.1| hypothetical protein LOC100273996 [Zea ma...		2.00E-45	#N/A	#N/A
ref|XP_001770491.1| predicted protein [Physcomitrella patens ...		2.00E-45	#N/A	#N/A
gb|EEC72223.1| hypothetical protein OsI_05329 [Oryza sativa I...		3.00E-45	#N/A	#N/A
ref|NP_186900.3| regulator of chromosome condensation (RCC1) ...		7.00E-45	#N/A	#N/A
ref|XP_002456994.1| hypothetical protein SORBIDRAFT_03g046900...		8.00E-45	#N/A	#N/A
ref|XP_002327568.1| predicted protein [Populus trichocarpa] >...		8.00E-45	#N/A	#N/A
ref|XP_002300931.1| predicted protein [Populus trichocarpa] >...		1.00E-44	#N/A	#N/A
ref|XP_002526126.1| Ran GTPase binding protein, putative [Ric...		2.00E-44	#N/A	#N/A
ref|XP_001761845.1| predicted protein [Physcomitrella patens ...		4.00E-44	#N/A	#N/A
gb|ABD96878.1| hypothetical protein [Cleome spinosa]	***Cleome spinosa***	**6.00E-44**	**#N/A**	**#N/A**

		Value		
Protein	**Species**	**Whole UVR8**	**C-terminal only**	**N-terminal only**
gb|EEE57593.1| hypothetical protein OsJ_07959 [Oryza sativa J...		7.00E-43	#N/A	#N/A
gb|EAY96235.1| hypothetical protein OsI_18130 [Oryza sativa I...		7.00E-43	#N/A	#N/A
ref|NP_001054420.1| Os05g0106700 [Oryza sativa (japonica cult...		8.00E-43	#N/A	#N/A
gb|EEC71342.1| hypothetical protein OsI_03406 [Oryza sativa I...		9.00E-43	#N/A	#N/A
gb|EEC73799.1| hypothetical protein OsI_08500 [Oryza sativa I...		2.00E-42	#N/A	#N/A
emb|CAO65111.1| unnamed protein product [Vitis vinifera]		3.00E-42	#N/A	#N/A
gb|EEC81974.1| hypothetical protein OsI_25886 [Oryza sativa I...		3.00E-42	#N/A	#N/A
ref|XP_002448811.1| hypothetical protein SORBIDRAFT_06g033680...		3.00E-42	#N/A	#N/A
ref|NP_680156.2| regulator of chromosome condensation (RCC1) ...		3.00E-42	#N/A	#N/A
ref|XP_002264093.1| PREDICTED: hypothetical protein [Vitis vi...		3.00E-42	#N/A	#N/A
ref|NP_001059575.1| Os07g0459400 [Oryza sativa (japonica cult...		4.00E-42	#N/A	#N/A
gb|AAL58903.1|AF462811_1 At1g76950/F22K20_5 [Arabidopsis thal...		6.00E-44	#N/A	#N/A
ref|NP_565144.1| PRAF1; Ran GTPase binding / chromatin bindin...		6.00E-44	#N/A	#N/A
gb|AAC00618.1| Unknown protein, contains regulator of chromos...		8.00E-44	#N/A	#N/A
ref|XP_002307065.1| predicted protein [Populus trichocarpa] >...		1.00E-43	#N/A	#N/A
gb|AAW78912.1| putative chromosome condensation factor [Triti...	***Triticum turgidum***	**2.00E-43**	**#N/A**	**#N/A**
ref|XP_002450904.1| hypothetical protein SORBIDRAFT_05g020900...		2.00E-43	#N/A	#N/A
ref|NP_001154232.1| zinc ion binding [Arabidopsis thaliana]		2.00E-43	#N/A	#N/A
gb|AAK84081.1|AF326781_2 putative chromosome condensation fac...	***Triticum monococcum***	**2.00E-43**	**#N/A**	**#N/A**
ref|XP_002440421.1| hypothetical protein SORBIDRAFT_09g000710...		2.00E-43	#N/A	#N/A
gb|AAW78916.1| putative chromosome condensation factor [Triti...	***Triticum aestivum***	**2.00E-43**	**#N/A**	**#N/A**
ref|XP_002454466.1| hypothetical protein SORBIDRAFT_04g031600...		2.00E-43	#N/A	#N/A
gb|EEE55253.1| hypothetical protein OsJ_03147 [Oryza sativa J...		4.00E-43	#N/A	#N/A
dbj|BAF16334.2| Os05g0106700 [Oryza sativa Japonica Group]		4.00E-43	#N/A	#N/A
ref|NP_001043984.1| Os01g0700200 [Oryza sativa (japonica cult...		5.00E-43	#N/A	#N/A
gb|EEE62040.1| hypothetical protein OsJ_16822 [Oryza sativa J...		6.00E-43	#N/A	#N/A
dbj|BAD07566.1| putative ZR1 protein [Oryza sativa Japonica G...		6.00E-43	#N/A	#N/A

Table 7.2 BLAST search results for UVR8 homologues in green plant species. Table shows proteins found to be most similar to Arabidopsis UVR8. Whole UVR8 denotes search using the full length sequence. C or N-terminal only shows results from search (adjusted to short sequences) for the 27 amino acid insertion and 32 amino acid region found at each terminus respectively.

APPENDIX IV
SEC COLUMN MOLECULAR WEIGHT CALCULATIONS

From running the column we can determine the gel phase distribution coefficient (K_{av}) using the following equation:

$$K_{av} = \frac{(Ve - V0)}{(Vc - V0)}$$

Where: V_0 = void volume (~5 ml),
V_C = column volume (240 ml).
Ve = (number of fractions × volume of fraction (0.3 ml)) + V_0

From calibration curve shown in Figure 5.3 and using equation of a straight line (y = mx + c) we know:

$$K_{av} = -0.01 \times Log_{Mr} - 0.085$$

Therefore:

$$10^{(K_{av} - 0.085)/-0.010} = Mr \text{ (i.e. the size of the protein or protein complex)}$$

REFERENCES

Afzal, Wood, *et al*. (2008). "Plant receptor-like serine threonine kinases: roles in signaling and plant defense." Mol Plant Microbe Interact **21**(5): 1-11.

Ahmad, M. and A. R. Cashmore (1993). "HY4 gene of A. thaliana encodes a protein with characteristics of a blue-light photoreceptor." Nature **366**(6451): 162-166.

Allan, A. C. and R. Fluhr (1997). "Two distinct sources of elicited reactive oxygen species in tobacco epidermal cells." Plant Cell **9**(9): 1559-1572.

Balogi, Z., O. Cheregi, *et al*. (2008). "A mutant small heat shock protein with increased thylakoid association provides an elevated resistance against UV-B damage in synechocystis 6803." J Biol Chem **283**(34): 22983-22991.

Barrier, M., C. D. Bustamante, *et al*. (2003). "Selection on rapidly evolving proteins in the Arabidopsis genome." Genetics **163**(2): 723-733.

Boccalandro, H. E., C. A. Mazza, *et al*. (2001). "Ultraviolet B radiation enhances a phytochrome-B-mediated photomorphogenic response in Arabidopsis." Plant Physiology. **126**(2): 780-788.

Britt, A. B. (1999). "Molecular genetics of DNA repair in higher plants." Trends in Plant Science **4**(1): 20-25.

Britt, A. B. (2004). "Repair of DNA damage induced by solar UV." Photosynthesis Research **81**(2): 105-112.

Brosche, N. and A. Strid (2003). "Molecular events following perception of ultraviolet-B radiation by plants." Physiologia Plantarum **117**(1): 1-10.

Brown, B. and G. Jenkins (2007). "UV-B Signaling Pathways with Different Fluence-Rate Response Profiles Are Distinguished in Mature Arabidopsis Leaf Tissue by Requirement for UVR8, HY5, and HYH." Plant Physiology **146**(2): 576-588.

Brown, B. A., C. Cloix, *et al*. (2005). "A UV-B-specific signaling component orchestrates plant UV protection." Proc Natl Acad Sci U S A **102**(50): 18225-18230.

Brown, B. A., L. R. Headland, *et al*. (2009). "UV-B action spectrum for UVR8-mediated HY5 transcript accumulation in Arabidopsis." Photochemistry and Photobiology **85**(5): 1147-1155.

Brown, B. A. and G. I. Jenkins (2008). "UV-B signaling pathways with different fluence-rate response profiles are distinguished in mature Arabidopsis leaf tissue by requirement for UVR8, HY5, and HYH." Plant Physiology **146**(2): 576-588.

Brown, D. E., A. M. Rashotte, *et al*. (2001). "Flavonoids act as negative regulators of auxin transport in vivo in arabidopsis." Plant Physiology **126**(2): 524-535.

Caldwell, M. M., C. L. Ballare, *et al*. (2003). "Terrestrial ecosystems increased solar ultraviolet radiation and interactions with other climatic change factors." Photochemical & Photobiological Sciences **2**(1): 29-38.

Casasoli, M., S. Spadoni, *et al*. (2008). "Identification by 2-D DIGE of apoplastic proteins regulated by oligogalacturonides inArabidopsis thaliana." Proteomics **8**(5): 1042-1054.

Casati, P. and V. Walbot (2003). "Gene expression profiling in response to ultraviolet radiation in maize genotypes with varying flavonoid content." Plant Physiology **132**(4): 1739-1754.

Casati, P. and V. Walbot (2004). "Crosslinking of ribosomal proteins to RNA in maize ribosomes by UV-B and its effects on translation." Plant Physiology **136**(2): 3319-3332.

Casati, P. and V. Walbot (2004). "Rapid transcriptome responses of maize (Zea mays) to UV-B in irradiated and shielded tissues." Genome Biol **5**(3): R16.

Casati, P., A. E. Stapleton, *et al*. (2006). “Genome-wide analysis of high-altitude maize and gene knockdown stocks implicates chromatin remodeling proteins in response to UV-B.” Plant J. **46**(4): 613-27.

Chalker-Scott, L. and J. D. Scott (2004). "Elevated ultraviolet-B radiation induces cross-protection to cold in leaves of Rhododendron under field conditions." Photochemistry and Photobiology **79**(2): 199-204.

Chapman, S., C. Faulkner, *et al*. (2008). "The photoreversible fluorescent protein iLOV outperforms GFP as a reporter of plant virus infection." Proc Natl Acad Sci U S A **105**(50): 20038-20043.

Christie, J. M. (2007). "Phototropin blue-light receptors." Annu Rev Plant Biol **58**: 21-45.

Christie, J. M. and G. I. Jenkins (1996). "Distinct UV-B and UV-A/Blue light signal transduction pathways induce Chalcone Synthase gene expression in Arabidopsis cells." Plant Cell **8**(9): 1555-1567.

Christie, J. M., M. Salomon, *et al*. (1999). "LOV (light, oxygen, or voltage) domains of the blue-light photoreceptor phototropin (nph1): binding sites for the chromophore flavin mononucleotide." Proc Natl Acad Sci U S A **96**(15): 8779-8783.

Clack, T., S. Mathews, *et al*. (1994). "The phytochrome apoprotein family in Arabidopsis is encoded by five genes: the sequences and expression of PHYD and PHYE." Plant Mol Biol **25**(3): 413-427.

Cleaver, J. E. (2001). "Xeroderma pigmentosum: the first of the cellular caretakers." Trends Biochem Sci **26**(6): 398-401.

Cloix, C. and G. I. Jenkins (2008). "Interaction of the Arabidopsis UV-B-specific signaling component UVR8 with chromatin." Mol Plant **1**(1): 118-128.

Correia, C. M., E. L. V. Areal, *et al*. (1998). "Intraspecific variation in sensitivity to ultraviolet-B radiation in maize grown under field conditions. I. Growth and morphological aspects." Field Crops Research **59**(2): 81-89.

Correia, Areal, *et al*. (1999). “Intraspecifc variation in sensitivity to ultraviolet-B radiation in maize grown under field conditions II. Physiological and biochemical aspects.” Field Crops Research **62**(2) 97-105.

Covington, M., J. Maloof, *et al*. (2008). "Global transcriptome analysis reveals circadian regulation of key pathways in plant growth and development." Genome Biol **9**(8): R130.

Culligan, K., A. Tissier, *et al*. (2004). "ATR regulates a G2-phase cell-cycle checkpoint in Arabidopsis thaliana." Plant Cell **16**(5): 1091-1104.

Culligan, K. M., C. E. Robertson, *et al*. (2006). "ATR and ATM play both distinct and additive roles in response to ionizing radiation." Plant J **48**(6): 947-961.

Debeaujon, I., A. J. Peeters, *et al*. (2001). "The TRANSPARENT TESTA12 gene of Arabidopsis encodes a multidrug secondary transporter-like protein required for flavonoid sequestration in vacuoles of the seed coat endothelium." Plant Cell **13**(4): 853-871.

Devlin, P. F. and S. A. Kay (2000). "Cryptochromes are required for phytochrome signaling to the circadian clock but not for rhythmicity." Plant Cell **12**(12): 2499-2510.

Dieterle, M., C. Buche, *et al*. (2003). "Characterization of a novel non-constitutive photomorphogenic cop1 allele." Plant Physiology **133**(4): 1557-1564.

Eisinger, W., T. E. Swartz, *et al*. (2000). "The ultraviolet action spectrum for stomatal opening in broad bean." Plant Physiology **122**(1): 99-106.

Ernst, H. A., A. N. Olsen, *et al*. (2004). "Structure of the conserved domain of ANAC, a member of the NAC family of transcription factors." EMBO Rep **5**(3): 297-303.

Eulgem, T., P. J. Rushton, *et al*. (2000). "The WRKY superfamily of plant transcription factors." Trends in Plant Science **5**(5): 199-206.

Favory, J., A. Stec, *et al*. (2009). "Interaction of COP1 and UVR8 regulates UV-B-induced photomorphogenesis and stress acclimation in Arabidopsis." EMBO J **28**(5): 591-601.

Feder, M. E. and G. E. Hofmann (1999). "Heat-shock proteins, molecular chaperones, and the stress response: Evolutionary and Ecological Physiology." Annual Review of Physiology **61**(1): 243-282.

Filiault, D. L., C. A. Wessinger, *et al*. (2008). "Amino acid polymorphisms in Arabidopsis phytochrome B cause differential responses to light." Proc Natl Acad Sci USA **105**(8): 3157-3162.

Franklin, K. A., V. S. Larner, *et al*. (2005). "The signal transducing photoreceptors of plants." Int J Dev Biol **49**(5-6): 653-664.

Fritsche, E., C. Schafer, *et al*. (2007). "Lightening up the UV response by identification of the arylhydrocarbon receptor as a cytoplasmatic target for ultraviolet B radiation." Proc Natl Acad Sci U S A **104**(21): 8851-8856.

Frohnmeyer, H. (2003). "Ultraviolet-B radiation-mediated responses in plants. Balancing damage and protection." Plant Physiology **133**(4): 1420-1428.

Frohnmeyer, H., L. Loyall, *et al*. (1999). "Millisecond UV-B irradiation evokes prolonged elevation of cytosolic-free Ca^{2+} and stimulates gene expression in transgenic parsley cell cultures." Plant J **20**(1): 109-117.

Fuglevand, G., J. A. Jackson, *et al*. (1996). "UV-B, UV-A, and blue light signal transduction pathways interact synergistically to regulate chalcone synthase gene expression in Arabidopsis." Plant Cell **8**(12): 2347-2357.

Fukuda, M., S. Asano, *et al*. (1997). "CRM1 is responsible for intracellular transport mediated by the nuclear export signal." Nature **390**(6657): 308-311.

Gitz, D. C. and L. Liu-Gitz (2003). "How do UV photomorphogenic responses confer water stress tolerance?" Photochemistry and Photobiology **78**(6): 529-534.

Groβ, S., A. Knebel, *et al*. (1999). "Inactivation of Protein-tyrosine Phosphatases as Mechanism of UV-induced Signal Transduction." J. Biol. Chem. **274**(37): 26378-26386.

Harmer, S. L., S. Panda, *et al*. (2001). "Molecular bases of circadian rhythms." Annu Rev Cell Dev Biol **17**: 215-253.

Hartmann, U., W. J. Valentine, *et al*. (1998). "Identification of UV/blue light-response elements in the Arabidopsis thaliana chalcone synthase promoter using a homologous protoplast transient expression system." Plant Molecular Biology **36**(5): 741-754.

Hectors K., E. Prinsen, *et al*. (2007) “Arabidopsis thaliana plants acclimated to low dose rates of ultraviolet B radiation show specific changes in morphology and gene expression in the absence of stress symptoms.” New Phytol **175**(2): 255-70.

Hideg, E., C. Barta, *et al*. (2002). "Detection of singlet oxygen and superoxide with fluorescent sensors in leaves under stress by photoinhibition or UV radiation." Plant Cell Physiol **43**(10): 1154-1164.

Hoang, N., J.-P. Bouly, *et al*. (2008). "Evidence of a light-sensing role for folate in Arabidopsis cryptochrome blue-light receptors." Mol Plant **1**(1): 68-74.

Holm, M., L. G. Ma, *et al*. (2002). "Two interacting bZIP proteins are direct targets of COP1-mediated control of light-dependent gene expression in Arabidopsis." Genes Dev **16**(10): 1247-1259.

Hutin, C., L. Nussaume, et al. (2003). “Early light-induced proteins protect Arabidopsis from photooxidative stress.” Proc Natl Acad Sci USA **100**(8): 4921-6.

Ioki, M., S. Takahashi, *et al*. (2008). "An unidentified ultraviolet-B-specific photoreceptor mediates transcriptional activation of the cyclobutane pyrimidine dimer photolyase gene in plants." Planta **229**(1): 25-36.

Izaguirre, M. M., C. A. Mazza, *et al*. (2007). "Solar ultraviolet-B radiation and insect herbivory trigger partially overlapping phenolic responses in Nicotiana attenuata and Nicotiana longiflora." Ann Bot **99**(1): 103-109.

Izaguirre, M. M., A. L. Scopel, *et al*. (2003). "Convergent responses to stress. Solar ultraviolet-B radiation and Manduca sexta herbivory elicit overlapping transcriptional responses in field-grown plants of Nicotiana longiflora." Plant Physiology **132**(4): 1755-1767.

James, A. B., J. A. Monreal, *et al*. (2008). "The circadian clock in Arabidopsis roots is a simplified slave version of the clock in shoots." Science **322**(5909): 1832-1835.

Jansen, M. A. K. (2002). "Ultraviolet-B radiation effects on plants: induction of morphogenic responses." Physiologia Plantarum **116**(3): 423-429.

Jansen, M. A. K., V. Gaba, *et al*. (1998). "Higher plants and UV-B radiation: balancing damage, repair and acclimation." Trends Plant Sci. **3**(4): 131-135.

Jenkins, G. I. (2009). "Signal transduction in responses to UV-B radiation." Annu Rev Plant Biol **60:** 407-31.

Jensen, LaCour, *et al*. (2001). "FYVE zinc-finger proteins in the plant model Arabidopsis thaliana : identification of PtdIns3P-binding residues by comparison of classic and variant FYVE domains." Biochem J. **359**(1): 165–173

Jiang, C.-Z., J. Yee, et al. (1997). "Photorepair mutants of Arabidopsis." Proc Natl Acad Sci U S A **94**(14): 7441-7445.

Jiao, Y., O. S. Lau, et al. (2007). "Light-regulated transcriptional networks in higher plants." Nat Rev Genet **8**(3): 217-230.

Jin, H. L., E. Cominelli, et al. (2000). "Transcriptional repression by AtMYB4 controls production of UV-protecting sunscreens in Arabidopsis." Embo Journal **19**(22): 6150-6161.

Jones, M. A., K. A. Feeney, et al. (2007). "Mutational analysis of phototropin 1 provides insights into the mechanism underlying LOV2 signal transmission." J Biol Chem **282**(9): 6405-6414.

Kaiserli, E. and G. I. Jenkins (2007). "UV-B promotes rapid nuclear translocation of the Arabidopsis UV-B-specific signaling component UVR8 and activates its function in the nucleus." Plant Cell **19**(8): 2662-2673.

Kaiserli, E., S. Sullivan, et al. (2009). "Domain swapping to assess the mechanistic basis of Arabidopsis phototropin 1 receptor kinase activation and endocytosis by blue light." Plant Cell **21**(10): 3226-3244.

Kalbina, I. and A. Strid (2006). "Supplementary ultraviolet-B irradiation reveals differences in stress responses between Arabidopsis thaliana ecotypes." Plant Cell and Environment **29**(5): 754-763.

Kalde, M., M. Barth, et al. (2003). "Members of the Arabidopsis WRKY group III transcription factors are part of different plant defense signaling pathways." Molecular Plant-Microbe Interactions **16**(4): 295-305.

Kevei, E., E. Schafer, *et al.* (2007). "Light-regulated nucleo-cytoplasmic partitioning of phytochromes." J Exp Bot **58**(12): 3113-3124.

Kilian, J., D. Whitehead, *et al.* (2007). "The AtGenExpress global stress expression data set: protocols, evaluation and model data analysis of UV-B light, drought and cold stress responses." Plant J **50**(2): 347-363.

Kim, B. C., D. J. Tennessen, et al. (1998). "UV-B-induced photomorphogenesis in Arabidopsis thaliana." Plant J **15**(5): 667-674.

Kimura, S., Y. Tahira *et al.* (2004). "DNA repair in higher plants; photoreactivation is the major DNA repair pathway in non-proliferating cells while excision repair (nucleotide excision repair and base excision repair) is active in proliferating cells." Nucleic Acids Research **32**(9): 2760-2767

Kircher, S., P. Gil, *et al.* (2002). "Nucleocytoplasmic partitioning of the plant photoreceptors phytochrome A, B, C, D, and E is regulated differentially by light and exhibits a diurnal rhythm." Plant Cell **14**(7): 1541-1555.

Kleine, T., P. Lockhart, *et al.* (2003). "An Arabidopsis protein closely related to Synechocystis cryptochrome is targeted to organelles." Plant J **35**(1): 93-103.

Kliebenstein, D. J. (2004). "Secondary metabolites and plant/environment interactions: a view through Arabidopsis thaliana tinged glasses." Plant Cell and Environment **27**(6): 675-684.

Kliebenstein, D. J., J. E. Lim, *et al.* (2002). "Arabidopsis UVR8 regulates ultraviolet-B signal transduction and tolerance and contains sequence similarity to human Regulator of Chromatin Condensation 1." Plant Physiology **130**(1): 234-243.

Kong, S. G., T. Suzuki, *et al.* (2006). "Blue light-induced association of phototropin 2 with the Golgi apparatus." Plant J **45**(6): 994-1005.

Kucera, B., G. Leubner-Metzger, *et al.* (2003). "Distinct ultraviolet-signaling pathways in bean leaves. DNA damage Is associated with β -1,3-glucanase gene induction, but not with flavonoid formation." Plant Physiol. **133**(4): 1445-1452.

Kudlicki, A., M. Rowicka, *et al.* (2007). "SCEPTRANS: an online tool for analyzing periodic transcription in yeast." Bioinformatics **23**(12): 1559-1561.

Landry, L. G., C. Chapple, *et al.* (1995). "Arabidopsis mutants lacking phenolic sunscreens exhibit enhanced ultraviolet-B injury and oxidative damage." Plant Physiol. **109**(4): 1159-1166.

Li, J. (2005). "Brassinosteroid signaling: from receptor kinases to transcription factors." Curr Opin Plant Biol. **8:** 526-531.

Li, J., T. M. Ou-Lee, *et al.* (1993). "Arabidopsis flavonoid mutants are hypersensitive to UV-B irradiation." Plant Cell **5**(2): 171-179.

Li, Q. H. and H. Q. Yang (2007). "Cryptochrome signaling in plants." Photochem Photobiol **83**(1): 94-101.

Lin, C. and D. Shalitin (2003). "Cryptochrome structure and signal transduction." Annual Review of Plant Biology **54**(1): 469-496.

Lin, C., H. Yang, *et al.* (1998). "Enhancement of blue-light sensitivity of Arabidopsis seedlings by a blue light receptor cryptochrome 2." Proc Natl Acad Sci U S A **95**(5): 2686-2690.

Long, J. C. and G. I. Jenkins (1998). "Involvement of plasma membrane redox activity and calcium homeostasis in the UV-B and UV-A blue light induction of gene expression in Arabidopsis." Plant Cell **10**(12): 2077-2086.

Mackerness, S. A. H., C. F. John, *et al.* (2001). "Early signaling components in ultraviolet-B responses: distinct roles for different reactive oxygen species and nitric oxide." Febs Letters **489**(2-3): 237-242.

Mackerness, S. A. H., S. L. Surplus, *et al.* (1999). "Ultraviolet-B-induced stress and changes in gene expression in Arabidopsis thaliana: role of signaling pathways controlled

by jasmonic acid, ethylene and reactive oxygen species." Plant Cell and Environment **22**(11): 1413-1423.

Matsushita, T., N. Mochizuki, *et al.* (2003). "Dimers of the N-terminal domain of phytochrome B are functional in the nucleus." Nature **424**(6948): 571-574.

Mazza, C. A., H. E. Boccalandro, *et al.* (2000). "Functional significance and induction by solar radiation of ultraviolet-absorbing sunscreens in field-grown soybean crops." Plant Physiology **122**(1): 117-125.

McKenzie, R. L., L. O. Bjorn, *et al.* (2003). "Changes in biologically active ultraviolet radiation reaching the Earth's surface." Photochem Photobiol Sci **2**(1): 5-15.

Mcnellis, T. W., A. G. Vonarnim, *et al.* (1994). "Genetic and molecular analysis of an allelic series of COP1 mutants suggests functional roles for the multiple protein domains." Plant Cell **6**(4): 487-500.

Meißner, D., A. Albert, *et al.* (2008). "The role of UDP-glucose:hydroxycinnamate glucosyltransferases in phenylpropanoid metabolism and the response to UV-B radiation in Arabidopsis thaliana." Planta **228**(4): 663-674.

Moissard G. and Voinnet O. (2006). "RNA silencing of host transcripts by cauliflower mosaic virus requires coordinated action of the four Arabidopsis Dicer-like proteins." Proc Natl Acad Sci U S A **103**(51): 19593–19598

Moore, J. D. (2001). "The Ran-GTPase and cell-cycle control." Bioessays **23**(1): 77-85.

Mortazavi, A., B. Williams, *et al.* (2008). "Mapping and quantifying mammalian transcriptomes by RNA-Seq." Nat Meth **5**(7): 621-628.

Nakajima, S., M. Sugiyama, *et al.* (1998). "Cloning and characterization of a gene (UVR3) required for photorepair of 6-4 photoproducts in Arabidopsis thaliana." Nucleic Acids Res. **26**(2): 638-44.

Olsen A., N., H. A. Ernst, *et al*. (2005). "NAC transcription factors: structurally distinct, functionally diverse." Trends in Plant Sciences **10**(2):79-87.

Ooka, H., K. Satoh, et al. (2003). "Comprehensive analysis of NAC family genes in Oryza sativa and Arabidopsis thaliana." DNA Res **10**(6): 239-247.

Oravecz, A., A. Baumann, *et al.* (2006). "CONSTITUTIVELY PHOTOMORPHOGENIC1 Is Required for the UV-B Response in Arabidopsis." Plant Cell **8**(18): 1975-1790.

Paul, N. D. and D. Gwynn-Jones (2003). "Ecological roles of solar UV radiation: towards an integrated approach." Trends in Ecology & Evolution **18**(1): 48-55.

Qian, J., J. Lin, *et al.* (2003). "Prediction of regulatory networks: genome-wide identification of transcription factor targets from gene expression data." Bioinformatics **19**(15): 1917-1926.

Quail, P. H. (2002). "Photosensory perception and signaling in plant cells: new paradigms?" Current Opinion in Cell Biology **14**(2): 180-188.

Renault, Nassar, *et al.* (1998). "The 1.7A˚crystal structure of the regulator of chromosome condensation (RCC1) reveals a seven-bladed propeller." Nature, **392**, 97-100.

Renault, Kuhlmann, *et al.* (2001). "Structural Basis for Guanine Nucleotide Exchange on Ran by the Regulator of Chromosome Condensation (RCC1) " Cell **105**; 245-255.

Ries, G., W. Heller, *et al.* (2000). "Elevated UV-B radiation reduces genome stability in plants." Nature **406**(6791): 98-101.

Rousseaux, M. C., A. L. Scopel, *et al.* (2001). "Responses to solar ultraviolet-B radiation in a shrub-dominated natural ecosystem of Tierra del Fuego (southern Argentina)." Global Change Biology **7**(4): 467-478.

Rozema, J., L. O. Bjorn, *et al.* (2002). "The role of UV-B radiation in aquatic and terrestrial ecosystems--an experimental and functional analysis of the evolution of UV-absorbing compounds." Journal of Photochemistry and Photobiology B: Biology **66**(1): 2-12.

Rozema, J., P. Boelen, *et al.* (2005). "Depletion of stratospheric ozone over the Antarctic and Arctic: Responses of plants of polar terrestrial ecosystems to enhanced UV-B, an overview." Environmental Pollution Forests Under Changing Climate, Enhanced UV and Air Pollution **137**(3): 428-442.

Safrany, J., V. Haasz, *et al.* (2008). "Identification of a novel cis-regulatory element for UV-B-induced transcription in Arabidopsis." Plant Journal **54**(3): 402-414.

Sakai, T., T. Kagawa, *et al.* (2001). "Arabidopsis nph1 and npl1: blue light receptors that mediate both phototropism and chloroplast relocation." Proc Natl Acad Sci U S A **98**(12): 6969-6974.

Sakamoto, K. and W. R. Briggs (2002). "Cellular and subcellular localization of phototropin 1." Plant Cell **14**(8): 1723-1735.

Sambrook, J., Fritsch, F. F. & Maniatis, T. (1989). "Molecular Cloning: A Laboratory Manual", Cold Spring Harbor Laboratory Press.

Sancar, A. (1994). "Structure and function of DNA photolyase." Biochemistry **33**(1): 2-9.

Sancar, A., L. A. Lindsey-Boltz, *et al.* (2004). "Molecular mechanisms of mammalian DNA repair and the DNA damage checkpoints." Annu Rev Biochem **73**: 39-85.

Sang, Y., Q. H. Li, *et al.* (2005). "N-terminal domain-mediated homodimerization is required for photoreceptor activity of Arabidopsis CRYPTOCHROME 1." Plant Cell **17**(5): 1569-1584.

Savenstrand, H., M. Brosche, *et al.* (2004). "Ultraviolet-B signaling: Arabidopsis brassinosteroid mutants are defective in UV-B regulated defence gene expression." Plant Physiology and Biochemistry **42**(9): 687-694.

Scarpeci, T. E., M. I. Zanor, *et al.* (2008). "Generation of superoxide anion in chloroplasts of Arabidopsis thaliana during active photosynthesis: a focus on rapidly induced genes." Plant Mol Biol. **66:** 361-378.

Seki, M., T. Umezawa, *et al.* (2007). "Regulatory metabolic networks in drought stress responses." Curr Opin Plant Biol. **10:** 296-302.

Selby, C. P. and A. Sancar (2006). "A cryptochrome/photolyase class of enzymes with single-stranded DNA-specific photolyase activity." Proc Natl Acad Sci U S A **103**(47): 17696-17700.

Seo, H. S., E. Watanabe, *et al.* (2004). "Photoreceptor ubiquitination by COP1 E3 ligase desensitizes phytochrome A signaling." Genes Dev **18**(6): 617-622.

Shalitin, D., H. Yang, *et al.* (2002). "Regulation of Arabidopsis cryptochrome 2 by blue-light-dependent phosphorylation." Nature **417**(6890): 763-767.

Shalitin, D., X. Yu, *et al.* (2003). "Blue light-dependent in vivo and in vitro phosphorylation of Arabidopsis cryptochrome 1." Plant Cell **15**(10): 2421-2429.

Shaner, N. C., G. H. Patterson, *et al.* (2007). "Advances in fluorescent protein technology." J Cell Sci **120**(Pt 24): 4247-4260.

Somers, D. E., P. F. Devlin, *et al.* (1998). "Phytochromes and cryptochromes in the entrainment of the Arabidopsis circadian clock." Science **282**(5393): 1488-1490.

Spalding, E. P. and K. M. Folta (2005). "Illuminating topics in plant photobiology." Plant, Cell & Environment **28**(1): 39-53.

Stratmann, J. (2003). "Ultraviolet-B radiation co-opts defense signaling pathways." Trends in Plant Science **8**(11): 526-533.

Surplus, S. L., B. R. Jordan, *et al.* (1998). "Ultraviolet-B-induced responses in Arabidopsis thaliana: role of salicylic acid and reactive oxygen species in the regulation of transcripts encoding photosynthetic and acidic pathogenesis-related proteins." Plant Cell and Environment **21**(7): 685-694.

Taiz, L. and E. Zeiger (1998). "Plant physiology." Sunderland, Mass., Sinauer Associates.

Takeuchi, Y., M. Murakami, *et al.* (1998). "The photorepair and photoisomerization of DNA lesions in etiolated cucumber cotyledons after irradiation by UV-B depends on wavelength." Plant and Cell Physiology **39**(7): 745-750.

Taki, N., Y. Sasaki-Sekimoto, *et al.* (2005). “12-oxo-phytodienoic acid triggers expression of a distinct set of genes and plays a role in wound-induced gene expression in Arabidopsis.” Plant Physiology. **139:** 1268-1283.

Tedetti, M. and R. Sempéré (2006). "Penetration of Ultraviolet Radiation in the Marine Environment. A Review." Photochemistry and Photobiology **82**(2): 389-397.

Tichtinsky, G., V. Vanoosthuyse, *et al.* (2003). "Making inroads into plant receptor kinase signaling pathways." Trends Plant Sci **8**(5): 231-237.

Tuteja, N., M. B. Singh, *et al.* (2001). "Molecular mechanisms of DNA damage and repair: Progress in plants." Critical Reviews in Biochemistry and Molecular Biology **36**(4): 337-397.

Ulm, R., A. Baumann, *et al.* (2004). "Genome-wide analysis of gene expression reveals function of the bZIP transcription factor HY5 in the UV-B response of Arabidopsis." Proc Natl Acad Sci U S A **101**(5): 1397-1402.

Wade, H. K., T. N. Bibikova, *et al.* (2001). "Interactions within a network of phytochrome, cryptochrome and UV-B phototransduction pathways regulate chalcone synthase gene expression in Arabidopsis leaf tissue." The Plant Journal **25**(6): 675-685.

Wargent, J., J. Moore, *et al.* (2009). "Ultraviolet radiation as a limiting factor in leaf expansion and development." Photochemistry and Photobiology **85**(1): 279-286.

Waters, E. R., Aevermann, W. D., *et al.* (2008). "Comparative analysis of the small heat shock proteins in three angiosperm genomes identifies new subfamilies and reveals diverse evolutionary patterns." Cell Stress and Chaperones **13**(2):127–142

Waterworth, W. M., Q. Jiang, *et al.* (2002). "Characterization of Arabidopsis photolyase enzymes and analysis of their role in protection from ultraviolet-B radiation." J. Exp. Bot. **53**(371): 1005-1015.

White, J. and E. Stelzer (1999). "Photobleaching GFP reveals protein dynamics inside live cells." Trends Cell Biol **9**(2): 61-65.

Xin, Z., Y. Zhao, *et al.* (2005). "Transcriptome analysis reveals specific modulation of abscisic acid signaling by ROP10 small GTPase in Arabidopsis." Plant Physiology **139**(3): 1350-1365.

Yamaguchi, R., M. Nakamura, *et al.* (1999). "Light-dependent translocation of a phytochrome B-GFP fusion protein to the nucleus in transgenic Arabidopsis." J Cell Biol **145**(3): 437-445.

Yang, F., L. G. Moss, *et al.* (1996). "The molecular structure of green fluorescent protein." Nat Biotechnol **14**(10): 1246-1251.

Yang, H. Q., R. H. Tang, *et al.* (2001). "The signaling mechanism of Arabidopsis CRY1 involves direct interaction with COP1." Plant Cell **13**(12): 2573-2587.

Yao, J., S. Roy-Chowdhury, *et al.* (2003). "AtSig5 is an essential nucleus-encoded Arabidopsis sigma-like factor." Plant Physiology **132**(2): 739-747.

Yi, C. L. and X. W. Deng (2005). "COP1 - from plant photomorphogenesis to mammalian tumorigenesis." Trends in Cell Biology **15**(11): 618-625.

Zhao, J. F., W. H. Zhang, *et al.* (2007). "SAD2, an importin beta-like protein, is required for UV-B response in Arabidopsis by mediating MYB4 nuclear trafficking." Plant Cell **19**(11): 3805-3818.